

***Drosophila* Hormone Receptor 96 (DHR96) Regulates Cellular Cholesterol Homeostasis**

by

Akila Gopalakrishnan

A thesis submitted in partial fulfillment of the requirements for the degree of

**Doctor of Philosophy**

in

Molecular Biology and Genetics

**Department of Biological Sciences  
University of Alberta**

© Akila Gopalakrishnan, 2015

## ABSTRACT

Cholesterol is well known for its adverse cardiovascular effects, however it has crucial cellular roles. For instance, cholesterol is a key component of eukaryotic cell membranes and constitutes the principle steroid hormone precursor in most animals. Cellular cholesterol concentrations have to be strictly controlled, since too much or too little can be fatal. Hence it is necessary to understand the molecular players that maintain cellular cholesterol homeostasis. Insects are sterol auxotrophs and thus obtain cholesterol or other suitable sterols exclusively from the diet. My data indicates that the nuclear receptor *DHR96* functions as a cellular cholesterol sensor to regulate cholesterol metabolism. While *DHR96* mutants are phenotypically normal on standard media, they arrest development as second instar larvae on diets with low, but sufficient amount of cholesterol to sustain normal development of wild type populations. I utilized *DHR96* mutants as a tool to characterize *Drosophila* sterol requirements, and carried out rescue experiments on lipid-depleted diets supplemented with different sterols to either entirely replace or partly substitute, for the principal functions of cholesterol in insects. My results suggest a novel unidentified function for cholesterol in insects, and that the prohormone alpha-ecdysone has a biological role in addition to its requirement for 20-hydroxyecdysone synthesis.

I identified that *DHR96* regulates the expression of several genes with predicted roles in cholesterol uptake, metabolism and transport. My data suggests that *DHR96* is required for the appropriate regulation of *Niemann-Pick type C-2c (Npc2c)*, at least in part through its function in the midgut. The *Drosophila* genome harbors eight *Npc2*-like genes. Mutations in the single human *NPC2* gene cause the fatal neurodegenerative Niemann-Pick Type C disease, characterized by cytotoxic cholesterol accumulation within organelles of nearly all tissues. I report the first observation that *Drosophila Npc2c* is transcriptionally regulated in a cholesterol-

and *DHR96*-dependent manner. Ubiquitous expression of *Npc2c-RNAi* cause developmental arrest phenotypes that cannot be rescued by cholesterol or the steroid hormone ecdysone. I triggered *Npc2c-RNAi* in a range of tissues and found that *Npc2c* function in the prothoracic gland (PG) and the midgut is necessary for viability. In the PG, loss-of-*Npc2c* function results in a dramatic downregulation of ecdysone biosynthetic enzymes, suggesting that *Npc2c* is vital for ensuring that cellular sterol levels are available for ecdysone synthesis. These data provide the first evidence to link a nuclear receptor in *Drosophila* to cholesterol homeostasis and to demonstrate that cholesterol regulates gene expression in *Drosophila*.

## ACKNOWLEDGMENTS

I am deeply grateful for the support and guidance of my advisor, Dr. Kirst King-Jones. Throughout my graduate work, Dr. King-Jones' insightful comments and advice have enormously helped develop my skills as a researcher, in delivering scientific presentations and teaching. I would like to thank Dr. Edan Foley and Dr. Heather McDermid for serving on my thesis committee. I sincerely thank them for the numerous discussions we have had and for their interest in my progress as a student in several aspects of research and scientific writing.

I express my earnest gratitude to my friends Jignesh, Aditi, Shishir and Aishwarya – whose humor and affection have supported me throughout my years in Edmonton. I am grateful to the many other friends I have been fortunate to meet and who have made my graduate life memorable and meaningful in their own different ways.

The work presented in this dissertation would not have been possible without the camaraderie with my lab colleagues and the generous support from other friends in my department. My heartfelt thanks to Mattéa, Emma, Nahbeel, Adam, Francesca, Ran, Jie, Brian, Pendleton, Niloofar, Cheryl, Manjeet, Morris, and Qiuxiang. I thank the departmental support staff, particularly, Ben, Jin-Xia, and Troy. I gratefully acknowledge the funding sources and the Departmental assistantships that have made this graduate work possible. I would like to thank all members in the *Drosophila* community, including the FlyGroup at the University of Alberta, for providing valuable reagents, comments and support for my projects.

I dedicate this dissertation to my parents and my husband. Their personal sacrifices and the unconditional love and support from thousands of miles away has been the foundation of my education, career and life.

## TABLE OF CONTENTS

<b>CHAPTER 1. INTRODUCTION</b>	<b>1</b>
1.1. Overview	2
1.2. Vertebrate cholesterol metabolic machinery	2
1.3. Cellular cholesterol: sources and pathways	3
1.4. Intracellular cholesterol transport	7
1.5. Nuclear receptors are crucial regulators of cholesterol metabolism	8
1.6. Insect sterol biology	10
1.7. Why does <i>Drosophila</i> need cholesterol?	13
1.8. Utilization of cholesterol by <i>Drosophila</i> for ecdysteroidogenesis	15
1.9. <i>Drosophila</i> Cholesterol biology	17
1.10. <i>DHR96</i> regulates <i>Drosophila</i> cholesterol metabolism genes	21
1.11. Project Objectives	25
<b>CHAPTER 2. MATERIALS AND METHODS</b>	<b>27</b>
2.1 Buffers	28
2.2. Culture media	29
2.2.1. LB (Luria Bertani) bacterial growth medium	29
2.2.2. Standard Fly Medium	29
2.2.3. Lipid-depleted media: LDYG and LDC424	30
2.3. <i>Drosophila</i> embryo collection	31
2.3.1. Embryo dechoriation	31
2.3.2. Population studies: setup	32
2.4. Larvae sample collections	32
2.5. RNA isolation	32
2.6. Quantitative Real time Polymerase Chain Reaction (qPCR)	33
2.7. High-throughput qPCR	34
2.8. Fly stocks	40
2.9. Filipin Staining	42
<b>CHAPTER 3.</b>	<b>43</b>
<b>USING <i>DHR96</i><sup>1</sup> MUTANTS AS TOOLS TO EXAMINE <i>DROSOPHILA</i> STEROL AND STEROID REQUIREMENTS</b>	<b>43</b>
3.1. <i>DHR96</i> <sup>1</sup> mutants arrest development in larval stages	44
3.2. <i>DHR96</i> <sup>1</sup> mutants are highly sensitive to cholesterol deprivation.	45
3.3. <i>DHR96</i> <sup>1</sup> mutant phenotype: a global defect in sterol metabolism?	47
3.4. Lipid-depleted C424 medium is a better alternative to LDYG.	50
3.5. Characterizing the cholesterol deficiency in <i>DHR96</i> <sup>1</sup> mutants	54
3.5.1. Testing the functional efficacy of supplemented sterol analogs	56
3.6. Do <i>DHR96</i> <sup>1</sup> mutants have an obligate requirement for cholesterol	57
3.7. Prohormone $\alpha$ -ecdysone has novel roles in independent of 20E production	61

<b>CHAPTER 4.</b>	<b>64</b>
<b>GENE EXPRESSION ANALYSIS OF THE CELLULAR RESPONSES TO DIETARY CHOLESTEROL</b>	<b>64</b>
4.1. Differences in dietary sterol composition trigger unique transcriptional responses	66
4.2. Cholesterol regulates gene expression in <i>Drosophila</i>	73
4.3. <i>High cholesterol</i> medium phenocopies the transcriptional response to <i>DHR96</i> mutation	76
4.4. Dietary sterol changes reverse the gene expression patterns of <i>DHR96</i> candidate targets that were induced by ectopic <i>DHR96</i> expression	92
4.5. Exploring the tissues that are most critical for <i>DHR96</i> function	97
 <b>CHAPTER 5.</b>	 <b>103</b>
<b>CHARACTERIZATION OF <i>DROSOPHILA</i> NIEMANN-PICK DISEASE TYPE C GENES: <i>Npc2c</i>, <i>Npc2d</i> and <i>Npc2e</i></b>	<b>103</b>
5.1. Phenotypic characterization of <i>Npc2d</i> and <i>Npc2e</i>	104
5.2. <i>Drosophila</i> gene <i>Npc2c</i> is essential for normal development	113
5.2.1. Ubiquitous <i>Npc2c</i> knockdown <i>in vivo</i>	113
5.3. Exploring the tissue-specific functions of <i>Drosophila Npc2c</i>	122
5.4. Midgut-specific knockdown of <i>Npc2c</i> has dose-dependent effects on development	124
5.4.1. Midgut-specific knockdown of <i>Npc2c</i> alleviates <i>DHR96<sup>1</sup></i> mutant phenotype on lipid-depleted media	129
5.5. A novel role for <i>Npc2c</i> in the prothoracic gland	133
5.5.1. Prothoracic gland-specific knockdown of <i>Npc2c</i> represses key ecdysone biosynthetic genes	138
5.5.2. Transcriptional regulation of <i>Npc2c</i> in the prothoracic gland	139
5.5.3. Validating the specificity of <i>Npc2c-RNAi</i> phenotypes	145
5.6. A model for <i>Npc2c</i> function	148
5.6.1. No obvious filipin-positive staining in <i>Npc2c-RNAi</i> animals	149
5.6.2. Prothoracic gland-specific <i>Npc1a-RNAi</i> recapitulates <i>Npc1a</i> mutant phenotypes	152
5.6.3. <i>Start1-RNAi</i> causes late larval developmental arrest that is fully rescuable to adult stages by cholesterol and 7DC	156
5.6.4. Are <i>Start1</i> and <i>Npc2c</i> necessary for the observed rescue of <i>Npc1a</i> mutants by cholesterol and 7DC?	161
5.7. Prothoracic gland-specific screen of the <i>Npc2</i> gene family	162
 <b>CHAPTER 6. DISCUSSION</b>	 <b>166</b>
6.1. <i>DHR96<sup>1</sup></i> mutants as a tool to study <i>Drosophila</i> sterol biology	167
6.2. Cholesterol regulates gene expression in <i>Drosophila</i>	171
6.3. <i>DHR96</i> controls cellular cholesterol homeostasis via Niemann Pick type C genes	174
6.4. Future directions	182
 <b>CONCLUSION</b>	 <b>184</b>
<b>BIBLIOGRAPHY</b>	<b>185</b>

**LIST OF TABLES**

<b>Table 2.1:</b> Primer sequences and UPL probe codes for quantitative real-time PCR.	35
<b>Table 4.1:</b> 55 Genes downregulated by 1% cholesterol in wild type.	78
<b>Table 4.2:</b> 73 Genes upregulated by 1% cholesterol in wild type.	79
<b>Table 4.3:</b> Summary of genes used for microfluidic qPCR and the effects of dietary lipids on their expression profiles.	80
<b>Table 4.4:</b> The transcriptional changes triggered by high cholesterol phenocopy the <i>DHR96<sup>l</sup></i> mutation.	89

## LIST OF FIGURES

<b>Figure 1.1:</b> Model of Vertebrate Cholesterol Transport	4
<b>Figure 1.2:</b> Representative images displaying cellular cholesterol accumulation phenotype of Niemann-Pick disease Type C	6
<b>Figure 1.3:</b> Phylogenetic tree comparing a subgroup of nuclear receptors in humans and <i>Drosophila</i> .	9
<b>Figure 1.4:</b> Sources of dietary sterols for steroid synthesis in <i>Drosophila</i> .	11
<b>Figure 1.5:</b> The onset of metamorphosis is initiated by the <i>Drosophila</i> neuropeptide prothoracicotropic hormone (PTTH).	13
<b>Figure 1.6:</b> Schematic showing <i>Drosophila</i> ring gland.	14
<b>Figure 1.7:</b> Protein sequence alignment of Npc2 proteins.	18
<b>Figure 1.8:</b> A hypothetical model of the key steps in <i>Drosophila</i> cholesterol biology.	19
<b>Figure 1.9:</b> High cholesterol phenocopies the transcriptional effects of the <i>DHR96</i> mutation.	21
<b>Figure 1.10:</b> Model for DHR96 function.	22
<b>Figure 3.1:</b> <i>DHR96<sup>l</sup></i> mutants arrest development as second instar larvae on Carolina 424 (C424) medium.	43
<b>Figure 3.2:</b> Validating the <i>DHR96<sup>l</sup></i> mutant lethal phenotype on an independent base medium.	45
<b>Figure 3.3:</b> <i>DHR96<sup>l</sup></i> mutants are rescued on LDYG medium by dietary cholesterol, ergosterol and stigmasterol.	47
<b>Figure 3.4:</b> Lipid-depleted C424 (LD) medium is a better alternative than LDYG.	49
<b>Figure 3.5:</b> Lipid-depleted C424 (LD) media fully recapitulates the <i>DHR96<sup>l</sup></i> mutant lethal phenotype and rescue by cholesterol without diminishing the viability of axenically reared wild type animals.	50
<b>Figure 3.6:</b> Chemical structures and molecular formula of sterols discussed in this chapter.	51
<b>Figure 3.7:</b> <i>DHR96<sup>l</sup></i> mutants can utilize desmosterol.	53
<b>Figure 3.8:</b> 20E is a biologically active sterol analog, sufficient to fully rescue	

<i>shroud-RNAi</i> animals on lipid-depleted (LD) medium.	54
<b>Figure 3.9:</b> 7-dehydrocholesterol is sufficient to rescue <i>DHR96<sup>l</sup></i> mutants to adulthood on lipid-depleted (LD) medium.	57
<b>Figure 3.10:</b> Prohormone alpha-ecdysone supports survival of <i>DHR96<sup>l</sup></i> mutants.	58
<b>Figure 3.11:</b> A unique combination of membrane sterols and ecdysteroids are sufficient to replace the dietary cholesterol requirement of wild type <i>Drosophila</i> .	61
<b>Figure 4.1:</b> Differentially expressed genes identified in the low cholesterol microarray.	65
<b>Figure 4.2:</b> Comparison of microarray data sets identified genes with roles in sterol biology.	66
<b>Figure 4.3:</b> Dietary cholesterol regulates cholesterol metabolism genes in a concentration- and <i>DHR96</i> -dependent manner.	70
<b>Figure 4.4:</b> A <i>high cholesterol</i> diet phenocopies the transcriptional responses caused by the <i>DHR96<sup>l</sup></i> mutation.	77
<b>Figure 4.5:</b> Exposure to high concentrations of dietary sterols result in unique sterol-specific transcriptional patterns.	84
<b>Figure 4.6:</b> Transcriptional profiles of the remaining 23 genes analyzed by microfluidics-based qPCR.	86
<b>Figure 4.7:</b> Dietary sterol changes reverse the gene expression patterns of <i>DHR96</i> candidate targets induced by ectopic expression of <i>DHR96</i> .	93
<b>Figure 4.8:</b> Midgut and fat body are the primary tissues critical for <i>DHR96</i> function.	97
<b>Figure 5.1:</b> Expression profiles of <i>Npc2d</i> , <i>Npc2e</i> and <i>Npc2c</i> on standard media.	104
<b>Figure 5.2:</b> Ubiquitous expression and/or ubiquitous <i>RNAi</i> -mediated knockdown of <i>Npc2d</i> and <i>Npc2e</i>	107
<b>Figure 5.3:</b> Tissue-specific <i>RNAi</i> -mediated knockdown of <i>Npc2d</i> and <i>Npc2e</i> cause no observable effects on survival or development on LD and SM	108
<b>Figure 5.4:</b> Test for genetic interaction between <i>DHR96</i> and <i>Npc2d/Npc2e</i> .	110
<b>Figure 5.5:</b> Validating the effectiveness of two independent <i>Npc2c-RNAi</i>	

transgenic lines.	112
<b>Figure 5.6:</b> <i>Npc2c-RNAi</i> phenotypes.	113
<b>Figure 5.7:</b> Ubiquitous <i>Npc2c-RNAi</i> using the VDRC#101583 transgenic line exhibits low penetrance and produces a range developmental phenotypes.	113
<b>Figure 5.8:</b> Summary of ubiquitous <i>Npc2c-RNAi</i> developmental phenotypes.	115
<b>Figure 5.9:</b> Ubiquitous knockdown of <i>Npc2c</i> (VDRC#31139) causes developmental arrest during larval stages.	116
<b>Figure 5.10:</b> Knockdown of <i>Npc2c</i> in the fat body, malpighian tubules and salivary gland has no observable effect on development or survival.	121
<b>Figure 5.11:</b> Midgut-specific knockdown of <i>Npc2c</i> causes partial developmental arrest.	124
<b>Figure 5.12:</b> Midgut-specific knockdown of <i>Npc2c</i> alleviates <i>DHR96<sup>l</sup></i> mutant phenotype on lipid-depleted media.	128
<b>Figure 5.13:</b> Partial rescue of the <i>DHR96<sup>l</sup></i> mutant phenotype by the midgut-specific knockdown of <i>Npc2c</i> .	130
<b>Figure 5.14:</b> Summary of the PG-specific <i>Npc2c-RNAi</i> developmental phenotypes.	133
<b>Figure 5.15:</b> Prothoracic gland-specific knockdown of <i>Npc2c</i> causes L3 developmental arrest and prolonged feeding.	134
<b>Figure 5.16:</b> Prothoracic gland-specific <i>Npc2c-RNAi</i> represses key ecdysone biosynthetic genes:	137
<b>Figure 5.17:</b> PG-specific <i>broad-RNAi</i> and <i>DHR96-RNAi</i> affect <i>Npc2c</i> -transcript levels.	139
<b>Figure 5.18:</b> PG-specific knockdown of <i>Npc2c</i> has no effects on the survival of <i>DHR96<sup>l</sup></i> mutants on lipid-depleted media.	140
<b>Figure 5.19:</b> Prothoracic gland-specific <i>broad-RNAi</i> represses <i>Npc1a</i> and <i>Start1</i> transcripts.	143
<b>Figure 5.20:</b> <i>Gbrowse</i> schematic view of <i>D.pseudoobscura</i> gene <i>Dpse\GAI7784</i> (631bp), ortholog of <i>Dmel</i> gene <i>CG3934</i> ( <i>Npc2c</i> ).	145
<b>Figure 5.21:</b> No obvious filipin-positive staining in <i>Npc2c-RNAi</i> animals.	149
<b>Figure 5.22:</b> Phenotypic characterization of <i>Npc1a</i> null mutants.	151
<b>Figure 5.23:</b> Prothoracic gland-specific <i>Npc1a-RNAi</i> is sufficient to fully recapitulate the <i>Npc1a</i> null mutant phenotype on yeast medium.	152
<b>Figure 5.24:</b> <i>Npc1a-RNAi</i> recapitulates <i>Npc1a</i> null mutant phenotype on	

lipid-depleted medium	153
<b>Figure 5.25:</b> Ubiquitous and prothoracic gland-specific knockdown of <i>Start1</i> cause developmental arrest on lipid-depleted (LD) medium.	156
<b>Figure 5.26:</b> Summary of results from the prothoracic gland-specific RNAi screen of the members of the <i>Npc2</i> gene family.	161
<b>Figure 5.27:</b> Prothoracic gland-specific knockdown of <i>Npc2g</i> is pupal lethal.	162
<b>Figure 6.1:</b> modENCODE tissue expression data of top candidate genes regulated by <i>DHR96</i> and cholesterol.	178
<b>Figure 6.2:</b> Promoter analysis of <i>Npc2c</i> upstream regions.	179
<b>Figure 6.3:</b> BLAST2 tool search result.	180

## LIST OF ABBREVIATIONS

20E - 20-hydroxyecdysone  
 7DC - 7-dehydrocholesterol  
 ABC - ATP-binding cassette  
 ABCA1 - ATP-binding cassette type A1  
 ABCG5 - ATP-binding cassette type G5  
 ABCG8 - ATP-binding cassette type G8  
 ACAT - acyl-CoA:cholesterol acyltransferase  
*act* – *actin*  
 AED - after egg deposition  
 apo – apolipoprotein  
*C. elegans* - *Caenorhabditis elegans*  
 C424 – Carolina 4-24 fly medium; also the *low cholesterol* medium  
 CA - corpora allata  
 CAR - Constitutive Active/Androstane Receptor  
 CC - corpus cardiacum  
 CETP - cholesteryl ester transfer protein  
*cg* - *collagen*  
 CLN3 - Ceroid lipofuscinosis protein  
 chol-ester – cholesteryl ester  
 DHR96 - *Drosophila* Hormone Receptor 96  
*DHR96<sup>l</sup>* – mutant allele of *DHR96* used for all studies described in this dissertation  
*Dib* - *Disembodied*  
 E –  $\alpha$  (alpha)-ecdysone  
 EcR - Ecdysone Receptor  
*egh* - *egghead*  
 ER - endoplasmic reticulum  
 ERK - extracellular-signal-regulated kinase  
 FANCL - Fanconi anemia, complementation group L  
 GCase - glucocerebrosidase  
 HDL - high-density lipoprotein  
*hh* – *hedgehog*  
*high cholesterol* medium - standard medium containing 1% w/v cholesterol  
 HMGCR - hydroxymethylglutaryl CoA reductase  
 IIS - insulin/insulin-like growth factor-1 (IGF-1) signaling  
 LD – lipid-depleted C424  
 LDL - low-density lipoprotein  
 LDL-R – LDL Receptor  
 LDYG - lipid-depleted yeast-glucose medium  
 LE – late endosome  
*Lip3* - *Lipase3*  
 LPL - lipoprotein lipase  
 LRP - LDL receptor-related protein  
 LXR - Liver X receptor  
 LYS – lysosome

M – molar  
MAPK - Mitogen-activated protein kinase  
*mex* - malic enzyme modifier  
MLN64 - Metastatic Lymph Node protein 64  
ng - nanogram  
NPC - Niemann-Pick Type C  
NPC1 - Niemann Pick disease Type C1  
NPC1a - Niemann Pick disease Type C, subfamily 1a  
NPC1b - Niemann Pick disease Type C, subfamily 1b  
NPC1L1 - Niemann-Pick C1-like 1  
NPC2 - Niemann Pick disease Type C2  
NPC2a - h - Niemann Pick disease Type C, subfamily 2a – 2h  
ORP1L - Oxysterol-binding protein-related protein 1L  
PG - prothoracic gland  
*Phm* – *Phantom*  
PL- phospholipids  
PTTH – prothoracicotropic hormone  
Raf - Rapidly Accelerated Fibrosarcoma  
Ras - Rat sarcoma  
rcf - relative centrifugal force  
RCT – Reverse Cholesterol Transport  
*sad* - *Shadow*  
*sd* – *scalloped*  
*shd* - *Shade*  
*sHh* - *sonic hedgehog*  
*spo* - *Spook*  
SREBP - Sterol Regulatory Element-Binding Protein  
*sro* - *Shroud*  
standard medium – standard cornmeal fly medium  
StAR - Steroid acute regulatory protein  
StART - Steroid acute regulatory protein-related lipid transfer  
SXR - Steroid and Xenobiotic Receptor  
TG – Triglyceride  
UAS - Upstream Activator Sequence  
USP - Ultraspiracle  
VDR - Vitamin D Receptor  
VLDL - very low-density lipoprotein  
w/v – weight by volume  
w/w – weight by weight  
YG – yeast-glucose medium  
µg – microgram  
µl – microliter  
µM - micromolar

**CHAPTER 1. INTRODUCTION**

## 1.1. Overview

Cholesterol is a major component of the western diet and has been associated for its adverse effects in prevalent diseases such as cardiac infarction, stroke, atherosclerosis, and neurodegenerative disorders such as Alzheimer's disease. However, cholesterol is a crucial molecule in many biological processes. At the cellular level, it is an essential component of eukaryotic cell membranes needed for preserving membrane fluidity, permeability, and microdomain organization [1], [2]. On an organismal level, cholesterol is required for covalent modifications of signaling proteins like Hedgehog (Hh) and is vital as the precursor of bile acids[3] that are important for intestinal absorption of dietary lipids. Cholesterol is a 27-carbon sterol that belongs to an important class of cyclical organic compounds called steroids. Cholesterol functions as the precursor to steroids such as pregnenolone, progesterone, aldosterone, testosterone, estradiol, cortisol, and vitamin D [4]–[6]. Since these steroids can function as hormones by binding to intracellular receptors to exert transcriptional regulation of responsive genes, they are collectively termed steroid hormones. Sterols such as campesterol, sitosterol and stigmasterol are plant-derived phytosterols, whereas ergosterol and zymosterol are the most commonly found fungal sterols. While the major animal sterols include cholesterol, 7-dehydrocholesterol, and coprosterol, cholesterol is physiologically the most important sterol in mammals.

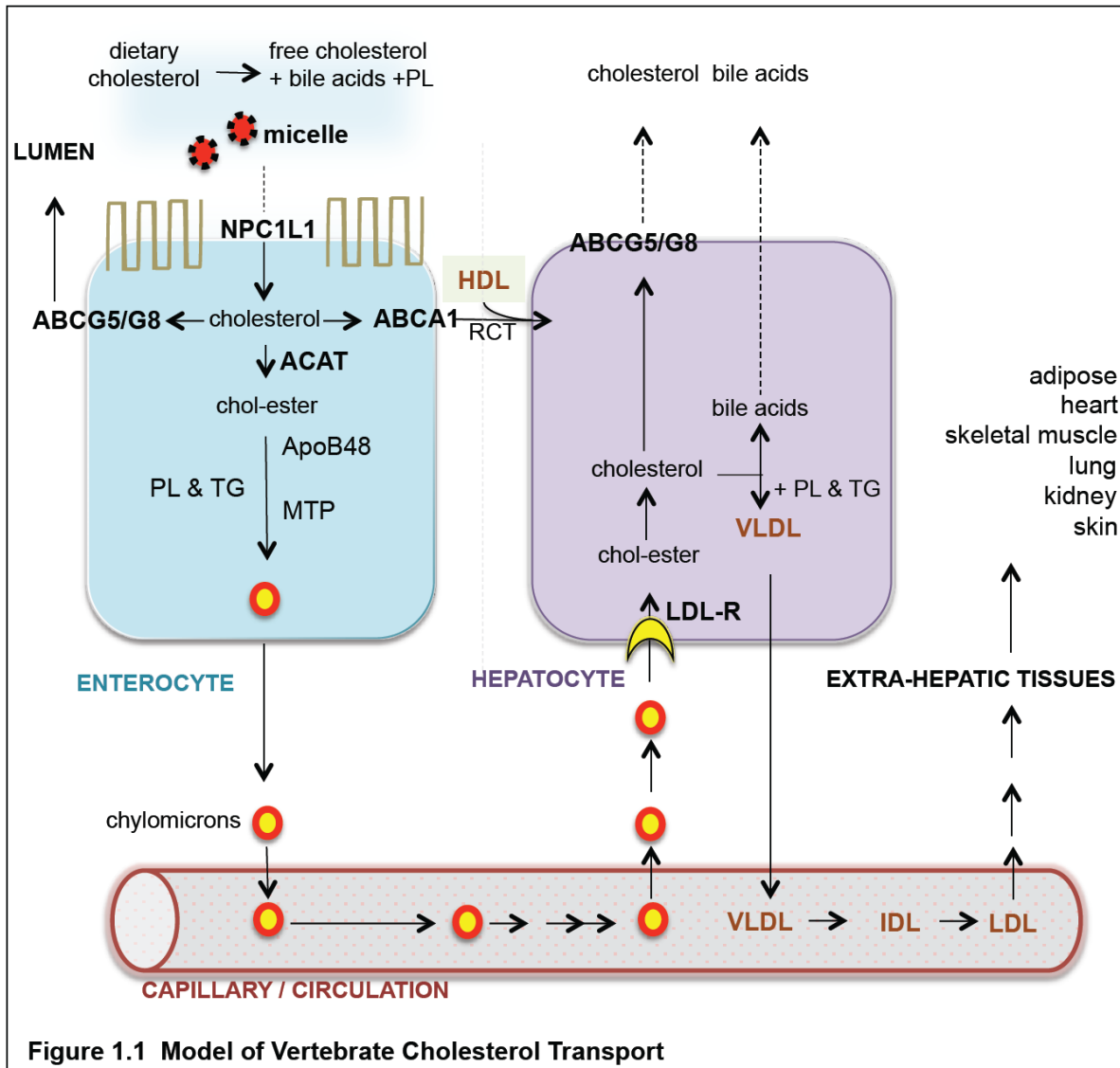
## 1.2. Vertebrate cholesterol metabolic machinery

Although the main biochemical pathways of cholesterol metabolism were identified several decades ago, we know relatively little about the aspects that regulate these processes. It is now well established that elevated plasma cholesterol levels are a risk for atherosclerosis. The whole body cholesterol balance is regulated by the net effects of endogenous cholesterol synthesis, dietary cholesterol absorption, and the biliary and fecal cholesterol excretion [7]–[9]. Among these processes, the regulation of cholesterol biosynthesis has been mainly studied within context to cardiovascular disease pathogenesis. For example, statin drugs have been well characterized to target the mevalonate-synthesizing enzyme hydroxymethylglutaryl CoA reductase (HMGCR) and thereby reduce circulating low-density lipoprotein cholesterol levels. In

contrast, our knowledge of how cellular cholesterol balance is maintained has been substantially behind. Although subcellular organelles have been shown to contain much different cholesterol concentrations, cells appear to have evolved specific homeostatic mechanisms to ensure that an optimal net cellular cholesterol level is maintained within strict limits. Misregulation of this cellular cholesterol homeostasis could lead to cytotoxicity [10] (due to excessive cholesterol) or cause detrimental effects such as cerebral haemorrhage [11], embryonic malformations, and behavioral disorders (due to cholesterol deficiency) [12]. Hence, there is a need to understand how cellular cholesterol is obtained, how it may be transported from the sites of synthesis to sites of utilization, and mainly, how these different processes are coordinately regulated to control fluctuations in cellular and systemic cholesterol levels.

### **1.3. Cellular cholesterol: sources and pathways**

There are two primary sources of mammalian cellular cholesterol. When cellular cholesterol levels drop, the transcription factor SREBP-2 (Sterol Regulatory Element-Binding Protein) is activated and subsequently transported into the nucleus to transcriptionally promote biosynthesis of cholesterol in the endoplasmic reticulum (ER). Cholesterol synthesized by the liver can then be packaged into plasma carriers called lipoproteins and transported to extra-hepatic tissues. The low-density lipoproteins (LDL) are the primary source of cholesterol for delivery to all tissues. The second source of cellular cholesterol comes from dietary absorption of cholesterol followed by receptor-mediated endocytosis of circulating LDLs. In mammals, the endogenous cholesterol synthesis and absorption of dietary cholesterol are coordinated - for example, inhibiting the synthetic pathway stimulates the uptake of circulating LDL-cholesterol from the blood via endocytosis. Such dynamic interaction between endogenous cholesterol synthesis and endocytosis is an approach to lower plasma cholesterol concentration and maintain it within optimal levels. As such, the LDL-endocytic pathway has been well characterized, however the intestinal absorption of cholesterol and the secondary intracellular processing of LDL-derived cellular cholesterol is a complex uncharacterized process that has been predicted to involve multiple interrelated degradative and synthetic pathways. In **Figure 1.1**, I summarize some of the major steps known to be involved in cholesterol absorption and secondary uptake of circulating LDLs. Modified and redrawn from *Ory (2004)* [13], *Lu et al., (2001)* [14] and *Takizawa (2010)* [15].



It has been hypothesized that within the intestinal lumen, bile acids solubilize cholesterol and fatty acids to form micelles that allow dietary cholesterol to diffuse through the surface of enterocytes, a process facilitated by the Niemann-Pick C1-like 1 (NPC1L1) protein (**Figure 1.1**). Within the enterocyte, the absorbed cholesterol can undergo one of the many fates: (1) cholesterol is excreted back into the lumen via the action of transporter proteins: ATP-binding cassette types G5- and G-8 (ABCG5 and ABCG8), (2) cholesterol could be effluxed from the enterocyte by ATP-binding cassette type A1 (ABCA1) transporter protein to high-density

lipoproteins (HDLs) for reverse cholesterol transport to the liver for utilization/excretion, or (3) the endoplasmic reticulum enzyme, acyl-CoA:cholesterol acyltransferase (ACAT2) esterifies free cholesterol and incorporates them into nascent chylomicron particles (with phospholipids (PL), triglycerides (TG) and lipid-binding apoproteins) that leave the intestine via the lymph and enter circulation. Chylomicrons then undergo substantial processing to form chylomicron remnants that primarily contain cholesteryl esters (chol-ester) and the protein component of lipoproteins called apolipoproteins (apoE and apoB-48). These remnants are then taken up by hepatocytes via interaction with the LDL receptor and/or LDL receptor-related protein (LRP), and subsequently their cholesterol is re-esterified and repackaged into very low-density lipoproteins (VLDLs). Circulating plasma VLDL then interacts with several proteins, including lipoprotein lipase (LPL) enzyme and cholesteryl ester transfer protein (CETP) to generate LDLs, which are thereafter endocytosed within target cells into late endosomes (LE) and lysosomes (LY). Recently, vesicular and non-vesicular pathways [16], [17] of intracellular cholesterol transport have been hypothesized as possible mechanisms to overcome cholesterol's hydrophobicity and the resulting hindrance across the aqueous compartments in the cell. Cholesterol may then be re-esterified (by ACAT) and stored within the cell.

Alternatively, it is predicted that the LDL-derived cholesterol might directly reach the endosome/lysosomal compartments where the luminal protein Niemann Pick disease Type C2 (NPC2) and the lysosomal membrane protein Niemann Pick disease Type C1 (NPC1) are located [18]. Recent biochemical and crystallographic analyses have identified a specific luminal domain of NPC1 to bind NPC2 at lysosomal-specific pH and that the binding strength strongly increases as NPC2 carries cholesterol, indicative of a directionality to this transfer [19]. The functional importance of these cholesterol transport proteins is implicated in the fatal Niemann-Pick Type C (NPC), an autosomal-recessive neurodegenerative disease. As a consequence of mutations in either NPC1 (95% of cases) or NPC2, cholesterol and several lipids such as sphingomyelin and glycolipids, progressively accumulate within lysosomes of neurons and nearly all other organs starting from early fetal development until death (of affected children or animal model [20], [21]. **(Figure 1.2)**. Affected patients demonstrate clinically progressive hepatosplenomegaly, lung dysfunction, and severe neurodegeneration in the brain. Typical neurological abnormalities such as vertical supranuclear gaze palsy, saccadic eye movement defects, cerebellar ataxia, dystonia and dysphagia [22] arise at different ages, but invariably become aggravated with age leading to

early death by childhood [23]. Patients with neurological early-onset develop symptoms faster and have an overall shorter lifespan than patients with adult-onset of neurodegeneration [23].

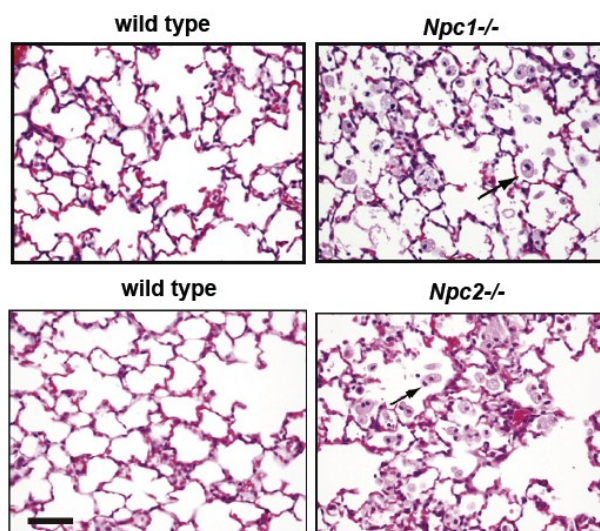


**Figure 1.2. Representative images displaying cellular cholesterol-accumulation phenotype of Niemann-Pick disease Type C.** Images on right side panels show representative histological sections of lung tissue in *Npc1*<sup>-/-</sup> and *Npc2*<sup>-/-</sup> mice. The arrow points to a lipid-laden macrophage within their alveoli. Data from Ramirez *et al* (2014).

Several disease-specific therapies have been tested in animal models using drugs such as Miglustat [24] and cholesterol-binding cyclodextrins [25]. However, such therapies relieve only a subset of specific disease symptoms, and currently there is no cure for the disease. NPC1 is a membrane-spanning protein located in the limiting membrane of late endosome/lysosome (LE/LY). Evidence suggests that NPC1 is responsible to transfer cholesterol from LE/LY to endoplasmic reticulum (ER) for esterification or to plasma membrane for efflux [22], however, it is unclear how NPC1 is regulated or how the balance between import/export of circulating cholesterol as governed by NPC1 relates to potential consequence in atherogenesis. On the other hand, NPC2 is a soluble, luminal lysosomal protein that has been shown to bind and release cholesterol very rapidly [19]. Few attempts have been made to study the molecular or biochemical aspects of cholesterol transport by NPC2. Although homologs of the NPC1 and NPC2 proteins exist in flies, worms, and yeast [26][27], little is still known about how mutations in either proteins correlated to the disease pathology and symptoms – and for example, how does the predicted functions of these proteins in cholesterol uptake, transport or metabolism relate to whole body physiology? In Chapters 4 and 5, I address how *Drosophila* NPC genes are transcriptionally regulated in response to dietary cholesterol.

#### 1.4. Intracellular cholesterol transport

The mechanisms by which cholesterol is transported intracellularly, e.g. from (the inside of) LE/LYS to mitochondria or endoplasmic reticulum, are not well understood. Preliminary studies have suggested that the vertebrate lysosomal protein Metastatic Lymph Node protein 64 (MLN64, also called StARD3- Steroid acute regulatory protein 3) may bind cholesterol via its StART (StAR-related lipid transfer) domain and subsequently tether to late endosomes (LE) to transport cholesterol to mitochondria. Two other cholesterol-binding proteins, the oxysterol-binding protein-related protein 1L (ORP1L)[28] and the neuronal ceroid lipofuscinosis protein (CLN3)[29] have also been recently reported to sense cholesterol levels within LE, induce LE-ER physical interactions and control dynamic movement of cellular cholesterol. The ATP binding cassette class A (ABCA) of cholesterol-binding proteins have been recently detected in LE compartments. Nearly 50% of the 48 human ABC transporter genes are linked to human disease conditions with abnormal lipid transport and/or homeostasis [30]. The ubiquitously expressed ABC protein - *ABCA1*, mutations in which cause the Tangier disease, is essential to generate high-density lipoprotein (HDL) particles (**Figure 1.1**). *ABCA1* plays a critical role in systemic cholesterol-efflux for the reverse cholesterol transport pathway in macrophages. Patients affected by the Tangier disease present significantly reduced levels of circulating HDL and ultimately develop atherosclerosis from aberrant tissue accumulation of cholesteryl esters [31]. On the other hand, another ABC protein - *ABCA3* is exclusively expressed in pulmonary pneumocytes and is reported to mediate the transport of cholesterol and phospholipids into lysosomal-like organelles called lamellar bodies that function as a storage pool for cholesterol-rich lung surfactants[32]. Thus different LE-specific cholesterol-binding proteins are likely associated with different steps of cholesterol transport based on their individual cellular context and future work will be necessary to identify cellular players of intracellular cholesterol transport. The work presented in this dissertation address the roles of nuclear receptors in regulating such cholesterol transporters to maintain cellular cholesterol homeostasis.

### 1.5. Nuclear receptors are crucial regulators of cholesterol metabolism

In vertebrates, cholesterol homeostasis is maintained by controlling dietary cholesterol absorption, modulating cellular influx and efflux of cholesterol, and via enzymatic control of key steps in the cholesterol biosynthetic pathway. In contrast to the SREBP family of transcription factors that regulate cholesterol biosynthesis in mammals, the liver X receptors (LXR) respond to high cellular cholesterol levels by directly binding specific cholesterol metabolites and triggering the induction of genes that promote cellular cholesterol trafficking and efflux[33]. My work concentrated on characterizing the role of a *Drosophila* nuclear receptor in the regulation of cholesterol metabolism. Nuclear receptors are ligand-regulated transcription factors that directly regulate gene expression of target genes primarily involved in processes like reproduction, development, and metabolism [34], [35]. These responses are mediated by binding to fat-soluble ligands such as sterols (cholesterol, oxysterols, bile acids) [44], steroids (vitamin A and D) [4], steroid hormones (androgens and estrogens) [38], [39], and a range of xenobiotics [40]. Nuclear receptors have emerged as promising therapeutic drug targets for human diseases such as cancers and metabolic syndrome. Nuclear receptors have been classified into six major subfamilies based on their phylogenetic relationships [41], [42]. While there are 48 nuclear receptor genes found in humans and 284 in *C. elegans*, the *Drosophila* genome contains only 21 genes [43]. Among subfamily I, the SXR (Steroid and Xenobiotic Receptor) and CAR (Constitutive Active/Androstane Receptor), which are human xenobiotic sensors; and VDR (Vitamin D Receptor), which regulates calcium homeostasis, have a single common ortholog in *Drosophila*, termed DHR96 (*Drosophila* Hormone Receptor 96) (**Figure 1.3**).

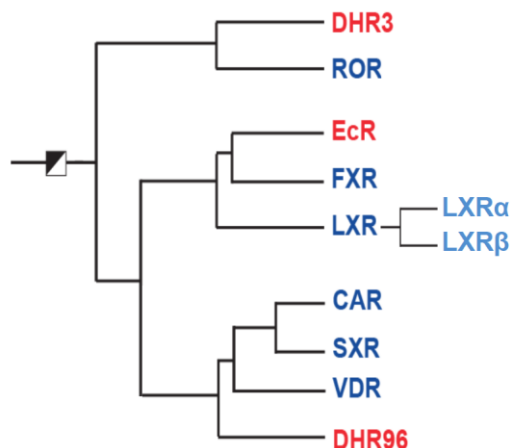


**Figure 1.3. Phylogenetic tree comparing a subgroup of nuclear receptors in humans and *Drosophila*.** Modified after Laudet *et al.*, 2005. This is a subgroup within Subfamily-I of nuclear receptors. Human nuclear receptors are shown in blue, fly receptors in red. LXR: Liver X Receptor. FXR: Farnesoid X Receptor. EcR: Ecdysone Receptor. CAR: Constitutive Androstane Receptor. SXR: Steroid and Xenobiotic Receptor. VDR: Vitamin D Receptor. DHR96: *Drosophila* Hormone Receptor 96. DHR3: *Drosophila* Hormone Receptor 3. ROR: retinoid-related orphan receptors (RORs).

Located within the subfamily-I is the vertebrate LXR $\alpha$  (NR1H3) and LXR $\beta$  (NR1H2), which are responsible to maintain cellular cholesterol homeostasis by regulating key steps in the biosynthesis, dietary uptake and cellular influx/efflux of cholesterol [44]–[46]. While LXR $\alpha$  is exclusively expressed in metabolically active tissues such as the liver, small intestine, kidney, macrophages, and adipose tissue [47], LXR $\beta$  is ubiquitously expressed, especially at higher levels in the developing brain [48], suggesting that the LXRs have different physiological functions. Cholesterol metabolites called oxysterols (particularly, 24(S), 25-epoxycholesterol) activate LXRs via direct binding and maintain cellular cholesterol concentrations by regulating expression of genes involved in the reverse cholesterol transport. As shown in **Figure 1.1** as RCT, in this process, cholesterol that is synthesized or deposited within peripheral cells is transported via high-density lipoproteins (HDL) and returned back to the liver for reuse or re-excretion into the bile. The cholesterol transporter *ABCA1*, also a LXR target, is the key regulator of this transport system[49]. Other LXR targets include several key enzymes in the cholesterol biosynthetic pathway such as squalene synthase [49], [50] and the complex ABCG5/ABCG8 that promote excretion of intestinal cholesterol into bile [51]. Curiously, LXR $\alpha$  activation by synthetic agonists induces expression of NPC1 and 2 proteins [46], and conversely, a siRNA-mediated knockdown of NPC1 and NPC2 leads to a strong reduction in basal and LXR-

induced cholesterol efflux [33], suggesting that LXR may directly target the NPC1/2 genes. Whether LXR $\alpha$  also transcriptionally regulates the gut-specific NPC1L1 (NPC1-Like 1) gene, which is critical for absorption of intestinal cholesterol, is debated. Nevertheless, the LXR activation-induced transcriptional regulation of genes involved in cholesterol trafficking and efflux has driven the development of novel cardiovascular disease treatments using molecules that can modulate LXR activity [52][53].

The work presented in this thesis has provided the first evidence that links a nuclear receptor in *Drosophila* to cholesterol homeostasis [54]. **My hypothesis is that *DHR96* functions as (i) a sensor for cholesterol and/or cholesterol metabolites and (ii) a central regulator of genes involved in dietary cholesterol uptake, metabolism and transport.** I demonstrate that DHR96 regulates fly orthologs of the human disease genes such as Niemann-Pick disease Type C (NPC1 and 2) that are involved in controlling cellular cholesterol homeostasis.

## 1.6. Insect sterol biology

A crucial distinction from vertebrates is that insects [55], and other invertebrates, such as *C. elegans* [56], cannot synthesize cholesterol [57]. This is because insects lack the enzyme squalene synthase and all successive enzymes of the mevalonate-cholesterol biosynthetic pathway that is well characterized in vertebrates. Historically, cholesterol has been studied in most insects as the precursor of the molting hormone - ecdysone [55]. A few known exceptions, include the *Drosophila pachea*, which requires  $\Delta 7$ -sterols such as 7-cholestenol and 7-campestenol[58], or the beetle *Xyleborus ferrugineus*, which requires ergosterol or 7-dehydrocholesterol for normal development. Under normal dietary conditions, cholesterol is the main insect sterol and satisfies all sterol requirements in most insects [59]. However, not all kinds of sterols can be utilized, since insects require specific sterol structures that can either be used directly for ecdysteroidogenesis or be converted to cholesterol from C28 - or C29 - sterols. Moreover, not all insects are capable of performing this conversion, a process that involves dealkylation of carbon-24 alkyl group of plant sterols (called phytosterols) to cholesterol via the enzymatic action of  $\Delta 24$ -reductase. Also, the extent to which they are capable of such conversions varies among the different species [60], [61]. For example, the house fly *Musca domestica* and the fruit fly *Drosophila melanogaster* lack  $\Delta 24$ -reductase and cannot dealkylate

phytosterols [57], whereas the yellow fever mosquito *Aedes aegypti* and the tobacco hornworm *Manduca sexta* are capable of dealkylation [61], suggesting that insect species have evolved to utilize a spectrum of sterols for survival and development.

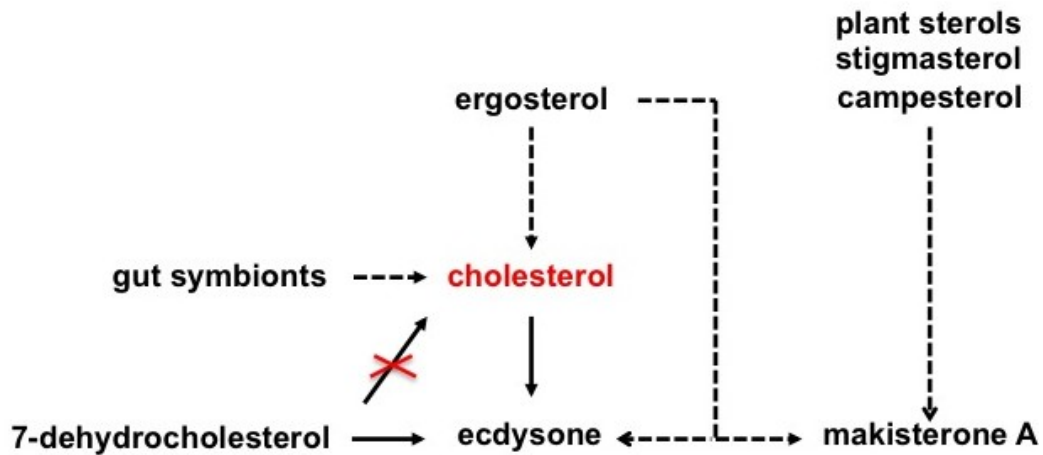


**Figure 1.4. Sources of dietary sterols for steroid synthesis in *Drosophila*.** Ecdysone is classically considered the major steroid hormone in *Drosophila melanogaster* [86]. It is synthesized from cholesterol through a series of enzymatic reactions, also involving the intermediate, 7-dehydrocholesterol. However, larvae raised on diets containing plant sterols (such as stigmasterol, campesterol) predominantly secrete makisterone A [128], [194] instead of ecdysone. On the other hand, larvae fed with yeast-based diets (mainly composed of ergosterol) have been shown to synthesize varying amounts of makisterone A [211] and ecdysone [89], the latter likely via dealkylation to cholesterol [128]. Gut microbial symbionts may also provide additional sources of sterols for *Drosophila* ADDIN CSL\_CITATION { "citationItems" : [ { "id" : "ITEM-1", "itemData" : { "DOI" : "10.1038/nmeth.2731", "ISSN" : "1548-7105", "PMID" : "24240321", "abstract" : "A critical requirement for research using model organisms is a well-defined and consistent diet. There is currently no complete chemically defined (holidic) diet available for *Drosophila melanogaster*. We describe a holidic medium that is equal in performance to an oligidic diet optimized for adult fecundity and lifespan. This holidic diet supports development over multiple generations but at a reduced rate. Over 7 years of experiments, the holidic diet yielded more consistent experimental outcomes than did oligidic food for egg laying by females. Nutrients and drugs were more available to flies in holidic medium and, similar to dietary restriction on oligidic food, amino acid dilution increased fly lifespan. We used this holidic medium to investigate amino acid-specific effects on food-choice behavior and report that folic acid from the microbiota is sufficient for *Drosophila* development.", "author" : [ { "dropping-particle" : "", "family" : "Piper", "given" : "Matthew D W", "non-dropping-particle" : "", "parse-names" : false, "suffix" : "" }, { "dropping-particle" : "", "family" : "Blanc", "given" : "Eric", "non-dropping-particle" : "", "parse-names" : false, "suffix" : "" }, { "dropping-particle" : "", "family" : "Leit\u00e7alves", "given" : "Ricardo", "non-dropping-particle" : "", "parse-names" : false, "suffix" : "" }, { "dropping-particle" : "", "family" : "Yang", "given" : "Mingyao", "non-dropping-particle" : "", "parse-names" : false, "suffix" : "" }, { "dropping-particle" : "", "family" : "He", "given" : "Xiaoli", "non-dropping-particle" : "", "parse-names" : false, "suffix" : "" }, { "dropping-particle" : "", "family" : "Linford", "given" : "Nancy J", "non-dropping-particle" : "", "parse-names" : false, "suffix" : "" }, { "dropping-particle" : "", "family" : "Hoddinott", "given" : "Matthew P", "non-dropping-particle" : "", "parse-names" : false, "suffix" : "" }, { "dropping-particle" : "", "family" : "Hopfen", "given" : "Corinna", "non-dropping-particle" : "", "parse-names" : false, "suffix" : "" }, { "dropping-particle" : "", "family" : "Souloukis", "given" : "George a", "non-dropping-particle" : "", "parse-names" : false, "suffix" : "" }, { "dropping-particle" : "", "family" : "Niemeyer", "given" : "Christine", "non-dropping-particle" : "", "parse-names" : false, "suffix" : "" }, { "dropping-particle" : "", "family" : "Kerr", "given" : "Fiona", "non-dropping-particle" : "", "parse-names" : false, "suffix" : "" }, { "dropping-particle" : "", "family" : "Pletcher", "given" : "Scott D", "non-dropping-particle" : "", "parse-names" : false, "suffix" : "" }, { "dropping-particle" : "", "family" : "Ribeiro", "given" : "Carlos", "non-dropping-particle" : "", "parse-names" : false, "suffix" : "" }, { "dropping-particle" : "", "family" : "Partridge", "given" : "Linda", "non-dropping-particle" : "", "parse-names" : false, "suffix" : "" } ], "container-title" : "Nature methods", "id" : "ITEM-1", "issue" : "1", "issued" : { "date-parts" : [ [ "2014", "1" ] ] }, "page" : "100-5", "title" : "A holidic medium for *Drosophila melanogaster*.", "type" : "article-journal", "volume" : "11" }, { "uris" : [ "http://www.mendeley.com/documents/?uuid=dc8ef5d2-99c4-4a45-8cdc-af1e2ea85e2f" ] }, { "id" : "ITEM-2", "itemData" : { "DOI" : "10.1242/jeb.101725", "ISSN" : "1477-9145", "PMID" : "24577449", "abstract" : "Animal nutrition is profoundly influenced by the gut microbiota, but knowledge of the scope and underlying mechanisms of the underlying animal-microbial interactions is fragmentary. To investigate the nutritional traits shaped by the gut microbiota of *Drosophila*, we determined the microbiota-dependent response of multiple metabolic and performance indices to systematically-varied diet composition. Diet-dependent differences between *Drosophila* bearing its unmanipulated microbiota (conventional flies) and experimentally deprived of its microbiota (axenic flies) revealed evidence for: microbial sparing of dietary B vitamins, especially riboflavin, on low-yeast diets; microbial promotion of protein nutrition, particularly in females; and microbiota-mediated suppression of lipid/carbohydrate storage, especially on high sugar diets. The microbiota also set the relationship between energy storage and body weight, indicative of microbial modulation of the host signaling networks that coordinate metabolism with body size. This analysis identifies the multiple impacts of the microbiota on the metabolism of *Drosophila*, and demonstrates that the significance of these different interactions varies with diet composition and host sex.", "author" : [ { "dropping-particle" : "", "family" : "Wong", "given" : "Adam C-N", "non-dropping-particle" : "", "parse-names" : false, "suffix" : "" }, { "dropping-particle" : "", "family" : "Dobson", "given" : "Adam J", "non-dropping-particle" : "", "parse-names" : false, "suffix" : "" } ] } ] }

Therefore since *Drosophila melanogaster* retrieves all of its sterol requirements – either directly or via appropriate sterol precursors, solely from the diet, I asked, what are the sterol requirements of *Drosophila*? In chapter 3, I address this question by using defined sterol-supplemented media to systematically characterize the requirement for dietary cholesterol in *Drosophila*. From a physiological standpoint, the cellular pool of endogenously synthesized cholesterol in vertebrate systems often confounds studies on the mechanisms of cholesterol transport and utilization. As such, a systemic sterol depletion in a mammalian model requires the use of techniques, such as: chemical extractions (to deplete cholesterol from cell/tissue extracts) [62], or the use of radiolabeled sterol diets [63], enzyme inhibitors that block cholesterol biosynthesis [64], or drug treatments (e.g. cyclodextrin to generate cholesterol-free products) [25], and other complex genetic manipulations which can perturb several shared developmental signaling and metabolic pathways [65]. In contrast, the absence of an endogenous cholesterol-biosynthetic pathway in *Drosophila* provides an ideal platform to investigate several open questions related to insect sterol biology: for instance, what are the physiological responses to varying levels of dietary cholesterol, what are the mechanisms regulating cholesterol uptake, transport and metabolism, and particularly, what are the cellular functions of cholesterol in insects?

### **1.7. Why does *Drosophila* need cholesterol?**

Sterols (predominantly, cholesterol) serve three known functions in *Drosophila*. Firstly, cholesterol mediates the C-terminal processing of the *Drosophila* hedgehog (hh) protein, a morphogen that has been implicated to regulate embryonic, larval and adult development [66], [67]. While cholesterol is known to covalently modify human sHh (sonic hedgehog) and thus facilitate the delivery of secreted Hh proteins within target tissues, the functional significance and requirement for cholesterol in regulating *Drosophila* Hh signaling activity has been debated [68]. Secondly, much like vertebrate cell membranes, a bulk of cholesterol constitutes a significant portion of the *Drosophila* membrane lipids and confers certain unique biophysical properties that are crucial to membrane potential, membrane domain organization [69], protein-lipid interactions and for normal functioning of membrane proteins [70], [71]. For instance, synthetic reduction in membrane cholesterol levels by chemical methods has been shown to

severely affect protein sorting and cell signaling, implying that membrane cholesterol has vital roles in vivo as well [65]. Recently, we are beginning to understand the mechanisms by which *Drosophila* might regulate membrane sterol levels and protect cells from variations in dietary cholesterol availability [72]–[75]. The third and the most well studied aspect of utilization of cholesterol in *Drosophila* is the synthesis of the molting hormone 20E (**Figure 1.5**).

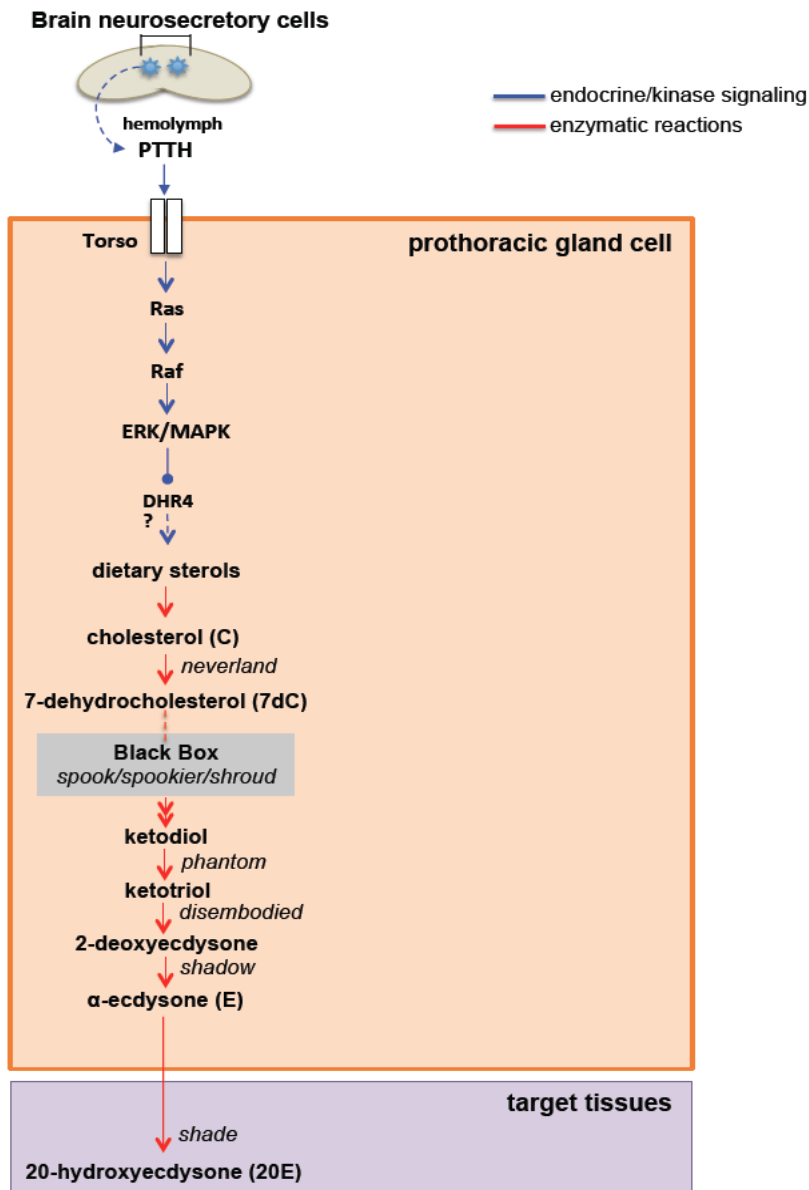


**Figure 1.5.** The onset of metamorphosis is initiated by the *Drosophila* neuropeptide prothoracicotrophic hormone (PTTH) which triggers the synthesis and release of ecdysone in the PG cells, and thereby controls the timing of developmental transitions and larval body size. PTTH is thought to bind its receptor Torso, to trigger ecdysone production via the Ras, Raf and ERK/MAPK pathway. Neuroendocrine signals are coordinated with several predicted nuclear transcription regulators to mediate the conversion of dietary derived plant or yeast sterols to cholesterol which reach the prothoracic gland cells to undergo a sequential conversion to ecdysone that is transported in the hemolymph to target tissues to synthesize 20E. **Ras**; Rat sarcoma, **RAF**; Rapidly Accelerated Fibrosarcoma, **ERK**; Extracellular signal-regulated kinase, **MAPK**; mitogen-activated protein kinase.

### 1.8. Utilization of cholesterol by *Drosophila* for ecdysteroidogenesis

Several tissues such as the ovaries, testes and epidermis utilize cholesterol for steroidogenesis, however only the prothoracic glands (PG) secrete the ecdysteroids (termed, molting hormones). During larval stages, ecdysteroids synthesis is activated in response to the release of the prothoracicotrophic (PTTH) hormone from the brain. Binding of PTTH to its receptor Torso triggers a MAP (Mitogen-activated protein) kinase pathway that ultimately stimulates ecdysteroid production. The major endocrine organ in *Drosophila* is the ring gland, which comprises the prothoracic gland (PG), the corpora allata (CA), and the corpora cardiaca (CC) (Figure 1.6).

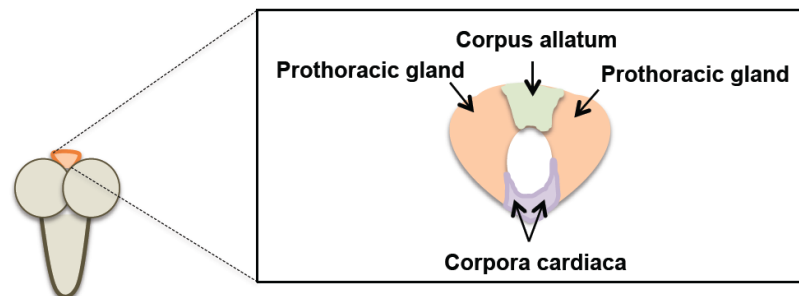


**Figure 1.6. Schematic showing *Drosophila* ring gland.**

The ring gland is located between the two brain hemispheres. It comprises the prothoracic gland (PG), corpus allatum (CA) and corpora cardiaca (CC).

In addition, nutritional cues that are integrated and relayed by the insulin/insulin-like growth factor-1 (IGF-1) signaling (IIS) pathway also impinge on the synthesis of ecdysteroids [119]. Although PPTH is found in adults, its exact role and significance in adults is unknown [79]. In

the larval PG cells, specific ER and mitochondrial cytochrome P450 (P450) enzymes encoded by a group of genes known as Halloween genes [80] then sequentially convert the dietary-derived cholesterol into the prohormone  $\alpha$ -ecdysone (E), which is then transformed to the active molting hormone 20-hydroxyecdysone (20E) in peripheral target tissues [81].

The first step in this 20E-synthesis pathway, which converts cholesterol to 7-dehydrocholesterol (7DC), requires a Rieske oxygenase called Neverland [82]. The details of successive conversion of 7DC to the 5 $\beta$ -ketodiol are still unclear and referred to as the 'Black Box'. However the black box is considered to harbor, the rate-limiting step of this pathway and require the function of at least two enzymes, called *Shroud* (*Sro*) and *Spook* (*Spo*) [83]. The P450 enzymes *Phantom* (*Phm*), *Disembodied* (*Dib*) and *Shadow* (*Sad*) catalyze the last three steps in the conversion of 5 $\beta$ -ketodiol to  $\alpha$ -ecdysone (E), which is then released from the PG and converted to molting hormone 20-hydroxyecdysone (20E) by another P450 enzyme called *Shade* (*Shd*) in peripheral tissues such as the fat body. The prothoracic gland degenerates during metamorphosis, and in female adult *Drosophila*, ovaries express *spo*, *phm*, *dib*, *sad* and *shd* to synthesize ecdysteroids that have essential roles in vitellogenesis and oogenesis [84]. In contrast, although they have been shown to produce ecdysteroids, little is known about the function of steroid hormones in adult *Drosophila* males, or the mechanisms and location of synthesis [85].

Pulses of 20E produced during the first and second instar larval stages trigger molting of the cuticle, whereas a high 20E titer pulse at the end of third instar initiates metamorphosis and triggers puparium formation [86]. The 20E steroid hormone binds to a heterodimer consisting of the Ecdysone Receptor (EcR) and Ultraspiracle (USP). When activated by its best characterized ligand, 20E, the 20E-EcR/USP receptor complex triggers stage- and tissue-specific transcription of primary 20E-response genes (e.g. E74, E75 and broad-complex) to orchestrate *Drosophila* development and metamorphosis [87]. While 20E is considered the classical - active molting hormone, ecdysone (E) has been shown to have physiological roles independent of 20E. A high titer of  $\alpha$ -ecdysone in the hornworm *Manduca* triggers neuroblast proliferation and optic lobe development [88]. Microarray analysis of RNA isolated from cultured *Drosophila* larval tissues revealed 55 genes that were transcriptionally regulated specifically as a response to  $\alpha$ -ecdysone, rather than 20E in cultured larval tissues, suggesting that  $\alpha$ -ecdysone may act as a hormone independent of 20E [87]. In **chapter 3, section 3.4**; I am presenting data supporting this idea. The PG cells have also been shown to synthesize the C28 ecdysteroid molting hormone -

makisterone A (C<sub>25</sub> hexahydroxy-ecdysone) when fed on cornmeal diets containing phytosterols such as campesterol [89]. However, the exact mechanisms of action or regulatory factors that control the synthesis of makisterone A or its physiological implications in development by its ability to function as a molting hormone are still unclear.

### **1.9. *Drosophila* Cholesterol biology**

The Dipteran insect *Drosophila melanogaster* has served for more than a 100 years as an excellent model system to study a variety of biological processes in development, metabolism and physiology. The availability of an extensive array of genetic tools, sequenced genome and the large collection of available RNAi-transgenics and mutants make *Drosophila* a highly versatile system to conduct experiments that explore the molecular basis and pathophysiology of several human diseases. Remarkably, *Drosophila* also has organs and cell types that perform cholesterol metabolism and homeostasis highly similar to their vertebrate counterparts [90]. For instance, analogous to the function of the microvilli located in the mammalian small intestine, the first site of dietary cholesterol absorption occurs in the *Drosophila* gut; a tubular organ that is functionally divided into three distinct compartments based on their developmental origins: the foregut, midgut and hindgut. Importantly, the gut is also vital for hosting immune responses directed at resident and pathogenic microorganisms [91], [92]. Likewise, the function of Malpighian tubules in insects is equivalent to the vertebrate kidney and is crucial to regulate osmoregulation and organic solute transport [93], metabolism [94], [95] and detoxification [96]. The adult Malpighian tubule functions as a tissue for defense against insecticides such as DDT, and to detect and mount a defense against bacterial invasion [97]. The *Drosophila* fat body cells function equivalent to the vertebrate adipose tissue and liver [98] by storing excess fat as triglycerides and cholesteryl esters that can be mobilized for energy production by the action of acid lipases (e.g. *Drosophila* Magro), which function orthologous to mammalian lipases (e.g. mammalian LipA). Similar to mammalian hepatocytes, a group of specialized cells in *Drosophila* called oenocytes (attached to the basal surface of cuticle), mobilize stored lipids within the fat body during long periods of dietary deprivation [99]. Under similar nutritional conditions, the mammalian pancreatic- $\beta$  cells secrete insulin to regulate energy and lipid metabolism. In *Drosophila*, there is no pancreas, but the insulin-producing cells (IPSc) located within the central brain, behave like the pancreatic- $\beta$  cells to secrete insulin-like peptides

(DILPs) that have been implicated to regulation of growth [78], circadian rhythms [96] and development [76]. In addition, the embryonic, larval and adult hearts of *Drosophila* have also been studied in context to cardiovascular diseases such as cardiomyopathy and arrhythmia [100], [101]. Besides organs and cells that perform similar functions, the *Drosophila* genome also encodes human orthologs of several key genes involved in the regulation of cholesterol homeostasis and metabolism. In the following paragraph, I illustrate few prominent examples to demonstrate the conservation of sterol metabolic pathways in *Drosophila*.

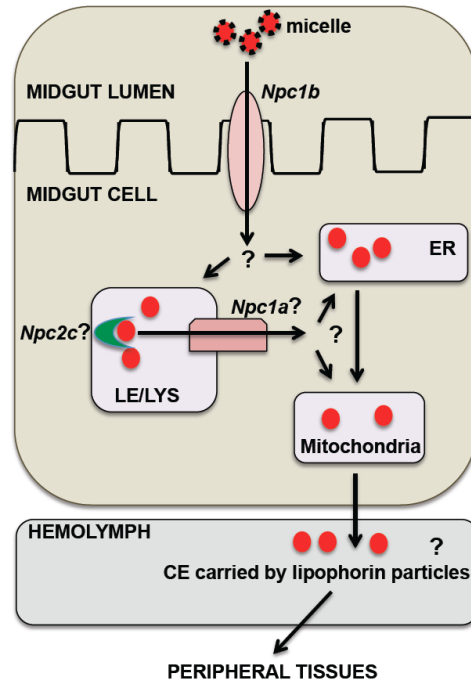
*Drosophila* harbors lipoprotein particles called lipophorins [102], [103] which are proposed to bind to LDL-like receptors called lipophorin receptors [104] and act as a reusable shuttle in lipid transport. Lipophorins mediate the storage of lipids in fat body cells (as lipid droplets), and under starvation conditions, mediate the transport of lipids in the hemolymph for redistribution to various tissues for utilization [105]. Other prominent similarities include: (i) cholesterol metabolising enzymes (e.g. Lip3, ACAT) and (ii) the orthologs of cellular cholesterol transporter proteins (e.g. ABCA1, NPC). *Lip3*, which encodes a cholesteryl ester hydrolase is responsible for breakdown of cholesteryl esters to promote intestinal cholesterol clearance [106]. In vertebrates, the enzyme acyl Co-A cholesterol acyl transferase (ACAT) catalyzes the formation of cholesteryl esters from cholesterol and fatty acyl-coenzyme A [107], and is strongly linked to the development of atherosclerosis [108]. Similarly, *Drosophila* encodes homologs of cholesterol transporters such as the Niemann-Pick disease Type C gene family (NPC1 and NPC2) and the ortholog of *ABCA1*, a vertebrate ATP-binding cassette protein that is required for cellular cholesterol clearance and efflux [49] (**Figure 1.1**).

*Npc1a* and *Npc1b* are the *Drosophila* homologs of mammalian *NPC1* and *NPC1L1*, respectively [109], although no studies have yet addressed how the transcriptional regulation of *Drosophila* NPC genes influences cellular cholesterol homeostasis. *Npc1b* is specifically required in midgut epithelium for dietary sterol absorption, similar to the role performed by the NPC1-like 1 (NPC1L1) protein in mammals. Conversely, *Npc1a* mRNA is enriched in embryonic and larval ring glands, and a *Drosophila* NPC disease model revealed that *Npc1a* mutants are lethal as first instar larvae, and are partially rescuable by feeding the molting hormone 20E [110]. *Npc1a* mutants accumulated excessive cholesterol in a punctate pattern, similar to the mammalian NPC phenotype. This has been explained by ‘sterol shortage model’ whereby loss of *Npc1a* blocks cellular cholesterol trafficking from LE/LY resulting in

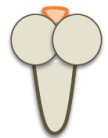
accumulation of excess free cholesterol in aberrant organelles and insufficient cholesterol availability as substrate for ecdysone synthesis. In contrast to the NPC1 homologs, eight genes with significant sequence similarity (**Figure 1.7**) to NPC2 have been described in *Drosophila*, named *Npc2a-h*. While *Npc2a* and *Npc2b* single mutants are viable, double mutants display a range of larval, pupal and adult lethality, that are rescuable by feeding ecdysone, cholesterol or 7-DC [111]. This suggests that these *Npc2* mutants can utilize sterol substrates when provided in excess in the diet, however, are unable to utilize normal sterol reserves. However, the exact molecular functions of these *Npc2* genes are unknown, and as such, there is no biochemical evidence to demonstrate if any of the *Drosophila* NPC2 proteins can bind cholesterol *in vitro* or *in vivo*. Thus based on the current knowledge of mammalian cholesterol biology and that several vertebrate sterol metabolic genes are conserved in *Drosophila*, I have created a simplified model of how cholesterol may be trafficked in *Drosophila* (**Figure 1.8**).



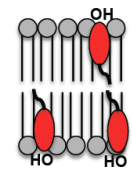
**Figure 1.7. Protein sequence alignment of *Npc2* proteins.** NPC2\_human, homo sapiens NPC2; CG3934, *Drosophila* NPC2c; CG12813, *Drosophila* NPC2d; CG31410, *Drosophila* NPC2e.



fat body  
(storage and utilization)



prothoracic gland  
(ecdysone synthesis)



cell membranes  
(structural integrity, signaling)

**Figure 1.8. A hypothetical model of the key steps in *Drosophila* cholesterol biology.**

Appropriate sterols are first absorbed within the midgut lumen and micelles of cholesterol then reach the midgut transmembrane protein, Niemann Pick disease type C1-b (*Npc1b*) to undergo secondary uptake into the midgut cells. Thereafter, it is predicted that cholesterol reaches the acidic environment within the endosomes (LE)/lysosome (LYS) via an uncharacterized pathway. Once internalised into the lysosomes, much similar to mammalian systems, the LDLP (low density lipophorin particle)[79] carrying cholesterol is likely acted upon by acid lipase enzymes (LAL) to release free unesterified cholesterol, which may thereafter be bound to *Npc1a* and/or one of the eight predicted *Npc2* proteins to be redistributed to other organelles, such as the ER, plasma membrane and mitochondria. Once within the endoplasmic reticulum (ER), cholesterol may be esterified (CE) and packaged so that it can be exported into the hemolymph, where lipophorin particles can then shuttle these CE to the respective peripheral tissues by binding via appropriate lipophorin receptors. This allows dietary-derived cholesterol to reach their destined peripheral tissues: fat body; for storage and metabolism, prothoracic gland; for ecdysone synthesis, or to cellular plasma membranes to maintain structural integrity and mediate signaling. Modified and redrawn from Dixit, *et al.*, 2007. Described in Chapter 5, my preliminary data suggests that the gene product of *Npc2c* is necessary for viability and that it may be involved in egressing free cholesterol from the LYS lumen to other organelles via its interaction with a specific LYS membrane protein, which is likely to be *Drosophila* *Npc1a* protein.

### 1.10. *DHR96* regulates *Drosophila* cholesterol metabolism genes

It is largely unclear how genes that are involved in cholesterol uptake, metabolism or transport are transcriptionally regulated in response to fluctuating dietary and/or cellular cholesterol levels, and how nuclear receptors are implicated in these processes. Our published data [54] and findings in this dissertation demonstrate that the *Drosophila* nuclear receptor *DHR96* functions as a critical regulator of cholesterol metabolism pathways, particularly via sensing declining cellular cholesterol levels.

The *Drosophila* nuclear receptor *DHR96* was first implicated to have a vital role in toxin metabolism [112]. Gas chromatography/mass spectrometry data has shown that a tagged version of full-length *DHR96* from a *Drosophila* cell line co-purifies with cholesterol, suggesting that *DHR96* is a receptor for cholesterol or similar molecules such as its metabolites [113]. On a standard cornmeal diet (called as ‘standard medium’ hereafter) commonly used in most *Drosophila* laboratories, *DHR96*<sup>1</sup> mutants were viable and displayed no obvious phenotypes. This suggested that *DHR96* is not required when animals are maintained on a sufficiently rich diet. Conversely, when reared on a low cholesterol medium (‘C424’) where wild type animals

are developing slower, but are still viable, *DHR96<sup>l</sup>* mutants arrested development as second larval instars and died within several days. Supplementing back cholesterol to this medium completely rescues these mutants to adulthood, whereas lipids such as oleic acid or desmosterol fail to do so, suggesting that underlying the *DHR96<sup>l</sup>* mutant lethal phenotype is cholesterol deficiency[54].

Mattea Bujold and Kirst King-Jones\* carried out genome-wide microarray studies on wild type and *DHR96<sup>l</sup>* mutants reared on standard medium, low-cholesterol, and *high cholesterol* media (which is standard medium containing 1% w/v cholesterol). The expression of several genes with known functions in vertebrate cholesterol metabolism including sterol transporters, metabolic enzymes such as fatty acyl transferases, cholesteryl esterases and lipases, were significantly misregulated in *DHR96<sup>l</sup>* mutants. By further mining these data sets (details are described in chapter 4, section 4.1), I identified that the expression of genes with predicted functions in cholesterol uptake, transport and metabolism were dependent on both *DHR96* function and dietary cholesterol levels. In addition, I observed that dietary cholesterol modulates *DHR96* function and induces transcriptional changes in genes that are predicted to function in pathways that maintain homeostatic control of cellular cholesterol levels (**Figure 1.9**). Cumulatively, the current model for *DHR96* function hypothesizes that low cellular cholesterol levels are sensed by DHR96 protein, which is thereby activated due to lack of an unknown ligand - which is cholesterol or a similar sterol metabolite (**Figure 1.9**). Activated DHR96 mediates genome wide transcriptional responses to overcome the cellular effects of dietary cholesterol deprivation and maintain cellular cholesterol homeostasis.

---

\* Matt ea Bujold, Akila Gopalakrishnan, Emma Nally and Kirst King-Jones Mol. Cell. Biol. 2010, 30(3):793.

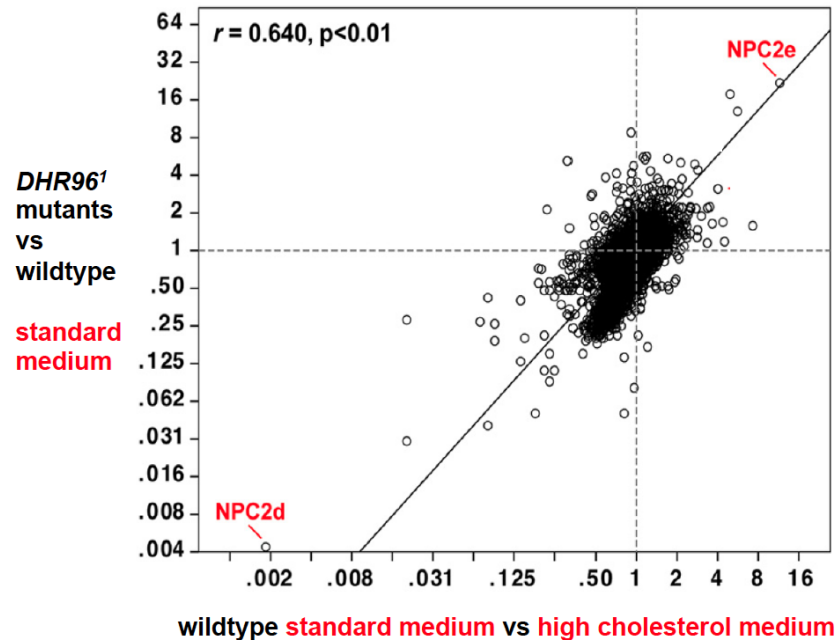
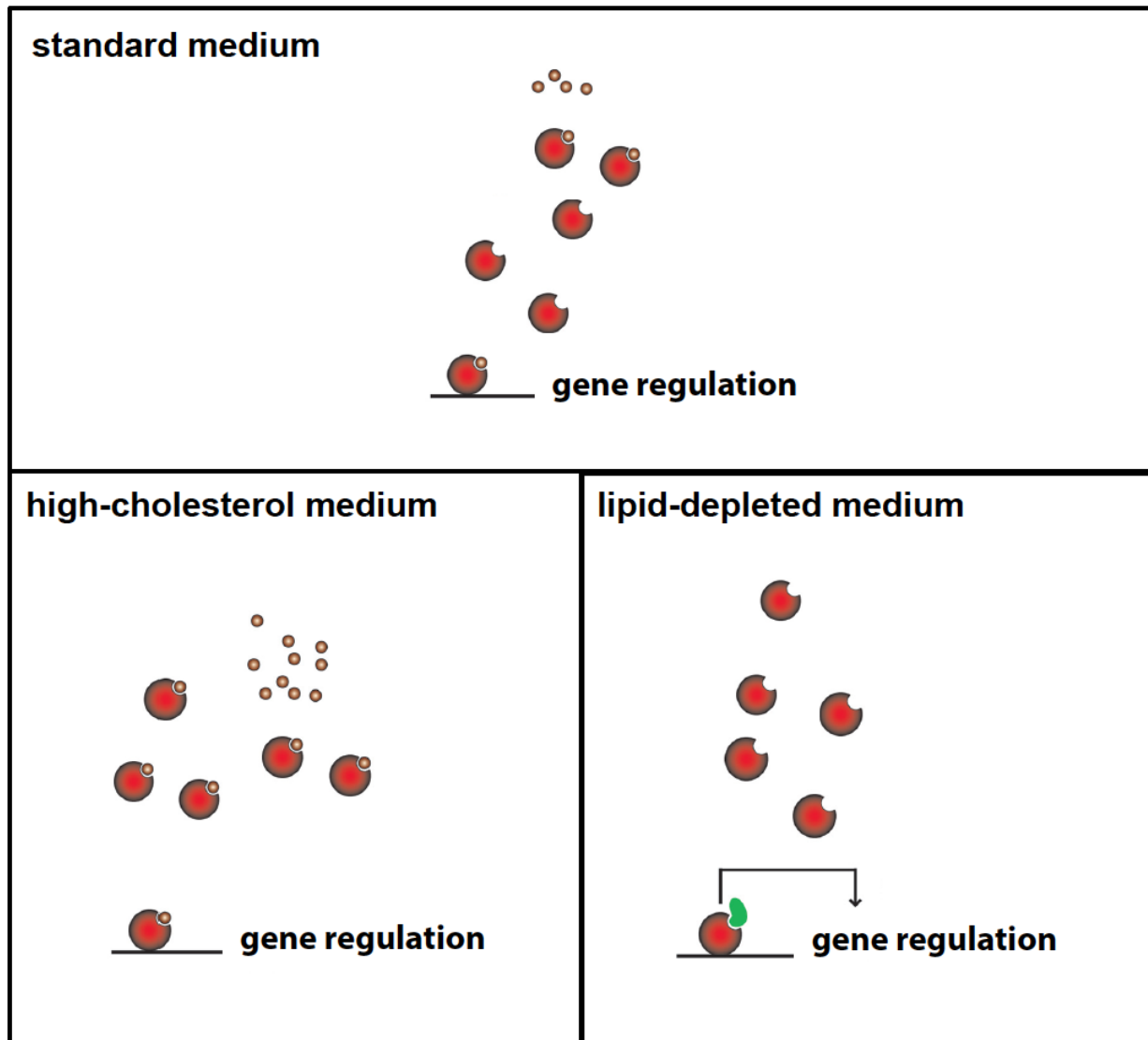


**Figure 1.9. High cholesterol phenocopies the transcriptional effects of the DHR96 mutation.** The statistical comparisons of two microarray data sets are shown. Axes indicate fold change values. X-axis indicates the effects of feeding *high cholesterol* medium (1% cholesterol) to wild type animals. The effects of the *DHR96<sup>1</sup>* mutation in animals reared on standard medium (0% cholesterol) are indicated on Y-axis. The correlation between the data sets are indicated by the *r* value, and their significance by the *P* value. *Npc2d* and *Npc2e*, ranked either by their significance or actual fold changes are the top repressed and induced genes by 'high cholesterol' in the wild type respectively, are also the most strongly repressed and induced genes in *DHR96<sup>1</sup>* mutants reared on standard medium. In summary, on a genome wide scale the *high cholesterol* medium phenocopies the transcriptional effects caused by the *DHR96* mutation. Figure from Bujold *et al* (2010).



 DHR96 protein    
  Ligand (cholesterol?)    
  Co-regulators

**Figure 1.10.** Model for DHR96 function. Standard medium conditions or the high-cholesterol medium containing abundant cholesterol, result in higher concentrations of the putative ligand which deactivate DHR96. Under conditions of lipid-depleted medium or low cholesterol, DHR96 protein is transcriptionally active by recruiting co-regulators (green).

### 1.11. Project Objectives

My research goal was to characterize the transcriptional regulatory network controlling cellular cholesterol homeostasis in the fruit fly, *Drosophila melanogaster*. In this dissertation, I describe the studies conducted to characterize the roles of the nuclear receptor DHR96 in regulating cholesterol metabolism.

1. *DHR96<sup>l</sup>* mutants are viable and display no obvious phenotypes when reared on a normal fly food diet, but arrest development when reared on a low-cholesterol diet. Hence it is essential to understand what function of cholesterol is rescued in *DHR96<sup>l</sup>* mutants and importantly why does *Drosophila* require cholesterol. I have addressed these questions in **Chapter 3** of my thesis - **Using *DHR96<sup>l</sup>* Mutants as Tools to Examine *Drosophila* Sterol and Steroid Requirements**. In this chapter, I detail the studies I have performed using *DHR96<sup>l</sup>* mutants as a tool to characterize *Drosophila* sterol requirements on lipid-depleted diets supplemented with different sterols to either entirely replace or partly substitute, for the principal functions of cholesterol in insects.
2. Nuclear receptors have been implicated to function as cellular sensors of key metabolites. To understand the cholesterol metabolic pathways controlled by *DHR96*, I identified candidate target genes that are transcriptionally regulated by *DHR96* and cholesterol. In **Chapter 4, Gene Expression Analysis of the Cellular Responses to Dietary Cholesterol**, I describe these gene expression studies that I conducted to validate the genome-wide transcriptional effects in response to changes in dietary cholesterol levels and to a *DHR96* mutation. By employing a transgenic line expressing *DHR96* ectopically, I test the hypothesis whether dietary sterols are sufficient to reverse the gene expression patterns of *DHR96* candidate targets.
3. Of all the candidate genes that I have identified, I describe my data in **Chapter 5, Characterization of *Drosophila* Niemann-Pick Disease Type C Genes: *Npc2c*, *Npc2d* and *Npc2e***, that DHR96 is required for appropriate regulation of its candidate target gene *Npc2c*, at least in part through its function in the midgut. I report that *Drosophila Npc2c* is transcriptionally regulated in a cholesterol- and DHR96-dependent manner. To understand the functional significance of the *Npc2* gene family in *Drosophila*, I describe

the results of phenotypic characterization using *RNAi* transgenic lines under standard and sterol-supplemented diets.

**CHAPTER 2. MATERIALS AND METHODS**

## 2.1 Buffers

All buffers listed below were made using Milli-Q ultrapure water unless indicated otherwise. v/v; volume per volume, w/v; weight per volume.

### **Tris-acetate-EDTA (TAE buffer) (50X)**

2 M Tris (Tris(hydroxymethyl)aminomethane)

500 mM EDTA (Ethylenediaminetetraacetic acid) (pH = 8.0)

5.71% glacial acetic acid (v/v)

### **Tris-EDTA (TE) buffer**

10 mM Tris (pH=7.4)

1 mM EDTA (pH=8.0)

### **DNA gel loading buffer (3x)**

15 mM Tris (pH=7.5)

18% glycerol (v/v)

0.075% bromophenol blue (w/v)

0.075% xylene cyanol (w/v)

### **Phosphate buffered saline (PBS) buffer (10X)**

1.4 M NaCl (Sodium chloride)

27 mM KCl (Potassium chloride)

100 mM Na<sub>2</sub>HPO<sub>4</sub>·7H<sub>2</sub>O (Sodium Monohydrogen Phosphate Heptahydrate)

14 mM KH<sub>2</sub>PO<sub>4</sub> (Monopotassium phosphate)

### **PBT buffer**

0.1% Tween-20 (v/v) in 1X PBS buffer

### **Plasmid Mini Preparations (Qiagen)**

1) P1 bacterial resuspension buffer: 10 mM Tris (pH=7.5) and 1 mM EDTA (pH=8.0)

2) P2 bacterial lysis buffer: 200 mM NaOH (Sodium hydroxide) and 1% SDS (w/v) (Sodium dodecyl sulfate)

3) P3 neutralization buffer: 3M potassium acetate (pH=5.5)

### **Buffers used from commercial kits (as per manufacturer's instructions)**

Plasmid Midi Preparations (Qiagen)

Gel Extraction kit (Qiagen)

PCR purification kit (Qiagen)

## **2.2. Culture media**

### **2.2.1. LB (Luria Bertani) bacterial growth medium**

For 500 ml:

5 g tryptone (Fischer)

2.5 g yeast extract (Sigma®)

5 g NaCl (Fischer)

7.5 g Agar (Sigma®) (for media plates)

### **2.2.2. Standard Fly Medium**

Yeast 17.3 g

Soy Flour 10 g

Cornmeal 73 g

Malt 46.1 g

Agar 6.3 g (Sigma®)

Molasses 77 ml

Propanoic Acid 2.9 ml (Sigma®)

Methyl Paraben 2.9 g (Sigma®)

Ethanol 10 ml

Autoclaved Milli-Q Water 1L

The above ingredients were individually weighed and mixed thoroughly with 1L Milli-Q water. The mixture was autoclaved on a 20-minute sterilization followed by 20-minute slow

exhaust cycle. When still warm (approx. 50 °C), the fresh medium was poured into vials (5 ml each) or bottles (20 ml each), as needed, or was supplemented with sterols (as described below).

**Sterol Supplementation:** To add sterols, a batch of freshly prepared standard medium was weighed to receive newly prepared ethanol solutions containing the appropriate amount of cholesterol, 7-dehydrocholesterol (7DC) or ecdysone. For 20E-, cholesterol- and 7DC-supplemented standard medium, 33 µl of a 10 mg/ml (in 100% molecular grade ethanol) stock each of a 20E (Steraloids Inc., C7980-000), cholesterol (Sigma®) or 7DC (Steraloids Inc. C3000-000) was added for every 1 ml of standard medium, bringing to a final concentration of 0.33 mg/ml. For higher concentrations 3.3 mg/ml and 6.6 mg/ml, the stock solutions were adjusted accordingly to keep the total sterol-ethanol volume constant. Control medium contained 33 µl of 100% ethanol. The supplemented sterols was mixed vigorously and immediately poured into vials (5 ml per vial) or larval collection petri dishes (5-20 ml per plate, based on size). The ethanol was allowed to evaporate (37.5°C for 5 h). For preparing high-cholesterol media, a batch of freshly prepared standard medium was weighed to receive 1% wet weight (w/v) cholesterol, canola oil (Crisco®), or tristearin (Sigma®) and immediately poured into vials (5 ml per vial) or larval collection petri dishes (5-20 ml per plate, based on size). For timing larvae to the mid-third-instar stage, I added 0.05% bromophenol blue to the medium and selected for larvae with dark-blue guts, representing ~ 18 hours prior to puparium formation. For larval sample collections, not more than 40 larvae were raised on each standard medium plate to avoid overpopulation.

### **2.2.3. Lipid-depleted media: LDYG and LDC424**

**Lipid depletion protocol:** To extract lipids, 200 g of ground C424 powder or yeast extract powder or agarose was transferred to a 4-liter Erlenmeyer flask and treated six times for 12 h each time with 1 liter of chloroform (modified from [73]). The lipid-depleted C424 or yeast extract or agarose was then air dried until no traces of chloroform were detectable. Finally, methyl paraben was added to a final concentration of 1% of the wet weight.

#### **2.2.3.1. Lipid-depleted yeast glucose medium (LDYG):**

(Recipe for each vial)

0.5 g lipid-depleted yeast extract

0.5 g glucose [Sigma®, D-(+)-Glucose  $\geq$ 99.5% (GC) G8270]

0.035 g lipid-depleted agarose [Sigma®, Agarose, low gelling temperature A9414]

0.05 g of Methyl Paraben [Sigma®]

The lipid-depleted yeast extract, glucose, agarose and methyl paraben were carefully weighed into each vial. To add sterols: ergosterol (Steraloids Inc., C5600-000), stigmasterol (Steraloids Inc., C3100-000), or cholesterol (Sigma®) each vial received a total of 200  $\mu$ l of ethanol containing the appropriate amount of sterol on the surface of 1 g of LD yeast glucose powder. After the ethanol was allowed to evaporate (37.5°C for 5 h), each vial was mixed vigorously with 5 ml water, heated to a quick boil in the microwave and cooled down until the medium was set.

#### **2.2.3.2. Lipid-depleted Carolina 424 medium (LDC424):**

The C424 (Carolina Biological Supply Company) medium, which is in form of flakes, was ground using a household blade grinder. Small batches were combined and thoroughly mixed to ensure equal distribution of methylparaben powder in C424. To make sterol supplemented LDC424, ergosterol, stigmasterol and all ecdysteroid precursors (i.e. cholesterol, 7DC,  $\alpha$ -ecdysone (Steraloids Inc., C8000-000) and  $\beta$ -ketodiol (a kind gift from Ryusuke Niwa) were dissolved in 100% ethanol (Sigma®), and added to each vial with 1 g C424 powder. After the ethanol was allowed to evaporate (37.5°C for 5 h), each vial was immediately mixed vigorously with 5 ml water until the medium was set.

### **2.3. *Drosophila* embryo collection**

3-5 day old females and males (20-25 flies each) were transferred to well-aerated egg cages that each contained freshly prepared yeast paste on grape juice agar plates. After an overnight egg-lay at 25°C, 1-2 h egg-laying windows were set up to collect embryos for staged larval sample collections and other phenotypic studies.

#### **2.3.1. Embryo dechoriation**

The protocol from CSH Protocols (2007; doi: 10.1101/pdb.prot4826) was modified. A batch of newly laid embryos from 3-5 day old parents fed with fresh yeast paste from a 3-4h egg collection schedule were carefully transferred from the agar plates to an egg basket. A glass

petri dish was partially filled with 50% freshly prepared bleach solution, in which the egg baskets containing the embryos were placed (such that the bleach was just below the rims of the basket) for 45 seconds – 1 minute. A Pasteur pipette was used to rinse the embryos gently in the bleach solution, and were constantly monitored under a dissecting microscope. When the dorsal appendages were dissolved in 80% of the embryos, the egg baskets were immediately placed in petri dishes containing the 1X embryo wash solution for 2-3 minutes, followed by two repetitions of gentle washing in sterile (autoclaved) MilliQ water for another 2-3 minutes each time. Note that the dechorionated embryos tend to float. The embryos were then carefully sorted and counted for sterol-supplementation studies.

#### **10X Embryo Wash Solution:**

7% (w/v) NaCl

0.5% (v/v) Triton-X-100

1-liter sterile MilliQ water

#### **2.3.2. Population studies: setup**

Unless otherwise mentioned, for all population studies, I transferred 50 normal or dechorionated *Drosophila* embryos to each vial containing C424, LDC424 or SM, and each condition was tested in triplicate. I scored the appearance of pupae every 24 h and maintained the vials until the pupae developed into adults.

#### **2.4. Larvae sample collections**

For *DHR96* overexpression studies, third instar control ( $w^{1118}$ ) and heat shock (*hs-DHR96*, obtained from K. King-Jones[112]) larvae staged at 4 h after the second-to-third instar larval molt were treated at 37°C for 1 h and allowed to recover at 25°C for 0-4 h. For qPCR on brain-ring gland complexes, third instar control ( $w^{1118}>dcr;phm-Gal4$ ) and *dcr;phm-Gal4 >broad-RNAi* or *>DHR96-RNAi* or *>Npc2c-RNAi* larvae staged at 4 h after the second-to-third instar larval molt were dissected in chilled PBS solution and proceeded to RNA isolation (described below).

#### **2.5. RNA isolation**

For 3rd instar whole body RNA, 8-10 staged larvae were homogenized in Trizol (Invitrogen) and immediately flash frozen in liquid nitrogen and stored at  $-80^{\circ}\text{C}$  until isolation of RNA. Total RNA was isolated from frozen larval samples using a modified protocol based on Trizol (Invitrogen), which utilized two repetitions of chloroform extraction and ethanol precipitation of RNA using 0.5 M LiCl. For brain-ring gland complexes, each sample constituted 12-15 brain ring-glands from staged larvae dissected in cold Phosphate Buffered Saline buffer. 500  $\mu\text{l}$  Trizol was added to each sample tube, vortexed well and flash frozen immediately for storage in  $-80^{\circ}\text{C}$ . 100  $\mu\text{l}$  of chloroform was added, shaken vigorously for 15 s and incubated at RT for 3 minutes, followed by centrifugation for 15 min at  $4^{\circ}\text{C}$  at 12,000 rcf. The upper aqueous phase was carefully transferred to a new sterol tube, 500  $\mu\text{l}$  isopropanol was added and the mixture was transferred to the columns provided in the RNeasy® Mini Kit (Qiagen) and the protocol was then followed further as per manufacturer's instructions. The extracted RNA was then quantified in a spectrophotometer (Nanodrop) and analyzed for quality using the Agilent 2100 bioanalyzer. cDNA was prepared from 1  $\mu\text{g}$  (for whole body preparations) or 500 ng (for brain ring gland complexes) using the High Capacity Reverse Transcriptase Kit (Applied Biosystems 4368814).

## **2.6. Quantitative Real time Polymerase Chain Reaction (qPCR)**

Real time qPCR primer design was performed using the Universal ProbeLibrary Assay Design Center (ProbeFinder: [lifescience.roche.com/universal-probelibrary-system-assay-design#ProbeFinder](http://lifescience.roche.com/universal-probelibrary-system-assay-design#ProbeFinder) Assay Design Software). The specificity of primers was assessed by alignment of the resulting sequences by performing BLASTN against the *Drosophila melanogaster* transcriptome. Primers were first validated by a standard melt-curve analysis using 5 dilutions in the ratio of 1:4 of a cDNA sample and step-wise temperature increase to confirm the presence of one melt curve peak such that the linear amplification is proportional to the corresponding dilution. At the melting temperature, the fluorescence peak maximum occurs, the double stranded PCR products dissociate, and the SYBR Green fluorescence drops significantly. Non-specifically amplified products or primer dimers melt at temperatures above or below that of the desired target gene product. For qPCR input reaction, cDNA was diluted to 1/20 (for whole body preparations) and 1/10 (for brain-ring

gland complexes). cDNA were amplified following the manufacturer's instructions using the KAPA SYBR® FAST qPCR Master Mix (2X) (KK4605) and analysed with StepOnePlus™ Real-Time PCR System (Applied Biosystems) according to the following thermal-cycling parameters: 2 min initial denaturation at 95 °C, followed by 40 cycles of 1 sec denaturation at 95 °C and 20 sec combined annealing/extension at 60 °C. The total run time was 40 min using this cycling protocol.

single reaction setup:

5 µl KAPA SYBR® FAST qPCR Master Mix (2X) (part no. KK4605)

2.5 µl Primer Mix (3.2 µM Forward/Reverse Mix)

2.5 µl Template cDNA (1/20)

10 µl Total

Each run included triplicates of test and control cDNA samples. Each sample was measured for the gene of interest and the reference (i.e. internal control) housekeeping gene - *ribosomal protein 49 (rp49)*. The cDNA concentration is quantified as a plot of the SYBR (green) fluorescence signal against the number of cycles in a log scale. The corresponding cycle number where the fluorescence exceeded the threshold (t), designated as the threshold cycle (Ct), was determined for each test sample and control cDNA sample (i.e. calibrator). The Ct value is proportional to the log of the initial amount of target sequence in input cDNA sample. A mean of the triplicate Ct values for each specific gene/each sample was calculated. Assuming that the amplification efficiency of the reference gene and target gene of interest were approximately equal, the relative fold change values of gene expression normalized to the calibrator was calculated [114] as follows:  $\Delta\Delta CT = (Ct(\text{target gene in control sample}) - Ct(\text{reference gene, } rp49 \text{ in control sample})) - (Ct(\text{target gene in test sample}) - Ct(\text{reference gene, } rp49 \text{ in test sample}))$ . The fold change value of target gene expression relative to the control (calibrator) in the test condition was calculated as  $2^{-\Delta\Delta CT}$  (base (2) is the efficiency of the amplification, where ideally it is doubled). By default, since  $\Delta\Delta CT$  of the calibrator equals zero, its fold change value (i.e.  $2^0$ ) is always one.

## **2.7. High-throughput qPCR**

High-throughput qPCR was performed on preamplified cDNA samples and analyzed on the 48.48 Dynamic Arrays™ Integrated Fluidic Circuits (IFCs) (Fluidigm Corporation

Biomark™ HD system, part no. BMK-M-48.48) where in each IFC is a network of fluid lines, NanoFlex™ valves and chambers. In this real-time PCR system, microfluidic chips undergo thermal cycling so that the expression of 48 genes is assayed across 48 samples, resulting in 2,304 parallel PCR reactions. Assays were designed using the web-based Probe Finder software from Roche Applied Science Universal ProbeLibrary (UPL) at: [www.universalprobelibrary.com](http://www.universalprobelibrary.com). This software shows a set of target-specific primer sequences and the matching UPL probe that is likely to be most effective. I used the Universal ProbeLibrary Single Probes #1 to #165 and all probes were pre-labeled with the reporter (FAM™) on 5' end and a dark quencher dye on 3' end. In this collection, each hydrolysis probe consists of 8-9 selective nucleotides that are highly prevalent within the transcriptome, thus allowing them to cover virtually all transcripts from the *Drosophila* transcriptome in the NCBI Reference Sequence Database. Nucleic acid analogues called Locked Nucleic Acids (LNA) have been incorporated within the sequence of these probes. In addition to the fact that most LNA nucleosides can base-pair efficiently with complementary nucleosides (similar to DNA and RNA), the presence of the 'locked' ribose conformation in LNAs results in enhanced binding strengths and base stacking. As a result, LNAs have increased thermal stability and higher specificity of detecting single-base mismatch, compared to standard DNA nucleotides. The following are the key steps involved:

**a) Preparing Primer Pair Mixes:** Custom primers were synthesized by Integrated DNA Technologies (IDT). Primer pairs for each assay were rehydrated to 100 µM stocks. 20 µl of each forward and reverse primer for each assay was added to 60 µl nuclease-free water, and combined to prepare a 100X Primer Pair Mix (20 µM each primer).

**b) Pre-amplification reactions:** For sample preparations, I used the equivalent of 5 ng of total RNA to amplify cDNA samples using the TaqMan Pre-Amp 2X Master Mix (Applied Biosystems, part no. 4391128) on the StepOnePlus Real-Time PCR System (Applied Biosystems, part no. 4376768) according to the following thermal-cycling parameters: 10 min initial denaturation at 95 °C, followed by 14 cycles of 15 sec denaturation at 95 °C and 4 min at 60 °C. All procedures were performed as per recommended by Fluidigm.

Each pre-amplification reaction consisted of:

2.5 µl cDNA

2.5 µl (4X) Multiplex Primer Mix (final concentration of each primer in this mix was 200 nM)

5 µl (2X) Taqman Pre-Amp Master Mix II (part no. 4391128)

10 µl Total

**c) Preparing Primer-Probe Mixes:**

Each primer mix – probe combination was pooled by mixing 2 µl of the 100X Primer Pair Mix for every 1 µl of the specific recommended UPL probe.

**d) Testing Pre-amplified products and Primer-Probe Mixes:**

The pre-amplified products were diluted 1:5 with nuclease-free water and validated on the 96-well format StepOnePlus™ Real-Time PCR System (Applied Biosystems, part no. 4376768) using a previously tested endogenous control gene (*rp49*) according to the following thermal-cycling parameters: 10 min initial denaturation at 95 °C, followed by 40 cycles of 15 sec denaturation at 95 °C and 1 min combined annealing/extension at 60 °C.

For 16 samples run in duplicate, the reaction conditions were:

20 µl 100x Primer Mix (400 nM final concentration)

4 µl Probe (100 nM final concentration)

160 µl nuclease-free water

200 µl TaqMan Universal Master Mix II (PN 4391128)

9.5 µl/ reaction + add 0.5 µl corresponding Pre-amplified sample/reaction.

The Primer – Probe Mixes were tested for new primer sets by thermal cycling (each pair) in duplicates on the StepOnePlus™ Real-Time PCR System (Applied Biosystems, part no. 4376768) using a previously tested endogenous control gene (*rp49*) according to the following thermal-cycling parameters: 10 min initial denaturation at 95 °C, followed by 40 cycles of 15 sec denaturation at 95 °C and 1 min combined annealing/extension at 60 °C.

250 µl cDNA Sample (~12.5ng of input template RNA / 10 µl qPCR reaction)

500 µl TaqMan Universal Master Mix II (part no. 4391128)

200 µl nuclease-free water

9.5 µl/ reaction + add 0.5 µl of corresponding Primer-Probe mix per reaction

In both aforementioned validation tests, the Pre-amplified samples or Primer-Pairs were considered a ‘fail’ if they demonstrated lower-than-expected/no Ct values, or failed to display sigmoidal shaped amplification curves.

**e) Preparing Assay Mixes:**

In a 96 well plate, prepare 10x Assay Mixes using Fluidigm, Dynamic Array (DA) Sample & Assay Loading Reagent Kit (part no. 85000800). Each 10X Assay mix reaction consisted of the following and the final concentration in the reaction was 400 nM Primer and 100 nM Probe:

(Volume per assay inlet)

3.25  $\mu$ l DA Assay Loading Reagent

1.95  $\mu$ l Primer – Probe mix

1.3  $\mu$ l Nuclease Free water

6.5  $\mu$ l Total

**f) Preparing Sample Mixes:**

The sample master mixes were prepared by the following recipe using ABI, TaqMan Universal PCR Master Mix without UNG Erase (part no. 4324018) and Fluidigm, DA Sample Loading Reagent (part no. 85000735): (Sample Mix for 48 samples)

200  $\mu$ l TaqMan Universal Master Mix

20  $\mu$ l DA Sample Loading Reagent

220  $\mu$ l Total

4  $\mu$ l of sample mix was dispensed to each of 48 wells on the left half of a 96 well plate. 2.5  $\mu$ l of Pre-amplified sample was added to each of the 48 wells. The plate was mixed by vortexing and spinning down. The chip was primed with the provided control line fluid (as per manufacturer's instruction Fluidigm BioMark™). The '113x Chip Prime' script (pre-programmed by manufacturer) was run on the NanoFlex™ 4-IFC Controller. For running the 48.48 Chip, the primed chip was removed and 5  $\mu$ l of the appropriate assay mix was loaded into the inlets on the left side of the chip, 5  $\mu$ l each of the appropriate sample mixes were loaded into the inlets on the right side of the chip. After removing any air bubbles with a clean pipette tip, the chip was placed into the NanoFlex™ 4-IFC Controller and the '113x Load mix' script (pre-programmed by manufacturer) was run to load the samples and assays into the chip. Once completed (~55 minutes later), the chip was then placed in the Biomark™ Real-time PCR System according to the following thermal-cycling parameters: 10 min initial denaturation at 95 °C, followed by 40 cycles of 15 sec denaturation at 95 °C

and 1 min combined annealing/extension at 60 °C. Each assay and sample of every individual real-time quantitative PCR result is displayed together as a heat map such that the colors on the heat map correspond to a specified range of Ct values. Also, the heat map legend displays those color-coded Ct values for every reaction corresponding to the position on the dynamic array. The raw data containing the Ct values were exported directly from the instrument in a Microsoft Excel format for fold change calculations. While the chip set up, number of replicates and choice of endogenous control genes were kept constant for all experiments, the composition of the samples varied depending on the particular experiment.

**g) Relative quantification:**

For each experimental condition, I tested four biological samples in triplicate. I included five housekeeping control genes per run: *rp49* (CG7939) (in triplicate, thus occupying three assay inlets), *α-tubulin 84B* (CG1913), *metallothionein A* (CG9470), *RNA polymerase II* 140-kDa subunit (CG3180), and *tropomyosin 1* (CG4898) (each of these 4 reference genes were tested in duplicates, thus occupying 8 assay inlets). The 48 assay inlets comprised a total of 11 control and 37 genes of interest. The  $\Delta C_t$  values for each gene were calculated as a mean of three technical replicates using each of 5 reference genes, i.e.  $\Delta C_t$  for every reference gene =  $C_t$  (target gene in each sample) –  $C_t$  (reference gene in that sample). These  $C_t$  values were then used to calculate the arithmetic mean of  $\Delta\Delta C_t$  values obtained for every assay in each of 4 biological replicates of calibrators and 4 test samples for every reference gene (=  $4*4*5 = 80$  total  $\Delta\Delta C_t$  values). Using the mean of  $\Delta\Delta C_t$  values for each reference gene, the fold change values for each gene were then calculated ( $2^{-\Delta\Delta C_t}$ ) to plot relative expression in graphs.

**Table 2.1 Primer sequences and UPL probe codes for quantitative real-time PCR.** This table lists the primer sequences I used for qPCR analysis. For the microfluidic-based qPCR, the listed UPL probe was used. In cases where the gene expression was analyzed by KAPA SYBR® FAST qPCR Master Mix (2x) (part no. KK4605) on the using StepOnePlus™ Real-Time PCR System (Applied Biosystems, part no. 4376768), the same primers were without the UPL probe.

Gene Name	Forward Primer Sequence 5'→3	Reverse Primer Sequence 5'→3	UPL Probe
<i>ACAT</i>	CACAAACTGAAACCGCACAG	CGACACGAAACAGAAGACCA	#24
<i>α-Tubulin 84B</i>	ACACTTCCAATAAAAACTCAATATGC	CCGTGCTCCAAGCAGTAGA	#3
<i>Atet</i>	CCAGACAGGAGCCAGTGC	GCCATTGCACAGGTTGTTT	#102
<i>β-Trypsin</i>	GAACATCGTCAGCCAGAGC	TTGATCTGGTTTCCGTAGCC	#69
<i>Brummer</i>	TGTCTCCTCTGCGATTTGC	CGTTCACCACCCTGAAGAAG	#44
<i>Cabut</i>	GGGAAAACAAGTTGGAAATCG	TCCCTCCATTTTTCTGACTCTT	#141
<i>CG1819</i>	AGCAAAAAGGAGTCCGGTATT	TGAAAAGCCGCCATTCTT	#84
<i>Cyp12d1-p</i>	GGTCCCGTTTCGATCTTCAA	GGTCTTGTGCTCCTCCGTTA	#75
<i>CYP28A5</i>	GACGCTTGTGTGCAGGAA	TTCGGTGCACAGTTTATTTCG	#103
<i>Cyt-b5-r</i>	TTCATACAAATGGGCACTCG	CCAGGTATATGGCAATGGGTA	#59
<i>DHR96</i>	TGGCCAAGAAGATTACAGCA	ACC TTT GAG TAG GGC CAC CT	#83
<i>Egghead</i>	AAACCCAAACATTCGGACAC	TCAGCTCTGTTTCTGGTCA	#143
<i>ε-Trypsin</i>	CGTATCGTCGGTGGTTATGA	CTGCAAGGACACCTGGTAGG	#159
<i>FANCL</i>	CGTCTGTTTGGAGGAGTGGT	AAA TGA GGT GGA CAG CTT CG	#158
<i>LpR1</i>	CGGATTCCGGCTTTATTG	AGCCAATGAGCAGGAGCA	#131
<i>LpR2</i>	ATGGGACGCCACACATTTAC	CAGATTTGAAGAGGGGGTTG	#153
<i>Lsp1-γ</i>	CGACAAGGCTCAATACGAGA	AACTCTCCCTTGGGAAGCA	#125
<i>Magro</i>	CAACGCCTTCATAATGTTTGC	TCTCGATCAGGACGCTCAT	#138
<i>MeF2</i>	CATCGCAGGAGGATAGGAAA	ACTTGCCTTGTGAAGGTC	#145
<i>Melted</i>	TTCGAAGTGATACGGACTGGT	ATTCTTCATCTGCAGCAACG	#66
<i>Mtn</i>	AAC TCA ATC AAG ATG CCT TGC	TTG CAG GAT CCC TTG GTG	#20
<i>Net</i>	TCCGGGAGTTACGACTCTTC	CGAGTGGTTCCAGCTGTTCT	#44
<i>Nol</i>	GCTACTGATCCAGCCACGA	GGCGAAGTGAAGTGGTG	#10
<i>Npc1a</i>	CCAAAGCAGGCTGAGTTCAT	CTCATCACCTTTCTTATTTTTCTGC	na
<i>Npc1b</i>	CCCCCTTCTACTGTTCGAA	AAG CGA AAG GCA GGT AAT CA	#146
<i>Npc2a</i>	ACAGTCGTCCACGGCAAG	ACACAGGCATCGGGATTG	na
<i>Npc2b</i>	ACAGTCGTCCACGGCAAG	ACACAGGCATCGGGATTG	#105
<i>Npc2c</i>	ACAGCACGCCAATTAGACAA	CGTTCGATTTGCACCATCA	#145
<i>Npc2d</i>	GGATTACTACTATCGCTGGCTGA	CCTCAAGCGGAAAAGGTTTA	#18
<i>Npc2e</i>	TTCTGGCCACAGTCAATGC	CCAGTGAAACGGCTTATTT	#120

<i>NPC2g</i>	GTCCGTACACCATCCGTTG	GTCGATGGTGAAGCAGCAG	#14
<i>NPC2h</i>	CAAGAGCGAGAACGTGGAG	CCAACGGATGGTGTATGGAT	#79
<i>Nubbin</i>	CGGGATAAATCGAAGGAAGC	AGTATTTGATGTGTTTGCGACTTT	#62
<i>Peste</i>	CGCAACTGGATCGATATGTTT	CTCGAATGATCGTGAATTGG	#72
<i>Phantom</i>	TAAAGGCCTTGGGCATGA	TTCTTTGCCTCAGTATCGAAAA	#19
<i>Prat2</i>	ATTTGGTCAGCTCGGTTCC	CCGACTCCCTGGCATAAC	#44
<i>Punch</i>	CAAGGGCTACGACCAGAGTC	GACCACCACCATTTCGTCAT	#153
<i>Rp49</i>	CGGATCGATATG CTA AGC TGT	GCG CTT GTT CGA TCC GTA	#105
<i>RPII140</i>	TGATGTACGACAACGAGGAAGA	GCC ACA GCT CGT GAG AGA T	#63
<i>Start1</i>	AAGGTGTTTGTGTTTCGATTGG	ACCCTACAGTCCAGGAACCA	na
<i>Thor</i>	CCAGATGCCCGAGGTGTA	AGCCCGCTCGTAGATAAGTTT	#22
<i>TM1</i>	GCG AGG AGT TCC ACA AGC	GTT CAG AGC GGC AAC CTC	#10
<i>TotC</i>	AATGAATGCCTCCATTTCTCTACT	CTCGTCAGAATAGCCCAAGC	#68
<i>CG4254</i>	TGAGAATTGTGAAAGCGAAAAA	TCTTGCAGACATCAGACACAGTT	#135
<i>CG10300</i>	GAGAAGTGGGTGCAGTTGCT	ACCACGAGTCCCATTCAAAA	#149
<i>CG10514</i>	CAGATTCCCAGTTTGCATCA	CACTACCGTAGAATGCAAAGCA	#10
<i>CG10531</i>	ACGATCGTGCCAACTTTGT	CATAGCCATAGGGAGCGAAC	#84
<i>CG11781</i>	TGGAATACTGTCGCACATCG	GTACCACTCAGGCCCAAATAC	#121
<i>CG16708</i>	CGTGCGTTTTCTGCTCAAC	TGTGCGATATACCTCTACAAAAGG	#29
<i>CG2065</i>	GCTGCTGGACGTATTGAAGA	GTTTTAATGAAACCTTGGGTGTG	#64
<i>CG7381</i>	AACCAGGCGACGAGGATT	GCCAAAATACGGCCAACA	#147

## 2.8. Fly stocks

Flies were cultured on standard cornmeal medium at 25°C. The *DHR96* mutant allele, *DHR96<sup>l</sup>*, was generated by King-Jones [112] by ends-in targeting method. It contains two deletions, one of which removes the translational start codon and the second of which removes exon four, the down-stream intron, and the splice acceptor site for exon 5, thus disrupting the ligand binding domain-coding region. Gal4 driver lines were obtained from labs indicated by the references: Ubiquitous expression: *actin (act-Gal4)* [115]-, Midgut: *malic enzyme modifier (mex-Gal4)* [116], Fat body: *combgap (cg-Gal4)* [117], Salivary gland: *scalloped (sd-Gal4)* [118], Malpighian tubules: *c42-Gal4* [119], and *c724-Gal4* [120]. For all genotypes involving a cross between the Gal4 driver and the UAS-responder

line, the genotype is written as follows: abbreviated name of the gene promoter used to drive Gal4 gene, followed by a '>' 'greater than' symbol, which is thereafter followed by the transgene fused to UAS responder. For example, the genotype *act>Npc2c-RNAi* denotes the progeny of the cross wherein the driver, *actin-Gal4* expresses *Npc2c-RNAi* (ubiquitously) in all tissues. For the control cross, unless otherwise mentioned, the abbreviated name of the gene promoter used to drive the transgene is followed by a '>' 'greater than' symbol, and is thereafter followed by '*w<sup>1118</sup>*', which is control stock, and the genetic background used for injection and transformation of the (responder) transgenic line. The *Npc2c*-fosmid (*Dpse\GA17784*, FlyFos046706) was kindly provided by the Pavel Tomancak lab and transgenic flies generated by Genetic Services Inc. The cDNA clones of *Npc2c*, *-Npc2d* and *Npc2e* were obtained from BDGP [121], subcloned into pUAST vector. Transgenic flies were generated using P-element mediated germline transformation (Best Gene Inc.) of the *w<sup>1118</sup>* strain (Bloomington Stock Center #3605). Codon usage in the transcript *Npc2c*-RA (discussed in Chapter 6, section 6.3) was modified with the introduction of silent mutations to render it resistant to RNAi-mediated knockdown, at the same time as minimizing the use of rare codons. 28 out of 166 codons were modified in the region targeted by *Npc2c<sup>GD6798</sup>*. This modified *Npc2c* transgene was synthesized (Biomatik, Inc.), subcloned into pBluescript II SK(+) and subsequently cloned into the destination vector pUASTB (Addgene, Alt Name/ID 18944). Transgenic flies were generated by Best Gene Inc. Other stocks were obtained from the Bloomington Stock Center, the Vienna *Drosophila RNAi* center, the Exelixis Collection, and the National Institute of Genetics (NIG-Fly).

cDNA sequence of *Npc2c* containing wobble bases:

```

ATGTCCAGCTTCAAGAAGTTATCCCTGTGCCTAGTGCTTTCTATCATGTGGACCTCGGTTGC
AGACAGCACGCCAATTAGACAATGTGCCGACAGCAACTATCCTCAGCCACTGATGGTGCAAA
TCGACGATTGTGACGCATTGCCCTGCGATTTGTGGAAGGGAACCGAGGCCAAAATCGACATC
CAATTTGTTGCCACTCGCAATACCATGAAGAAGCTGTCCGCCGAGGTGCATCTGACCTCCCT
GGGCGTGACCATCCCCTACGACCTGGAGGCCTCCCGCGGCAACGTGTGCAGCAACCTGCTGC
ATGGCGCCTACTGCCCCCTGGACGCCGCGGAGGACGTGACCTACCAGCTACTGCTGCCCGTC
ACCACCAATCAGCCCGAGGTGCCACGCGTCTGGAGGTTCCGCTGCTGGACTCCGACGACGA
GAACCGCGTGGTGTCTTCTGCTTCCCTGGCTGACACTCGGGTCAAGAAGCCCAGATCGGCAGTTT
AG

```

1	ATG	TCC	AGC	TTC	AAG	AAG	TTA	TCC	CTG	TGC	CTA	GTG	CTT	TCT	ATC	ATG	TGG	ACC	TCG	GTT	60
1	Met	Ser	Ser	Phe	Lys	Lys	Leu	Ser	Leu	Cys	Leu	Val	Leu	Ser	Ile	Met	Trp	Thr	Ser	Val	20
61	GCA	GAC	AGC	ACG	CCA	ATT	AGA	CAA	TGT	GCC	GAC	AGC	AAC	TAT	CCT	CAG	CCA	CTG	ATG	GTG	120
21	Ala	Asp	Ser	Thr	Pro	Ile	Arg	Gln	Cys	Ala	Asp	Ser	Asn	Tyr	Pro	Gln	Pro	Leu	Met	Val	40
121	CAA	ATC	GAC	GAT	TGT	GAC	GCA	TTG	CCC	TGC	GAT	TTG	TGG	AAG	GGA	ACC	GAG	GCC	AAA	ATC	180
41	Gln	Ile	Asp	Asp	Cys	Asp	Ala	Leu	Pro	Cys	Asp	Leu	Trp	Lys	Gly	Thr	Glu	Ala	Lys	Ile	60
181	GAC	ATC	CAA	TTT	GTT	GCC	ACT	CGC	AAT	<u>ACC</u>	<u>ATG</u>	<u>AAG</u>	<u>AAG</u>	CTA	TCA	GCC	GAA	<u>GTG</u>	<u>CAT</u>	<u>CTG</u>	240
61	Asp	Ile	Gln	Phe	Val	Ala	Thr	Arg	Asn	Thr	Met	Lys	Lys	Leu	Ser	Ala	Glu	Val	His	Leu	80
241	<u>ACC</u>	<u>TCG</u>	<u>CTG</u>	<u>GGA</u>	<u>GTG</u>	<u>ACC</u>	<u>ATA</u>	<u>CCC</u>	<u>TAT</u>	<u>GAC</u>	<u>CTA</u>	<u>GAA</u>	<u>GCC</u>	<u>TCC</u>	<u>CGT</u>	<u>GGC</u>	<u>AAT</u>	<u>GTG</u>	<u>TGC</u>	<u>AGC</u>	300
81	Thr	Ser	Leu	Gly	Val	Thr	Ile	Pro	Tyr	Asp	Leu	Glu	Ala	Ser	Arg	Gly	Asn	Val	Cys	Ser	100
301	<u>AAT</u>	<u>CTG</u>	<u>CTC</u>	<u>CAT</u>	<u>GGC</u>	<u>GCC</u>	<u>TAC</u>	<u>TGT</u>	<u>CCC</u>	<u>CTG</u>	<u>GAT</u>	<u>GCT</u>	<u>GGC</u>	<u>GAG</u>	<u>GAT</u>	<u>GTG</u>	<u>ACC</u>	<u>TAC</u>	<u>CAG</u>	<u>CTG</u>	360
101	Asn	Leu	Leu	His	Gly	Ala	Tyr	Cys	Pro	Leu	Asp	Ala	Gly	Glu	Asp	Val	Thr	Tyr	Gln	Leu	120
361	<u>CTC</u>	<u>CTG</u>	<u>CCA</u>	<u>GTC</u>	<u>ACC</u>	<u>AAC</u>	<u>CAG</u>	<u>CCG</u>	<u>GAG</u>	<u>GTG</u>	<u>CCC</u>	<u>ACG</u>	<u>CGC</u>	<u>CTA</u>	<u>GAA</u>	<u>GTT</u>	<u>CGT</u>	<u>CTG</u>	<u>CTG</u>	420	
121	Leu	Leu	Pro	Val	Thr	Thr	Asn	Gln	Pro	Glu	Val	Pro	Thr	Arg	Leu	Glu	Val	Arg	Leu	Leu	140
421	<u>GAC</u>	<u>TCC</u>	<u>GAT</u>	<u>GAC</u>	<u>GAG</u>	<u>AAT</u>	<u>CGA</u>	<u>GTG</u>	<u>GTG</u>	<u>TCC</u>	<u>TGT</u>	<u>TTC</u>	<u>CTG</u>	<u>GCC</u>	<u>GAC</u>	<u>ACT</u>	<u>CGG</u>	<u>GTC</u>	<u>AAG</u>	<u>AAG</u>	480
141	Asp	Ser	Asp	Asp	Glu	Asn	Arg	Val	Val	Ser	Cys	Phe	Leu	Ala	Asp	Thr	Arg	Val	Lys	Lys	160
481	CCC	AGA	TCG	GCA	GTT	TAG															498
161	Pro	Arg	Ser	Ala	Val	End															165

The yellow highlighted sequence is the predicted region targeted by the siRNA - *Npc2c*<sup>GD6798</sup> (VDRC #31139). Wobble bases were modified so that the longest stretch was not more than 16 nucleotides. Underlined sequence denotes the stretch of unchanged nucleotides. The codons modified are denoted as (handwritten) bases above the corresponding nucleotides. A total of 28 codons were modified. Alternative codons were selected based on [122].

## 2.9. Filipin Staining

For filipin staining of free sterols, tissues were fixed in 4% paraformaldehyde for 30 minutes, washed twice in chilled PBS, and stained with 50 µg/ml Filipin III (Sigma®) in PBS solution in dark for 1h at room temperature on a shaker. Samples were then washed twice with PBS before mounting them in Mowoil/DABCO mounting medium. Images were captured on a Nikon C1 plus confocal microscope.

**CHAPTER 3.****USING *DHR96<sup>1</sup>* MUTANTS AS TOOLS TO EXAMINE *DROSOPHILA* STEROL AND STEROID REQUIREMENTS**

### 3.1. *DHR96*<sup>l</sup> mutants arrest development in larval stages

The vertebrate liver X receptors (LXRs) are phylogenetically closely related to *Drosophila* DHR96 [123], suggesting that DHR96 might function similar to LXRs and control cellular and/or systemic cholesterol levels in *Drosophila*. Hence, a loss of *DHR96* function (via a mutation) could abrogate cellular cholesterol homeostasis, raising the question of how *DHR96*<sup>l</sup> mutants might respond to low or high levels of dietary cholesterol, and whether these dietary differences could manifest in phenotypic effects. We<sup>†</sup> reported the first observation that *DHR96*<sup>l</sup> mutants are second instar larval lethal on the Carolina 424 ('C424') medium [54], but viable and phenotypically normal on a standard fly medium. The C424 medium is derived from dried potato tuber flakes and its sterol composition has been analyzed [124] and shown that C424 contains ~10 times less cholesterol than the experimental optimum [125]. Therefore we consider the C424 as a naturally poor source of cholesterol, i.e. 'low cholesterol medium'.

The inability of *DHR96*<sup>l</sup> mutants to survive on the C424 medium might indicate a fundamental defect to properly retrieve a vital nutrient from the diet. *DHR96*<sup>l</sup> mutants are rescued to adulthood specifically by feeding cholesterol and not the molting hormone (20E), or yeast extract (which is a water-based extract, rich in amino acids, salts and sugars, but contains very few yeast lipids). This suggested that the observed lethality of *DHR96*<sup>l</sup> mutants was based on the scarcity of dietary cholesterol. To address the underlying cause for the *DHR96*<sup>l</sup> mutant lethality, I employed three main approaches:

- (1) I validated this mutant phenotype (**Figure 3.1**) with an independent base medium.
- (2) Since the differences between the C424 and SM are complex, I re-examined the phenotypes of *DHR96*<sup>l</sup> mutants on a lipid-depleted C424 medium (also called 'LD') to directly test the effectiveness of cholesterol supplementation.
- (3) Since *DHR96*<sup>l</sup> mutants were rescued specifically by dietary cholesterol, I asked what aspect of cholesterol function was deficient in the *DHR96*<sup>l</sup> mutants.

---

<sup>†</sup> Mattéa Bujold, Akila Gopalakrishnan, Emma Nally and Kirst King-Jones Mol. Cell. Biol. 2010, 30(3):793.

Figure 3.1.

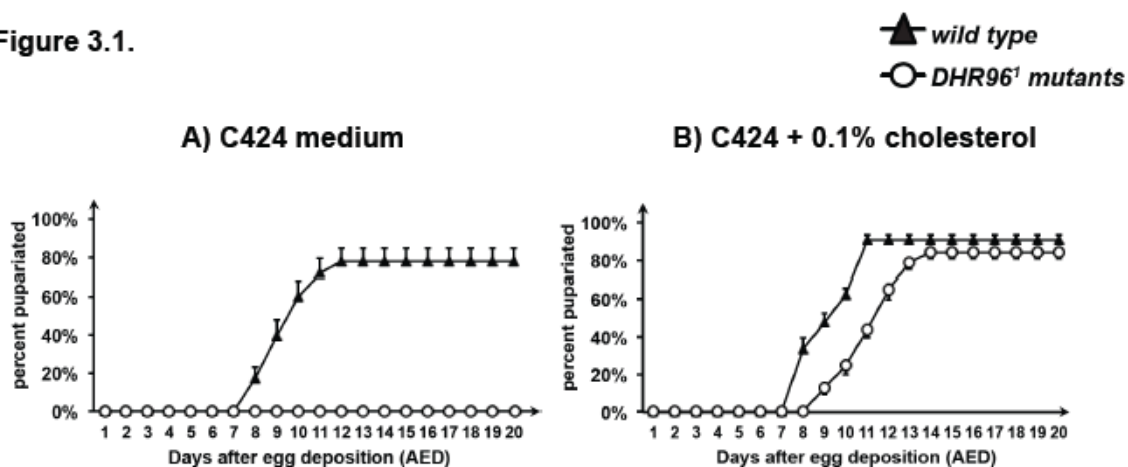


**Figure 3.1. *DHR96*<sup>1</sup> mutants arrest development as second instar larvae on Carolina 424 (C424) medium.**

*DHR96*<sup>1</sup> mutants were raised on Carolina 424 (C424), a potato-based medium. 50 embryos, each of wild type (triangles) and *DHR96*<sup>1</sup> mutants (circles) were planted on four replicate cultures of C424 medium, or C424 supplemented with 0.1% (wet weight) cholesterol. Survival was measured directly by scoring for pupae daily for 20 days after egg deposition (AED). *DHR96*<sup>1</sup> mutants arrest development as second larval instars on C424 medium. 0.1% cholesterol rescues *DHR96*<sup>1</sup> mutants albeit resulting in 2-3 day development delay and reduced survival than controls. Error bars represent standard deviation calculated from quadruplicates.

### 3.2. *DHR96*<sup>1</sup> mutants are highly sensitive to cholesterol deprivation.

To explore the phenotypic response of *DHR96*<sup>1</sup> mutants to low or high levels of dietary cholesterol, I raised populations of four replicate cultures each containing 50 age-matched embryos of *DHR96*<sup>1</sup> mutants and wild type (*Canton S*, hereafter *CanS*) on C424 medium, and C424 medium containing 0.1% cholesterol. The embryos were scored daily and the percentage of emerging pupae was calculated until day 20 AED (after egg deposition). In the survival graphs shown in **Figure 3.1**, X-axis indicates the time course represented as number of days AED, while the Y-axis indicates the percentage of animals that had pupariated. Although not shown in the data, it is to note that 100% of the pupae developed normally and eclosed into healthy, viable adults. On C424 medium ~80% of wild type animals pupariated, while 100% of *DHR96*<sup>1</sup> mutants arrested development as L2 and subsequently failed to survive past day 4-5 AED. Due to the naturally low sterol content of

the C424 medium, ~20% of the wild type also arrested development as L2s, which never developed further nor survived past day 4-5 AED. Supplementing the C424 medium with 0.1% cholesterol fully rescued *DHR96<sup>l</sup>* mutants to adulthood, which on the other hand demonstrated a 2-3 day developmental delay in pupariation relative to wild type animals. Feeding 0.1% cholesterol also boosted wild type survival by ~15% which suggested that, in addition to other nutrients, a significant amount of cholesterol or a certain sterol metabolite is the main nutrient missing from the C424 medium, and that shortage of dietary sterol has a direct effect on the normal larval development and growth. These survival curves thus validated the original phenotypic observation of *DHR96<sup>l</sup>* mutants on the low cholesterol C424 medium and their rescue to adult stages by 0.1% cholesterol supplementation.

To rule out any bias in the choice of fly media, I employed the yeast-glucose (YG) medium to verify the mutant phenotype using an independent base medium. To be absolutely sure that all possible sterol sources were eliminated from this diet, I subjected the ingredients – i.e. yeast extract and agarose, to rigorous lipid-depletion by chloroform extraction. Due to the hardening property of agarose and dryness associated with using the chemically purified yeast extract, this ‘lipid-depleted yeast-glucose medium’ (LDYG) posed significantly harsher survival conditions. On LDYG (**Figure 3.2**), merely ~10% of wild type animals pupariated by day 10-13 AED and developed into healthy adults, while the remaining ~90% of the population failed to survive past L2 stages. On the other hand, 100% of *DHR96<sup>l</sup>* mutants failed to survive past L2, which recapitulated the original phenotype observed on C424 medium. Therefore, in spite of the high lethality of wild type animals on LDYG, I continued using this medium because it provided an additional assay to validate the lethal phenotype of *DHR96<sup>l</sup>* mutants on sterol-depleted diets. Supplementing LDYG with 0.1% cholesterol boosted wild type and *DHR96<sup>l</sup>* mutant survival to ~75% and ~60%, respectively, as pupae that developed normally and eclosed into healthy, viable adults. Similar to our observation on C424 medium, rescued *DHR96<sup>l</sup>* mutants demonstrated a 2-3 day delay relative to wild type developmental timing. Thus, despite the harsher conditions for survival, the LDYG medium fully recapitulated the larval arrest phenotype of *DHR96<sup>l</sup>* mutants and their complete rescue to adult stages by cholesterol supplementation.

Figure 3.2.

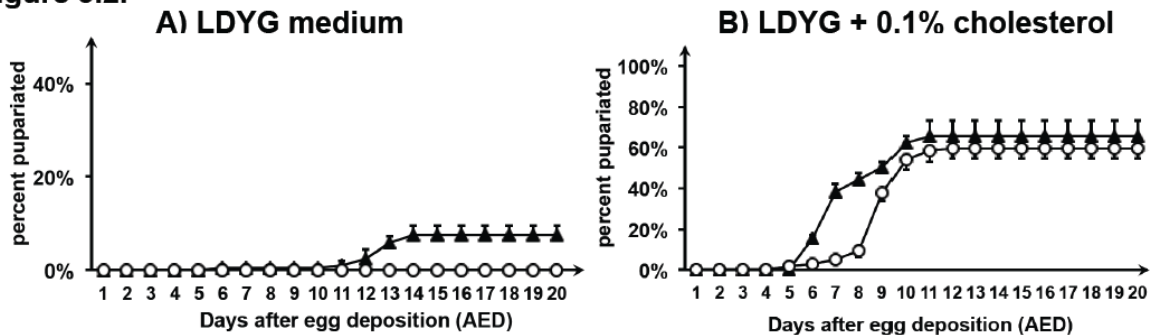


**Figure 3.2. Validating the *DHR96<sup>1</sup>* mutant lethal phenotype on an independent base medium.**

To validate the underlying nutritional deficiency causing the observed lethality of *DHR96<sup>1</sup>* mutant on C424 medium, 50 embryos, each of wild type (triangles) and *DHR96<sup>1</sup>* mutants (circles) were planted on four replicate cultures of lipid-depleted yeast-glucose (LDYG) medium, or LDYG supplemented with 0.1% (wet weight) cholesterol. Survival was measured directly by scoring for pupae daily for 20 days after egg deposition (AED). Error bars represent standard deviation calculated from the replicates. *DHR96<sup>1</sup>* mutants arrest development as second larval instars also on LDYG medium. However due to its composition, LDYG reduced overall percentage of wild type survivors as well.

### 3.3. *DHR96<sup>1</sup>* mutant phenotype: a global defect in sterol metabolism?

Since insects are cholesterol auxotrophs, they are obligated to either ingest dietary cholesterol directly, or like the tobacco hornworm *Manduca sexta* ingest suitable plant sterols, called phytosterols that can be dealkylated to cholesterol [61][126]. *Drosophila melanogaster* is however incapable of dealkylation and depends solely on dietary cholesterol for synthesizing ecdysone to complete normal development [55]. While some plant sterols have been shown to substitute entirely for cholesterol in the wild type (e.g. ergosterol, 7-dehydrocholesterol), most other sterols cannot be dealkylated and are thus incapable of replacing cholesterol (e.g. desmosterol, sitosterol) [55], [57]. However, work by others [127]–[129] have shown that 20-hydroxyecdysone may not necessarily be the only functional molting hormone in *Drosophila melanogaster*. The C28 ecdysteroid, makisterone A has been detected in *Drosophila* larvae and importantly, wild type ring glands have been shown to secrete 20-deoxymakisterone A *in vivo* [128]. Interestingly, while *Drosophila* larvae reared on a cholesterol-containing medium exclusively secreted 20E, larvae that were raised on diets containing plant sterols such as campesterol and sitosterol, secreted nearly

similar levels of both makisterone A and 20-hydroxyecdysone [89]. Hence, the phenotypic rescue of *DHR96<sup>l</sup>* mutants by cholesterol supplementation also raised the question whether the lethality associated with the *DHR96<sup>l</sup>* mutation arose from a global defect in sterol homeostasis, or a specific defect in cholesterol metabolism. Hence, I wanted to test the ability of sterols, other than cholesterol, to restore viability in *DHR96<sup>l</sup>* mutants on LDYG medium (**Figure 3.3**). I tested the abilities of ergosterol, the main yeast sterol, and stigmasterol, a widespread plant sterol. Both sterols contain the 3' hydroxyl group, alkyl side chain and the cyclic planar ring structure, making them structurally highly similar to cholesterol, presumably capable of partially or fully replacing the requirement for cholesterol by *DHR96<sup>l</sup>* mutants.

I supplemented LDYG with 32, 80, 200 and 500 µg each of ergosterol, stigmasterol or cholesterol (as control). The embryos used for these survival curves were obtained from parents that were fed with live yeast paste, which is a sterol-rich medium. Moulds, bacteria and yeasts which adhere to the embryo's exochorion often remain adhered in spite of removing the flies and eggs from any contact with yeasts [130]. To abolish the possibility of external sterol contamination in the form of yeast spores, I manually removed the chorion membrane of wild type and *DHR96<sup>l</sup>* embryos by bleach treatment, to ensure that no traces of sterol-containing media remained attached to the embryos. This allowed scoring the percentage of survivors axenically. In the absence of supplemented sterol, 100% of the dechorionated wild type and *DHR96<sup>l</sup>* embryos failed to survive on LDYG and arrested as L2 which continued to feed, without further development, until their death 4-5 days AED. Of the sterol concentrations tested on LDYG, wild type required a minimum of 32 µg sterols, while *DHR96<sup>l</sup>* mutants required a minimum of 200 µg supplemented sterols to support survival of at least ~20% of their populations (**Figure 3.3**). Incremental increases of sterol concentrations progressively boosted the percentage of wild type and *DHR96<sup>l</sup>* mutant survivors, indicating that dietary sterol availability is critical for *Drosophila* development and survival. At their maximum concentrations, cholesterol, stigmasterol and ergosterol rescued ~30%, ~70%, ~65% of *DHR96<sup>l</sup>* mutants to pupal stages, indicating that *DHR96<sup>l</sup>* mutants can efficiently use a range of dietary sterols such as ergosterol and stigmasterol for complete development and survival.

Figure 3.3.

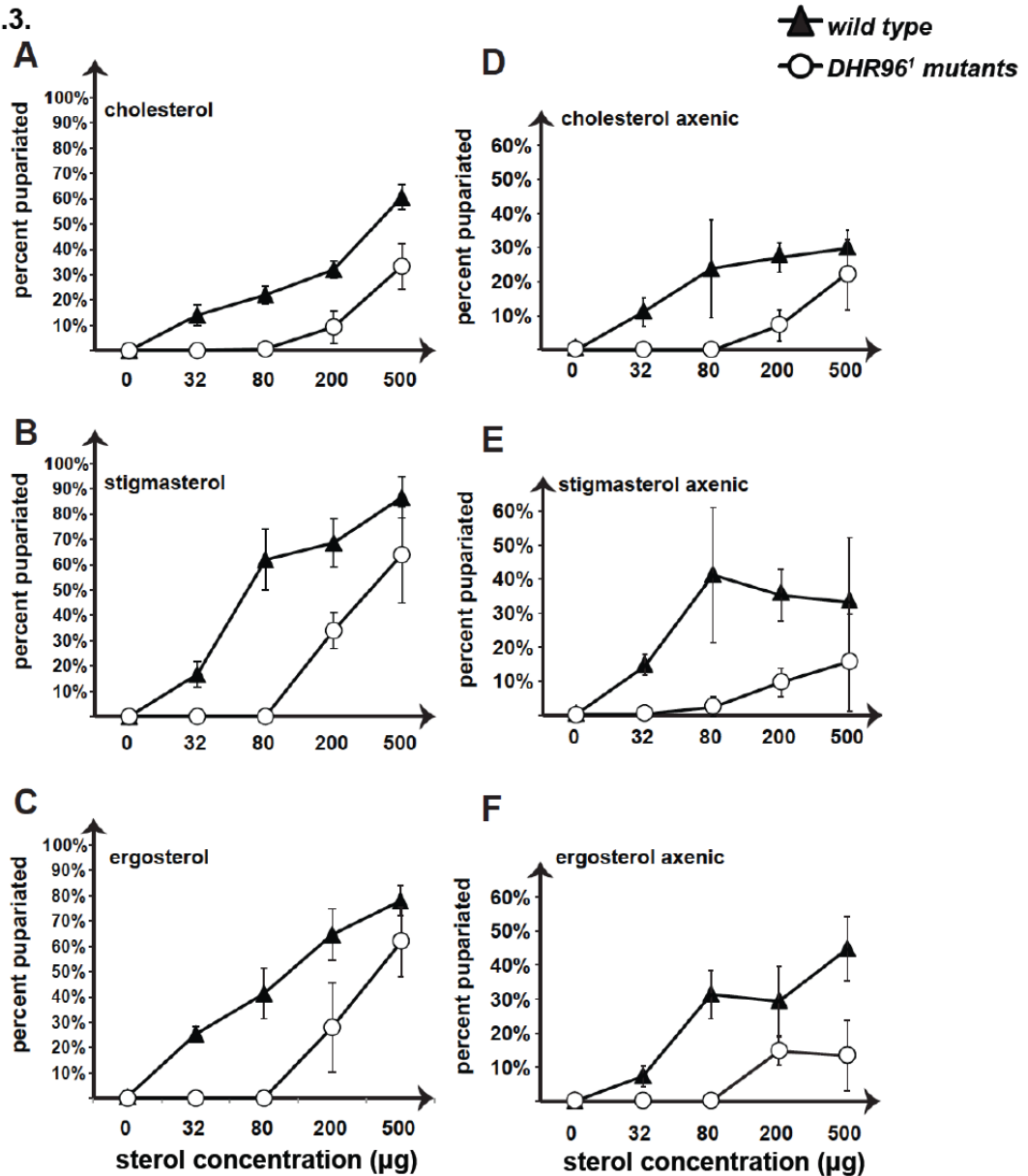


**Figure 3.3. *DHR96*<sup>1</sup> mutants are rescued on LDYG medium by dietary cholesterol, ergosterol and stigmasterol.** Here, I used lipid-depleted yeast-glucose medium (LDYG) to test the abilities of dietary cholesterol, ergosterol and stigmasterol to rescue *DHR96*<sup>1</sup> mutants. 50 embryos, each of wild type (triangles) and *DHR96*<sup>1</sup> mutants (circles) were planted on four replicate cultures of lipid-depleted yeast-glucose (LDYG) medium containing 32, 80, 200 or 500 µg of each of cholesterol, ergosterol or stigmasterol (X-axis). Survival was measured directly by scoring for pupae daily for 20 days after egg deposition (AED). Error bars represent standard deviation calculated from the replicates. While dechoriation of embryos greatly reduce the actual survival numbers, the general trend of survival of wild type and *DHR96*<sup>1</sup> mutants in response to different sterols is constant, with stigmasterol being the most effective sterol.

Previously, it has been shown that [128] ring glands dissected from *Drosophila melanogaster* larvae grown on an ergosterol-containing medium only secreted 20E, which suggested that the C-28 sterol (containing 28 carbon atoms), ergosterol, is likely to be dealkylated to cholesterol. If this hypothesis were true, then the observed rescue of *DHR96<sup>l</sup>* mutants by ergosterol reflects a systemic defect in cholesterol metabolism. In contrast, the observed rescue by stigmasterol is likely to result by the synthesis of the ecdysteroid makisterone A, and not 20E – since cumulative evidence suggests that *Drosophila melanogaster* cannot dealkylate C29 plant sterols (such as stigmasterol and sitosterol) to cholesterol [61], [128], [131]–[133]. *DHR96<sup>l</sup>* mutants do not suffer a mere hormonal defect, since supplementing 20E (the active molting hormone) at several different concentrations to LD media consistently fails to rescue these mutants (**Figure 3.8**). Thus, the rescue by stigmasterol suggests that *DHR96<sup>l</sup>* mutants can utilize stigmasterol and metabolize it to an intermediate that might be able to functionally replace cholesterol.

Importantly, although not indicated in the data, 100% of these rescued pupae continued to develop normally and eclosed into healthy, viable adults by 9-12 days AED. On the other hand, although axenic embryos greatly reduced the survival numbers since the dechoriation procedure directly affected survival numbers, the general trend of wild type and *DHR96<sup>l</sup>* mutant survival in response to the three sterols remained identical to that observed with embryos with intact chorionic membranes (left panels, **Figure 3.3**), with stigmasterol producing highest number of survivors, followed by ergosterol and finally by cholesterol which intriguingly produced the least number of survivors. Taken together, my results indicated while *DHR96<sup>l</sup>* mutants can utilize dietary sterols for survival, they possess a much higher threshold for dietary sterol requirements than wild type animals. The fact that these differences in sterol requirements phenotypically manifest only on lipid-depleted diets strengthen my hypothesis that ***DHR96<sup>l</sup>* mutants suffer from an inherent failure to sense and cope with the drop in cellular cholesterol levels as a result of dietary cholesterol deprivation.**

### **3.4. Lipid-depleted C424 medium is a better alternative to LDYG.**

The LDYG medium is a hard-textured medium that comprises multiple chloroform-treated ingredients, such as agarose (materials & methods 2.1.2), demanding ample hydration. The

harshness of this LDYG medium combined with the fact that I reared these embryos axenically, i.e. by removing the chorion membrane, significantly affected wild type survival. Since these limitations could not be fixed by modifying the LDYG recipe, I created a lipid-depleted version of the already mentioned C424 medium, where I subjected the medium to rigorous and repeated chloroform extraction. Since this lipid-depleted medium could be readily constituted with water, it presented a virtually lipid-free environment that was also not harsh for wild type animals to complete growth and development. Hence this lipid-depleted diet represented a minimal medium to which I could then supplement defined amounts of cholesterol to test for rescue of *DHR96<sup>1</sup>* mutants.

To determine if this LD medium can be better alternative to LDYG medium, I monitored the survival trend of 50 axenic wild type and *DHR96<sup>1</sup>* mutant embryos on LD supplemented with or without 0.1% cholesterol (**Figure 3.4**). While ~75% wild type animals were viable, 100% of *DHR96<sup>1</sup>* mutants recapitulated the L2 arrest phenotype observed on C424, and were completely rescued to adults by 0.1% cholesterol supplementation. Additionally, supplementing LD with 200 or 500µg of cholesterol (**Figure 3.5**) produced nearly twice as many *DHR96<sup>1</sup>* mutant survivors achieved under identical cholesterol concentrations on LDYG (**Figure 3.3**). Importantly, in contrast to the LDYG where irrespective of embryo dechoriation, wild type animals consistently failed to survive in the absence of supplemented sterol, the LD medium allowed for ~10% of dechorionated wild type embryos to complete development as normal adults. From then on, I have exclusively used this lipid-depleted C424 medium (hereafter referred to as ‘LD’) for all experiments described in this dissertation.

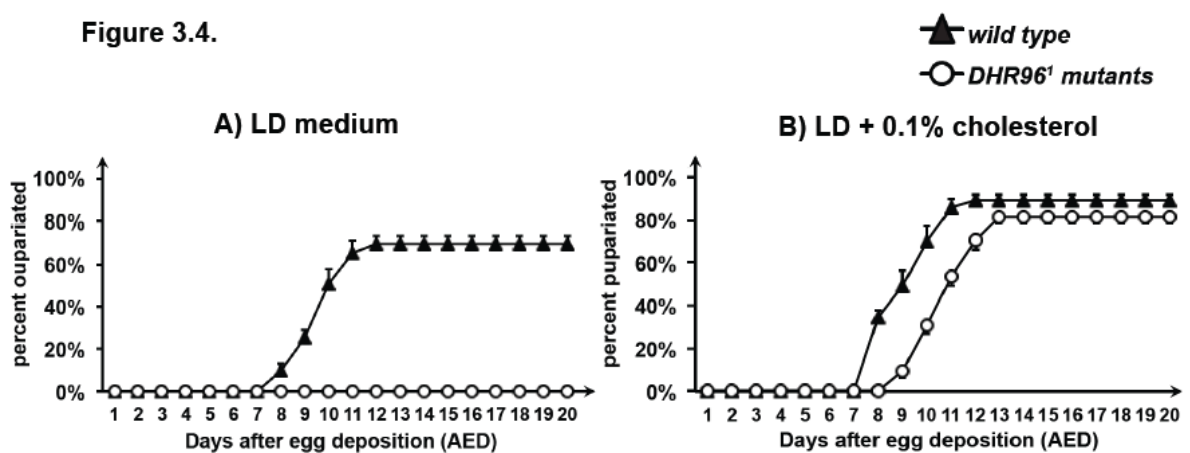


**Figure 3.4. Lipid-depleted C424 (LD) medium is a better alternative than LDYG.** C424 medium subjected to rigorous lipid depletion by chloroform extraction constituted the Lipid-depletedC424 (LD) medium. Compare data to Figure 3.2. 50 embryos, each of wild type (triangles) and *DHR96<sup>1</sup>* mutants (circles) were planted on four replicate cultures of LD medium or LD supplemented with 0.1% (wet weight) cholesterol, were each seeded with 50 de-chorionated axenic embryos of wild type (triangles) and *DHR96<sup>1</sup>* mutants (circles). Survival was measured directly by scoring for pupae daily for 20 days after egg deposition (AED). Error bars represent standard deviation calculated from the replicates.

**Figure 3.5.**

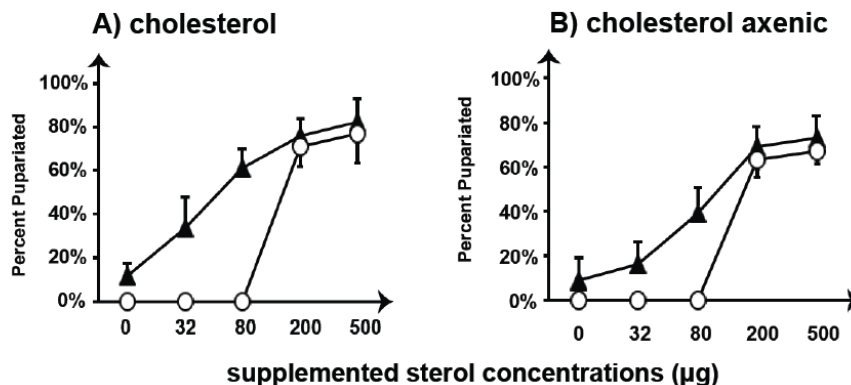
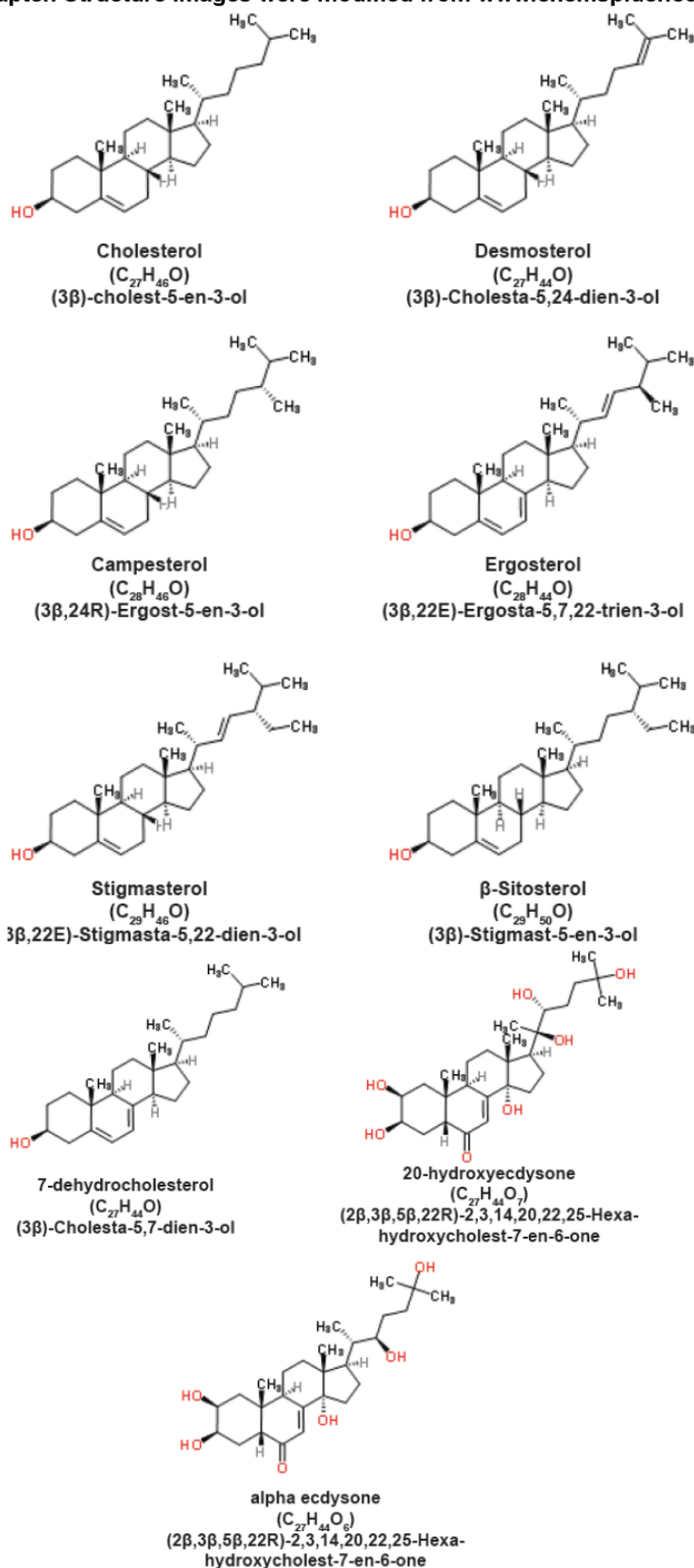


**Figure 3.5. Lipid-depletedC424 (LD) media fully recapitulates the *DHR96<sup>1</sup>* mutant lethal phenotype and rescue by cholesterol without diminishing the viability of axenically reared wild type animals.** 50 embryos, each of wild type (triangles) and *DHR96<sup>1</sup>* mutants (circles) were planted on four replicate cultures of lipid-depletedC424 (LD) medium containing 32, 80, 200 or 500µg of cholesterol were seeded with 50 dechorionated axenic embryos of wild type (triangles) and *DHR96<sup>1</sup>* mutants (circles). Survival was measured directly by scoring for pupae daily for 20 days after egg deposition. Error bars represent standard deviation calculated from the replicates.

Figure 3.6. Chemical structures and molecular formula of sterols discussed in this chapter. Structure images were modified from [www.chemspider.com/](http://www.chemspider.com/).



### 3.5. Characterizing the cholesterol deficiency in *DHR96<sup>l</sup>* mutants

To define the underlying cause for *DHR96<sup>l</sup>* mutant lethal phenotype on LD medium, I asked **what function of cholesterol was being rescued in these animals?** Based on the currently known functions of insect cholesterol, cholesterol is required in bulk amounts in the plasma membranes for preserving structural integrity and is thus vital for normal growth processes [134]. The orchestrated pulses of active ecdysteroids that drive larval molting, development and metamorphosis are initiated by the synthesis of 20E from cellular cholesterol in the prothoracic gland [135]. The third known function of insect cholesterol is to covalently modify signaling proteins such as Hedgehog (hh) [68], [136], [137]. Since insects are cholesterol auxotrophs that meet all their cholesterol requirements exclusively via nutritional intake, dietary cholesterol depletion could thus drastically reduce membrane and cellular sterol levels. Consequently, this impedes the abilities of insects to complete normal development due to reduced 20E synthesis, or via directly affecting *hh* signaling. Yet, it is possible that other unknown functions of cholesterol exist. To identify which function of cholesterol or a metabolite thereof is affected in *DHR96<sup>l</sup>* mutants, I fed wild type and mutant larvae with a wide range of sterol analogs that were predicted to structurally replace cholesterol function in the membranes or functionally usable as substrates for the biosynthesis of any required cholesterol-derived hormones and signaling molecules.

Desmosterol, a sterol structurally highly similar to cholesterol (**Figure 3.6**), is reported to functionally replace cholesterol in *Drosophila* membranes [2]. To test if *DHR96<sup>l</sup>* mutants have an exclusive bulk membrane cholesterol defect or a failure to synthesize 20E hormone, I supplemented LD medium with desmosterol (to replace cholesterol in the membranes) or the active hormone, 20E (to substitute for the hormone synthesis function of cholesterol), respectively. Using this approach, I could test whether these sterols when administered individually or in combination could support *DHR96<sup>l</sup>* mutant survival on LD.

My findings indicated that, at several concentrations tested, desmosterol alone could not sustain development of *DHR96<sup>l</sup>* mutants to adulthood. However, identical levels of desmosterol when provided in combination with trace amounts of cholesterol attained an even better rescue compared to identical concentrations of cholesterol alone (**Figure 3.7**), which provides the first evidence that *Drosophila* can utilize desmosterol *in vivo*, and

indicating that it is however insufficient to sustain growth and development on lipid-depleted diets. On the other hand, a combination of desmosterol with 20E (without any added cholesterol) failed to rescue *DHR96<sup>1</sup>* mutants. This suggests that despite providing sufficient amount of desmosterol, which may partly substitute for the membrane function of cholesterol, *DHR96<sup>1</sup>* mutants were still deficient in retrieving an essential cholesterol metabolite.

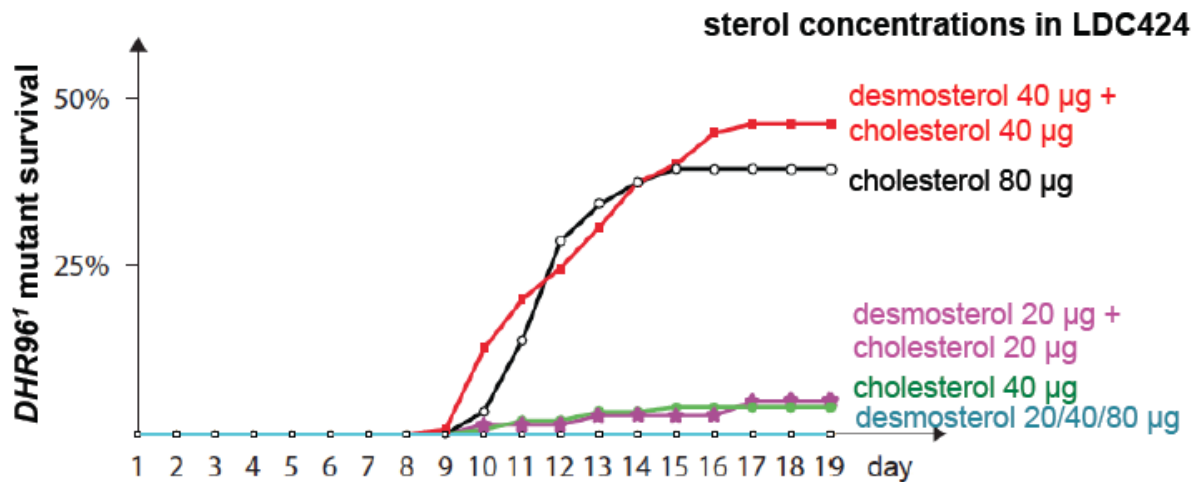


**Figure 3.7. *DHR96<sup>1</sup>* mutants can utilize desmosterol.** Viability study of *DHR96<sup>1</sup>* mutants on lipid-depleted C424 media supplemented with different concentrations of desmosterol and cholesterol. **Desmosterol cannot be metabolized in *Drosophila*, but may be used for structural purposes. This experiment shows that *DHR96* mutants can indeed utilize desmosterol for non-metabolic functions** (presumably desmosterol is used to replace cholesterol in plasma membranes). *DHR96* mutants require ~80 micrograms of total sterol content per vial to reach ~40-50% survival rates, either in the form of pure cholesterol (white circles) or 50% each of cholesterol and desmosterol (black squares). 80 µg of desmosterol alone yields no survivors (white squares), similarly, 20 µg and 40 µg desmosterol or no sterol at all are also insufficient for survival (all white squares). In contrast, 40 µg of cholesterol results in ~5% survivors (green circles), similar to the survival rates when a combination of 20 µg cholesterol and 20 µg desmosterol is used (pink stars). Increasing cholesterol concentrations to 80 µg per vial improves viability to ~40% (black, circles), comparable to survival rates when 40 µg cholesterol is used in conjunction with 40 µg desmosterol (red, squares). Work done in collaboration with Nahbeel Premji.

### 3.5.1. Testing the functional efficacy of supplemented sterol analogs

It was highly likely that the *DHR96<sup>1</sup>* mutants arrested development as L2 due to a hormonal deficiency. Hence I tested this scenario using LD supplemented with varying levels of 20E hormone. To demonstrate that the supplemented 20E is functional, I used the *phantom* (*phm*)-*Gal4* driver to trigger *shroud-RNAi*, specifically in the prothoracic gland cells (**Figure 3.8**). *Shroud* is an ecdysone biosynthetic gene, which encodes a cytochrome P450 enzyme that catalyzes the conversion of 7dC to 5 $\beta$ -ketodiol [138] (**Figure 1.5**). While the controls *phm-Gal4>w<sup>1118</sup>* appeared phenotypically normal and viable on LD, 100% of PG-specific *sro-RNAi* were larval lethal and subsequently rescuable to adult stages by 20E. Since a knockdown of *sro* would have caused a concomitant block in the 20E pathway, supplementing dietary cholesterol would be predicted to not rescue the *sro-RNAi* phenotype. While 10  $\mu$ g of 20E failed to rescue the *sro-RNAi* larvae, incremental increases to 50, 100 and 180  $\mu$ g of 20E progressively increased the effectiveness of the rescue of *sro-RNAi* to adulthood demonstrating that the supplemented synthetic 20E hormone is functional and can be utilized by *Drosophila*.

**Figure 3.8.**

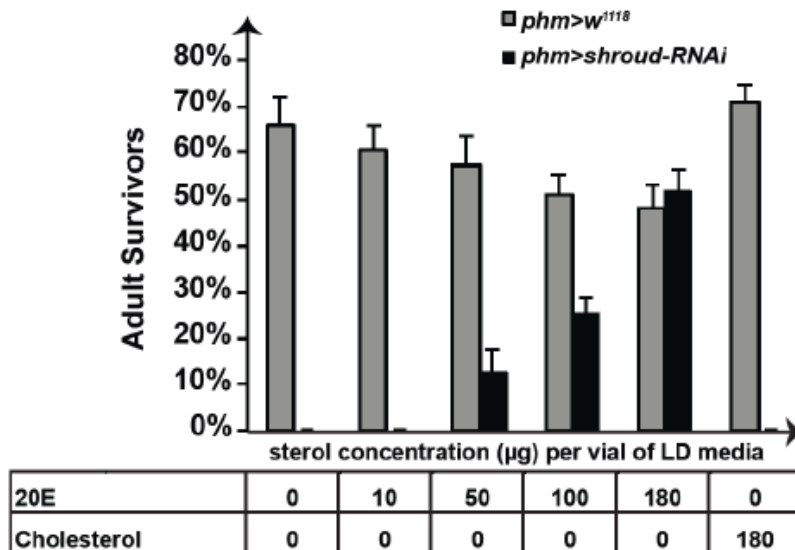


**Figure 3.8. 20E is a biologically active sterol analog, sufficient to fully rescue *shroud-RNAi* animals on lipid-depleted (LD) medium.**

*Shroud* is one of the ecdysone biosynthetic genes, which encode P450 enzymes which catalyze the intermediate steps in the conversion of 7dC (7-hydrocholesterol) to 5 $\beta$ -ketodiol. PG-specific *shroud-RNAi* causes larval arrest phenotype that is completely rescuable to adult stages by 20E supplementation. Hence *shroud-RNAi* was utilized to test the efficacy of the 20E used in our studies. 50 embryos each of *phm>w<sup>1118</sup>* (grey) and *phm>shroud-RNAi* (black) animals were raised on lipid-depleted (LD) medium containing 20E (20-hydroxy ecdysone) or cholesterol. Error bars represent standard deviation calculated from 4 replicates at each sterol concentration tested. *phm-Gal4* transgene drives expression in the prothoracic gland.

### 3.6. Do *DHR96<sup>l</sup>* mutants have an obligate requirement for cholesterol

Collectively, my data indicated that although the bulk membrane desmosterol, and the 20E hormone were beneficial, neither of them could sustain growth and development of *DHR96<sup>l</sup>* mutants on LD. Hence I asked: what function of cholesterol was being rescued in *DHR96<sup>l</sup>* mutants reared on LD. Can cholesterol be replaced altogether by a combination of cholesterol-derived metabolites, or do *DHR96<sup>l</sup>* mutants have an obligate requirement for cholesterol itself, perhaps as a substrate for a signaling pathway critical for normal growth and development on lipid-depleted diets. In the 20E biosynthetic pathway, the first step is the conversion of the substrate cholesterol into 7-dehydrocholesterol (7DC), followed by sequential synthesis of 20E from its prohormone;  $\alpha$ -ecdysone in the target tissues. My expectation was that if cholesterol was utilized directly, say to modify hedgehog protein, or that cholesterol has other independent and novel cellular functions, then supplementing LD with 7-dehydrocholesterol will likely fail to rescue *DHR96<sup>l</sup>* mutants. On the other hand, as shown in **Figure 3.9**, 7-dehydrocholesterol is sufficient fully rescue *DHR96<sup>l</sup>* mutants to adulthood on LD at concentrations identical to that of cholesterol, suggesting that a cholesterol metabolite located within the 20E pathway might have a previously uncharacterized vital role in sustaining survival and development of *DHR96<sup>l</sup>* mutants on LD.

To identify which cholesterol metabolite could fully substitute the cholesterol requirement in *DHR96<sup>l</sup>* mutants on LD, I reared 50 age-matched, dechorionated wild type

(grey bars) and *DHR96*<sup>l</sup> mutant (black bars) embryos, with each genotype in 26 replicates, on LD supplemented with specific concentrations of desmosterol, 20E, cholesterol,  $\alpha$ -ecdysone or 7DC (as listed in the Table on X-axis of **Figure 3.10**). On LD medium, ~70% of wild type animals were viable, and 100% of *DHR96*<sup>l</sup> mutants arrested as L2s. On the other hand, ~80% of both wild type and *DHR96*<sup>l</sup> mutants were viable as healthy adults on standard medium, whereas ~20% of their populations were larval lethal due to the effects of dechoriation. Supplementing LD with 80  $\mu$ g of cholesterol boosted wild type and *DHR96*<sup>l</sup> mutant survivors to ~80% and ~70% respectively. An attempt to replace the supplemented cholesterol by combining 80  $\mu$ g of desmosterol and 10  $\mu$ g of 20E to LD failed to rescue *DHR96*<sup>l</sup> mutants, and caused an additional ~20% lethality in wild type, possibly due to an excess of unutilized supplemented sterols.

Given that *Drosophila* is a cholesterol auxotroph, I asked whether this dietary cholesterol requirement was in bulk or trace amounts. Remarkably, adding back a minute amount of cholesterol, i.e. 1  $\mu$ g, in combination with desmosterol and 20E was sufficient to rescue ~30% of *DHR96*<sup>l</sup> mutants to adult survivors on LD. This highlighted the need to address what aspect of cholesterol function in *DHR96*<sup>l</sup> mutants was rescued by this trace amount. Hence I attempted to replace this trace amount of cholesterol with other intermediates from the cholesterol-based 20E pathway. Strikingly, replacing the 1  $\mu$ g cholesterol with 1  $\mu$ g of 7DC (i.e. in combination with 80  $\mu$ g of desmosterol and 10  $\mu$ g of 20E), was also sufficient to rescue *DHR96*<sup>l</sup> mutants on LD. In an unexpected finding, I observed that substituting this trace amount of cholesterol with 1  $\mu$ g of the prohormone  $\alpha$ -ecdysone (in the same combination with desmosterol and 20E) was sufficient to sustain growth and development of ~25% of *DHR96*<sup>l</sup> mutants to adult stages.

The larval lethality phenotype of *DHR96*<sup>l</sup> mutants is a highly reproducible phenotype that has been validated in over 500 independent replicates conducted by several researchers in our lab. The finding that a combination of alpha-ecdysone ( $\alpha$ -ecdysone), desmosterol and 20E can support normal growth and development of *DHR96*<sup>l</sup> mutants on LD medium is thus a highly significant phenotypic rescue.

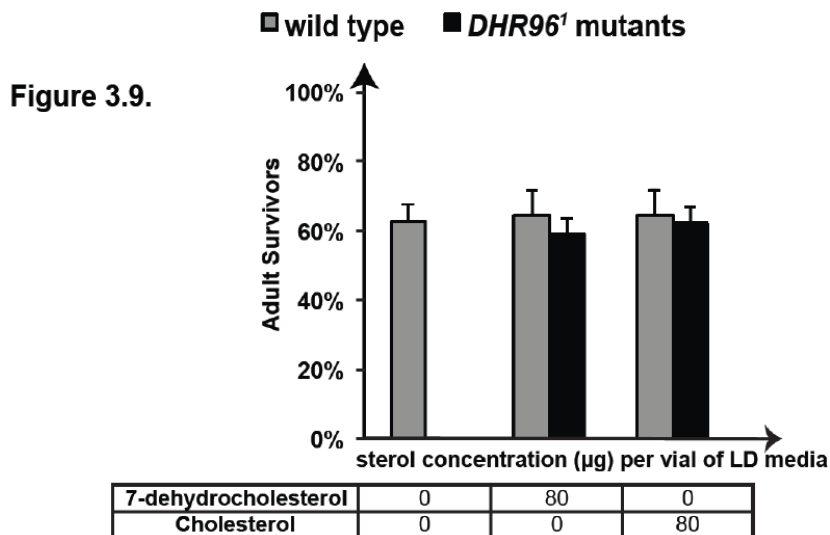


**Figure 3.9. 7-dehydrocholesterol is sufficient to rescue *DHR96'* mutants to adulthood on lipid-depleted (LD) medium.** Survival graphs of wild type (grey) and *DHR96'* mutants (black) on lipid-depleted (LD) medium supplemented with 7-dehydrocholesterol or cholesterol. Error bars represent standard deviation calculated from 5 replicates for each sterol tested, with each replicate containing 50 de-chorionated axenic embryos.

Figure 3.10.

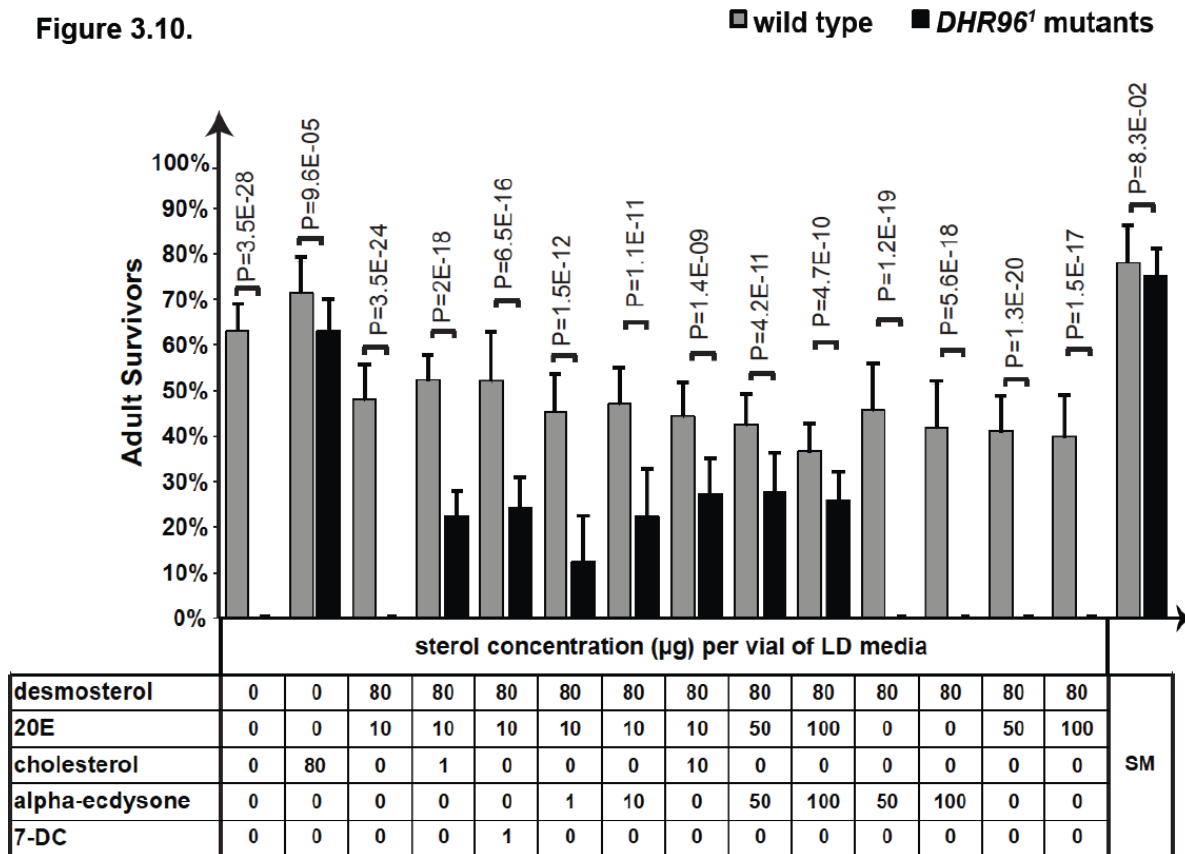


**Figure 3.10. Prohormone alpha-ecdysone supports survival of *DHR96* mutants to adulthood on lipid-depleted (LD) medium (or) *DHR96* mutants are rescued to adulthood on lipid-depleted (LD) medium containing putative functional analogs of cholesterol.**

Survival graphs of wild type (grey) and *DHR96*<sup>1</sup> mutants (black) animals on standard medium (SM) or on lipid-depleted (LD) medium supplemented with specific sterols (the total amount of sterol per vial is the sum of the individual concentrations as indicated in the table below the X-axis). *P* values represent results from an unpaired Student's *t* Test. Error bars represent standard deviation calculated from 26 replicates for each dietary condition with each replicate containing 50 dechorionated axenic embryos. 20E; 20-hydroxyecdysone.

Keeping the combination of 80 µg desmosterol and 10 µg 20E constant, and increasing the concentration of α-ecdysone to 10 µg resulted in a further ~10% increase in *DHR96*<sup>1</sup> mutant survival, in a manner that was strikingly identical to supplementing 10 µg cholesterol (adjacent column to the right), strongly suggesting that α-ecdysone is somehow utilized by *DHR96*<sup>1</sup> mutants to complete adult development on LD diets. Although, the historical understanding of the prohormone α-ecdysone has been confined to its role as the

penultimate precursor of 20E, given that  $\alpha$ E can also bind the ecdysone receptor (EcR) [139] and regulates developmental timing and body size [140], my finding that 20E supplementation along with  $\alpha$ -ecdysone is more effective than feeding 20E alone, suggests that there may exist a critical balance between the relative concentrations of these two steroid hormones in relation to their binding affinities and competition for the hormone receptor, likely, EcR.

To test if a relative balance exists between 20E and  $\alpha$ E, I further increased both 20E and  $\alpha$ -ecdysone to 50 or 100  $\mu$ g each, while maintaining desmosterol constant at 80  $\mu$ g. However, this resulted only in a moderate increase to ~40% survivors, with no significant difference between the percentage of survivors between the 50  $\mu$ g and 100  $\mu$ g ecdysteroids concentrations. Arguably, it was possible that the supplemented  $\alpha$ E was merely being converted to 20E. To test this scenario, I individually supplemented 50  $\mu$ g and 100  $\mu$ g each of either  $\alpha$ E or 20E (with 80  $\mu$ g desmosterol) (**Figure 3.10**, far right column), and found that neither ecdysteroid were capable of supporting *DHR96<sup>l</sup>* mutant development on LD, suggesting that  $\alpha$ -ecdysone has a novel cellular function in addition to 20E synthesis. Although a PG-specific knockdown of *DHR96* resulted in no obvious developmental defects (**Chapter 4, Figure 4.8G**), the fact that a specific combination of ecdysteroids can alleviate the *DHR96<sup>l</sup>* mutant phenotype revealed a new possibility that DHR96 may have an autonomous or non-autonomous function in the prothoracic gland (PG).

### **3.7. Prohormone $\alpha$ -ecdysone has novel roles in independent of 20E production**

As cholesterol auxotrophs, wild type animals have an obligate requirement for dietary cholesterol to complete development, which explained why only ~85% of wild type were viable on LD medium, which in addition, worsened to ~10% on LDYG (**Figure 3.2**). Within a given population where larvae are competing for dietary sources that support survival, larval carcasses represent abundant sources of maternally derived sterols and other critical nutritional reserves. Thus, scavenging on these sterols can provide a substantial survival advantage on LD. To thus eliminate the effects of sterol contamination resulting from sterol sources in carcasses, I used one embryo per vial of LD medium and reared the embryos axenically (i.e. by removing their chorion). Since *DHR96<sup>l</sup>* mutants fail to survive even in

populations, I confined my preliminary studies on understanding the functional significance of  $\alpha$ -ecdysone using wild type single embryos.

I reared 35 single, age-matched and dechorionated wild type embryos in individual vials containing LD medium (**Figure 3.11**). 100% of these independently raised embryos failed to develop past L2, which confirmed my hypothesis that carcasses pose a source of dietary sterols that can be absorbed and metabolized to support normal development on LD. Secondly, this verified that the sterol depletion in LD medium was effective. Thirdly, adding back 80  $\mu\text{g}$  of cholesterol was sufficient to rescue  $\sim 60\%$  of these embryos to phenotypically healthy adult flies, as one would expect for a cholesterol auxotroph.

To investigate the functional significance of  $\alpha$ -ecdysone in supporting *Drosophila* development, I reared these single wild-type embryos on LD medium supplemented with different combinations of desmosterol, 20E, and  $\alpha$ -ecdysone. I used sterols at concentrations identical to those that fully rescued *DHR96<sup>l</sup>* mutants to adult stages on LD medium. The stacked columns in **Figure 3.11** represent the number of single wild type embryos, across 35 replicates, that have either: arrested development as larvae or pupae (white bars), or have completed development to healthy adult flies (black bars). Embryos were reared on LD medium supplemented with different sterols that were tested in concentrations as shown in the table (below X-axis) and on standard medium (far right column).

While 100% of the individually reared wild type embryos were L2 larval lethal on LD medium, supplementing 80  $\mu\text{g}$  of cholesterol to LD rescued  $\sim 60\%$  wild type embryos to healthy adult flies and the rest  $\sim 40\%$  arrested development as L2s. For all sterol combinations discussed hereafter, the concentration of supplemented desmosterol was kept at a constant 80  $\mu\text{g}$ . I observed that 50  $\mu\text{g}$  or 100  $\mu\text{g}$  of 20E failed to rescue wild type embryos (third column from left, **Figure 3.11**). In a striking contrast, 50  $\mu\text{g}$  and 100  $\mu\text{g}$  of  $\alpha$ -ecdysone were capable of rescuing  $\sim 22\%$  and  $\sim 60\%$ , respectively, of wild type L2s to healthy adults. Curiously, combining 50  $\mu\text{g}$  each of 20E and  $\alpha$ -ecdysone somehow failed to achieve a complete rescue, in spite of the previous rescue by 50  $\mu\text{g}$  of  $\alpha$ -ecdysone. On the other hand, combining 100  $\mu\text{g}$  each of 20E and  $\alpha$ -ecdysone boosted adult survivors to  $\sim 45\%$  on LD, which was seemingly less effective than the rescue achieved by 100  $\mu\text{g}$  of  $\alpha$ -ecdysone alone (i.e. without 20E).

As such, this complete rescue of individual wild type embryos to adulthood by a combination of desmosterol and  $\alpha$ -ecdysone without any supplemented cholesterol, is strongly consistent with my previous rescue of *DHR96<sup>l</sup>* mutant populations at identical sterol concentrations. In summary, my findings suggest that the prohormone  $\alpha$ -ecdysone may have independent developmental roles in addition to synthesizing the classical molting hormone, 20E.

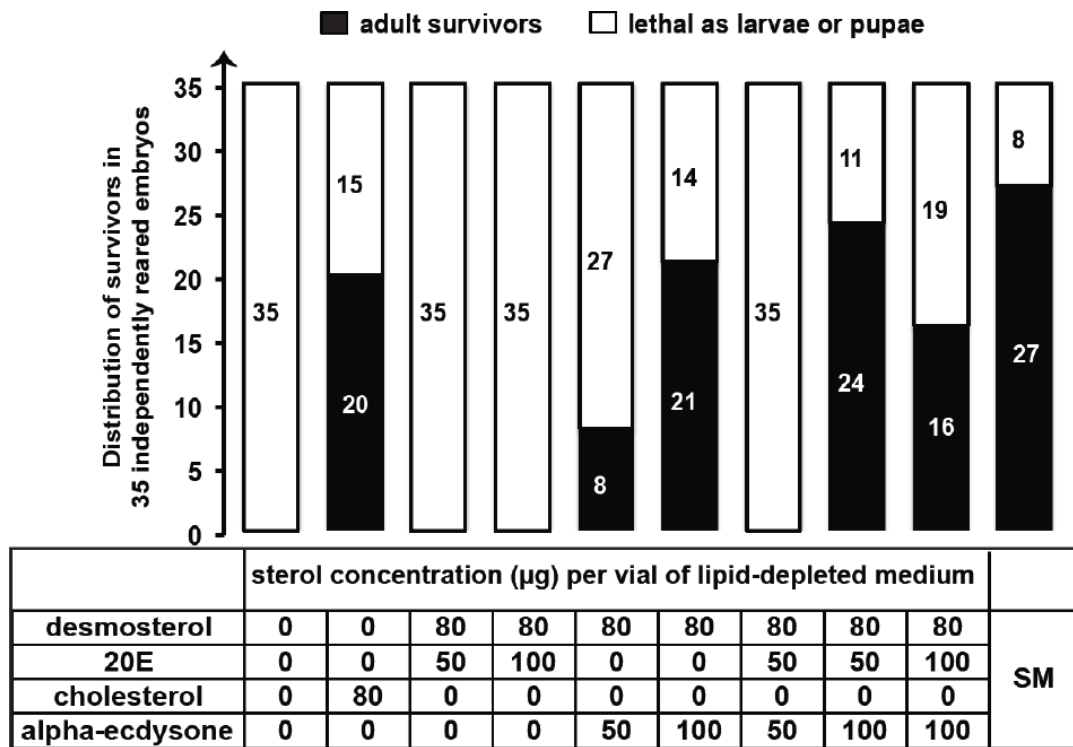


**Figure 3.11. A unique combination of membrane sterols and ecdysteroids are sufficient to replace the dietary cholesterol requirement that is mandatory for survival of wild type *Drosophila melanogaster* on lipid-depleted medium.** Stacked columns represent the number of single wild type embryos out of 35 independently reared replicates, each containing one embryo per vial, that developmentally arrested as larvae or pupae (white) or survived as adult flies on standard medium (SM), or on lipid-depleted (LD) medium supplemented with specific sterols. The total sterol amount per vial is the sum of the individual concentrations as indicated in the table below the X-axis. 20E; 20-hydroxyecdysone.

**CHAPTER 4.****GENE EXPRESSION ANALYSIS OF THE CELLULAR RESPONSES TO  
DIETARY CHOLESTEROL**

Results presented in this chapter are partially reflected in the following publication:

*Mattéa Bujold, Akila Gopalakrishnan, Emma Nally and Kirst King-Jones. Mol. Cell. Biol. 2010, 30(3):793. DOI: 10.1128/MCB.01327-09.*

The preliminary findings described in this chapter were experiments performed by M. Bujold and K. King Jones. M. Bujold collected and processed samples for the *low cholesterol microarray* (Figure 4.1, 4.3.1), and *high cholesterol microarray* (Figure 4.4, Tables 4.1 and 4.2) and K. King Jones analyzed all microarray data. In guidance with K. King Jones, I shortlisted the candidate genes and performed the follow-up validation experiments (Figures 4.2, 4.5, Table 4.3) and I collaborated with M. Bujold to standardize the working protocol and data analyses for the microfluidic qPCR experiments (Figures 4.3.1 and 4.3.2). I performed all steps in the experimental design, sample collections, setup, and data analysis of the microfluidic qPCR shown in Figures 4.5, 4.6, Table 4.4. Unless otherwise mentioned, all other data figures are my original work.

#### 4.1. Differences in dietary sterol composition trigger unique transcriptional responses

Several studies on vertebrate models have established a role for nuclear receptors to function as cellular sensors of key metabolites [5], [141]–[143]. A physiological change that disturbs normal cellular levels of such metabolites could accordingly activate or inactivate specific nuclear receptors [64], [144]. When activated, nuclear receptors target the promoter regions of specific genes that are functionally involved in cellular pathways that utilize those metabolites [145]–[147]. To understand the metabolic pathways controlled by *DHR96*, I needed to first narrow down the list of candidate genes that might be transcriptionally regulated by *DHR96*. One way to do this was to analyze the genome-wide transcriptional effects of a *DHR96* mutation.

To better understand the gene expression profiles underlying the *DHR96<sup>l</sup>* mutant lethality on the *low cholesterol* ‘C424’ medium, M. Bujold used Affymetrix 2.0 microarrays to conduct, what we refer to as, the *low cholesterol microarray* (summarized in **Figure 4.1A**). In this microarray analysis, we compared the transcriptional patterns in the *DHR96<sup>l</sup>* mutant and wild type L2 larvae that were raised throughout development on the following food sources: (i) **C424 instant fly medium**, which mainly contains trace amounts of phytosterols that cannot be metabolized into cholesterol [148] and thus signifies a low cholesterol, suboptimal medium, and (ii) **standard medium (hereafter, SM)**, composed mainly of yeast, which produces ergosterol [89] that can be effectively utilized by *Drosophila* for complete development (ergosterol data represented in **Figure 3.3**, Chapter 3), and thus signifies a nutritionally sterol abundant medium. Specifically, array data were filtered for genes that demonstrated statistically significant expression differences, i.e.  $\geq 2$  (fold change values) for upregulated genes and  $\leq 2$  (fold change values) for downregulated genes,  $P < 0.01$  (**Figure 4.1**) between the following criteria: I) wild type vs. *DHR96<sup>l</sup>* mutants on each media type, and II) C424 vs SM for each genotype (**Figure 4.1**, dotted lines). Interestingly, the vertebrate homologs of top differentially regulated genes in these gene sets had previous links to known sterol metabolic pathways (**Figure 4.2**).

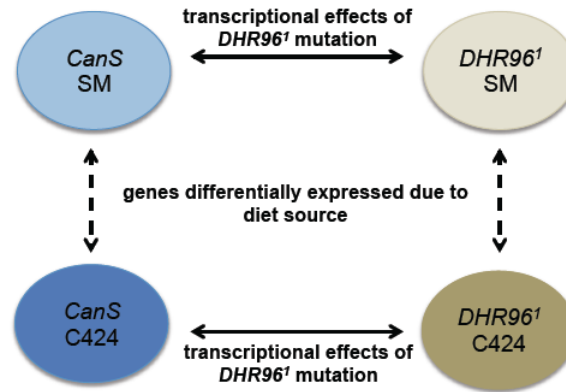
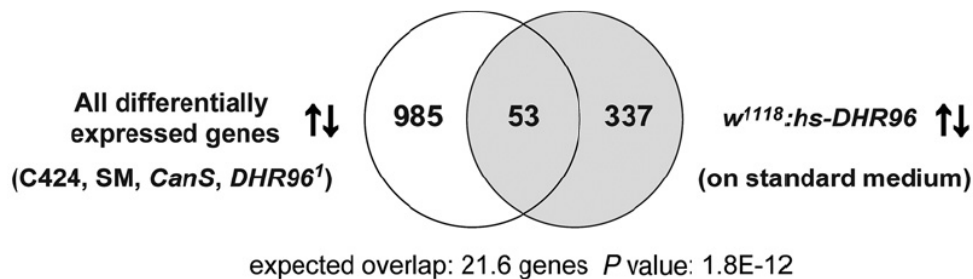


**Figure 4.1. Differentially expressed genes identified in the *low cholesterol* microarray.** Here, we compared four Affymetrix data sets (conducted by M. Bujold): *CanS* (*CanS*) and *DHR96*<sup>1</sup> mutant animals, each raised on standard medium (SM) or Carolina 424 medium (C424). The solid and dashed, double-headed black lines indicate the cross-comparisons performed. This allowed us to identify a total of 1038 genes that were differentially expressed between the aforementioned data sets and that demonstrated a minimum 2-fold induction or repression ( $P < 0.01$ ). While comparing *CanS* to *DHR96*<sup>1</sup> mutants data sets on any particular media refined the gene list for genes potentially regulated by *DHR96*, comparing the genome-wide profiles of the top affected genes within a single genotype raised on SM or C424, was critical to enriching the gene list for genes that specifically responded to dietary differences.

To refine the gene set so that it represents selective genes that are transcriptionally modulated by *DHR96*, I further compared the aforementioned *DHR96*-loss-of-function array dataset to that of an earlier published *DHR96*-gain-of-function array [112] (**Figure 4.2**). The latter dataset comprised 390 genes that were significantly misregulated in response to the ectopic *DHR96* expression in wild type animals raised on SM (detailed in section 4.2). This meta-analysis comparing expression patterns of the same genes between the loss- and gain-of-*DHR96* functions, revealed a highly significant overlap of 53 genes ( $P$  value,  $1.8E-12$ ) (**Figure 4.2**) that were doubly dependent on *DHR96* function, as well as, the dietary differences between C424 and SM (**Figure 4.3 A-D**, black bars).



**Genes found in overlap with roles in sterol biology:**

Gene Name	CG	controls vs: <i>hs-DHR96</i>		<i>DHR96</i> <sup>1</sup>		<i>DHR96</i> <sup>1</sup>		pr. function	human homolog
		Medium: SM	FC	p	SM	FC	p		
<i>ABCA1</i> *	CG17118	-2.5	2.0E-04	1.5	1.8E-02	1.9	1.3E-03	sterol/lipid transport	<i>ABCA1/3</i>
<i>ACAT</i> *	CG8112	-2.9	2.1E-05	1.6	4.1E-03	1.8	1.5E-03	cholesterol metabolism	<i>ACAT1/2</i>
<i>Cyp301a1</i>	CG8587	-1.7	2.4E-04	1.2	>0.05	-6.2	8.7E-04	steroid metabolism	<i>Cyp P450 family 27/24</i>
<i>hedgehog</i>	CG4637	-1.6	2.7E-05	1.4	>0.05	2.5	1.9E-03	signaling	<i>sonic hedgehog</i>
<i>NPC1b</i>	CG12092	-2.9	6.4E-04	4.1	8.2E-06	-2.1	1.0E-03	cholesterol transport	<i>NPC1L1</i>
<i>NPC2c</i>	CG3934	-6.3	1.1E-06	-2.6	9.0E-03	1.9	4.9E-02	sterol/lipid binding	<i>NPC2</i>
<i>NPC2d</i>	CG12813	-4.1	1.4E-05	-77.0	9.5E-12	-1.1	>0.05	sterol/lipid binding	<i>NPC2</i>
<i>NPC2e</i>	CG31410	-1.6	6.2E-04	4.2	1.0E-07	1.0	>0.05	sterol/lipid binding	<i>NPC2</i>

**Figure 4.2. Comparison of microarray data sets identified genes with roles in sterol biology.** Two microarray data sets were compared. The first set harbored 1,038 differentially expressed genes obtained from an analysis of either wild-type or mutant L2 larvae that were reared on C424 and standard medium (SM). The second set contained a list of 390 genes that were affected in response to ectopic expression of *DHR96* (*hs-DHR96* transgenic line). The resulting overlap (53 genes) contained ~2.5-fold more genes than one would expect, on average, when random sets of the same size are compared. This enrichment is significant, as indicated by the  $P$  value derived from a  $X^2$  calculation. The arrows indicate up- and downregulated genes. The table lists genes with known or predicted functions with links to sterol biology. An asterisk indicates that the gene name is not listed in Flybase. CG, computed gene; FC, fold change; P,  $P$  value, based on Student's  $t$ -test calculated by the LIMMA software package; pr. function, predicted function. Controls for the gain-of-function array were *w*<sup>1118</sup> larvae, whereas controls for the *low cholesterol* C424/SM array were *CanS* larvae. Figure modified from Bujold *et al*, 2010.

We validated the *low cholesterol* microarray data using qPCR and found that four genes demonstrated striking transcriptional patterns: *Npc1b*, *Npc2c*, *CG8112*, and *CG1718*.

*Npc1b*, a member of the Niemann Pick disease Type C gene family-1, is most closely related to the human *NPC1L1*, that has been implicated to mediate a crucial step in the intestinal absorption of cholesterol. As shown in **Figure 4.3**, on SM, the expression of *Npc1b* was roughly 4-fold higher in *DHR96<sup>l</sup>* mutants in comparison to wild type. A significant induction of *Npc1b* in *DHR96<sup>l</sup>* mutants may suggest that intestinal cholesterol uptake occurs at a much lower rate in *DHR96<sup>l</sup>* mutants than in wild type. We have earlier reported [54] that *DHR96<sup>l</sup>* mutants demonstrated lower whole body cholesterol levels than wild type animals when raised on the C424 medium, and conversely, exhibited higher than wild type total-cholesterol levels when raised on standard and *high cholesterol* media. The observation that changes in dietary cholesterol levels also altered circulating total cholesterol strongly suggested that *DHR96<sup>l</sup>* mutants might have no difficulty in effectively absorbing dietary cholesterol. However, given that *DHR96<sup>l</sup>* mutants accumulate cholesterol when raised on media containing relatively higher cholesterol concentrations, when wild type animals failed to do so, suggested that the cholesterol uptake process is not properly regulated in *DHR96<sup>l</sup>* mutants. It is plausible that increased *Npc1b* expression in *DHR96<sup>l</sup>* mutants could account for the observed higher cholesterol levels in *DHR96<sup>l</sup>* mutant animals raised on standard or *high cholesterol* medium (**Figure 4.3A**). However, *Npc1b* expression in *DHR96<sup>l</sup>* mutants remains unaffected to differences in sterol sources – C424 versus SM, which strongly suggested that DHR96 might directly regulate the response of *Npc1b* to dietary sterols. When we looked at the transcriptional effects of dietary differences alone, we noticed that *Npc1b* was ~4 fold induced in wild type animals raised on C424 medium relative to their expression on SM. The most likely explanation is that on C424 medium (where dietary sterols are scarce), a higher *Npc1b* expression could imply increased intestinal cholesterol absorption and trafficking (Chapter 1, **Figure 1.1**), so that cellular cholesterol balance can be restored and animals can complete normal development on this medium.

In contrast to *Npc1b*, the wild type *Npc2c* mRNA levels were drastically lower (~10 fold) on C424 medium than SM (**Figure 4.3B**), raising the possibility that under conditions of cholesterol scarcity, repressing *Npc2c* function is advantageous to conserve cellular cholesterol, suggesting that *Npc2c* is involved in trafficking and redistributing the absorbed cellular cholesterol to respective cellular destinations for utilization (**Chapter 1, Figure**

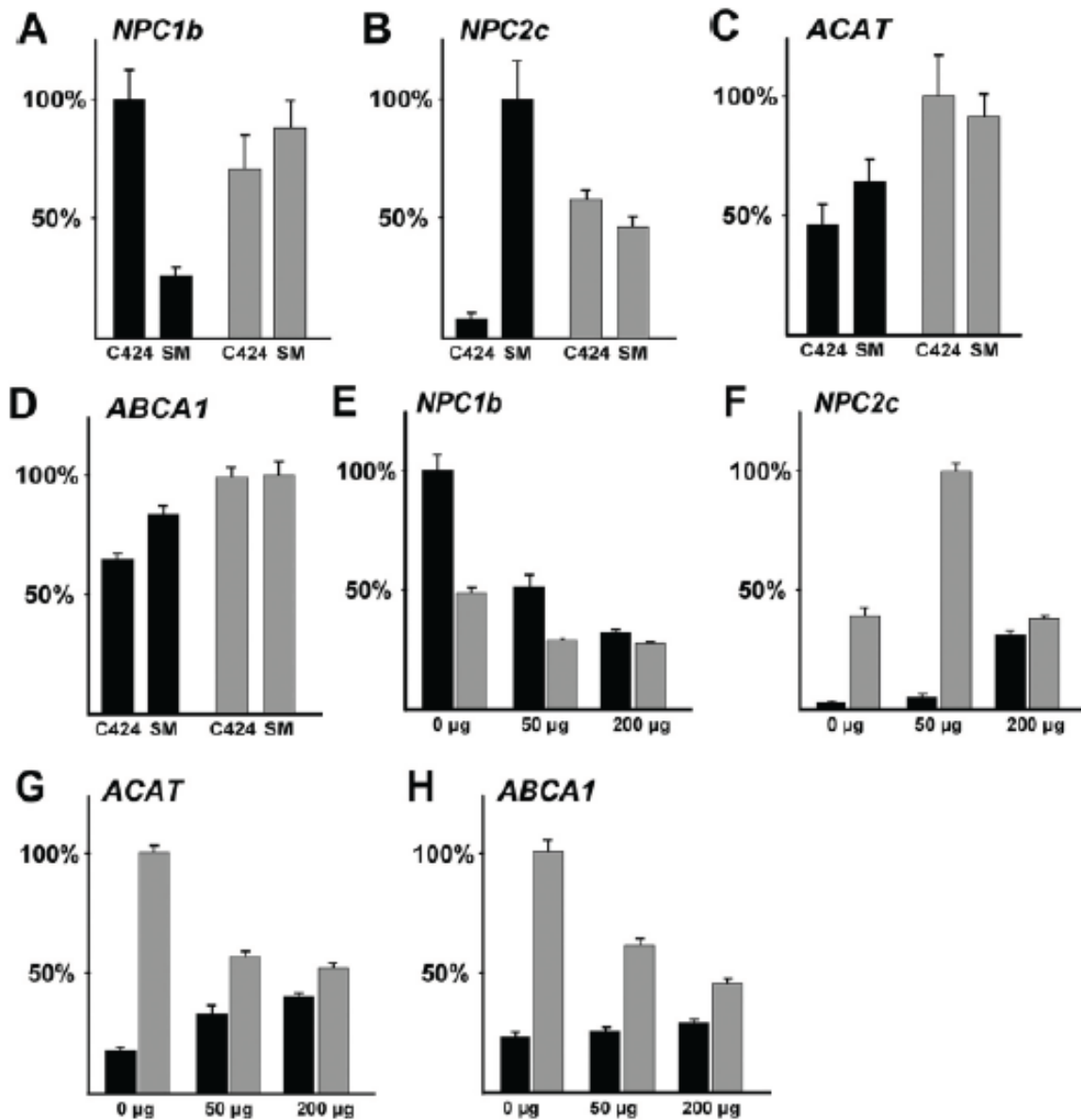
**1.1).** As such, while *Npc1b* is likely involved in dietary cholesterol uptake to promote cellular cholesterol reserves, *Npc2c* might be involved in utilizing cellular cholesterol for membranes, hormone synthesis or other uncharacterized metabolic functions. In addition, *Npc2c* levels were ~2-fold higher in wild type animals than in *DHR96<sup>l</sup>* mutants on SM (**Figure 4.3B**), which strengthened our hypothesis that when sufficient dietary sterols are absorbed, *Npc2c* function takes prominence to actively transport the absorbed cholesterol to respective cellular destinations. On the same lines, our observation that *DHR96<sup>l</sup>* mutants failed to alter *Npc2c* transcripts when reared on different media strongly suggests that DHR96 regulates *Npc2c* transcriptional response to cholesterol.

In a manner that appeared less pronounced than *Npc1b* and *Npc2c* were the expression profiles of *ACAT* and *ABCA1* that were ~1.4-fold and ~1.3-fold repressed in wild type animals when raised on C424 medium than when raised on SM (**Figure 4.3 C and D**). *Drosophila ACAT* is predicted to esterify free cellular cholesterol for storage and future utilization. Published literature [108] [149] and BLAST search revealed that CG8112 (which we refer to here as ACAT), is most closely related to mammalian *ACAT-1* and *-2* genes, which are both key cellular enzymes that are responsible for esterifying free cholesterol to protect cells from cytotoxicity. It is likely that *ACAT* levels are reduced on the low cholesterol medium to maximize the utilization and minimize the storage of diet-derived sterols, since feeding larvae are dependent on the cholesterol-derived ecdysone hormone and other metabolites for development and survival. Similarly, BLAST analysis reveals that CG1718 is most closely related to the human ABC-transporter protein ABCA3, and to a lesser degree to *ABCA1*, which are ATP-binding cholesterol transporters localized to either late endosomes or plasma membranes, respectively. While *ABCA1* is expressed ubiquitously as a key regulator of the reverse cholesterol transport, ABCA3 proteins are detected mainly in lungs, where it likely functions as a lipid pump for transporting phospholipids and cholesterol into lysosomal-like organelles called lamellar bodies [150]. It is likely that CG1718 is the single fly ortholog of both human genes, and we refer to it as *ABCA1* from here on, since our data (**Figures 4.2 and 4.3**) strongly suggest that CG1718 has a critical role in *Drosophila* to maintain cholesterol homeostasis. However, it is to note that *ABCA3* is listed as the predicted human ortholog of CG1718 in Flybase. The observation (**Figure 4.3**) that *ABCA1* is moderately ~1.3-fold repressed in wild type animals

on C424 medium presumably reflects an overall reduction in the expression of certain genes that promote efflux cellular cholesterol for utilization by tissues. This suggests that physiological conditions of acute sterol shortage, such as the C424 medium, triggers a deliberate shift in the transcriptional pattern of genes involved in conserving use of the absorbed dietary sterols for immediate critical requirements such as survival and development. Consequently, this might cause the observed repression of predicted cholesterol transporters (e.g. *Npc2c*, *ABCA1*, CG31148).

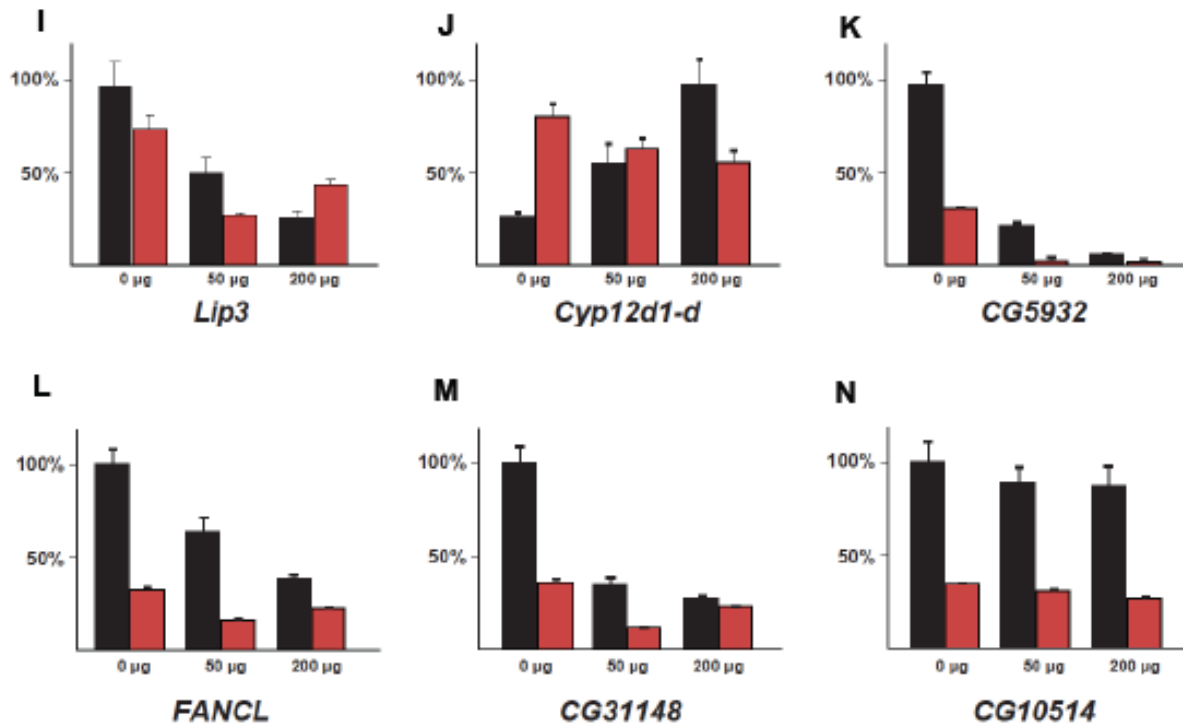
Taken together, our results suggest that the differences in sterol compositions and concentrations between C424 and SM are responsible for the transcriptional responses in genes *Npc1b*, *Npc2c*, ACAT, and *ABCA1* that are associated with different aspects of sterol homeostasis. On the other hand, the transcript levels of all 4 genes remained unaffected in a *DHR96<sup>l</sup>* mutant background, which strongly suggested that **DHR96 regulates their transcriptional response to dietary sterol differences.**

Figure 4.3 (Panels A-N)



**Figure 4.3. Dietary cholesterol regulates cholesterol metabolism genes in a concentration- and *DHR96*-dependent manner.**

(A to D) Staged L2 larvae were collected from either untreated C424 medium or a standard medium (SM). (E to H) Staged L2 larvae were collected from lipid-depleted C424 medium that was supplemented with either 0  $\mu$ g, 50  $\mu$ g, or 200  $\mu$ g cholesterol per gram (dry weight). For each gene, the highest expression level was normalized to 100%. Black bars, wild type (*CanS*); gray bars, *DHR96* mutants. The error bars indicate standard errors.



**Figure 4.3. (contd. I-N)** Staged second instar larvae were collected from lipid-depleted C424 medium that was supplemented with either 0 µg, 50 µg or 200 µg cholesterol per gram (dry weight, 1 g per vial). Total RNA was reverse-transcribed and subjected to qPCR analysis whereby every data point is based on four biological samples each tested in triplicate. For each gene, the highest expression level was normalized to 100%. Black: wild type (*CanS*), red: *DHR96* mutants. Error bars indicate standard error. *FANCL*: *Fanconi anemia complementation group L*. Figure adapted from Bujold *et al*, 2010.

#### 4.2. Cholesterol regulates gene expression in *Drosophila*

It is likely that differences between C424 medium and a standard fly medium are rather complex, and could lead to transcriptional changes in several genes involved in diverse insect metabolic pathways. Originally, we used C424 because it is a plant-based medium representing a dietary source that only contains trace amounts of plant sterols (and thus no source of cholesterol). However, the C424 medium is inherently a minimal medium compared to the SM we use for everyday fly maintenance. Therefore, C424 differs not just with respect to cholesterol, but also with presumably an entire range of nutrients from SM. Nonetheless, two lines of evidence suggest that a critical distinction between these two media is the sterol concentration and composition. One is that *DHR96*<sup>1</sup> mutants raised on

C424 medium can be fully rescued to adulthood by supplementing dietary cholesterol. Secondly, our microarray analyses have clearly shown that the wild type expression profiles of genes with known or predicted functions with links to sterol biology require *DHR96* for proper regulation. For this reason, it became crucial to identify those genes that responded in a *DHR96*-dependent manner specifically to changes only in dietary cholesterol (and not other nutrients). To create an absolute minimal medium using the C424 as base medium, I developed the lipid-depleted C424 medium (called, 'LD medium'), repeated chloroform extraction ensured complete elimination of dietary nutrients including all sterol. This represented a defined minimal medium to which dietary cholesterol or any other nutrients can be reliably supplemented in precise concentrations. By rearing larvae on this medium, we could thus characterize the transcriptional effects specific to dietary cholesterol.

To test directly which genes respond to dietary cholesterol, wild type and *DHR96<sup>l</sup>* mutant L2 larvae were reared on LD medium supplemented specifically with 0, 50 or 200  $\mu\text{g}$  of cholesterol per vial (which corresponded to 0%, 0.00083%, and 0.0033% cholesterol (wet weight), respectively). The above concentrations were chosen for the following reasons: the 0  $\mu\text{g}$  represented an absolute minimal medium where nearly ~85% wild type populations completed normal development, while *DHR96<sup>l</sup>* mutants arrested as L2. Supplementing 50  $\mu\text{g}$  cholesterol to LD medium was sufficient to produce distinct transcriptional effects in wild type (**Figure 4.3. E-H**), but was insufficient to rescue *DHR96<sup>l</sup>* mutants. On the other hand, 200  $\mu\text{g}$  represented an optimal medium that was both sufficient to support the development of *DHR96<sup>l</sup>* mutants on par with wild type animals, suggesting that this concentration may be suitable to investigate the transcriptional patterns of genes with predicted roles in cholesterol metabolism.

From the 53 genes that overlapped between the *low cholesterol* array and the *DHR96*-overexpression array (shown in **Figure 4.2**), a subset of 34 genes were found to be implicated in lipid and cholesterol metabolism pathways based on published literature and gene ontology files. Since these genes displayed distinct expression changes that overlapped (*P* value, 1.8E-12) between: (i) dietary differences between C424 and SM types, (ii) a loss of *DHR96* function, and (iii) *DHR96* gain-of-function, I expected this gene set to be highly enriched for genes that were doubly dependent on *DHR96* and the dietary sterol composition. Using a microfluidics-based qPCR method, the expression patterns of these 34

genes were analyzed (by M. Bujold) in response to a gradient of increasing dietary cholesterol concentrations. This provided a method to identify genes that responded specifically to dietary cholesterol and test if their responses were dependent on *DHR96* function. The complete list of the 34 selected genes and their predicted functions are summarized in Table 4.3. Strikingly, among the 34 genes tested, the same four genes, *ACAT*, *ABCA1*, *Npc2c*, and *Npc1b* responded to changes in dietary cholesterol concentrations (**Figure 4.3E to H**).

In wild type animals, *Npc1b* mRNA levels were ~3-fold repressed by increasing dietary cholesterol from 0  $\mu\text{g}$  to 200  $\mu\text{g}$ , similar to the trend (i.e. repression) observed on SM versus C424 (**Figure 4.3A**), which supported the hypothesis that *Npc1b* promotes cellular cholesterol levels under low cholesterol conditions and that beyond a certain threshold of cellular cholesterol, a homeostatic control regulates *Npc1b* to protect cells from excess cholesterol uptake. *Npc1b* levels in *DHR96*<sup>l</sup> mutants were however 50% lower than in controls (**Figure 4.3E**), likely because mutants fail to sense the sterol paucity in the absence of *DHR96* and thus fail to induce *Npc1b*. In contrast, *Npc2c* and *ACAT* transcripts were incrementally induced with increasing dietary cholesterol levels, which fully recapitulated our observations on the sterol-rich SM relative to C424 (**Figure 4.3B-C**), suggesting that these genes had vital roles in controlling cellular cholesterol balance, likely by means of transporting intracellular cholesterol for tissue-specific cholesterol utilization. Although *ABCA1* failed to be induced under increasing cholesterol levels on LD, *DHR96*<sup>l</sup> mutants displayed ~4-fold higher *ABCA1* transcripts than wild type on un-supplemented LD medium, which is more pronounced than the ~1.6-fold induction on C424 (**Figure 4.3D**). Subsequently, this induction in *ABCA1* transcripts was lost in *DHR96*<sup>l</sup> mutants at higher cholesterol levels, which is in contrast to **Figure 4.3D** where a change from C424 to SM had no difference on *ABCA1* transcripts in *DHR96*<sup>l</sup> mutants. This could mean that loss of *DHR96* relieves the regulatory control *ABCA1*, which supports our observation that wild type raised on SM or *DHR96*<sup>l</sup> mutants raised on either media types consistently displayed high *ABCA1* expression. Alternatively, since wild type *ABCA1* transcripts were induced on SM, but not on LD supplemented with 200  $\mu\text{g}$  cholesterol, it is likely that *ABCA1* responds to higher range of sterol or sterol metabolites that could have been outside these tested concentrations.

In addition, the following lipid metabolism genes were repressed by cholesterol (**Figure 4.3 I-N**). *Lip3* encodes a predicted cholesterol ester hydrolase. CG5932, which encodes a gastric lipase has been demonstrated to be directly regulated by DHR96 [151]. Both *Lip3* and CG5932 function to increase cellular cholesterol by breakdown of stored lipids and cholesteryl esters. Hence a concomitant repression in wild type *Lip3* and CG5932 with increasing cholesterol levels is suggestive of homeostatic regulatory mechanism to protect from excess of cellular cholesterol. CG31148, encodes a lysosomal acid  $\beta$ -glucocerebrosidase (GCCase) with predicted roles in sphingolipid metabolism. This *Drosophila* homolog is ~49% similar to the human GCCase gene, mutations in which cause the neurodegenerative Gaucher's disease that is characterized by an aberrant accumulation of glucosylceramide [152]. Recently, intracellular cholesterol levels have been reported to modify glucocerebrosidase activity [153], which can partly explain the observed repression, although we do not know the functional significance of this repression in *Drosophila*. *FANCL* (*Fanconi anemia, complementation group L*) encodes a predicted ubiquitin E3 ligase [115], [154], whose function in regulating cholesterol homeostasis in *Drosophila* is still unknown. *Cyp12d1*, a mitochondrial cytochrome P450 gene is induced by cholesterol supplementation (**Figure 4.3J**). Given that it is closely related to *Cyp301a1* that is predicted to function in 20E biosynthesis pathway, it is likely that *Cyp12d1* induction is involved in metabolizing cellular cholesterol for a related hormonal function. In contrast, CG10514, a gene encoding a DUF227 domain (domain of unknown function 277), was not significantly affected by changes in the medium but demonstrated consistently lower levels of expression in *DHR96*<sup>1</sup> mutants regardless of the dietary sterol content, reflecting a *DHR96*-dependent regulation.

Taken together, these results indicated that cholesterol modulates the expression of key cholesterol metabolism genes: *Npc1b*, *Npc2c*, ACAT, and *ABCA1*, and that DHR96 is necessary to mediate these observed responses to cholesterol.

### **4.3. High cholesterol medium phenocopies the transcriptional response to *DHR96* mutation**

Genes with putative functions in known vertebrate cholesterol metabolic pathways thus appear to respond to a range of dietary cholesterol concentrations via distinct

transcriptional patterns. Based on the nature of those predicted cellular functions, I hypothesized that a class of genes that responded exclusively to a certain range of dietary cholesterol might fail to demonstrate that transcriptional response at a cholesterol concentration outside of that range. Therefore, as a converse strategy to our earlier analysis of transcriptional responses on diets containing either no cholesterol (i.e. lipid-depleted LD medium) or trace amounts of plant sterols (C424 medium), M. Bujold reared wild type (*CanS*) and *DHR96<sup>1</sup>* mutant animals on: SM (SM), and SM supplemented with 1% wet weight cholesterol; which we refer to as the *high cholesterol* diet, and measured the gene expression changes using high throughput qPCR. This allowed us to: (i) to identify the transcriptional effects of feeding a *high cholesterol* medium to wild type animals, and (ii) to determine if *DHR96* is necessary to mediate the observed transcriptional responses to the *high cholesterol* diet.

**Choice of *high cholesterol* concentration:** Feeding larvae with cholesterol at concentrations considerably higher than normal physiological needs is likely to trigger pronounced changes in the expression of genes involved in sequestering, transporting and metabolizing cholesterol, which can aid in gene discovery. Works by others [155]–[157] have supplemented standard cornmeal-agar media with cholesterol concentrations ranging from 0.2 mg/mL – 1 mg/mL to perform various phenotypic rescue studies. The 1% *high cholesterol* medium contains 10 mg of cholesterol per mL of SM. I have also tested a range of *high cholesterol* concentrations for potential toxicity. Specifically, I followed the development of wild type and *DHR96<sup>1</sup>* mutant embryos to adulthood on SM containing 0%, 0.5%, 1%, or 5% w/w cholesterol. While the 5% concentration greatly reduced the survival of both wild type and *DHR96<sup>1</sup>* mutants by ~90%, I observed no adverse effects on the survival or developmental timing of wild type or *DHR96<sup>1</sup>* mutants in the 1% and 0.5% (w/w) cholesterol diets. In contrast, supplementing the SM with an equivalent 1% wet weight of the fatty acids: oleic acid or linoleic acid failed to support development. Hence, we used the 1% (w/w) cholesterol added to SM to represent the *high cholesterol* diet.

M. Bujold conducted microarray analysis (Affymetrix2) on mid-wandering L3 samples collected from wild type and *DHR96<sup>1</sup>* mutants that were raised throughout development on SM, or on SM to which cholesterol had been added to 1% wet weight. We filtered the four data sets: wild type±1% cholesterol and *DHR96<sup>1</sup>* mutants ±1% cholesterol

for significant fold changes differences ( $\geq 2$  for upregulated genes and  $\leq 2$  for downregulated genes,  $P < 0.01$ ). By this filtering, we found that in the wild type, 73 genes were induced by *high cholesterol* and that 55 genes were repressed by *high cholesterol* (Tables 4.1 and 4.2). **We observed a unique correlation between the transcriptional effects of a *high cholesterol* medium to the consequences of the *DHR96* mutation alone (Chapter 1, Figure 1.9).** Strikingly, 53 out of the 55 genes repressed by *high cholesterol* in the wild type, displayed corresponding lower levels of expression in *DHR96*<sup>l</sup> mutants that were raised on SM without any added cholesterol. Similarly, 72 of the 73 genes in wild type that were induced by *high cholesterol* were likewise induced in *DHR96*<sup>l</sup> mutants in spite of being reared on SM with out any added cholesterol. Comparing the top 102 genes that were significantly upregulated in the *DHR96*<sup>l</sup> mutants to the set of the 73 cholesterol-induced genes in the wild type, revealed 13 overlapping genes, which is nearly 33 times higher than expected by random chance alone ( $P = 6.9E-90$ ) (Figure 4.4). Similarly, a comparison between the 43 genes that are downregulated in *DHR96*<sup>l</sup> mutants to the 55 genes that were repressed by *high cholesterol* ( $P < 10E-999$ ) revealed an interesting overlap of 22 genes (Figure 4.4). These data suggested that administrating high dietary cholesterol phenocopies many of the transcriptional effects caused by a loss of *DHR96* function. Even more notable was our finding that the fold change values were similar in magnitude and direction under both conditions: i.e., feeding *high cholesterol* to wild type and feeding SM to *DHR96*<sup>l</sup> mutants. The genes that were significantly affected in response to *high cholesterol* and *DHR96*<sup>l</sup> mutation are summarized in Tables 4.1-4.4.

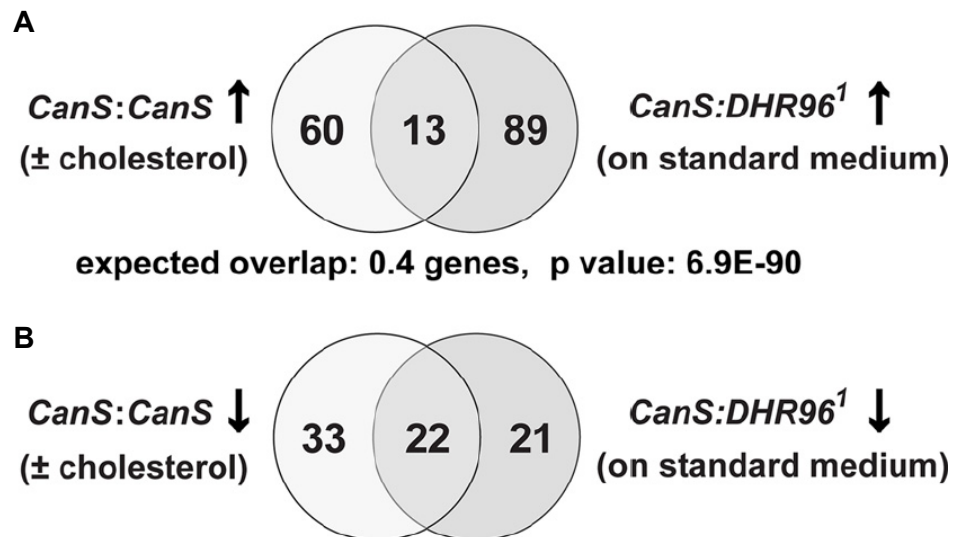


**Figure 4.4. A high-cholesterol diet phenocopies the transcriptional response caused by the *DHR96<sup>1</sup>* mutation.** (A) Comparison of microarray data sets representing 73 genes upregulated in response to high cholesterol (left circle) or 102 upregulated due to a mutation in the *DHR96* gene (right circle). The *P* value indicates the significance of the overlap, based on a  $\chi^2$  test. (B) Analysis similar to that in panel A; however, here the data sets comprise 55 genes downregulated in response to high cholesterol (left circle) and 43 genes downregulated in *DHR96<sup>1</sup>* mutants that were maintained on standard medium. Average expected overlaps and *P* values based on  $\chi^2$  calculations are indicated. Microarray analyses were done by Kirst King-Jones.

**Table 4.1. 55 Genes downregulated by 1% cholesterol in wild type.** This table summarizes genes downregulated in wild type (*CanS*) when treated with 1% dietary cholesterol using Affymetrix *Drosophila* 2.0 microarrays. Data was analyzed with gcrma and limma by Kirst King-Jones. Included are fold changes for *CanS* (1%) vs. *CanS* (0%) as well as *DHR96* (0%) vs. *CanS* (0%). Selection criteria for this list are a p value <0.01 and a fold change < -1.5. Genes are ranked by fold change in the column representing the response to cholesterol in wild type, with the most strongly downregulated gene in row 1.

row	probe set	Gene Symbol	FC CanS +/- 1% C	p-value	FC DHR96 vs CanS	p-value
1	1633050_at	CG12813 (NPC2d)	-556.05	3.54E-08	-233.32	1.18E-07
2	1631446_at	Chf9	-43.04	3.74E-07	-27.14	1.07E-06
3	1631558_at	Cpr65Ax2	-13.04	4.18E-03	-3.61	8.56E-02
4	1636402_at	CG10081	-11.79	8.87E-03	-20.63	2.87E-03
5	1636583_at	CG5932	-10.80	7.81E-03	-5.04	4.44E-02
6	1641622_at	Lcp65Ae	-10.09	9.60E-03	-3.75	9.09E-02
7	1634815_at	CG31104	-6.98	9.71E-03	-7.35	8.50E-03
8	1641136_at	Cpr78Cc	-6.40	4.76E-03	-4.92	1.07E-02
9	1636387_at	CG10300	-4.65	4.31E-05	-8.59	3.29E-06
10	1625235_at	CG13325	-4.60	3.05E-03	-4.60	3.05E-03
11	1635467_a_at	CG7381	-4.44	3.92E-04	2.14	1.91E-02
12	1638132_at	CG10184	-3.58	1.58E-03	-2.04	3.16E-02
13	1639268_at	CG13324	-3.18	6.43E-03	5.21	7.64E-04
14	1638182_at	CG5999	-3.07	6.78E-04	-3.32	4.29E-04
15	1638903_at	CG5724	-3.04	5.53E-07	-2.88	8.17E-07
16	1631072_at	CG9512	-2.89	4.56E-04	-1.61	3.59E-02
17	1640065_at	GstE7	-2.85	4.03E-05	-1.76	2.66E-03
18	1622946_at	CG6908	-2.70	8.65E-04	-1.49	7.42E-02
19	1633492_at	hgo	-2.55	6.80E-03	-1.50	1.57E-01
20	1625042_at	CG31288	-2.52	7.40E-03	-2.54	7.09E-03
21	1637319_at	FancI	-2.49	3.41E-06	-6.43	1.07E-08
22	1623769_at	CG7322	-2.45	4.56E-03	-1.50	1.19E-01
23	1628474_at	CG16712	-2.39	7.10E-03	-1.55	1.11E-01
24	1634697_at	CG32667	-2.32	6.81E-03	-1.85	3.00E-02
25	1627180_at	Cyp4d14	-2.31	1.03E-03	-1.21	2.97E-01
26	1634152_at	GstD5	-2.29	7.21E-03	-1.36	2.22E-01
27	1628657_at	GstE9	-2.26	6.29E-03	-1.95	1.74E-02
28	1627869_at	Jon25Bi	-2.19	5.19E-03	-2.77	1.09E-03
29	1633684_at	CG32444	-2.17	1.31E-05	-1.79	1.12E-04
30	1633471_at	Prx2540-2	-2.14	2.79E-03	-1.22	3.01E-01
31	1623840_at	CG18607	-2.11	7.03E-03	-1.34	1.99E-01
32	1630212_at	CG2065	-2.08	8.40E-03	-2.04	9.47E-03
33	1638246_at	CG5804	-2.04	6.72E-03	-1.33	1.85E-01
34	1630109_at	Hsc70-4	-1.86	3.94E-03	-1.04	8.26E-01
35	1641052_at	Jon66Ci	-1.77	8.89E-03	-1.42	7.16E-02
36	1629853_at	CG3699	-1.77	8.86E-04	-1.42	1.33E-02
37	1638038_at	CG4335	-1.76	9.42E-04	-1.67	1.71E-03
38	1633503_at	CG12171	-1.76	6.94E-03	-1.68	1.03E-02
39	1640466_s_at	CG6543	-1.74	3.13E-03	-1.96	9.83E-04
40	1625265_at	CG9119	-1.71	2.30E-03	-1.37	3.31E-02
41	1629009_at	Cyp28a5	-1.71	1.63E-04	-2.08	1.61E-05
42	1635800_at	CG5431	-1.69	6.47E-04	-1.69	6.83E-04
43	1630624_s_at	CG10151	-1.69	2.65E-03	-1.93	6.29E-04
44	1630505_a_at	Cyp311a1	-1.65	8.42E-03	-1.65	8.39E-03
45	1626664_at	CG3285	-1.64	4.12E-03	-1.13	3.58E-01
46	1631533_at	Cyp6a22	-1.64	6.93E-03	-1.24	1.63E-01
47	1630429_s_at	CG11889	-1.62	8.17E-04	-1.01	9.28E-01
48	1630802_at	Cyp6d4	-1.60	3.33E-03	-1.97	3.20E-04
49	1627854_at	CG9914	-1.58	5.80E-04	-1.54	8.77E-04
50	1626248_at	CG18547	-1.53	7.69E-03	-1.19	1.89E-01
51	1639553_at	CG9987	-1.53	4.54E-03	-1.14	2.75E-01
52	1641650_at	alpha-Est5	-1.53	1.09E-03	-1.18	9.39E-02
53	1633036_s_at	CG32495	-1.51	6.50E-03	-1.31	4.42E-02
54	1632342_a_at	CG33080	-1.51	2.82E-03	-1.41	7.82E-03
55	1624185_at	CG1041	-1.50	7.66E-03	-1.26	8.17E-02

**Table 4.2. 73 Genes upregulated by 1% cholesterol in wild type.** This table summarizes genes upregulated in wild type (*CanS*) when treated with 1% dietary cholesterol using Affymetrix *Drosophila* 2.0 microarrays. Data was analyzed with gcrma and limma by Kirst King-Jones. Included are fold changes for *CanS* (1%) vs. *CanS* (0%) as well as *DHR96* (0%) vs. *CanS* (0%). Selection criteria for this list are a p value <0.01 and a fold change >1.5. Genes are ranked by fold change in the column representing the response to cholesterol in wild type, with the highest value at position 1.

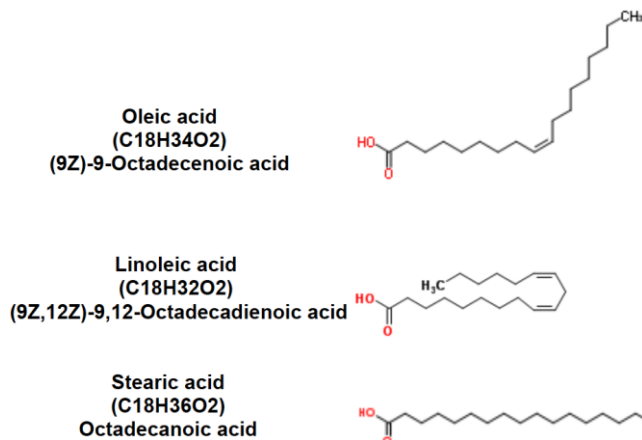
row	probe set	Gene Symbol	FC <i>CanS</i> +/- 1% C	p-value	FC <i>DHR96</i> vs <i>CanS</i>	p-value
1	1623732_at	CG31410 (NPC2e)	11.59	1.21E-07	21.82	1.85E-08
2	1627895_at	CG18404	5.63	5.62E-03	12.96	5.05E-04
3	1627236_e_at	—	4.50	6.11E-04	1.18	5.67E-01
4	1629559_e_at	Atet	4.03	1.33E-06	3.12	6.56E-06
5	1634075_at	dp	3.65	8.14E-03	1.65	2.20E-01
6	1636132_at	—	3.35	3.41E-03	1.16	6.42E-01
7	1637253_e_at	CG17570	3.03	7.68E-03	1.90	7.75E-02
8	1635766_at	Fs(2)Ket	2.83	7.53E-04	1.29	2.45E-01
9	1626028_at	CG4783	2.71	2.70E-03	4.89	1.26E-04
10	1632177_at	hth	2.51	9.85E-04	1.36	1.34E-01
11	1631621_e_at	esh	2.47	4.53E-03	2.08	1.36E-02
12	1634980_e_at	CG18490	2.37	5.35E-03	1.58	8.39E-02
13	1635909_at	cic	2.37	9.61E-04	1.27	2.03E-01
14	1623605_a_at	cbt	2.35	4.25E-03	1.78	2.94E-02
15	1633512_at	toy	2.35	4.40E-03	1.37	1.92E-01
16	1639306_e_at	CG17090	2.24	9.37E-04	1.59	2.03E-02
17	1639785_e_at	dpld	2.23	1.81E-03	1.41	9.16E-02
18	1628489_at	dally	2.19	6.98E-03	1.46	1.23E-01
19	1624067_at	CG6704	2.15	5.52E-03	1.02	9.15E-01
20	1638568_s_at	H	2.10	2.16E-04	1.22	1.37E-01
21	1627446_at	net	2.08	1.50E-05	2.21	8.11E-06
22	1637144_a_at	Map205	2.06	6.31E-05	1.47	4.06E-03
23	1625471_e_at	CG4928	2.01	9.22E-03	1.31	2.33E-01
24	1629944_at	CG12814	2.00	8.53E-03	1.30	2.35E-01
25	1633801_s_at	CG9171	2.00	1.06E-03	1.52	1.73E-02
26	1631303_e_at	NK7.1	1.98	1.07E-03	1.68	5.64E-03
27	1627101_at	scyl	1.95	7.92E-05	1.74	3.04E-04
28	1638432_a_at	CG10082	1.94	1.24E-03	1.41	3.68E-02
29	1631280_at	CG9095	1.90	7.03E-03	1.64	2.43E-02
30	1624839_at	h	1.89	5.42E-04	1.48	9.69E-03
31	1627784_at	—	1.89	5.22E-03	1.54	3.37E-02
32	1633794_a_at	Pino	1.89	6.20E-03	2.11	2.47E-03
33	1639330_e_at	Tao-1	1.88	3.95E-03	1.14	4.39E-01
34	1628435_at	—	1.84	2.04E-03	1.46	2.45E-02
35	1641685_at	Edc3	1.81	3.66E-04	1.59	1.80E-03
36	1631534_at	sfl	1.81	8.16E-05	1.52	9.63E-04
37	1634573_a_at	—	1.80	3.51E-03	1.29	1.22E-01
38	1626899_at	GATAd	1.79	6.34E-03	1.21	2.62E-01
39	1640457_e_at	Bsg	1.78	4.93E-04	1.20	1.13E-01
40	1639414_at	Snoo	1.76	9.91E-03	1.56	2.94E-02
41	1624059_at	CG32223	1.75	8.38E-03	1.21	2.67E-01
42	1624021_a_at	dlg1	1.72	6.60E-04	1.14	2.47E-01
43	1634579_at	CG4747	1.70	2.93E-03	1.27	9.44E-02
44	1623812_at	CG10943	1.68	6.47E-03	2.46	2.10E-04
45	1628729_at	—	1.68	9.79E-03	1.24	2.06E-01
46	1634146_at	CG42258	1.68	7.94E-03	1.33	9.03E-02
47	1629479_a_at	fok	1.67	9.60E-03	1.30	1.21E-01
48	1640280_at	lola	1.66	5.20E-03	1.31	8.26E-02
49	1624321_at	Rac2	1.66	8.79E-03	1.49	2.65E-02
50	1624780_at	DereCG2995	1.66	6.06E-03	1.49	2.03E-02
51	1634771_a_at	CG8184	1.64	3.46E-03	1.30	6.76E-02
52	1629396_e_at	CG8486	1.64	2.17E-03	1.21	1.34E-01
53	1640817_at	zornin	1.63	7.61E-03	1.53	1.57E-02
54	1625594_e_at	Pka-R2	1.63	1.28E-03	1.33	2.41E-02
55	1633253_s_at	CG2991	1.63	6.67E-04	1.30	2.05E-02
56	1630396_at	CG4360	1.63	6.76E-04	1.16	1.41E-01
57	1627191_a_at	ena	1.62	2.48E-03	1.29	5.56E-02
58	1628778_at	itp	1.62	7.98E-04	1.32	1.78E-02
59	1634509_e_at	fwd	1.61	3.05E-03	1.11	4.12E-01
60	1636363_s_at	Mapmodulin	1.61	2.74E-03	-1.08	5.11E-01
61	1631321_s_at	His1:CG31617	1.59	6.41E-03	1.03	8.20E-01
62	1638741_at	—	1.59	7.78E-03	1.28	1.03E-01
63	1637487_at	Dcp-1	1.58	3.07E-04	1.96	1.80E-05
64	1640547_at	mew	1.57	3.68E-04	1.28	1.30E-02
65	1626766_s_at	daw	1.56	1.07E-04	1.32	2.32E-03
66	1628784_at	CG16817	1.56	1.90E-03	1.03	8.04E-01
67	1639054_e_at	—	1.54	8.51E-03	1.47	1.48E-02
68	1641104_e_at	Eaat1	1.53	5.67E-03	1.20	1.44E-01
69	1633443_e_at	CG2082	1.53	3.50E-03	1.26	5.92E-02
70	1631524_a_at	hth	1.51	1.46E-04	1.50	1.63E-04
71	1636099_e_at	mb1	1.51	4.28E-03	1.37	1.70E-02
72	1639064_e_at	Akt1	1.51	2.80E-03	1.29	3.07E-02
73	1632485_a_at	Nak	1.51	1.47E-03	1.29	1.80E-02

**Table 4.3. Summary of genes used for microfluidic qPCR and the effects of dietary lipids on their expression profiles.** I selected these genes based on loss- and gain-of function *DHR96* microarray studies, predicted gene functions as well as published work. The table summarizes the molecular functions and expression profiles of affected genes in wild type animals (*CanS*) and *DHR96*<sup>1</sup> mutants reared on standard cornmeal medium containing 1% (wet weight) of three different fats: cholesterol (C), canola oil (CA) or tristearin (TS). The gene expression values represent fold changes based on data generated with the Biomark Fluidigm arrays. The arrows denote up- or downregulation higher or lower than 1.5-fold. \*\* name not official yet – only used in this publication. *Atet*: ABC transporter expressed in trachea, *ABCG4*: ATP-binding cassette sub-family G member 4, *ABCA1*: ATP-binding cassette sub-family C member 1, *NPC1*: Niemann Pick type C-1, *NPC2*: Niemann-Pick type C-2, *VLDL*: very low density lipoprotein receptor, *ACAT*: Acyl coenzyme A:cholesterol acyltransferase, *CERKL*: Ceramide Kinase-like, *GPAT*: Glutamine phosphoribosylpyrophosphate amidotransferase, *TTPA*: Tocopherol Transfer Protein Alpha, *FANCL*: Fanconi anemia-complementation group L, *RNAPII*: RNA Polymerase II). Note: *ABCA1* was tested separately on a 96-well qPCR instrument (StepOnePlus, ABI) using SYBR Green as a fluorescent dye.

Gene ID	Molecular Function/Activity	Human Homolog	WT ( <i>CanS</i> )			<i>DHR96</i> <sup>1</sup>		
			C	CA	TS	C	CA	TS
<i>Atet</i>	ATPase Coupled Transport	ABCG4	↑					
<i>ABCA1</i> **	ATPase Coupled Transport	ABCA1/ABCA3	↑					
CG1819	ATPase Coupled Transport	ABCA12	↑		↓			↑
CG11781	Membrane Transport	Transmembrane Protein 93						
<i>NPC1b</i>	Intestinal Cholesterol absorption/transport	<i>NPC1L1</i>	↑		↓	↑		
<i>NPC2a</i>	Sterol Transport	<i>NPC2</i>				↓	↑	↑
<i>NPC2d</i>	Sterol Transport	<i>NPC2</i>	↓					
<i>NPC2e</i>	Sterol Transport	<i>NPC2</i>	↑	↑				
<i>NPC2g</i>	Sterol Transport	<i>NPC2</i>	↓	↓				
<i>NPC2h</i>	Sterol Transport	<i>NPC2</i>	↓	↑	↑			
<i>peste</i>	Fatty Acid Transport	Scavenger Receptor Class B, member 2	↑	↓	↓	↑		
<i>LPR1</i>	Lipid (Lipoprotein) Transport	VLDL-b	↑	↑	↑			
<i>LPR2</i>	Lipid (Lipoprotein) Transport	VLDL-a						
<i>ACAT</i> **	Sterol O-Acyltransferase	<i>ACAT1/2</i>					↑	
CG5932	Triacylglycerol Lipase	Gastric Lipase A (LIPA)	↓		↓	↓	↑	
<i>brummer</i>	Triacylglycerol Lipase	Patatin-Like Phospholipase Domain						
<i>Lip3</i>	Cholesteryl ester hydrolase	Acid Lipase	↓				↑	
CG31148	Glucosylceramidase, Sphingolipid metabolism	Beta-Glucocebrosidease		↑		↑	↑	↑
CG15533	Sphingomyelin Phosphodiesterase	Sphingomyelin Phosphodiesterase 1	↑		↓	↑		
<i>egghead</i>	Sphingolipid metabolism	-						
CG10514	Choline Kinases	-						
CG16708	Ceramide Kinase, Sphingolipid metabolism	<i>CERKL</i>	↓	↑	↑	↓	↑	↑
<i>Prat2</i>	Amidophosphoribosyl Transferase	<i>GPAT</i>	↓		↑			
<i>FANCL</i>	E3 Ubiquitin Ligase	<i>FANCL</i>						
CG2065	Short-Chain Dehydrogenases	3-Hydroxyacyl-CoA Dehydrogenase II	↓	↓				
<i>Cyp12d1</i>	Detoxification, Steroid metabolism	Cytochrome P450, 27A1		↑	↑			
<i>TotC</i>	Stress Response	-	↑	↑	↑			
CG10300	Carrier Vitamin E Binding	<i>TTPA</i>	↓	↑		↑		
<i>DHR96</i>	Transcriptional regulation, Xenobiotic response	VITAMIN D Receptor (VDR)	↓	↓	↓	n/a	n/a	n/a
<i>Net</i>	Transcriptional regulation	Neurogenic Differentiation 1						
CG4783	Insect development?	-	↑	↑	↑			
<i>Thor</i>	Translational regulation (developmental events)	eIF4e-Binding Protein 2				↓		
<i>Brat</i>	Translation repressor activity	-						
<i>Nubbin</i>	Transcriptional regulation	POU Class 2 Homeobox 1						
<i>Mmp1</i>	Metallo-endopeptidase	Matrix Metallopeptidase 1						↓
<i>Nol</i>	Larval neurogenesis (Secreted glycoprotein?)	-	↓	↓				

To validate the *high cholesterol microarray* data and importantly, to distinguish transcriptional responses that were specific to administering dietary cholesterol, I employed microfluidics-based qPCR technique (Fluidigm), which allowed for simultaneous analyses each sample for the expression of 37 genes (excluding controls). Since a high overlap of differentially expressed genes were identified between the transcriptional effects of *high cholesterol* and *DHR96<sup>l</sup>* mutation, I selected the 34 genes based on their significance, fold change values within these overlap, predicted functions in published literature, and gene ontology files (**Table 4.3**).

To identify cholesterol-specific transcriptional responses, I reared wild type and *DHR96<sup>l</sup>* mutant embryos on SM supplemented with or without 1% wet weight of the following lipids: (a) cholesterol, (b) canola oil; or (c) tristearin. Canola oil is a mixture of triglycerides and fatty acids such as oleic and linoleic acid, and being plant-based is likely to



contain trace amounts of plant sterols [158], while tristearin is a triglyceride of stearic acid that has been reported to cause no toxicity in *Drosophila* [159]. Since plant sterols or fatty acids such as oleic acid and stearic acid cannot be converted to cholesterol in *Drosophila*, these dietary lipids served as ideal controls to test for the transcriptional effects of a non-sterol fat. RNA samples were isolated from staged wandering L3 larvae.

The top-affected genes are shown in **Figure 4.5 (A-L)**. *Npc2d* was the most strongly repressed (~100 fold down), while *Npc2e* was the most strongly induced gene (~40 fold up) specifically in response to cholesterol, but not by canola oil or tristearin. This suggested that *Npc2d* and *Npc2e* are regulated by cholesterol, likely to perform opposing functions in cellular sterol transport. *LpRI* (LDL-receptor-related protein), which encodes a homolog of the low-density lipoprotein receptor protein family, is ~2.5-fold upregulated by cholesterol and ~5-fold induced by canola oil and tristearin, suggesting that this gene responds to a wide range of lipids. *Atet* (ABC transporter expressed in trachea), a putative ATP-binding cassette containing cholesterol transporter, is ~2-fold induced in response to cholesterol, canola oil

and tristearin. In a similar fashion, albeit to a lesser degree, *egh* (egghead) which encodes a  $\beta$ -1,4-mannosyltransferase with a putative function in glycosphingolipid biosynthesis, is  $\sim$ 1.5-fold induced in response to all three fats. These expression patterns suggested that *LpR1*, *Atet* and *egh* are transcriptionally regulated lipid genes, with no apparent specificity to cholesterol. On the other hand, *Cyp12d-1*, which encodes a homolog of the cytochrome P450-dependent monooxygenase enzymes, has predicted functions in insecticide resistance [96][160], and is  $\sim$ 2.5-fold induced in the wild type, specifically in response to cholesterol, but not to canola oil or tristearin (Figure 4.6E). The transcriptional pattern of *CG5932* (*Magro*) a midgut-specific gastric triacylglyceride lipase, is strongly repressed  $\sim$ 10-fold in the wild type, in a specific response to cholesterol, revealing a novel function for this lipase in cholesterol homeostasis, which is in contrast to its known historical function in triglyceride metabolism [151]. Later work by Seiber *et al.*, suggested that *CG5932* is a direct target of DHR96. Surprisingly, three genes with predicted roles in sphingolipid metabolism (**Figures H, I & J**), namely *CG31148*, which encodes a putative glucosylceramidase activity, *CG15533*, predicted to code for a sphingomyelin phosphodiesterase and *CG16708*, a encoding a predicted D-erythrosphingosine kinase, are misregulated in *DHR96<sup>l</sup>* mutants, irrespective of the dietary sterol supplemented. This indicates that DHR96 may exert transcriptional control of sphingolipid metabolism, much like its vertebrate ortholog LXR $\alpha$ . Similar to sterols, sphingolipids play important roles in plasma membranes and cell signaling, and both lipid classes are enriched within membrane signaling microdomains called lipid rafts. Moreover, similar to cholesterol, sphingolipids also accumulate within cells in patients affected by the Niemann-Pick type C disease. Thus, it is likely that a homeostatic control of both sphingolipids and cholesterol might occur via shared pathways.

In contrast to the induction of gene expression, some genes (**Figures 4.5 K & L**) displayed a significant repression in response to high cholesterol. *CG10300*, a predicted retinaldehyde-binding protein with putative roles in cellular alpha-tocopherol transport, is  $\sim$ 2-fold repressed specifically in response to cholesterol, but not to canola oil or tristearin. On the other hand, *FANCL*, a predicted ubiquitin E3 ligase is consistently and strongly repressed  $\sim$ 4-fold in response to cholesterol, but failed to be repressed in response to canola oil or tristearin. In humans, defects in *FANCL* are a cause of Fanconi anemia (FA), an

autosomal recessive disorder characterized by a cellular defect in DNA repair causing progressive bone marrow failure and increased cancer susceptibility [161]. This is the first report of a Fanconi ubiquitin ligase to be misregulated in a nuclear receptor mutant. Not much is known currently how *FANCL* expression and physiological pathways are regulated. Based on the observations that FA complex is implied in DNA repair perhaps via SWI/SNF chromatin remodeling complex, it is likely that *FANCL* might also be involved with DHR96 to gain access to target genes to enable nuclear functions such as transcription and DNA repair. Future work on Fanconi Anemia complex is needed to understand the observed repression of *FANCL* in response to cholesterol.

It is important to note that the expression of all of the 12 aforementioned genes **remained unchanged in *DHR96*<sup>1</sup> mutants irrespective of cholesterol supplementation**, strongly suggesting that their response to dietary cholesterol is directly or indirectly regulated via DHR96.

The expression patterns of the remaining 23 (of the total 34) genes, tested in wild type and *DHR96*<sup>1</sup> mutants, in response to feeding with dietary cholesterol, canola oil or tristearin are shown in **Figure 4.6 (A-W)**. Genes such as *ACAT* and *Npc1b* that showed drastic and significant gene expression differences in wild type animals in responses dietary differences between SM versus LD media, or in LD media supplemented with trace amounts of cholesterol, failed to display such distinct transcriptional patterns in response to *high cholesterol* concentrations. This supported my hypothesis that variation in a certain optimal cholesterol threshold is somehow sensed by the cell and orchestrates the transcription of appropriate cholesterol-metabolizing genes so that cellular cholesterol levels can be returned back within optimal limits.

Figure 4.5 (Page 1/2)

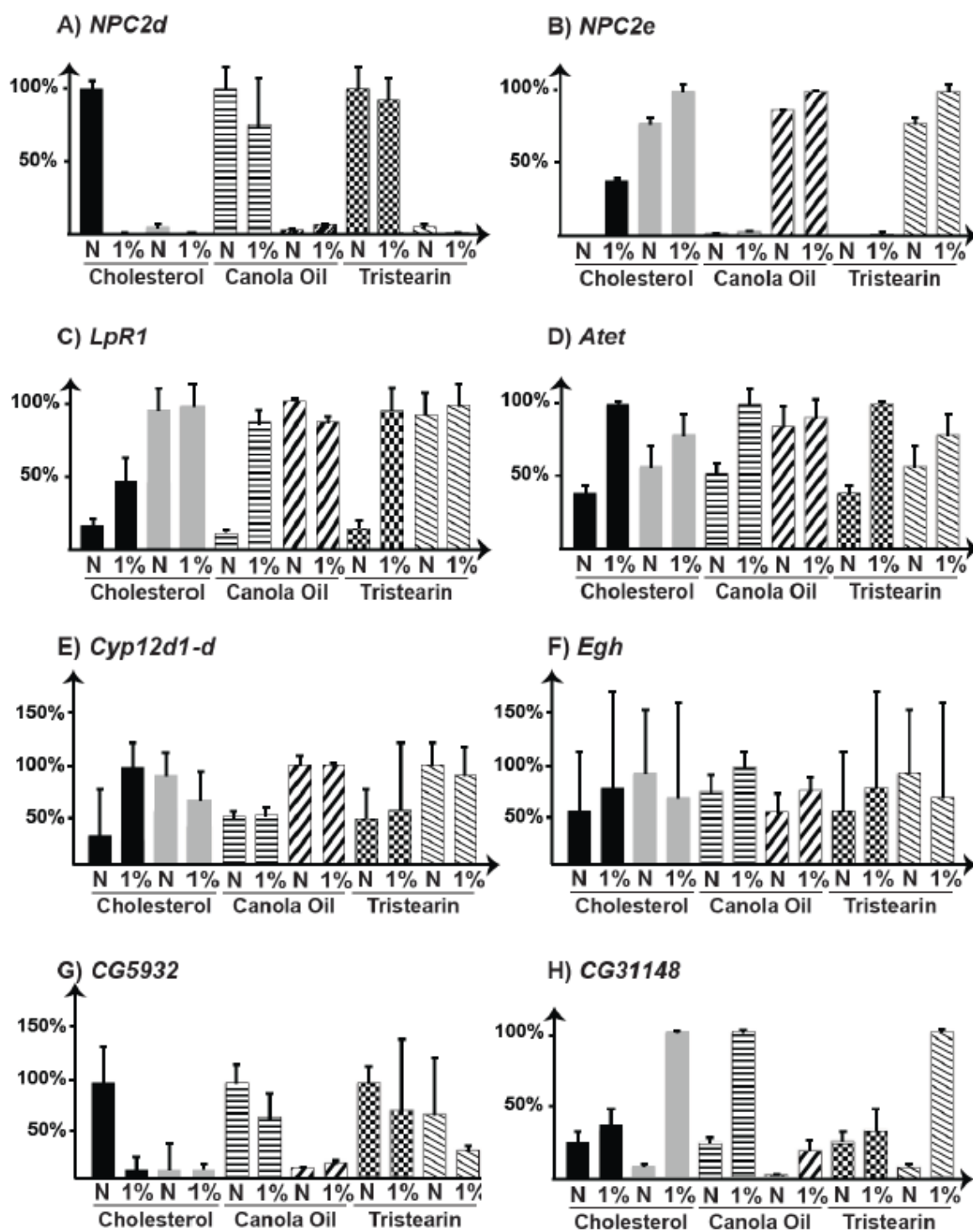
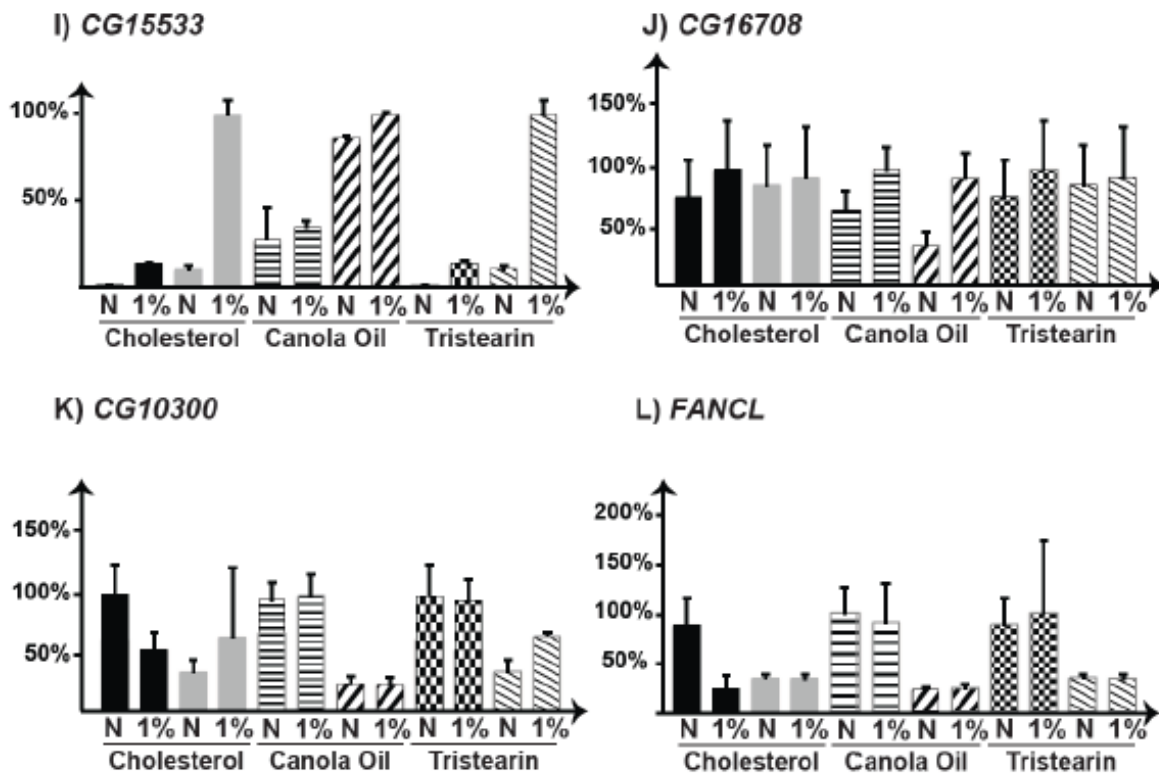
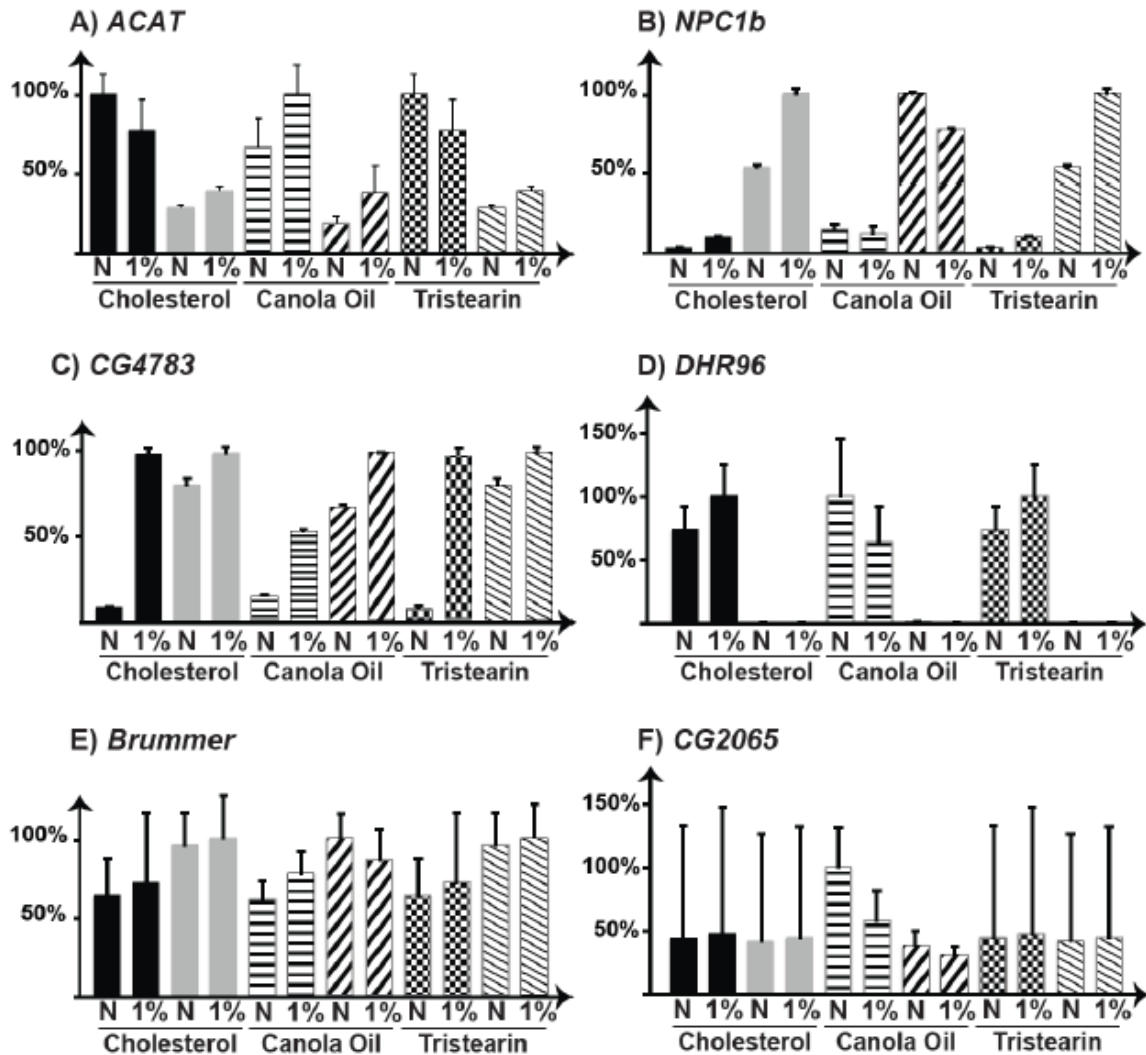


Figure 4.5 (Page 2/2)



**Figure 4.5. Exposure to high concentrations of dietary sterols result in unique sterol-specific transcriptional patterns.** Panels A-L are qPCR data of the top 12 genes with significant fold change differences between wild type when raised on media containing different lipids. The relative fold change values of the respective gene are represented on the X-axis and the nutritional conditions tested on Y-axis. Staged mid-L3 larvae wild type and *DHR96*<sup>1</sup> mutants were collected on standard medium or standard medium that contained either 1% cholesterol, 1% canola oil, or 1% tristearin. *Npc2d* and *Npc2e*, Niemann Pick Type C subfamily -2d, and -2e; *LpR1*, LDL-receptor-related protein; *ATET*, ABC transporter expressed in trachea; *egh*, egghead; *FANCL*; Fanconi anemia complex, subunit Fancl. For each gene, the highest expression level among wild type and *DHR96*<sup>1</sup> mutants for every lipid tested was normalized to 100%. The error bars indicate standard errors. N, standard medium with no added lipid and 1%, representing standard medium supplemented with 1% weight of cholesterol, canola oil or tristearin.

Figure 4.6 – Page 1/4



**Figure 4.6. Transcriptional profiles of the remaining 23 genes analyzed by microfluidics-based qPCR.** The relative fold change values of the respective gene are represented on the X-axis and the nutritional conditions tested on Y-axis. Staged mid-L3 larvae wild type and *DHR96<sup>1</sup>* mutants were collected on standard medium or standard medium that contained either 1% cholesterol, 1% canola oil, or 1% tristearin. For each gene, the highest expression level among wild type and *DHR96<sup>1</sup>* mutants for every lipid tested was normalized to 100%. The error bars indicate standard errors. N, standard medium with no added lipid and 1%, representing standard medium supplemented with 1% weight of cholesterol, canola oil or tristearin.

Figure 4.6 – Page 2/4

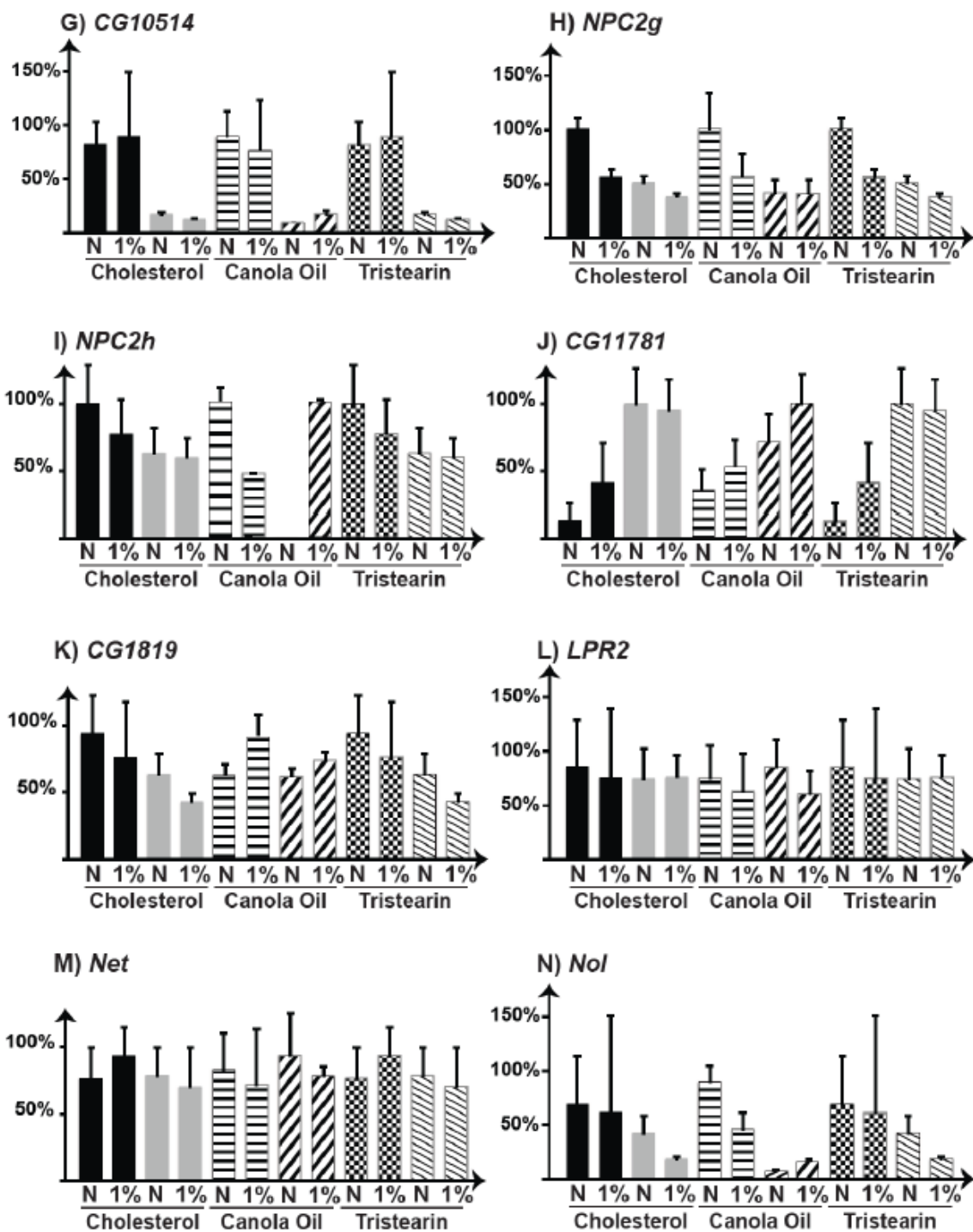


Figure 4.6 – Page 3/4

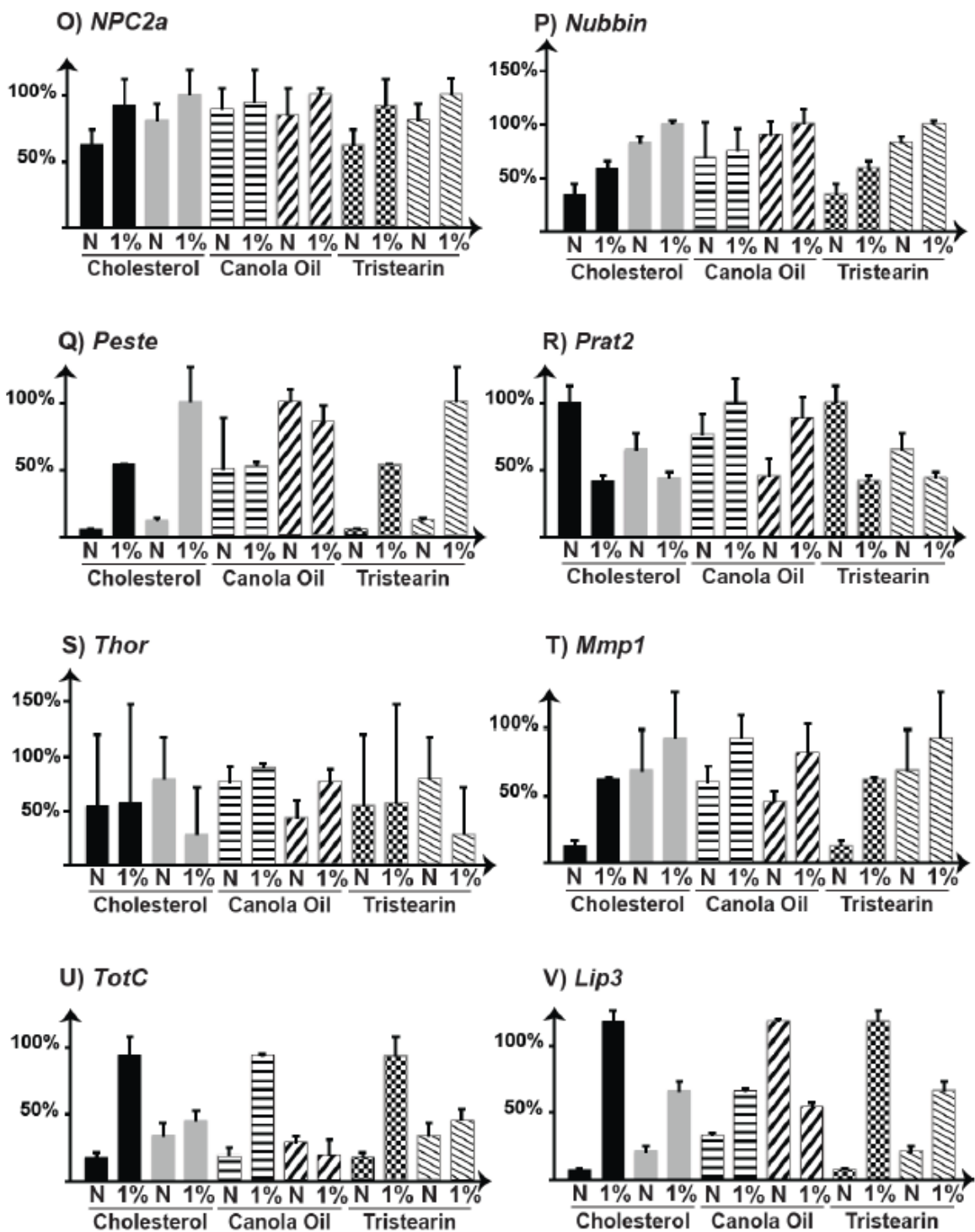
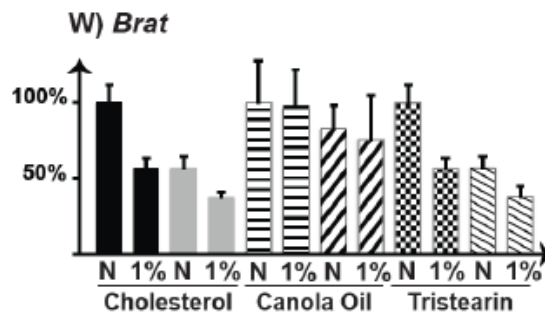


Figure 4.6 – Page 4/4



**Table 4.4. The transcriptional changes triggered by high cholesterol phenocopy the *DHR96<sup>1</sup>* mutation.** Both tables represent qPCR analysis of 34 genes in samples that were isolated from larvae reared on standard medium plus/minus 1% cholesterol. qPCR is based on the Fluidigm Biomark instrument using 5 internal control genes per sample. Fold changes are averages of eight independent samples, standard error is indicated as “SE”. To facilitate the comparison between the two tables, genes are grouped in different columns, depending on whether the gene was found to be induced (>1.5 fold change, shown in blue), repressed (<-1.5fold change, shown in red) or considered to not change significantly (<1.5 and >-1.5fold changes). Genes are sorted top to bottom starting with the most strongly downregulated gene.

## High cholesterol

FC	SE	induced	repressed	neutral
0.00	0.00		NPC2d	
0.13	0.01		CG5932	
0.31	0.05		Nol	
0.43	0.08		CG2065	
0.47	0.09		CG11314	
0.53	0.16		Prat2	
0.57	0.20		CG10300	
0.64	0.23		CG16708	
0.69	0.16		CG11315	
0.71	0.23			CG10514
0.71	0.32			Mmp1
0.77	0.36			Brat
0.77	0.36			FancL
0.80	0.51			CG31148
0.84	0.46			ACAT
0.86	0.34			Thor
0.90	0.33			Egh
0.93	0.47			CG11781
0.94	0.42			Nubbin
0.98	0.28			LpR2
1.11	0.40			CG1819
1.16	0.51			Cyp12d1
1.23	0.78			Brummer
1.28	0.59			NPC2a
1.37	0.55			Net-RA
1.42	0.39			Peste
1.52	0.47	NPC1b		
2.35	0.71	TotC		
2.92	0.50	Atet		
3.13	1.17	CG15533		
3.30	1.20	LpR1		
4.13	0.75	Lip3		
5.01	0.53	CG4783		
32.09	2.21	NPC2e		

*CanS* (0%) controls vs. *CanS* (1% cholesterol)

Mutation in *DHR96*

FC	SE	induced	repressed	neutral
0.04	0.00		NPC2d	
0.14	0.02		Nol	
0.15	0.01		CG5932	
0.15	0.01		CG10514	
0.18	0.05		CG31148	
0.32	0.08		FancL	
0.33	0.05		ACAT	
0.39	0.05		CG2065	
0.44	0.07		CG11314	
0.49	0.13		CG10300	
0.64	0.16		CG11315	
0.70	0.25			Brat
0.77	0.28			CG16708
0.79	0.33			Mmp1
0.84	0.22			CG1819
0.93	0.42			Thor
0.97	0.50			Prat2
0.99	0.51			Egh
1.01	0.39			LpR2
1.05	0.43			Net-RA
1.39	0.53			NPC2a
1.54	0.54	Brummer		
1.59	0.46	Nubbin		
1.67	0.42	Peste		
1.73	0.61	Atet		
1.80	0.63	TotC		
1.81	0.60	Lip3		
2.09	0.66	Cyp12d1		
2.55	0.27	CG11781		
3.67	1.21	CG15533		
6.31	0.54	CG4783		
7.41	0.69	NPC1b		
13.21	2.09	LpR1		
97.34	4.62	NPC2e		

*CanS* vs. *DHR96<sup>1</sup>* mutants on standard medium

#### 4.4. Dietary sterol changes reverse the gene expression patterns of DHR96 candidate targets that were induced by ectopic *DHR96* expression

I identified that feeding a *high cholesterol* medium to wild type animals transcriptionally phenocopies the *DHR96<sup>l</sup>* mutation. Simply put, this may suggest that *DHR96<sup>l</sup>* mutants “think” that they are on a *high cholesterol* diet. An observation that supports this idea is the original phenotype of *DHR96<sup>l</sup>* mutants on lipid-depleted diets. *DHR96<sup>l</sup>* mutants presumably fail to recognize or sense their reduced cellular sterol levels attributed by the LD medium, likely because the transcriptional profile of DHR96 targets, that are linked to cholesterol metabolism, mimic that of a *high cholesterol* scenario and thus fail to trigger the necessary transcriptional patterns to cope with the cholesterol paucity. It was intriguing that *DHR96<sup>l</sup>* mutants have always been viable on SM, but not on LD medium. Taking this with the fact that dietary cholesterol recapitulates *DHR96<sup>l</sup>* mutant expression patterns in wild type animals, strongly suggested that cholesterol inactivates and/or downregulates DHR96. Given that DHR96 can bind to cholesterol, this may indicate that DHR96 is either directly inactivated by a cholesterol metabolite, or cholesterol might transcriptionally downregulate *DHR96*, likely through an autoregulatory mechanism. M. Bujold analyzed *DHR96* expression in wild-type larvae [54] reared on different medium types supplemented with or without with cholesterol, and found that *DHR96* was repressed roughly 4-fold by cholesterol in L2 larvae reared on LD medium supplemented with as little as 50 µg per vial. Similarly, wild-type L3 larvae reared on SM displayed two-fold-higher expression of *DHR96* than L3 larvae reared on *high cholesterol* (1%) medium. Together, these data suggested that cholesterol downregulates *DHR96* transcription in a concentration-dependent manner. Since our microarray data showed us that DHR96 itself mediates responses to dietary cholesterol, it is possible that DHR96 is controlled by an autoregulatory feedback loop.

To determine the genome-wide transcriptional effects of ectopic *DHR96* expression, (**Figure 4.2**), King-Jones *et al.*, conducted a gain-of-function microarray on staged control animals (*w<sup>1118</sup>*) and transgenic animals carrying the *DHR96* gene under the control of a heat-inducible promoter (*'hs-DHR96'*) [112]. Samples were collected for each of control and *hs-*

*DHR96* animals at 4h recovery after heat treatment. 390 genes demonstrated significant expression changes ( $\geq 1.5$  for upregulated genes and  $\leq 1.5$  for downregulated genes,  $P < 0.01$ ) between controls and *hs-DHR96* transgenic animals. Strikingly, roughly ~80% (308 genes) of this gene set were downregulated due to this ectopic expression of *DHR96*.

To test the possibilities that dietary cholesterol modulates *DHR96*, I made use of this *hs-DHR96* transgenic line to address two questions: (1) what are the transcriptional responses to ectopic *DHR96* expression on LD (where *DHR96* protein is presumably active), and (2) do these transcriptional patterns become reversed or unresponsive when *DHR96* is ectopically expressed under conditions of abundant cholesterol (i.e. SM, where *DHR96* is presumably inert)? For example, genes with previous published roles in vertebrate cholesterol biology, i.e. *ABCA1*, *Npc1b*, and *ACAT* are genes that were all downregulated (~3-fold), in *hs-DHR96* transgenic animals on SM. Thus, if dietary cholesterol were to regulate *DHR96* function, then it is likely that differences in cholesterol content between LD vs SM override the transcriptional effects of ectopically expressed *DHR96*. I expected to observe that the ectopic expression of *DHR96* on LD medium reverses the overall expression trend (fold changes) of these putative *DHR96* target genes. **Figure 4.7** represents the results of a quantitative real time PCR (qPCR) analysis of 7 genes tested on larval whole body RNA samples that were collected from controls (*w*<sup>1118</sup>) and *hs-DHR96* transgenic animals. To differentiate the immediate versus delayed transcriptional effects of heat shock-induced *DHR96* expression, I collected staged control and *hs-DHR96* heat-treated larvae at exactly 0h and 4h after recovery from the heat treatment. Fold changes are relative to their respective control expression at 0 h on SM. The *hs-DHR96* transgene induced *DHR96* transcripts by ~200-fold on SM and ~130-fold on LD, demonstrating that the transgene is functional. At the end of the 4h recovery from heat shock, *DHR96* transcripts dropped ~10-fold.

Upon heat treatment at 4h recovery (**Figure 4.7, next page**), *ACAT* transcripts were mildly repressed in *hs-DHR96* animals on SM, however about 2-fold induced on LD medium. Similarly, *FANCL* - which encodes a predicted ubiquitin E3 ligase, was strongly induced only on LD medium and not on SM, suggesting that ectopic *DHR96* expression affects *FANCL* transcripts under conditions where we hypothesize *DHR96* is active. The 4h time point appeared to allow longer time for recovery from the heat treatment and as such,

was sufficient to validate the expression patterns of the top genes *ACAT*, *FANCL*, *Npc2c*, and *DHR96* based on the microarray reported previously in King-Jones *et al.* Hence for other genes, I quantified the expression pattern on SM versus LD media for the 4h time point only. Fold changes were calculated relative to their respective control expression at the 4h time point (i.e. 4h after recovery from heat treatment).

Figure 4.7.

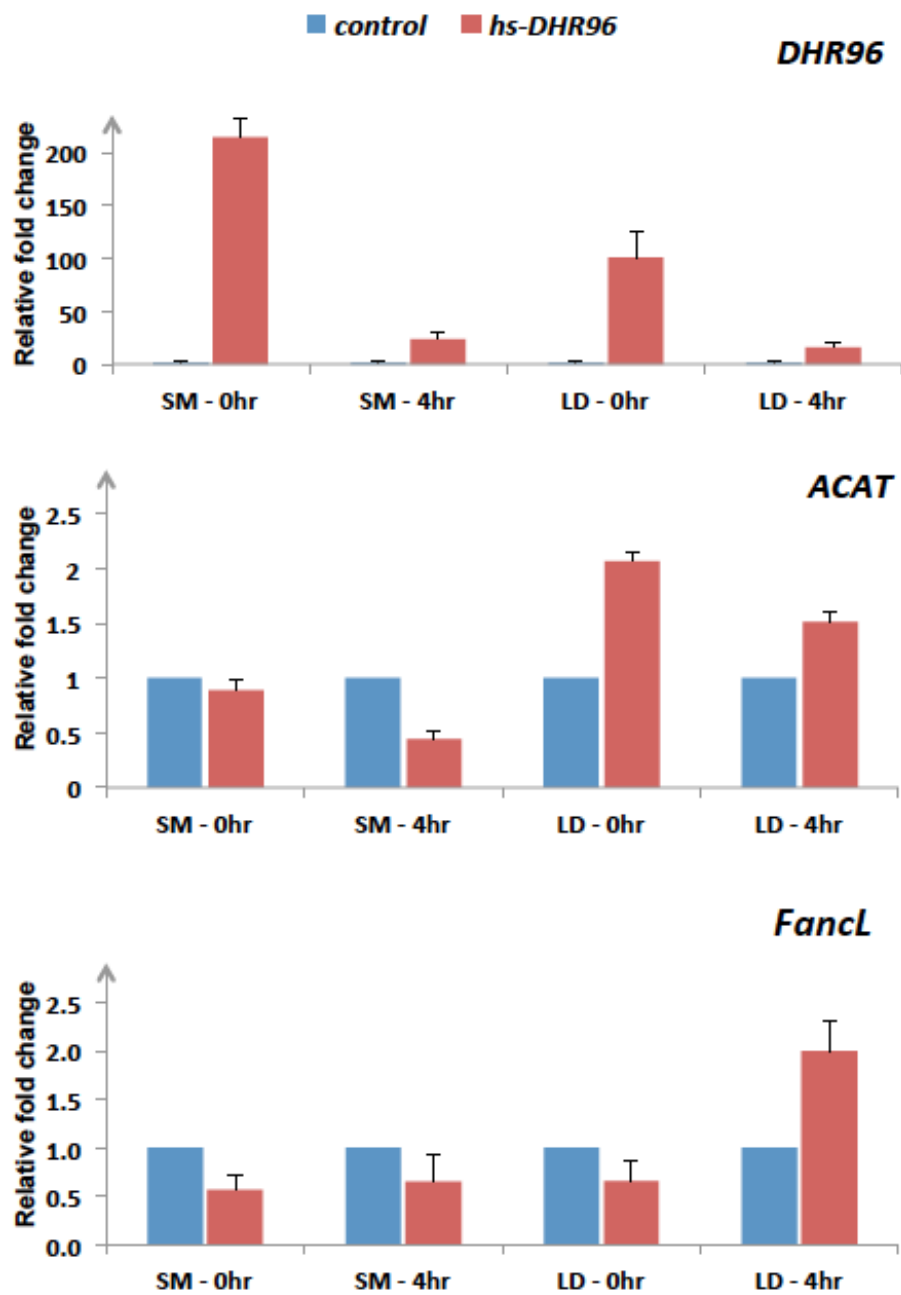
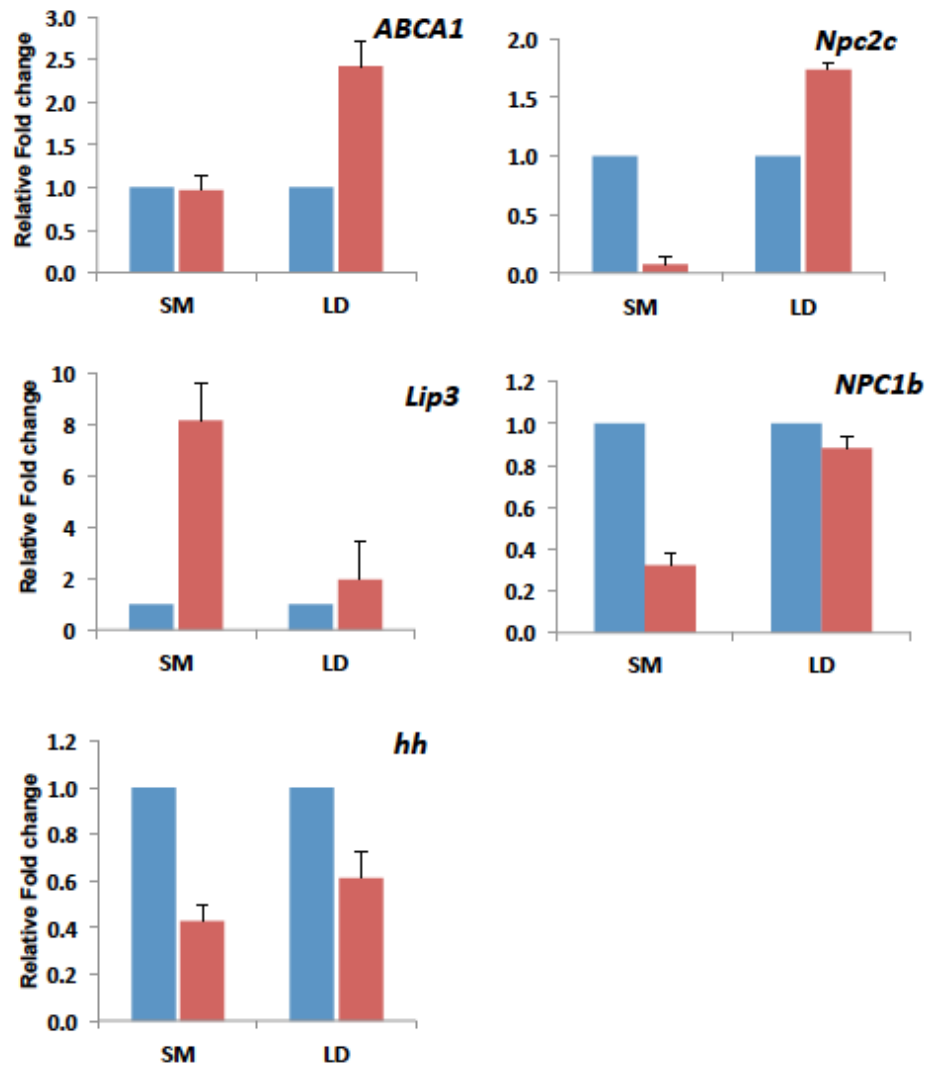


Figure 4.7. (Contd.)



**Figure 4.7: Dietary sterol changes reverse the gene expression patterns of DHR96 candidate targets induced by ectopic expression of DHR96.** The qPCR data demonstrates the transcript levels of *DHR96*, *ACAT*, *FANCL*, *ABCA1*, *Npc2c*, *Npc1b*, *Lip3* and *hh*, in *w<sup>1118</sup>* and *hs-DHR96* animals. Hours (on X-axis) are relative to the recovery time after heat-shock, and fold changes are relative to the control of 0-hr or 4-hr time points. *w<sup>1118</sup>* animals reared at identical conditions served as controls. For the genes *ABCA1*, *Npc2c*, *Npc1b*, *Lip3* and *hh*, expression levels were quantified only in the 4-hr time point samples. Gene expression patterns in controls are represented by blue bars, while expression of the same genes in *hs-DHR96* animals are shown by red bars, respectively on SM and LD. Error bars represent 95% confidence intervals, and *P* values were calculated with the unpaired Student's *t*-Test. *ACAT*: acyl coA acyl transferase, *NPC2c*: Niemann Pick disease Type C-2c, *ABCA1*-ATP Binding Cassette A1, *hh*: *hedhehog*, *Lip3*: Lipase; cholesteryl ester hydroloase, *NPC1b*: Niemann Pick disease Type C-1b, *FANCL*: ubiquitin E3 ligase.

In line with the microarray [112] that was conducted on SM, *ABCA1* transcript levels showed no significant difference in response to ectopic *DHR96* expression, however were ~2.5-fold induced on LD. A similar, but more dramatic pattern was observed with *Npc2c* transcripts which were strongly down regulated by ectopic *DHR96* expression on SM but 2-fold induced by the same transgenic line when expressed on LD medium. On the other hand, *DHR96* expression caused an ~8-fold induction of *Lip3* transcripts on SM, and a concomitant ~4-fold repression on LD medium. *Npc1b*, which was nearly 5-fold repressed on SM, is distinctly de-repressed on LD medium – supporting my hypothesis that dietary cholesterol modulates *DHR96*-dependent expression of these genes. The 2.5-fold repression of *Hedgehog (hh)* in response to *DHR96* overexpression failed to display any significant difference between SM and LD, suggesting that dietary changes do not affect *hh* regulation.

Thus, ectopic expression of *DHR96* regulates downstream candidate targets of *DHR96* under lipid-depleted conditions; but fails to trigger those distinct expression changes under conditions of abundant cholesterol, such as the SM; presumably due to the inactivation and/or downregulation of *DHR96* by dietary cholesterol. Taken together, this qPCR data fits my hypothesis that dietary sterol differences regulates *DHR96*-mediated transcriptional control of key cholesterol metabolizing genes such as *ACAT*, *ABCA1*, *Npc2c* and *Npc1b*. A follow-up based on the same experimental design using LD medium with defined amounts of cholesterol will aid in distinguishing whether cholesterol can modulate transcriptional responses to ectopic *DHR96* expression.

#### **4.5. Exploring the tissues that are most critical for *DHR96* function**

The underlying reason for *DHR96<sup>l</sup>* mutant lethality on LD medium is still unknown. One way to understand the *DHR96<sup>l</sup>* mutant phenotype was to identify the tissue-specific roles of *DHR96*. King-Jones *et al.*, (2006) [112] carried out immunostaining of tissues isolated from wild type L3 larvae reared on SM, and detected *DHR96* protein exclusively in the larval fat body, midgut, salivary glands and Malpighian tubules. Using tissue-specific *DHR96-RNAi* knockdown, I asked if we could determine which of these four tissues were most important for the *DHR96<sup>l</sup>* mutant phenotype. I used the following tissue-specific *Gal4* drivers (**Figure 4.8 A-G**): *actin (act)* [115]-, *malic enzyme modifier (mex)* [116]-, *collagen (cg)*- [117], *scalloped (sd)* - [118], *c42*- [119], and *c724*- [120] to trigger *DHR96-RNAi* ubiquitously or

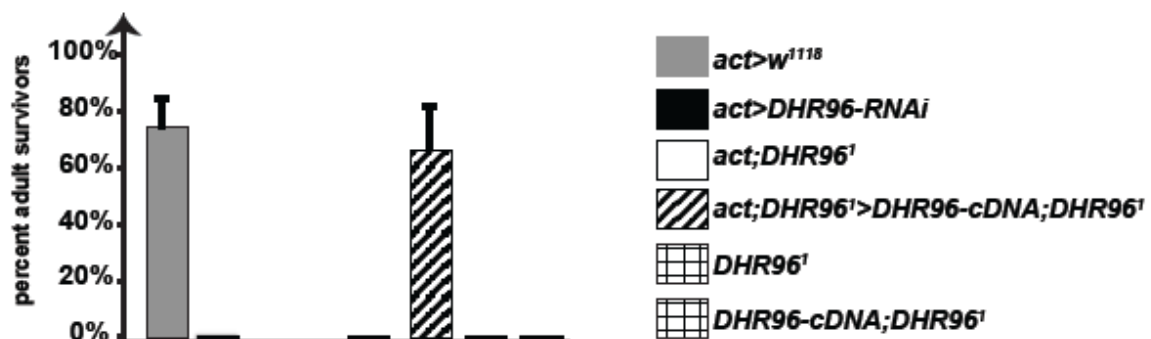
specifically in the midgut, fat body, salivary gland, the principal and stellate cells of Malpighian tubules, respectively. In **Chapter 3**, I reported that *DHR96<sup>l</sup>* mutants can be rescued to adulthood on lipid-depleted medium supplemented with a combination of ecdysteroids and membrane sterol, other than cholesterol. Hence, I additionally employed the phantom (*dcr;phm*)-*Gal4* [79] to test if *DHR96* had a critical function in the prothoracic gland and whether that function is correlated with the mutant lethal phenotype.

By triggering *DHR96-RNAi* (2 copies of *UAS-DHR96-RNAi* transgenes) in specific tissues, I wanted to identify which knockdown of *DHR96* in which tissue(s) most recapitulated the L2 larval arrest of *DHR96<sup>l</sup>* mutant on lipid-depleted (LD) medium. For instance, if a midgut-specific *DHR96* knockdown were sufficient to phenocopy the mutant lethality, it may suggest that *DHR96<sup>l</sup>* mutants suffer from a defect in the absorption and transport of dietary cholesterol. Similarly, a fat body or a malpighian tubule-specific knockdown of *DHR96* that recapitulates the mutant lethality phenotype is suggestive of broad defects in metabolism, excretion, and/or detoxification. As a reverse strategy, I employed a transgenic line carrying the full-length *DHR96-cDNA* under UAS control (constructed by K. King-Jones), to ectopically express *DHR96* in specific tissues of the *DHR96<sup>l</sup>* mutant. The expectation from this strategy was to determine the tissue(s) (if any) in which the expression of a *DHR96-cDNA* transgene might be sufficient to fully rescue *DHR96<sup>l</sup>* mutants reared on LD medium. The following four controls were tested in triplicates on LD medium: (i) every individual *Gal4* driver crossed to *w<sup>1118</sup>*, (ii) every individual *Gal4* driver recombined into the *DHR96<sup>l</sup>* mutant background, (iii) the *DHR96-cDNA* overexpression transgene recombined into the *DHR96<sup>l</sup>* mutant background, and (iv) *DHR96<sup>l</sup>* mutant. A population of 50 age-matched embryos of the aforementioned controls and experimental genotypes were monitored every day for 15-18 days to calculate the percentage of total adult survivors (**Figures 4.8 A-G**). Due to the nature of its nutritional content, the LD medium consistently produced only ~80% adult survivors in the control *w<sup>1118</sup>* population. The remaining ~20% of their population arrested development as L2 larvae and failed to survive past day 4 AED.

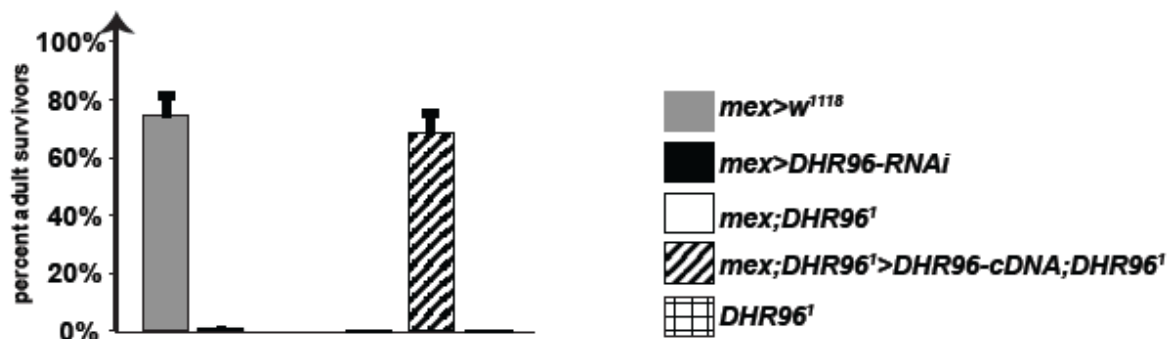
**Figure 4.8: Midgut and fat body are the primary tissues critical for *DHR96* function.**

Columns represent the percentage of adult survivors on lipid-depleted (LD) medium. *DHR96*<sup>1</sup> mutants (indicated by large grid bars, rightmost column) arrest development as second instar larvae on LD medium. Ubiquitous (A) and tissue-specific *Gal4* drivers (B-G) were used to express *DHR96-RNAi* transgene in the wild type, or the *DHR96-cDNA* transgene in the *DHR96*<sup>1</sup> mutants. The controls *Gal4* driver >*w*<sup>1118</sup> and *Gal4* driver alone in *DHR96*<sup>1</sup> mutant background are indicated by solid grey bars and solid white bars, respectively for each tissue-specific driver. Each tissue-specific driver was crossed to *UAS-DHR96-RNAi* (solid black bars), and each driver recombined to the *DHR96*<sup>1</sup> mutant background was further crossed to *UAS-DHR96-cDNA* transgenic line that was also recombined to the *DHR96*<sup>1</sup> mutant (diagonal black stripes). 50 embryos of each of the aforementioned tissue specific *DHR96-RNAi* or *DHR96-cDNA* transgenic lines were transferred to lipid-depleted (LD) medium. Error bars represent standard deviation calculated from 3-4 replicates (each containing 50 embryos). *cg-*, *mex-*, *c42-*, *c724*, *sd*, *dcr;phm-Gal4* transgenes drive expression specifically in the fat body, midgut, principal cells of malpighian tubules, secondary cells of malpighian tubules, salivary gland cells and prothoracic gland cells respectively. *act-Gal4* transgene drives expression ubiquitously.

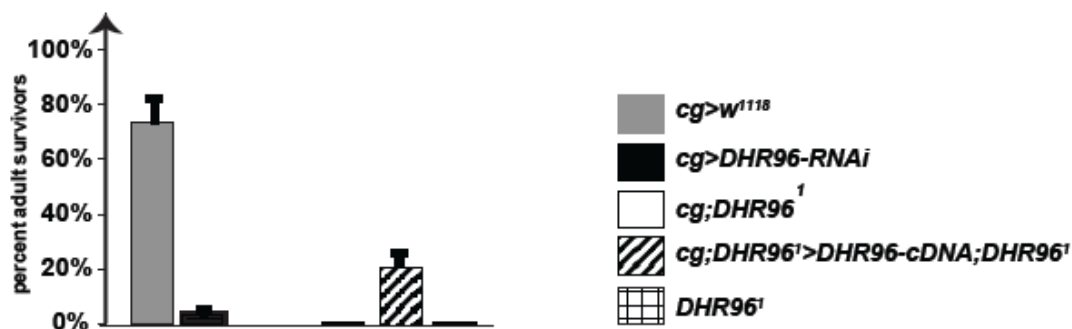
**A) Ubiquitous**



**B) Midgut**



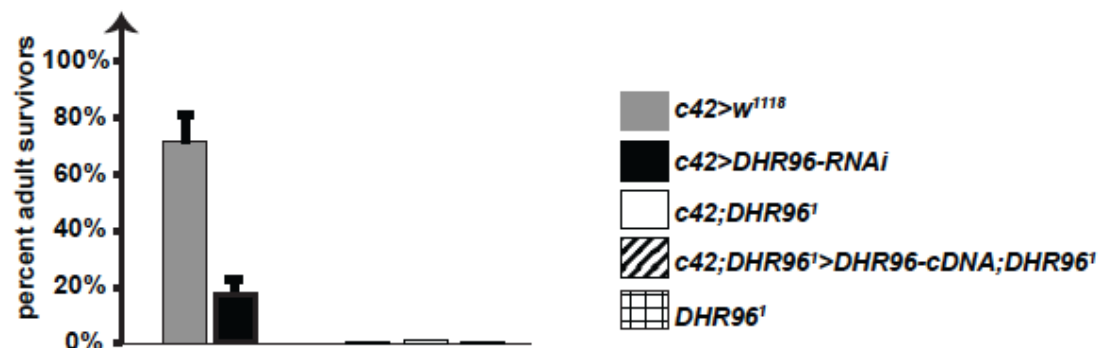
## C) Fat body



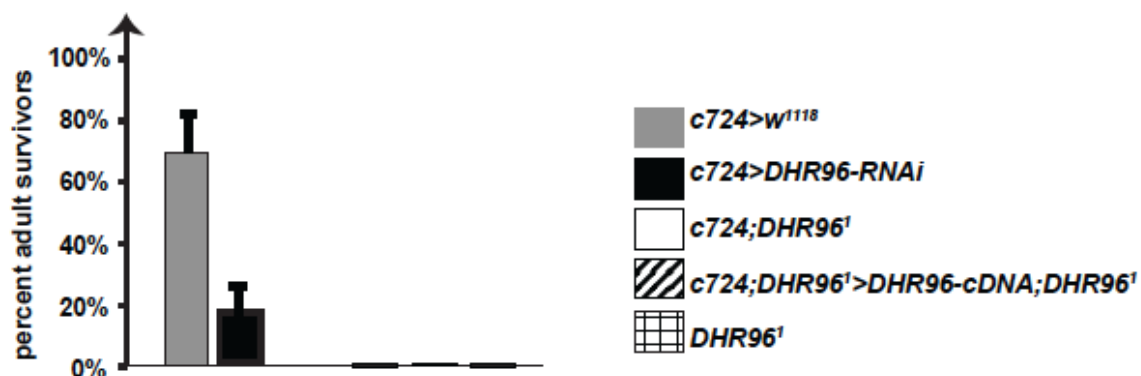
## D) Salivary gland



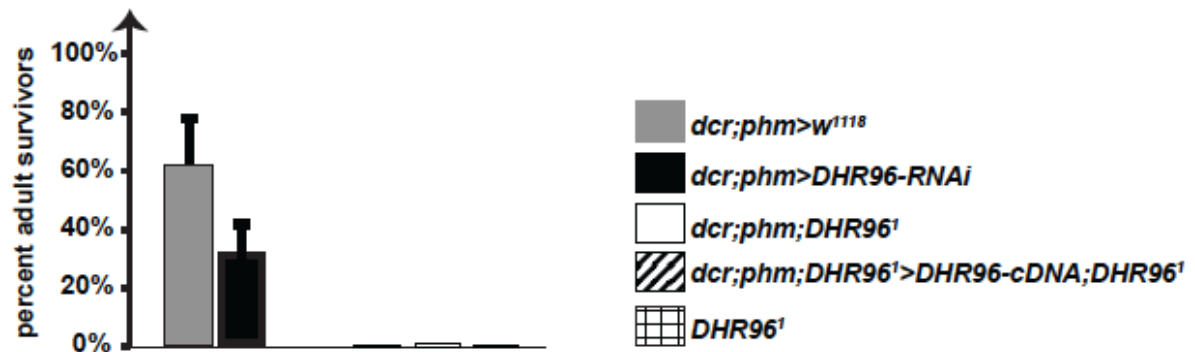
## E) Malpighian tubule (primary cells)



## F) Malpighian tubule (secondary cells)



### G) Prothoracic gland



I used the ubiquitous driver *actin (act)-Gal4* as shown in **Figure 4.8A** to demonstrate the effectiveness of the *DHR96-RNAi* transgenic line to knockdown *DHR96*. While the *Gal4* driver control cross (*act-Gal4>w<sup>1118</sup>*) was viable and resulted in healthy adults on LD medium, ubiquitous knockdown of *DHR96-RNAi* caused 100% of the population to arrest as L2, with no observed escaper to either L3, pupal or adult stages. Likewise in the complementary approach, ubiquitous expression of *DHR96-cDNA* completely restored survival of the larval-lethality seen in *DHR96<sup>1</sup>* mutants reared on LD medium. The transgenic animals containing the *act-Gal4* and *DHR96-cDNA* transgenes alone in the *DHR96<sup>1</sup>* mutant background were 100% L2-lethal on LD medium, indicating that the *DHR96*-transgenic constructs were working.

The midgut data demonstrated the most striking results, as shown in **Figure 4.8B**, since a midgut-specific *DHR96-RNAi* was sufficient to fully recapitulate the *DHR96<sup>1</sup>* mutant phenotype by resulting in 100% larval lethality. Conversely, expression of *DHR96* specifically in the midgut cells of *DHR96<sup>1</sup>* mutants was sufficient to rescue 100% of *DHR96<sup>1</sup>* mutant embryos to adulthood on LD medium, indicating that *DHR96* has vital roles in regulating dietary cholesterol absorption and transport. In a similar observation, although to a lesser degree, the fat body-specific knockdown of *DHR96* strongly reduced survival wherein ~95% arrested as L2 larvae and ~5% survived to adults. Likewise, the expression of the *DHR96-cDNA* in the fat body of *DHR96<sup>1</sup>* mutants, rescued ~30% of the *DHR96<sup>1</sup>* mutant population to healthy adults, while ~70% of the mutant population remained arrested as L2 larvae that continued to survive on LD medium until day 4 AED.

In contrast, knockdown of *DHR96* specifically in the Malpighian tubules, or in the salivary gland cells, only partially phenocopied *DHR96<sup>l</sup>* mutant lethality. Previous studies [93], [162] have described that the production of urine in *Drosophila* and other Dipterans require the combined activity of two tubule cell types: principal (type I) and secondary or stellate (type II). Principal cells, the major cell type, transport potassium ions into the lumen [163], while the stellate cells allow the consequent movement of chloride ions and water [164]. The selective transport of these metabolites occurs via the activity of ion-transporters that are hormonally regulated by diuretic peptides [165], [166]. However little is known about the transcriptional control, pathways and tissue-specific factors that regulate the function of these cell types. To explore if *DHR96* might have distinct roles in the tubules, I triggered *DHR96-RNAi* and *-cDNA* constructs in the tubule principal cells by *GAL4* line *c42*, or in tubule stellate cells by *GAL4* line *c724*. In contrast to the severe lethality observed with midgut-specific knockdown, *DHR96-RNAi* in either tubule cell types only moderately affected survival, resulting in ~20% adult survivors on LD medium. Moreover, expression of the *DHR96-cDNA* specifically in these tissues of *DHR96<sup>l</sup>* mutants failed to rescue the *DHR96<sup>l</sup>* mutant phenotype, suggesting that DHR96 regulates genes in diverse metabolic pathways and that lethality phenotype on lipid-depleted conditions may arise due to impaired pathways in sterol uptake and/or transport via the midgut and fat body. In addition, the expression of *DHR96-RNAi* or *-cDNA* constructs in the salivary glands and in prothoracic glands neither fully recapitulated nor alleviated the *DHR96<sup>l</sup>* mutant L2 larval lethality on LD medium, suggesting that DHR96 is most critical in tissues where early steps in sterol uptake and utilization are dynamically regulated in response to changing cellular cholesterol levels.

**CHAPTER 5.****CHARACTERIZATION OF *DROSOPHILA* NIEMANN-PICK DISEASE TYPE C  
GENES: *Npc2c*, *Npc2d* and *Npc2e***

In Chapter 4, I described the rationale for conducting *low cholesterol* and *high cholesterol* microarrays to identify genes with roles in *Drosophila* sterol biology (**Figure 4.2B**). This led to a refined subset of genes that were doubly responsive to: (a) dietary cholesterol differences, and (b) a mutation in the nuclear receptor gene, *DHR96*. Four of the genes: *Npc1b*, *Npc2c*, *Npc2d* and *Npc2e* belong to the Niemann Pick Disease Type C family of cholesterol transporters, vertebrate homologs of which are implicated in the neurodegenerative disease Niemann Pick Type C. While *Npc1b* has been characterized to be critical for dietary sterol absorption in midgut epithelium [109], no studies have yet addressed the functional significance of *Npc2c*, *Npc2d*, or *Npc2e*.

### 5.1. Phenotypic characterization of *Npc2d* and *Npc2e*

On a genome-wide scale, *Npc2d* (~100 fold repressed) and *Npc2e* (~40 fold induced) are the most strongly responding genes when fed a *high cholesterol* medium to wild type animals, as well, in *DHR96<sup>l</sup>* mutants reared on standard medium (SM) without any added cholesterol (**Chapter 4, Figure 4.5A-B**). Notably in *DHR96<sup>l</sup>* mutants, *Npc2d* and *Npc2e* were also the top-affected genes across the genome, exhibiting a similar degree of fold change values and statistical significance (**Chapter 4, Table 4.3**). Moreover, *Npc2d* and *Npc2e* mRNA levels in *DHR96<sup>l</sup>* mutants remained unchanged irrespective of whether *DHR96<sup>l</sup>* mutants were fed diets containing *high cholesterol* or not. This led to my hypothesis that upon cellular uptake, dietary cholesterol modulates *DHR96* function, which in turn transcriptionally regulates downstream targets to maintain cellular cholesterol homeostasis. Moreover, since *DHR96<sup>l</sup>* mutants arrest development on lipid-depleted diets and are rescued specifically by cholesterol supplementation, genes identified in this overlap represent candidate *DHR96* targets, and can provide important links to understanding the underlying reason for *DHR96<sup>l</sup>* mutant lethality on LD medium.

I hypothesized that if *DHR96* exerted regulatory control over the transcriptional response of *Npc2d* and *Npc2e* to cholesterol, then changes in dietary cholesterol levels, which modulate *DHR96* expression [54], or a loss of *DHR96* function via a mutation will likely trigger comparable gene expression patterns. Hence, I wanted to test if the larval lethality phenotype of *DHR96<sup>l</sup>* mutants on lipid-depleted media is associated with the misregulation of *Npc2d* and *Npc2e*. Evidence for a positive epistatic interaction between the

*Npc* genes and *DHR96* would strengthen my hypothesis that *Npc2d* and *Npc2e* represent direct targets of DHR96. To genetically explore the phenotypic effects of reversing *Npc2d* and *Npc2e* expression in *DHR96<sup>l</sup>* mutants, I generated *DHR96<sup>l</sup>* mutant and control transgenic lines that expressed the following *Npc2d*- and *Npc2e*- specific constructs containing the Upstream Activator Sequence(s) (UAS) to achieve spatial control of target gene expression when crossed to appropriate Gal4 drivers containing gene-specific promoters: (1) full length *Npc2d*- and *Npc2e*- cDNA constructs to overexpress the genes in an ectopic manner, and (2) *RNAi* constructs (Vienna *Drosophila RNAi* Center) to achieve knockdown of *Npc2d*- and *Npc2e*- gene expression. In short, I attempted to recapitulate the *DHR96<sup>l</sup>* mutant expression patterns of *Npc2d* and *Npc2e*, in control animals, in order to examine whether these transcriptional changes may be able to partially phenocopy the larval lethality of *DHR96<sup>l</sup>* mutants observed on lipid-depleted media. More importantly, I asked if reversing the respective expression patterns of *Npc2d* and *Npc2e*, i.e. knockdown of *Npc2e* and overexpression of *Npc2d* in *DHR96<sup>l</sup>* mutants, either individually or in combination, would alleviate *DHR96<sup>l</sup>* mutant lethality on lipid-depleted medium (**Figure 5.3**).

While the individual *Npc2d* knockdown (VDRC #31095, **Figure 5.1A**) caused 80% reduction in *Npc2c* mRNA levels, it also negatively impacted *Npc2e* and *Npc2c* transcripts. Similar was the case with *Npc2e-RNAi* (VDRC #100445, **Figure 5.1C**), but not with *Npc2c* knockdown (VDRC #31139 (*Npc2c<sup>GD6798</sup>*), **Figure 5.1F**), which repressed *Npc2c* transcripts over 90% without any effects on *Npc2d* or *Npc2e*. On the other hand, the individual overexpression constructs of *Npc2d* and *Npc2e* caused a significant and specific induction of *Npc2d* and *Npc2e* transcripts only (**Figure 5.1B and D**). Oddly, combining *Npc2e* overexpression with *Npc2d-RNAi* resulted in a 5-fold repression of *Npc2d* (**Figure 5.1E**), and a 3.5-fold repression of *Npc2c*, similar to the transcriptional effects of ubiquitous *Npc2d-RNAi* alone, raising the possibility whether effects of *Npc2d-RNAi* interfered with the transcriptional effects of *Npc2e* expression in spite of the overexpression by *actin*-promoter driver. Since the qPCR primers were verified to confirm that each primer pair uniquely targets their corresponding *Npc2*-specific transcripts only, it seemed less likely that the observed transcriptional responses were due to non-specificity of primer binding (**Chapter 6, Figure 6.2**). Alternatively, since *Drosophila* harbors 8 *Npc2*-like genes it is likely that

these *Npc2* genes may function redundantly, and are mutually regulated, likely via shared regulatory elements.

**Figure 5.1**

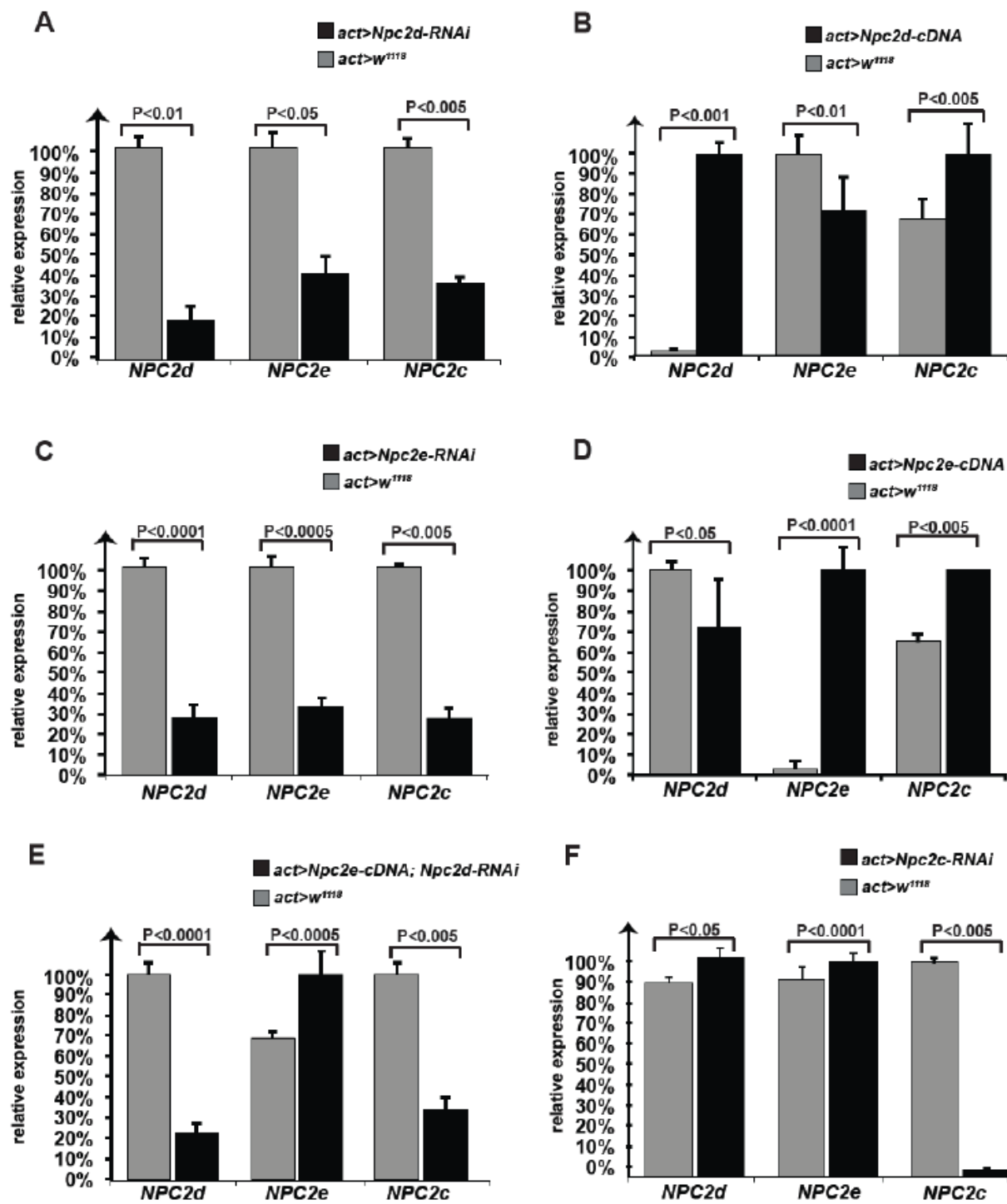


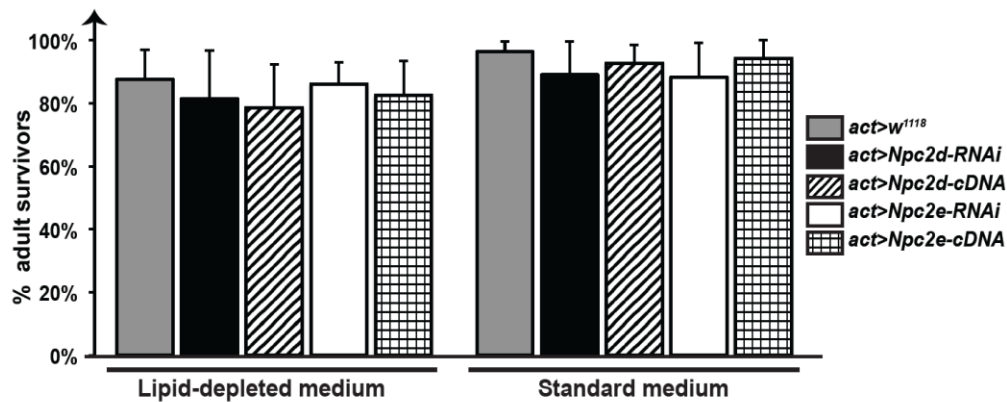
**Figure 5.1 Expression profiles of *Npc2d*, *Npc2e* and *Npc2c* on standard media.** Note: For all samples detailed below, whole body RNA was collected from third instar wandering larvae staged at 40 h after L2/L3 molt on standard media. Error bars represent 95% confidence intervals, and *p* values were calculated with the unpaired Student's *t*-test. All bar graphs represent qPCR data showing transcript levels of *Npc2d*, *Npc2e* and *Npc2c* transcripts in: ubiquitous expression of (A) *Npc2d*-RNAi, (B) *Npc2d*-cDNA, or (C) *Npc2e*-RNAi, (D), *Npc2e*-cDNA, (E) *Npc2e*-cDNA recombined with *Npc2d*-RNAi, and (F) *Npc2c*-RNAi, respectively. Fold changes are relative to the respective expression *Npc2d*, *Npc2e* and *Npc2c* in the control *actin-Gal4 > w<sup>1118</sup>*, as shown in grey bars.

To test if these transcriptional changes manifested in observable phenotypic effects, I quantified the percentage of adult survivors in the following genetic classes: controls (i.e. the specific-Gal4>*w<sup>1118</sup>*) and the individual RNAi-mediated knockdown of *Npc2d* /*2e* on the SM and LD media. The SM is a relatively abundant source of dietary sterols, and our data [54] indicates that SM is sufficient to transcriptionally downregulate *DHR96* compared to the responses on LD. Hence, I included the LD medium in the likelihood that *Npc2d* /*2e* knockdown/expression-related phenotypes that were unnoticeable on SM might manifest under lipid-depleted conditions, where we propose that *DHR96* is active.

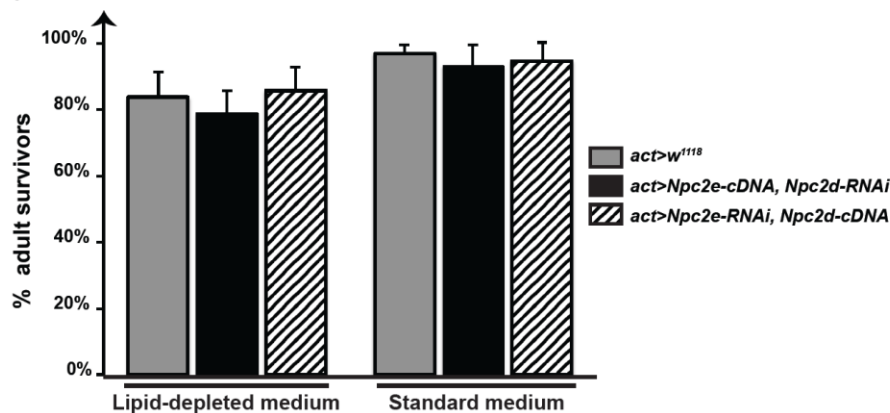
The RNAi-mediated knockdown of *Npc2d* and *Npc2e*; whether ubiquitously or in specific larval tissues (based on modENCODE and FlyAtlas data) had no significant effects on survival or development timing on LD or SM (**Figure 5.2**). Even more, doubling the number of copies of the UAS-*Npc2d* /*2e*-RNAi, and the midgut Gal4-driver (the tissue where *Npc2d* and *Npc2e* transcripts are maximally expressed; modENCODE and FlyATLAS data) still had no obvious phenotypic effects (**Figure 5.3**). Conversely, I selectively reversed the expression patterns of *Npc2d* and *Npc2e* that were observed in *DHR96<sup>l</sup>* mutants by recombining the *Npc2d*-cDNA overexpression and *Npc2e*-RNAi knockdown transgenes in a *DHR96<sup>l</sup>* mutant background. **Figure 5.4** shows the percentage of adult survivors resulting from the ubiquitous expression of the two aforementioned transgenes in the *DHR96<sup>l</sup>* mutant background. The act-Gal4 driver was also crossed back into a *DHR96<sup>l</sup>* mutant background. The controls: i.e. *act>w<sup>1118</sup>* and the individual UAS-*Npc2d*-cDNA/UAS-*Npc2e*-RNAi double transgenic animals; produced viable adults on lipid-depleted medium. All the aforementioned controls and experimental genotypes were

viable and produced healthy adult survivors on SM. Controls and UAS-containing transgenic animals: *Npc2d* -cDNA and *Npc2e-RNAi* crossed back into the *DHR96<sup>l</sup>* mutant background, were 100% L2 lethal on lipid-depleted medium. However, transgenic combinations of the UAS-*Npc2d* -cDNA/UAS-*Npc2e-RNAi* failed to rescue *DHR96<sup>l</sup>* mutant larval arrest on lipid-depleted medium (**Figures 5.4**). It is likely that the *DHR96<sup>l</sup>* mutants are lethal on lipid-depleted diets is a result of a complex transcriptional network affecting several direct target genes of DHR96. While the expression of certain genes could ‘drive’ the phenotypic consequence, transcriptional patterns of other misregulated genes may result from secondary physiological responses. My data indicates that modifying the expression patterns of two putative DHR96 targets, *Npc2d* or *Npc2e* is insufficient to phenocopy, at least in part, the critical functions of DHR96 on lipid-depleted conditions.

Figure 5.2



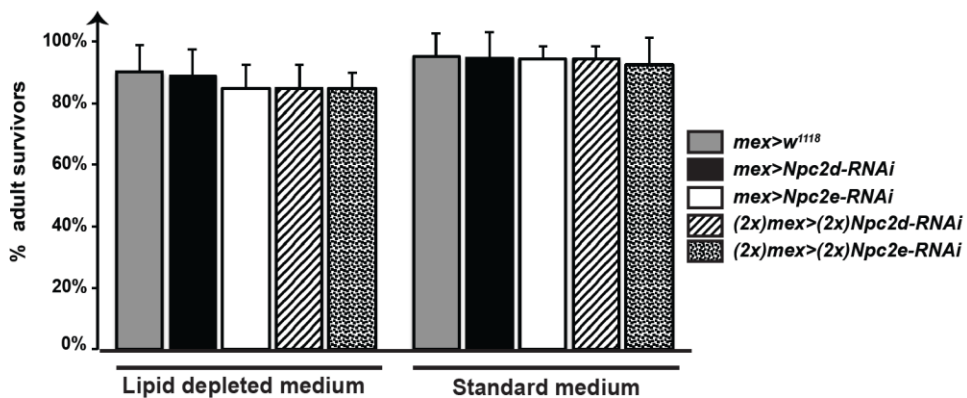
B)



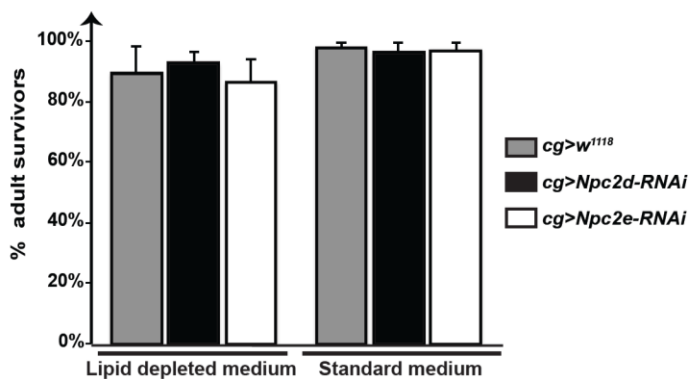
**Figure 5.2: Ubiquitous expression of *Npc2d* and *Npc2e* and/or ubiquitous RNAi-mediated knockdown of *Npc2d* and *Npc2e* cause no observable effects on survival or development under lipid-depleted and standard media conditions. (A)** Columns represent the percentage of adult survivors in each of the following genetic backgrounds: *act>npc2d-RNAi*; solid black bars, *act>npc2d-cDNA*; black stripes, *act>npc2e-RNAi*; solid white bars, *act>npc2e-cDNA*; grids, respectively. **(B)** Columns represent the percentage of adult survivors in each of the following genetic backgrounds: *act>npc2e-cDNA, npc2d-RNAi*; solid black bars, *act>npc2d-cDNA, npc2e-RNAi*; black stripes, respectively. Controls are *act>w<sup>1118</sup>* and are indicated by grey bars. 50 embryos of each of the aforementioned genotypes were transferred to either lipid-depleted (LD) medium, or standard medium (SM). Error bars represent standard deviation calculated from 3-4 replicates (each containing 50 embryos). *act-Gal4* transgene drives expression ubiquitously.

Figure 5.3

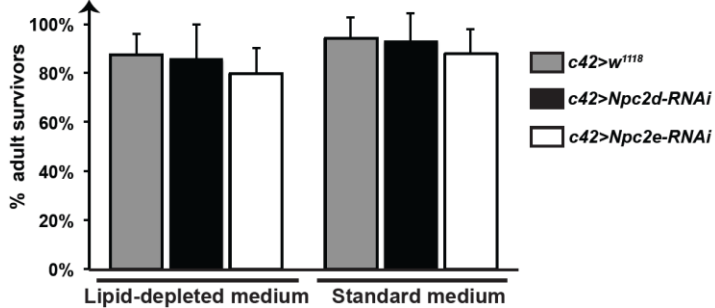
## A) Midgut



## B) Fat body



## C) Malpighian tubules (primary cells)



## D) Malpighian tubules (secondary cells)

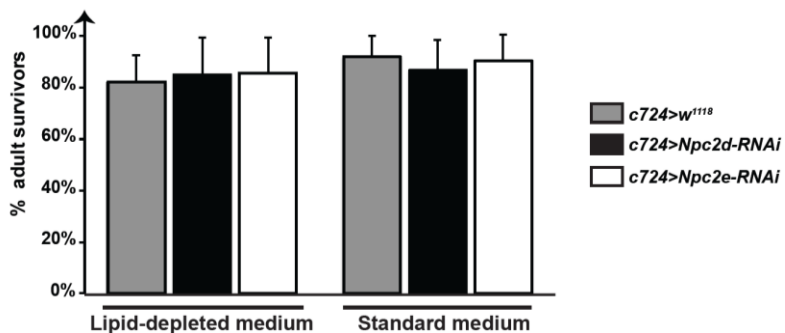


**Figure 5.3: Tissue-specific RNAi-mediated knockdown of *Npc2d* and *Npc2e* cause no observable effects on survival or development under lipid-depleted and standard media conditions.** Columns represent the percentage of adult survivors of tissue specific knockdown of *Npc2d* and *Npc2e* in the midgut (**A**), fat body (**B**), malpighian tubules (**C,D**), respectively. Controls *act>w<sup>1118</sup>* are indicated by solid grey bars. 50 embryos of each of the aforementioned genotypes were transferred to either lipid-depleted (LD) medium, or standard medium (SM). For midgut-specific knockdown (**A**), the copies of the *mex-Gal4* and *RNAi* transgenes were doubled to achieve stronger mRNA knockdown. Error bars represent standard deviation calculated from 3-4 replicates (each containing 50 embryos). *cg-*, *mex-*, *c42-*, *c724-Gal4* transgenes drive expression specifically in the fat body, midgut, principal cells of malpighian tubules, and secondary cells of malpighian tubules, respectively.

Figure 5.4

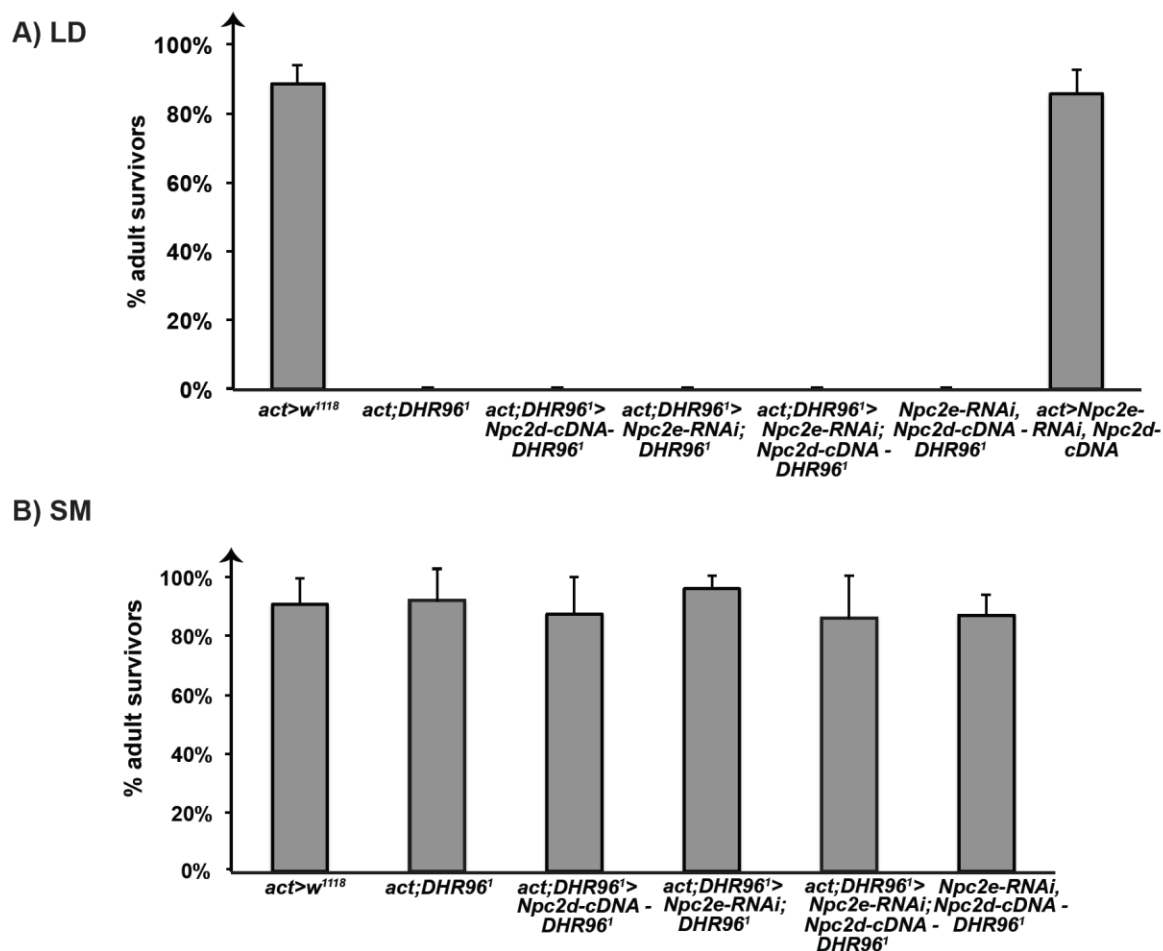


**Figure 5.4: Test for genetic interaction between *DHR96* and *Npc2d/Npc2e*.** Columns represent the percentage of adult survivors in each of the respective genetic backgrounds as indicated on the X-axis labels. 50 embryos of each genotype were transferred to lipid-depleted (LD) medium (**A**), or standard medium (SM) (**B**). Error bars represent standard deviation calculated from 3-4 replicates (each containing 50 embryos). *act-Gal4* transgene drives expression ubiquitously.

## 5.2. *Drosophila* gene *Npc2c* is essential for normal development

*Npc2c* was shortlisted among a selective gene set containing genes that demonstrated significant expression changes between wild type and *DHR96*<sup>l</sup> mutants in response to dietary differences between standard and low cholesterol media (detailed in chapter 4, **section 4.1**). Moreover, when this gene set was compared to a set of 390 genes that were significantly affected by ectopic *DHR96* expression, *Npc2c* was again identified in this overlap subset of 53 genes (**Figure 4.2**, *P* value, 1.8E-12). Specifically, upon ectopic expression of *DHR96*, the whole body expression levels of *Npc2c* underwent a characteristic reversal in the direction of fold changes when the fly media was switched from SM to LD medium, indicating that the observed *Npc2c* transcriptional response is *DHR96* dependent. Finally, our data (**Figure 4.3, Chapter 4**) indicates that gradual increases in cholesterol supplementation to lipid-depleted medium incrementally induced wild type *Npc2c* expression. However in *DHR96*<sup>l</sup> mutants, *Npc2c* was unresponsive to dietary cholesterol changes, suggesting that *Npc2c* is regulated by *DHR96* to adapt to changing cholesterol levels for its subsequent trafficking and metabolism. Hence my follow up studies focused on characterizing *Drosophila Npc2c* function, using: (1) *Npc2c-RNAi* transgenic lines: VDRC #31139 (*Npc2c*<sup>GD6798</sup>) and #101583 (*Npc2c*<sup>KK103904</sup>), and (2) two media types: LD and SM. Wild type *Npc2c* expression increases upon increasing dietary cholesterol levels; hence I used both lipid-depleted medium (where *Npc2c* is lowly expressed and we hypothesize *DHR96* protein is active) and SM (*Npc2c* transcripts are ~10–fold higher (**Figure 3.2**), and where *DHR96* protein is presumably inactive).

### 5.2.1. Ubiquitous *Npc2c* knockdown *in vivo*

I have used vertically stacked columns to show the distribution of *Npc2c-RNAi* phenotypes among the various developmental stages. Each stacked column (shown in **Figures 5.8 to 5.12, 5.15 and 5.21**) represent the proportion of adult survivors versus the proportion of animals that failed to develop beyond larval and/or pupal stage in a population of 100 age-matched *Npc2c-RNAi* embryos monitored daily for 15 days. The data represented in every column is an average of 3-4 populations, and standard deviations are represented as error bars. Unless otherwise mentioned, animals that are described to have

‘arrested development’ failed to develop any further, yet were phenotypically normal in appearance and survived in that specific developmental stage for about 10 days AED. I used two independent *RNAi* transgenic lines: *Npc2c*<sup>GD6798</sup> (VDRC line #31139) and *Npc2c*<sup>KK103904</sup> (VDRC line #101583).

The *Npc2c*<sup>KK103904</sup> caused moderate repression of *Npc2c* transcripts (**Figure 5.5**) and resulted in partial lethality phenotypes with incomplete penetrance. On SM, ~40% of the progeny eclosed to viable adults, and the remaining ~15%, ~30% and ~15% of the population, respectively, failed to develop beyond the L2, L3 and pupal stages (**Figure 5.9**). Interestingly, surviving larvae, pupae or adults were considerably larger in size than controls (**Figure 5.6**), revealing a novel role for *Npc2c* in the CNS. On LD medium (**Figure 5.7**) that normally resulted in ~10-15% L2 lethality in controls, had no additional adverse effects on the survival of *Npc2c-RNAi* animals, suggesting that the observed phenotype does not result from a mere dietary nutrient unavailability. On the other hand, the *Npc2c*<sup>GD6798</sup> achieved >90% knockdown of *Npc2c* transcripts (**Figure 5.5**) and produced a L3 arrest phenotype with complete penetrance (**Figure 5.8**). Hence, I used this line for all subsequent *in vivo* *Npc2c* phenotypic studies.

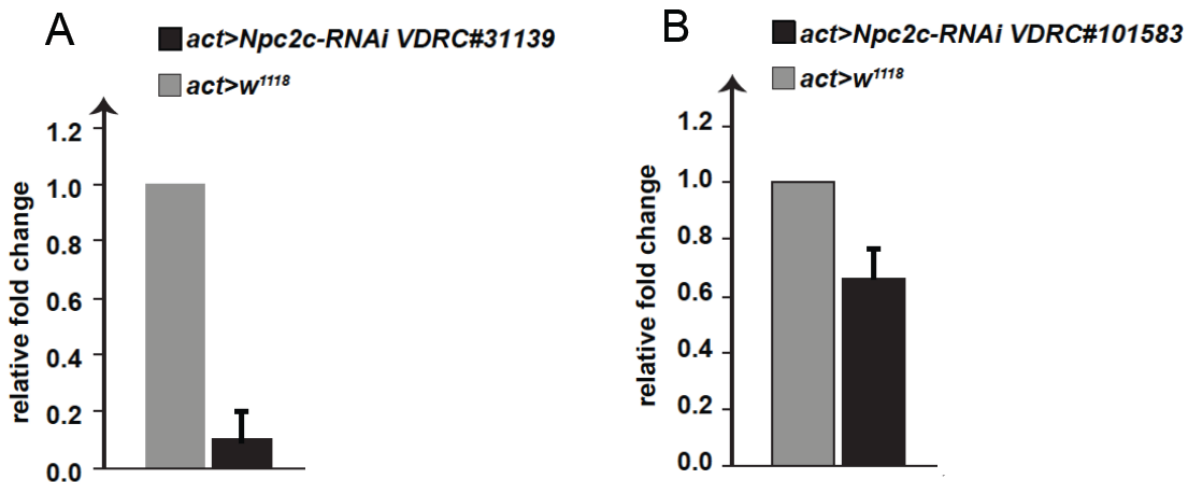


**Figure 5.5. Validating the effectiveness of two independent *Npc2c-RNAi* transgenic lines.** Whole body RNA was collected from wandering L3 larvae from the control *actin-Gal4>w<sup>1118</sup>* and the two *actin-Gal4>Npc2c-RNAi* lines (A) VDRC#31139 (B) VDRC#101583. Animals were staged at 40 h after L2/L3 molt on standard media. Error bars represent 95% confidence intervals, and *p* values were calculated with the unpaired Student's *t*-test. All bar graphs represent qPCR data showing transcript levels of *Npc2c*. Fold changes are relative to the respective expression of *Npc2c* in the control *act-Gal4 > w<sup>1118</sup>*, as shown in grey bars. The VDRC line#31139 achieved more effective knockdown of *Npc2c*.

Figure 5.6

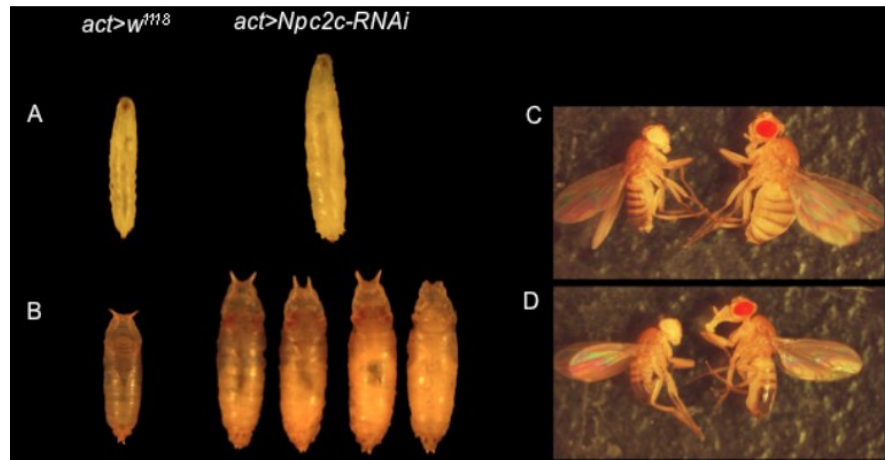


**Figure 5.6. *Npc2c-RNAi* phenotypes.** Images **A-D** depict the enlarged body size phenotypes of *act>Npc2c-RNAi* using the **VDRC#101583** on SM. **(A)** mid-L3; **(B)** pupae; **(C)** male & **(D)** female adult flies.

**Figure 5.7. Ubiquitous *Npc2c-RNAi* using the VDRC#101583 transgenic line exhibits low penetrance and produces a range developmental phenotypes.** Stacked columns represent the proportion of adult survivors in a population versus the proportion of animals that do not develop beyond larval or pupal stages, as indicated: L1; solid white bars, L2; diagonal black stripes, L3; grids, pupae; solid black bars, adults; solid grey bars, respectively. 100 embryos of each genotype, as listed on the X-axis, were transferred to either lipid-depleted (LD) media **(A)**, or LD media supplemented with 100 $\mu$ g 20E **(B)**, 200 $\mu$ g cholesterol **(C)**, or 200 $\mu$ g 7DC **(D)**, **(E-H)** 100 embryos of each genotype, as listed on the X-axis, were transferred to either standard media (SM) **(E)**, or SM supplemented with 1.65mg each of 20E **(F)**, cholesterol **(G)**, or 7DC **(H)**. These populations were scored daily for 12 days by counting the number of viable animals at every developmental stage. Error bars represent standard deviation calculated from 4-5 replicates (each containing 100 embryos). 20E; 20-hydroxyecdysone, 7DC; 7-dehydrocholesterol, *act-Gal4* transgene drives expression ubiquitously.

**(Figure 5.7. next page)**

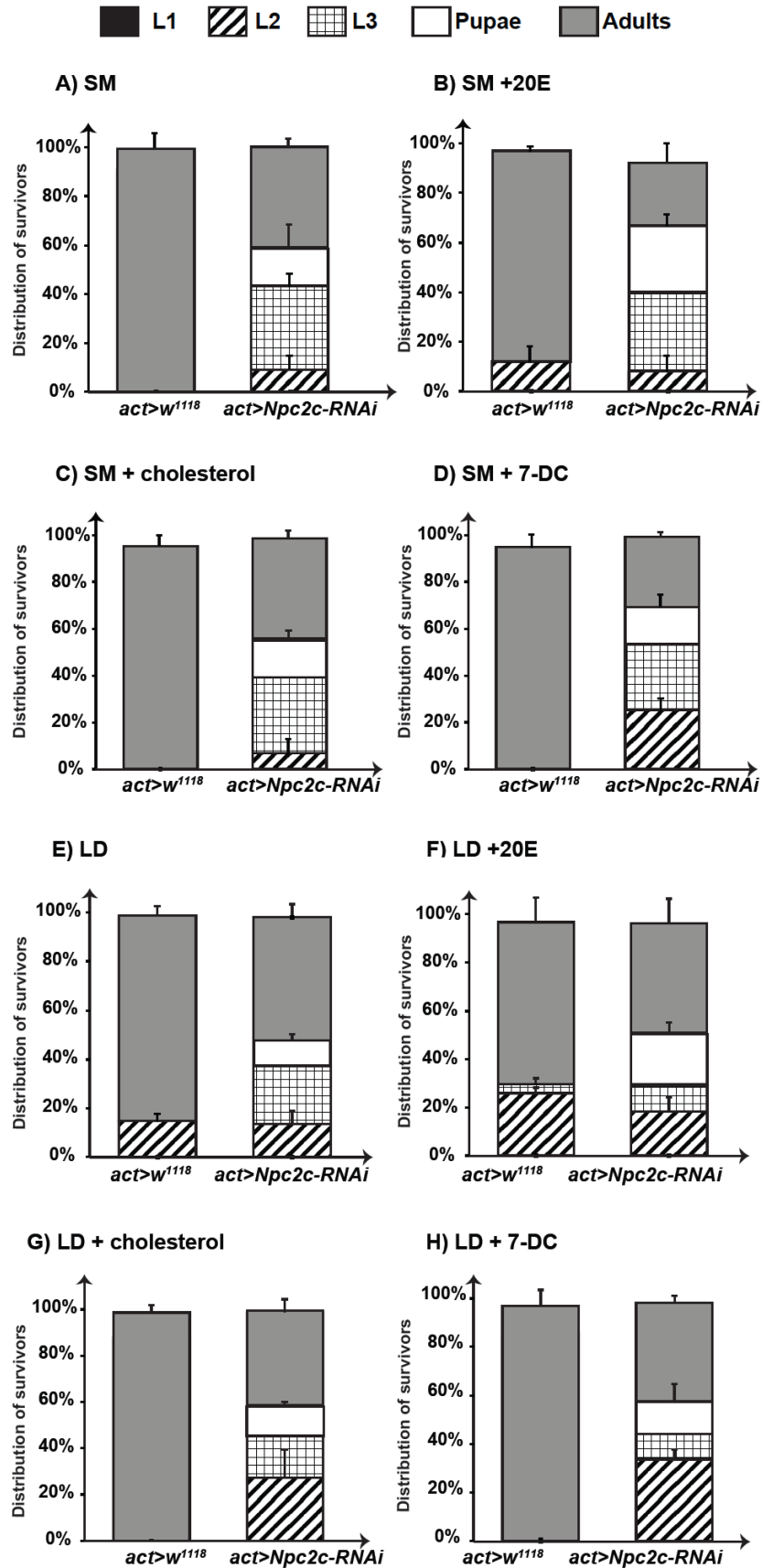
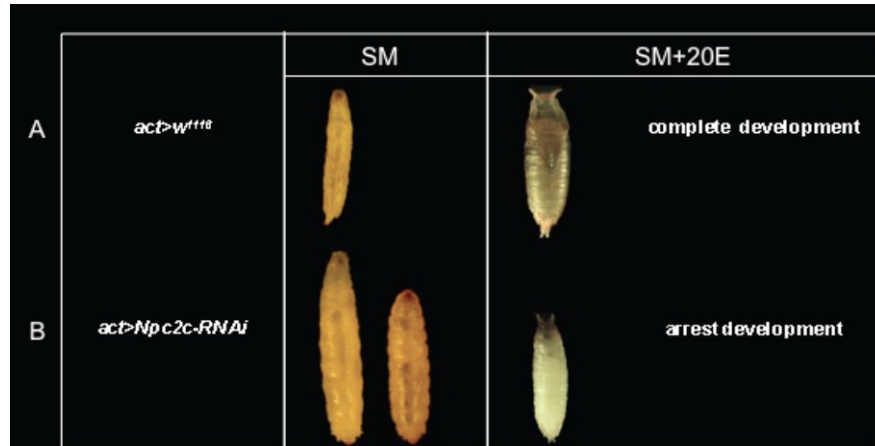


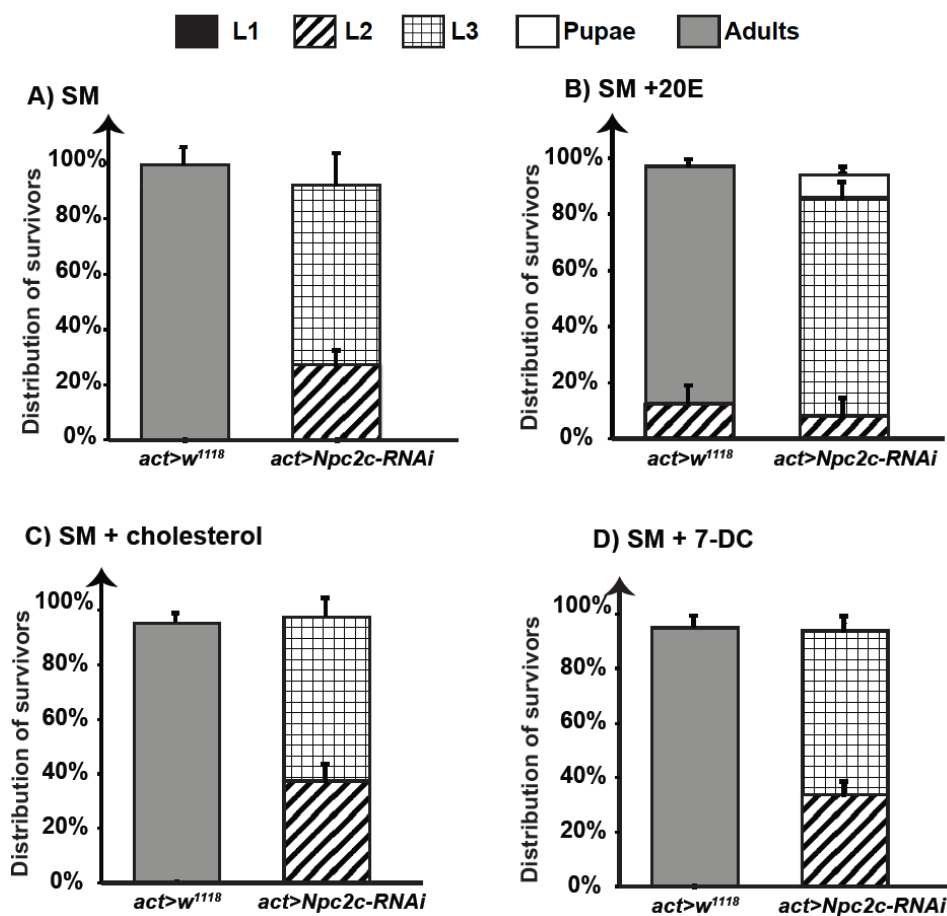
Figure 5.8

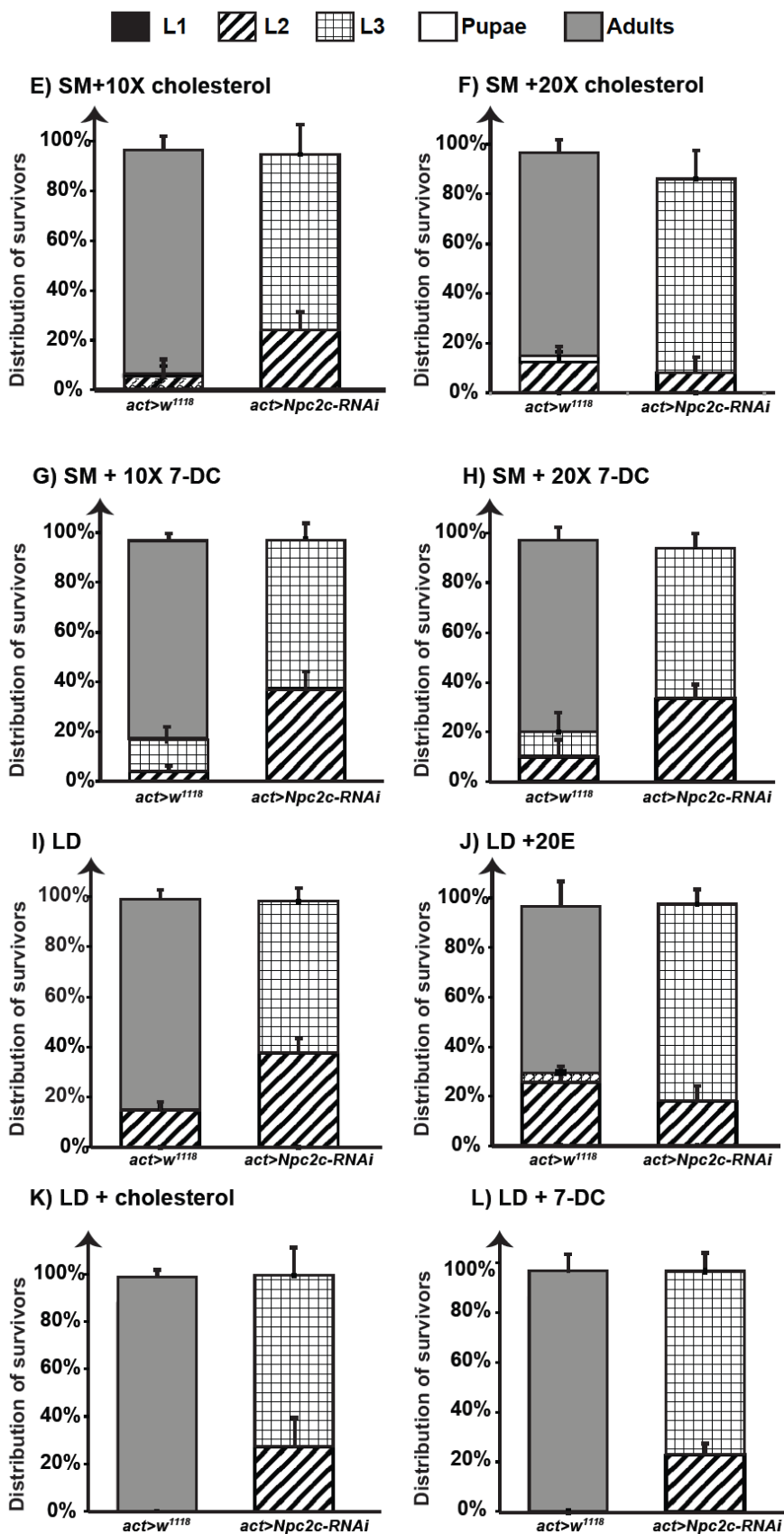


**Figure 5.8. Summary of ubiquitous *Npc2c-RNAi* developmental phenotypes.** A & B are representative images of the larval arrest phenotypes of the ubiquitous knockdown of *Npc2c* using the **VDRC#31139**, when raised on standard medium (SM) or SM supplemented with 0.33mg 20E which partially rescues these giant L3 to pupal stages that never eclose to adult flies. 20E; 20-hydroxyecdysone, *act-Gal4* transgene drives expression ubiquitously.

**Figure 5.9: Ubiquitous knockdown of *Npc2c* (VDR#31139) causes developmental arrest during larval stages.** Stacked columns represent the proportion of adult survivors in a population versus the proportion of animals that do not develop beyond larval or pupal stages, as indicated: : L1; solid white bars, L2; diagonal black stripes, L3; grids, pupae; solid black bars, adults; solid grey bars, respectively. **(A-D)** 100 embryos of each genotype, as listed on the X-axis, were transferred to either standard media (SM) **(A)**, or SM supplemented with 1.65mg each of 20E **(B)**, cholesterol **(C)**, or 7DC **(D)**. **(E-H)** 100 embryos of each genotype, as listed on the X-axis, were transferred to standard media supplemented with higher sterol concentrations: 16.5mg of cholesterol **(E)**, or 33mg of cholesterol **(F)**, 16.5mg of 7DC **(G)**, or 33mg 7DC **(H)**. **(I-L)** 100 embryos of each genotype, as listed on the X-axis, were transferred to either lipid-depleted (LD) media **(I)**, or LD media supplemented with 100 $\mu$ g 20E **(J)**, 200 $\mu$ g cholesterol **(K)**, or 200 $\mu$ g 7DC **(L)**. These populations were scored daily for 12 days by counting the number of viable animals at every developmental stage. Error bars represent standard deviation calculated from 4-5 replicates (each containing 100 embryos). 20E; 20-hydroxyecdysone, 7DC; 7-dehydrocholesterol, *act-Gal4* transgene drives expression ubiquitously.

(Figure 5.9. continued on next page)





On SM, the majority of animals that ubiquitously expressed *Npc2c-RNAi* (#31139) failed to develop beyond L3 (**Figure 5.9**). The remainder ~30% of *Npc2c-RNAi* animals which arrested as L2, also failed to survive after day 5 AED. The L3 animals however continued to survive, without further development, and ~8% of them transformed into ‘giant larvae’ (**Figure 5.7**), strongly implying a role for *Npc2c* in pathways that regulate larval development and metamorphosis. To test if animals displayed a development arrest due to impaired availability of molting hormone, I supplemented SM with 20-hydroxyecdysone (20E), and its precursors, cholesterol (C) or 7-dehydrocholesterol (7DC). At all concentrations tested, i.e. 1.65 mg of each sterol (**Figure 5.9 A-D**) or higher (**Figure 5.9 E-H**) was unable to fully rescue the larval arrest phenotype to adult stages, suggesting that mere scarcity of dietary sterols is likely not responsible for the observed developmental defect. On the other hand, supplementing 1.65mg of 20E accelerated growth by a day, and partially rescued ~7% of *Npc2c-RNAi* animals to pupae that never eclosed. Although the **partial rescue** could indicate a hormonal deficiency, it is likely that the dietary-derived molting hormone is incapable of mimicking the *in vivo* ecdysone pulses and its downstream signaling effects during development and metamorphosis. Alternatively, it is likely that these dietary sterols are not available in a specific structural form or subcellular location, so that cells may utilize appropriate sterols for membrane function, signaling, steroid synthesis, or other unknown functions.

In control populations, while 1.65 mg of 20E accelerated growth by 1-2 days and caused lethality in ~10% L2, 1.65 mg of C or 7DC produced no toxic effects on the viability of controls. I also observed a mild-to-moderate degree of toxicity with 16.5mg of C, which caused ~2% pupal and ~5% L3 lethality in controls. Expectedly, 33mg of C demonstrated higher toxicity and caused developmental arrest of ~4% and ~16% of the population as pupae and L3, respectively. It is possible that synthetic sterols are not available in the biological form for proper absorption, or that synthetic dietary sterols in excess of the optimal physiological needs could result in toxicity due to reduced clearance and utilization. Alternatively, uptake of synthetic sterols may interfere with the uptake and metabolism of other dietary nutrients. These factors may partially explain why some sterol analogs are incapable of functionally substituting for *in vivo* sterol/sterol intermediates. Animals in all phenotypic classes continued to survive in their respective stages until day 10-13 AED,

while rest of their population eclosed as normal healthy adults. In comparison, 7DC demonstrated higher toxicity. In controls, 16.5 mg of 7DC caused developmental arrest of ~5% of the population as pupae, ~10% as L3 and ~5% as L2. 33 mg of 7DC caused developmental arrest as ~10% L3 and ~10% L2, which continued to survive in these stages until day 10-13 AED, while the rest ~80% of the population developed into normal healthy adults. However, in *Npc2c-RNAi* animals, this range of lethality due to sterol toxicity was not observed and the *Npc2c* knockdown phenotype remained consistent, appearing to override the likely effects of toxicity.

On lipid-depleted medium, ~15% of the control *act>w<sup>1118</sup>* populations arrested as L2 and failed to survive past day 4 AED, resulting in a net ~85% adult survivors, likely because of lack of essential nutrients, particularly the critical dietary sterols. Supplementing LD medium with 200 µg of C or 7DC was sufficient to boost survival of controls to ~100% normal healthy adults, which is in line with the fact that *Drosophila* is a cholesterol auxotroph and dietary cholesterol is an obligate requirement for normal growth and development. In contrast to controls, ~60% and ~40% of ubiquitous *Npc2c-RNAi* animals arrested as L3 and L2, respectively, and continued to survive in these stages until day 10-13 AED. In contrast to the partial rescue that was observed on SM containing 20E, adding back 100µg of 20E to LD (**Figure 5.9 I-L**) failed to rescue the L3 arrest of *Npc2c-RNAi* animals to any degree, further strengthening the inference that the observed developmental arrest phenotype is not a mere consequence of ecdysteroid deficiency. Rather, based on our knowledge that the cholesterol transporter mammalian NPC2 binds a range of cholesterol-related molecules, such as cholesterol precursors, plant sterols, oxysterols, cholesterol sulfates, cholesterol acetates, and 5- $\alpha$ -cholestan-3-one; it is likely that the *Npc2c* - knockdown phenotype is a result of cellular inability to utilize a special class of sterols or metabolites, not limited to cholesterol, and which have critical metabolic functions in addition to steroid synthesis and development. Similar to our observation on SM, 100 µg each of C or 7DC also failed to rescue the *Npc2c-RNAi* phenotype. In controls, 100µg of 20E-related toxicity caused ~25% L2 and ~3% L3 arrest, whereas 200 µg each of C or 7DC produced no adverse toxic effects on viability. Thus, on both sterol-supplemented SM and lipid-depleted medium, ubiquitous knockdown of *Npc2c* adversely affected larval development at the late-L3 stage, indicating that *Npc2c* is an essential *Drosophila* gene.

Supplementing the media with the molting hormone or its precursors, cholesterol and 7-dehydrocholesterol failed to achieve phenotypic rescue to adult stages, suggesting that *Npc2c* is required to utilize the supplemented dietary sterols and presumably, other sterol classes as well, for cellular functions that extend beyond transporting cellular cholesterol for ecdysteroid production.

### 5.3. Exploring the tissue-specific functions of *Drosophila Npc2c*

Although it appeared that *Npc2c-RNAi* animals exhibited a systemic sterol defect that manifested in a developmental phenotype, I wanted to gain a better understanding of the cellular functions of *Npc2c*, based on the tissues it was most expressed in. The FlyAtlas Anatomical Expression data indicates that based on the microarray signal intensities, *Npc2c* is most highly expressed in the larval and adult midgut, followed by expression in larval and adult central nervous system and fat body, Malpighian tubules, and salivary gland, suggesting that *Npc2c* may have overlapping roles in tissues that actively absorb, transport and metabolize dietary sterols. To understand what function of *Npc2c* is indispensable for wild type survival on SM and LD, I triggered tissue-specific *Npc2c-RNAi* and asked in which tissue was *Npc2c* knockdown sufficient to recapitulate the larval arrest phenotypes associated with the ubiquitous *Npc2c-RNAi*. Furthermore, I used defined sterol diets to test if these tissue-specific *RNAi* phenotypes were influenced by dietary cholesterol conditions. If such an apparent correlation were evident, it would strengthen my hypothesis that *Npc2c* has critical tissue-specific functions in cellular cholesterol uptake and metabolism. The phenotypic results shown in **Figure 5.10** indicated that irrespective of the dietary sterol content, knockdown of *Npc2c* in the fat body, malpighian tubules and salivary gland cells failed to affect survival or developmental progression and thus exhibited no observable phenotypes in the progeny. In contrast, the knockdown of *Npc2c* in two tissues was sufficient to phenotypically impair larval development and survival: (a) the midgut (Figure 5.11), which is critical for dietary sterol absorption, and (b) the prothoracic gland (Figure 5.15), a component of the ring gland is the site of ecdysteroid production.



**Figure 5.10: Knockdown of *Npc2c* in the fat body, malpighian tubules and salivary gland has no observable effect on development or survival**

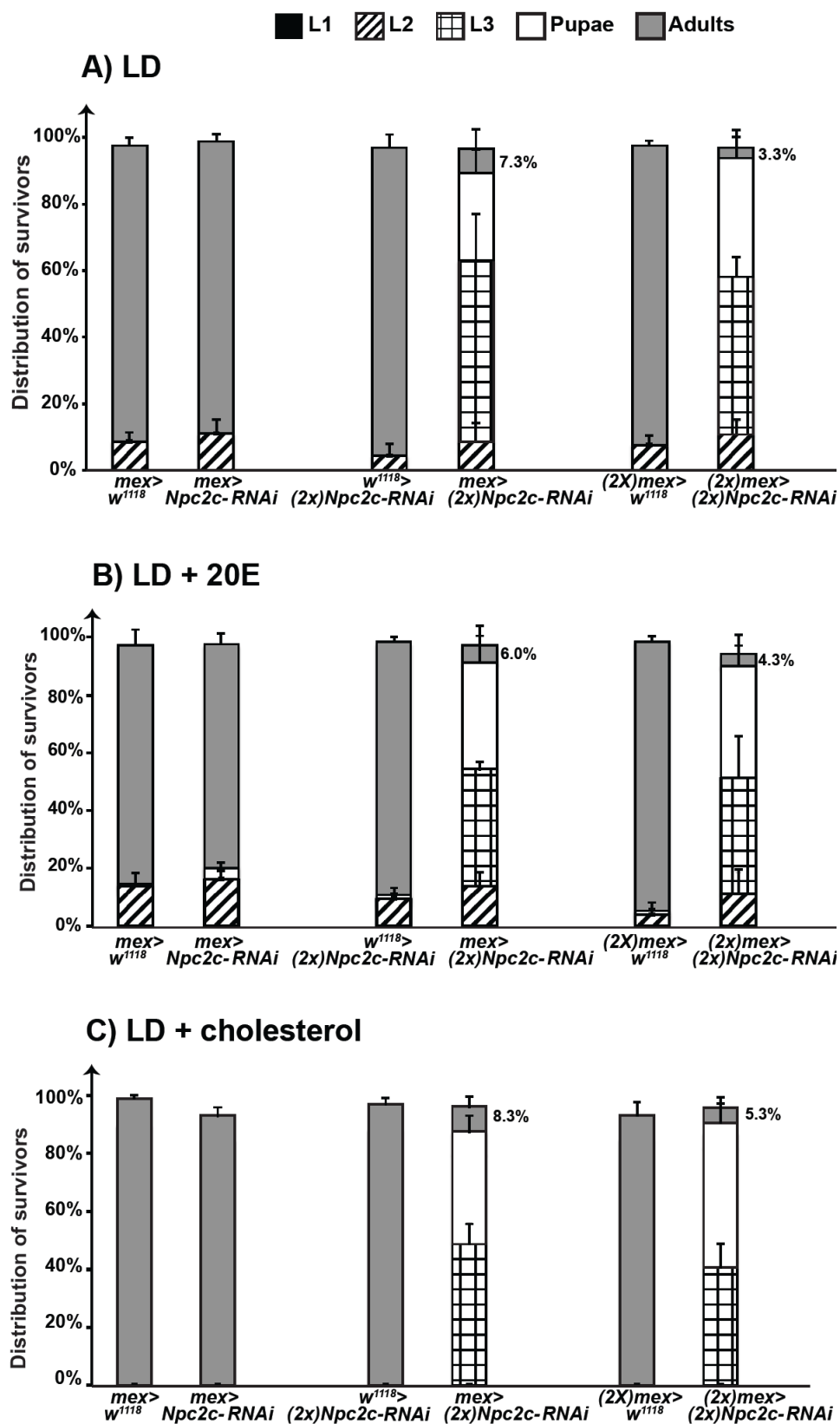
Stacked columns represent the proportion of adult survivors in a population versus the proportion of animals that do not develop beyond larval or pupal stages, as indicated: L1; solid black bars, L2; diagonal black stripes, L3; grids, pupae; solid white bars, adults; solid grey bars, respectively. 100 embryos of each genotype, as listed on the X-axis, were transferred to either standard medium (SM) or lipid-depleted (LD) media. These populations were scored daily for 12 days by counting the number of viable animals at every developmental stage. Error bars represent standard deviation calculated from 3 replicates (each containing 100 embryos). *cg-*, *c42-*, *c724-* and *sd-Gal4* transgenes drive expression specifically in the fat body, principal and secondary cells of malpighian tubules, and in the salivary gland.

#### 5.4. Midgut-specific knockdown of *Npc2c* has dose-dependent effects on development

I used the malic enzyme modifier (*mex*)-*Gal4* to achieve midgut-specific *Npc2c-RNAi*, as shown in **Figures 5.11 to 5.13**. Single copies of each of the *mex-Gal4* driver and the UAS-*Npc2c-RNAi* transgenes produced no observable lethality or developmental defects in progeny raised on lipid-depleted or SM. However, using two copies of the *RNAi* transgene (with one copy of the driver) resulted in severe larval and pupal lethality in ~85% (on LD media) to 92% (on SM) of the progeny. Whereas, doubling both the UAS-*Npc2c-RNAi* and *mex-Gal4* transgenes produced a dose-dependent lethality effect causing ~97% of the progeny to arrest development in larval and pupal stages irrespective of whether they were reared on the sterol-rich SM or lipid depleted media. In contrast to the complete penetrance observed in *act>Npc2c-RNAi* larvae, the proportion of *mex>Npc2c-RNAi* animals that did not demonstrate developmental defects consistently eclosed into phenotypically normal viable adult flies. Presumably the high expression of *Npc2c* transcripts in the midgut could cause variability in RNAi-silencing effects because higher amounts of dsRNA are required to effectively knockdown *Npc2c*. If *Npc2c* function within the midgut was linked to the first step in the uptake of dietary cholesterol (or other related sterols), I hypothesized that the observed developmental arrest phenotypes arose from a systemic unavailability of cholesterol for a variety of cellular functions including, but not limited to, membrane organization, signaling and ecdysteroid synthesis in the prothoracic gland. To test these possibilities, I supplemented LD and SM with 20E (molting hormone), 7DC (structurally similar to cholesterol and found in membranes) and cholesterol (C) itself. Specifically, I supplemented SM with 20E, C or 7DC (1.65 mg each; **Figure 5.11F**), or LD media with

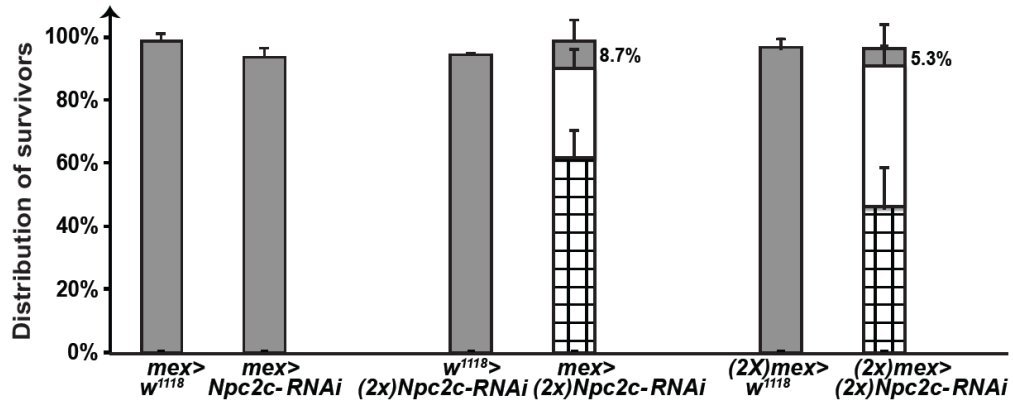
100 µg of 20E, and 200 µg of C and 7DC (**Figure 5.11 B-D**). In line with my observations with *act>Npc2c-RNAi* animals, all the aforementioned supplemented sterols failed to rescue any of the larval or pupal arrest phenotypes of *mex>Npc2c-RNAi* animals, indicating an indispensable sterol-related function for *Npc2c* within the midgut. Moreover, the phenotypic effects of *Npc2c-RNAi* are dependent on the dosage and strength of the *RNAi* effect, but independent of the sterol content in the media, suggesting that *Npc2c* function in the midgut is necessary for not only for cellular uptake of sterols from supplemented diets, but also in subsequent intracellular trafficking of absorbed sterols. In summary, the midgut-specific knockdown of *Npc2c* causes a late-larval lethality, and that this developmental arrest phenotype is unlikely to be a consequence of a mere sterol-derived ecdysone deficit.

Figure 5.11

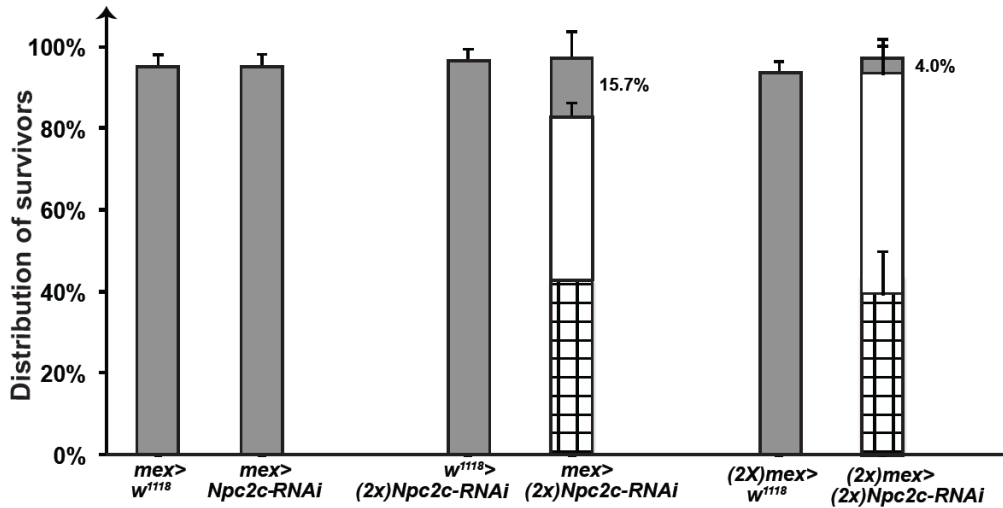


L1
  L2
  L3
  Pupae
  Adults

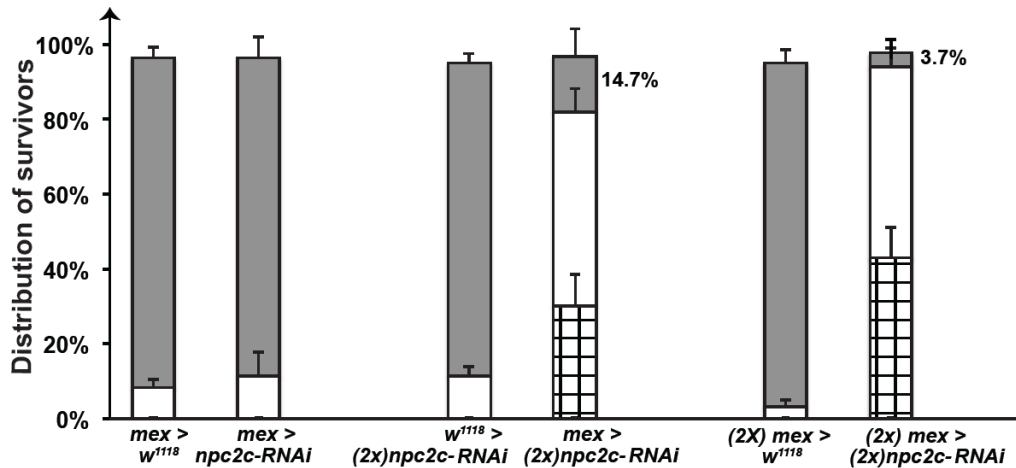
### D) LD + 7-dehydrocholesterol



### E) SM



### F) SM+20E



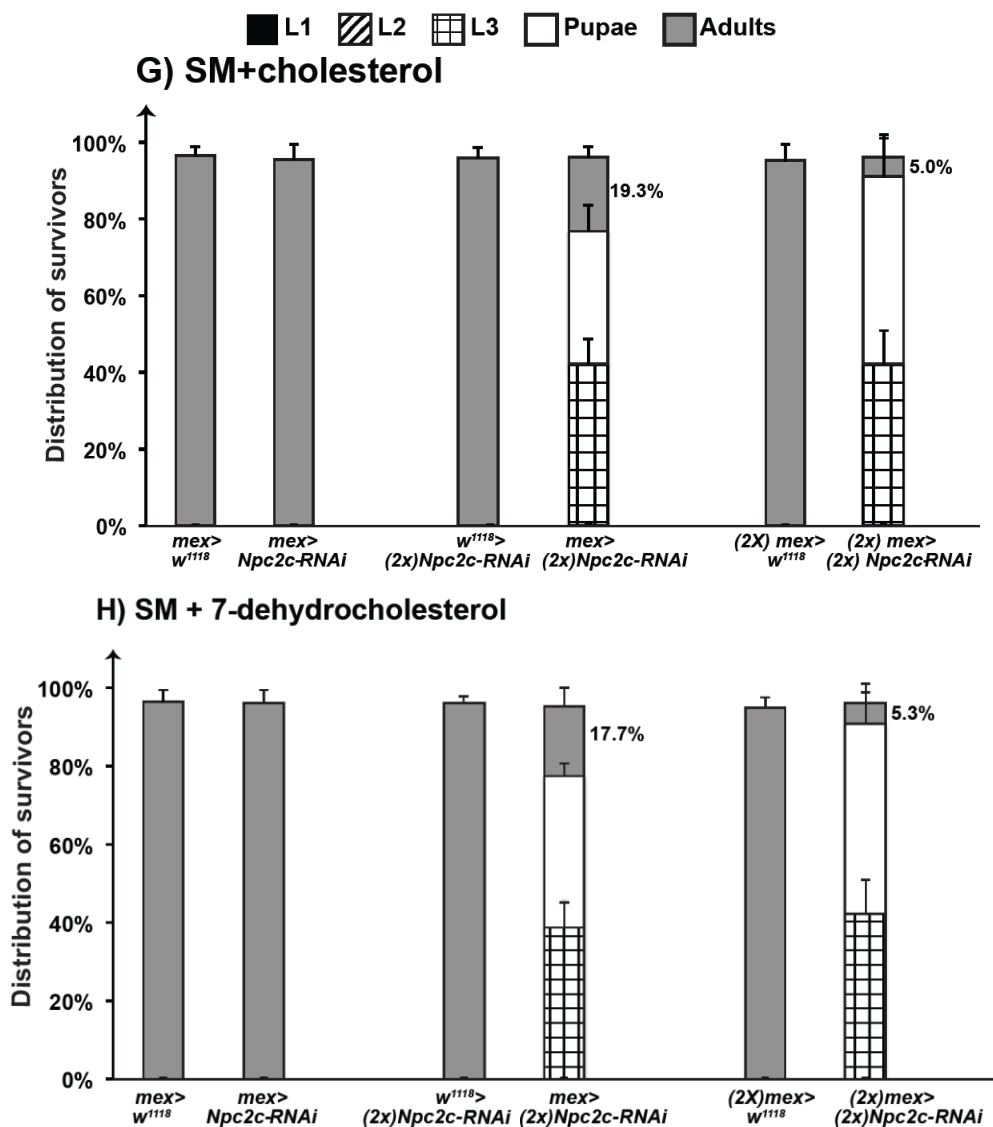


**Figure 5.11. Midgut-specific knockdown of *Npc2c* causes partial developmental arrest.** Stacked columns represent the proportion of adult survivors in a population versus the proportion of animals that do not develop beyond larval or pupal stages, as indicated: L1; solid white bars, L2; diagonal black stripes, L3; grids, pupae; solid black bars, adults; solid grey bars, respectively. **(A-D)** 100 embryos of each genotype, as listed on the X-axis, were transferred to either lipid-depleted (LD) media **(A)**, or LD media supplemented with 100 $\mu$ g 20E **(B)**, 200 $\mu$ g cholesterol **(C)**, or 200 $\mu$ g 7DC **(D)**. **(E-H)** 100 embryos of each genotype, as listed on the X-axis, were transferred to either standard media (SM) **(E)**, or SM supplemented with 1.65mg each of 20E **(F)**, cholesterol **(G)**, or 7DC **(H)**. Error bars represent standard deviation calculated from 3-4 replicates (each containing 100 embryos). 20E; 20-hydroxyecdysone, 7DC; 7-dehydrocholesterol, *mex-Gal4* transgene drives expression in the midgut.

#### 5.4.1. Midgut-specific knockdown of *Npc2c* alleviates *DHR96<sup>l</sup>* mutant phenotype on lipid-depleted media

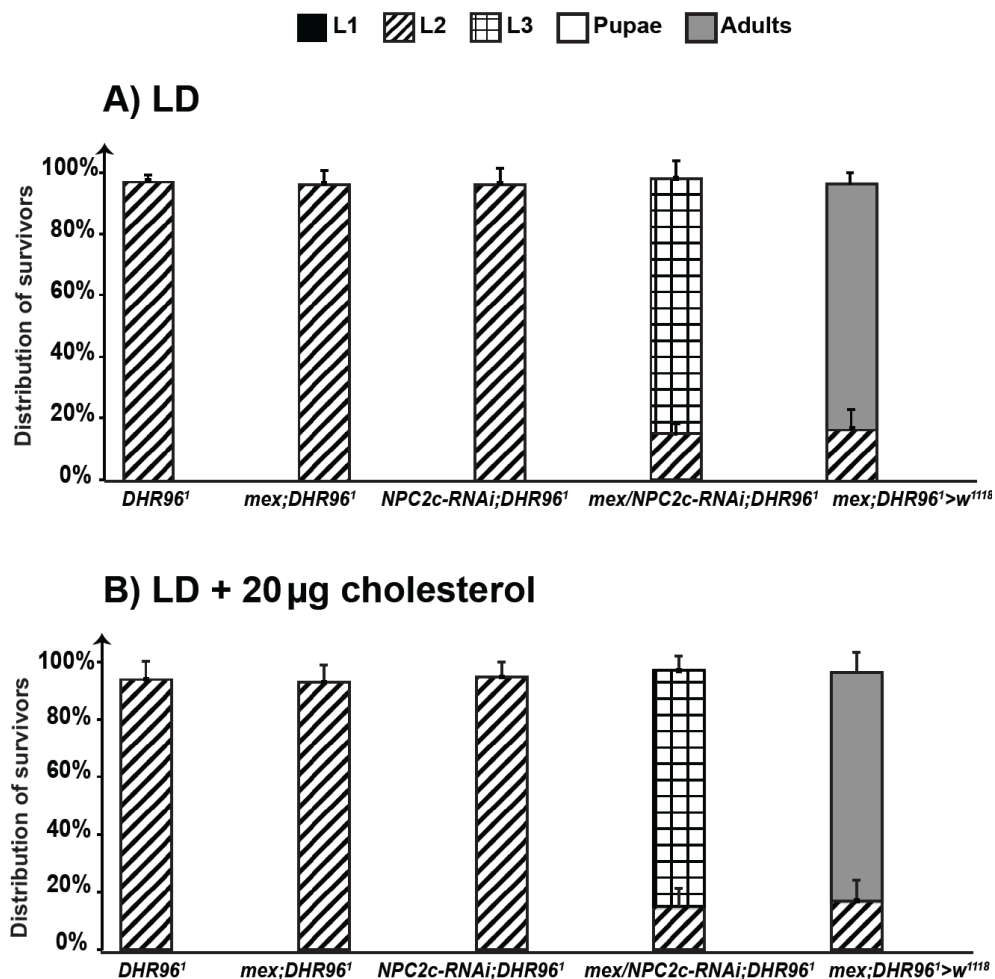
*Npc2c* expression is 5-fold induced in *DHR96<sup>l</sup>* mutants in comparison to wild type expression levels on lipid-depleted medium. Importantly, midgut-specific knockdown of *DHR96* was sufficient to fully recapitulate the *DHR96<sup>l</sup>* mutant phenotype on lipid-depleted media. Taking these observations together with the FlyAtlas RNA Seq data demonstrated that the tissue with highest expression of *Npc2c* was the midgut. Hence, I asked whether: (1) *DHR96* regulates *Npc2c* expression in the midgut, and (2) if the observed failure to repress *Npc2c* on LD medium is associated with the *DHR96<sup>l</sup>* mutant larval lethality.

To address this possible genetic interaction between *DHR96* and *Npc2c* in the midgut, I recombined the UAS-*Npc2c-RNAi* and *mex-Gal4* transgenes individually into the *DHR96<sup>l</sup>* mutant background and tested if the midgut-specific knockdown of *Npc2c* in *DHR96<sup>l</sup>* mutants might alleviate *DHR96<sup>l</sup>* mutant survival on LD medium (**Figures 5.12 and 5.13**). 100 age-matched embryos of each of the genotypes discussed below were transferred to LD medium. The total proportion of adult survivors compared to the proportion of animals that failed to develop beyond each larval or pupal stage are represented in vertically stacked columns. Each of the transgenic stocks; i.e. *Npc2c-RNAi;DHR96<sup>l</sup>* and *mex>DHR96<sup>l</sup>* fully recapitulated the *DHR96<sup>l</sup>* mutant phenotype, i.e. 100% L2 arrest. In a surprising finding, *mex-Gal4-DHR96<sup>l</sup>>Npc2c-RNAi -DHR96<sup>l</sup>* partially rescued ~80% of *DHR96<sup>l</sup>* mutants to L3, which followed normal developmental timing, i.e. molted 3 days AED and initiated wandering by day 5 AED. Although a partial rescue, **this** is the first observed rescue of *DHR96<sup>l</sup>* mutants on LD medium without any supplemented cholesterol. However, these rescued L3 animals were smaller in size (**Figure 5.13**), failed to pupariate and never completed development to adult stages. Since I did not observe a full survival rescue, I asked whether knocking down *Npc2c* could rescue *DHR96<sup>l</sup>* mutants by lowering cholesterol requirements needed to support *DHR96<sup>l</sup>* mutant development on LD medium. Hence, I raised *mex-DHR96<sup>l</sup>>Npc2c-RNAi -DHR96<sup>l</sup>* animals on LD medium containing cholesterol concentrations that have consistently failed to rescue *DHR96<sup>l</sup>* mutants, i.e. 20 µg and 40 µg. As positive and negative controls, I supplemented LD with 80

$\mu\text{g}$  of cholesterol and 100  $\mu\text{g}$  of 20E, respectively. These concentrations are identical to those that were used to rescue *DHR96<sup>l</sup>* mutants (detailed in **chapter 3**).

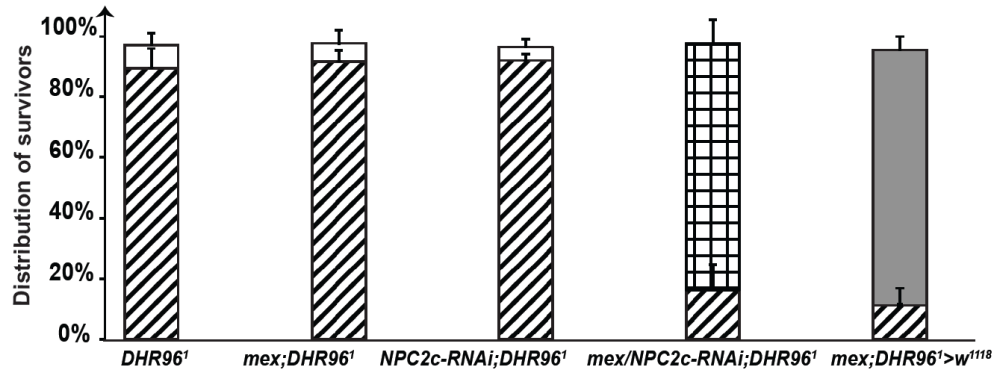
In a manner identical to *DHR96<sup>l</sup>* mutant phenotype, 20  $\mu\text{g}$  and 40  $\mu\text{g}$  of cholesterol, and 100  $\mu\text{g}$  of 20E also failed to rescue *mex-Gal4;DHR96<sup>l</sup>>Npc2c-RNAi -DHR96<sup>l</sup>* animals on LD medium (**Figure 5.12**), while 80  $\mu\text{g}$  fully rescued *DHR96<sup>l</sup>* mutants to adults (**Figure 5.12 D**). Taken together, my results demonstrate that the midgut-specific knockdown of *Npc2c* partially rescues *DHR96<sup>l</sup>* mutants to mid-wandering L3 stages on LD medium, suggesting that predicted cellular cholesterol transport function of *Npc2c* in midgut cells is transcriptionally linked to *DHR96* function, thus providing a homeostatic link between dietary cholesterol and the transcriptional control of cholesterol metabolism in the midgut.

**Figure 5.12**

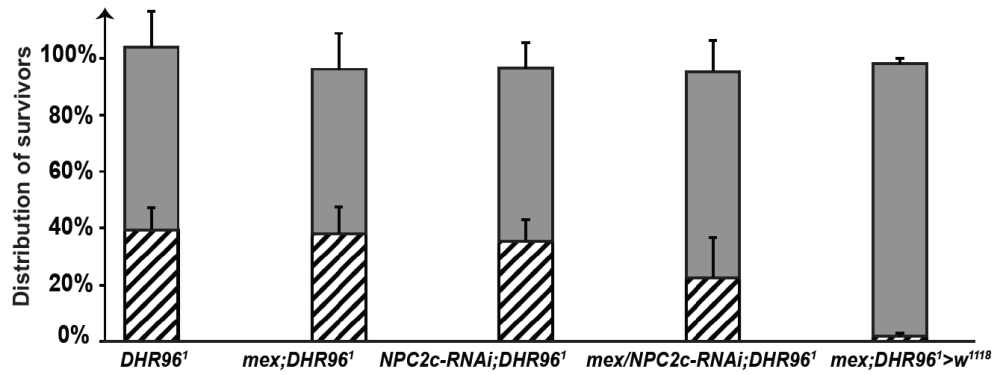


■ L1    ▨ L2    ▩ L3    □ Pupae    ■ Adults

### C) LD + 40 µg cholesterol



### D) LD + 80 µg cholesterol



### E) LD + 100 µg 20E

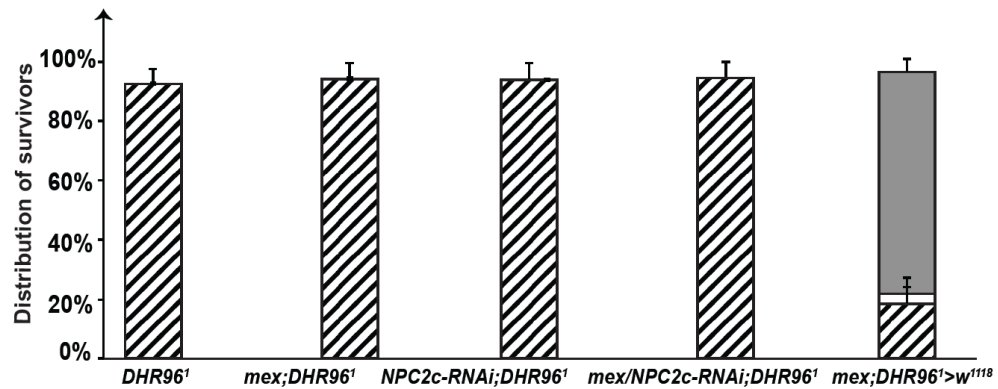


**Figure 5.12. Midgut-specific knockdown of *Npc2c* alleviates *DHR96*<sup>1</sup> mutant phenotype on lipid-depleted media.** Stacked columns represent the proportion of adult survivors in a population versus the proportion of animals that do not develop beyond larvae or pupal stages, as indicated: : L1; solid white bars, L2; diagonal black stripes, L3; grids, pupae; solid black bars, adults; solid grey bars, respectively. (A-E) 100 embryos of each genotype, as listed on the X-axis, were transferred to either lipid-depleted (LD) media (A), or LD media supplemented with 20µg cholesterol (B), 40µg cholesterol (C), 200µg cholesterol (D), or 100µg 20E (E). *DHR96*<sup>1</sup> animals arrest development as L2 on LD media and are partially rescued to L3 stage on LD media when combined with a midgut-specific knockdown of *Npc2c*. Error bars represent standard deviation calculated from 3-4 replicates (each containing 50 embryos). 20E; 20-hydroxyecdysone, 7DC; 7-dehydrocholesterol, *mex-Gal4* transgene drives expression in the midgut, *DHR96*<sup>1</sup>; *DHR96*<sup>1</sup> mutant.

Figure 5.13.

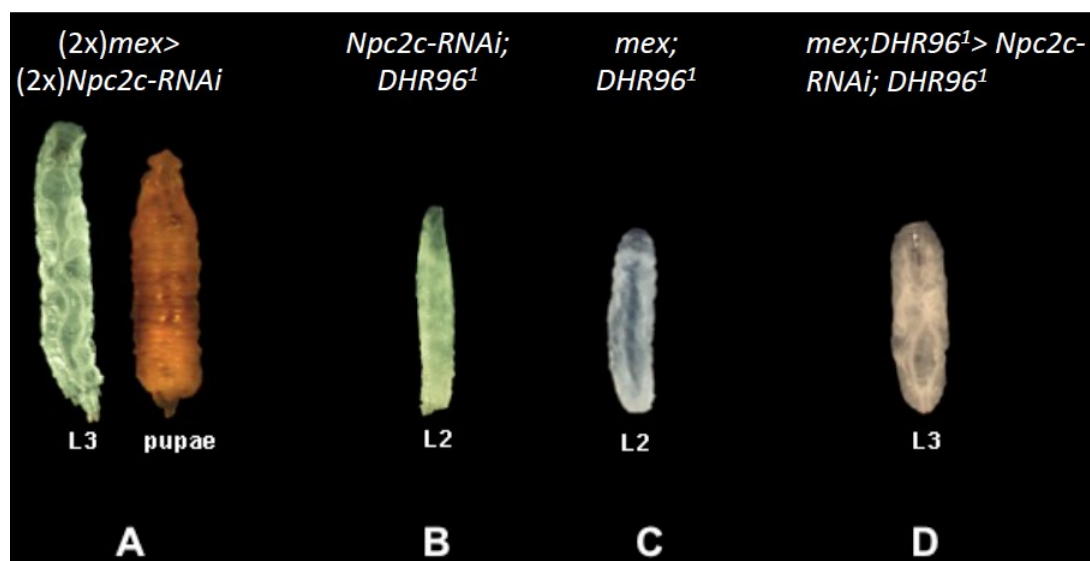


**Figure 5.13. Partial rescue of the *DHR96*<sup>1</sup> mutant phenotype by the midgut-specific knockdown of *Npc2c*.**

On lipid-depleted medium, the midgut-specific knockdown of *Npc2c* transcripts containing two copies of the respective driver (*mex-Gal4*) and responder (*UAS-Npc2c-RNAi*) transgenes arrest development in the late L3 and pupal stages (A). On the other hand, the *Npc2c-RNAi* (B) or the *mex-Gal4* (C) transgenic controls, both carrying the *DHR96*<sup>1</sup> mutation, fail to develop past early-mid L2 larva. Expression of midgut-specific *Npc2c-RNAi* in *DHR96*<sup>1</sup> mutants (D) partially rescued the developmental arrest phenotype of *DHR96*<sup>1</sup> mutants to L3 stages, suggesting possible epistatic interactions between *DHR96* and *Npc2c*. These rescued L3 animals however continued to wander by day 6 AED but never pupariated. *mex-Gal4* transgene drives expression specifically in the midgut.

### 5.5. A novel role for *Npc2c* in the prothoracic gland

The *Drosophila* neuropeptide prothoracicotrophic hormone (PTTH) triggers synthesis and release of ecdysone in the PG cells, and thereby controls the timing of developmental transitions and larval body size [79]. Previous studies [167] [168] indicated that PTTH binds its receptor Torso, to trigger ecdysone production via the Ras, Raf and ERK/MAPK\* pathway. PG-specific knockdown of *torso* reportedly caused a 5.8-day delay in pupariation. This resulted in excessive growth and giant-sized pupae, which subsequently eclosed into viable and fertile adults after 3 days [168]. In a different line of studies, Ou *et al.*, (unpublished data) have conducted ring gland-specific microarrays from L3 animals that were staged at -18h and -8h before puparium formation. These time points were chosen since they correlate with the low and high ecdysone pulses, respectively, of the PTTH signal during the L3 stage [79]. Results from this array showed that, at both time points tested, the constitutively active form of *Ras* (the downstream target of PTTH), i.e. *Ras<sup>v12</sup>*, repressed *Npc2c*, while the PG-specific knockdown of the PTTH receptor *torso*, relieved the repression (**Figure 5.29** and **Chapter 1 - Figure 1.3**). This raised the question whether PTTH signaling might regulate *Npc2c* expression within the PG. A similar trend, yet of lower magnitude of fold-change values was also observed with *Npc2h*, but not in any other *Npc2* gene family (**Figure 5.29**), suggesting that these *Npc2* genes might have similar functions in this tissue. The single vertebrate homolog of the 8-member *Drosophila Npc2* gene family is a known lysosomal luminal protein with direct roles in cellular sterol transport [19], [169]–[173]. Since the ubiquitous knockdown of only *Npc2c* (among the 8-member *Npc2* gene family) resulted in a developmental arrest (data not shown), I focused my attention to *Npc2c* and tested the hypothesis that if *Npc2c* functions in a manner similar to vertebrate NPC2 in the lysosomal organelles of PG cells, then it represents one of the final steps in a pathway that is critical to transport cholesterol out of the lysosomes to make it available for ecdysone synthesis in the PG.

To characterize *Npc2c* function in the prothoracic gland, I triggered prothoracic gland (PG)-specific knockdown of *Npc2c* on SM (**Figure 5.15**). It resulted in ~80% and ~20% of the population to arrest as L3 and L2, respectively, that continued to survive at

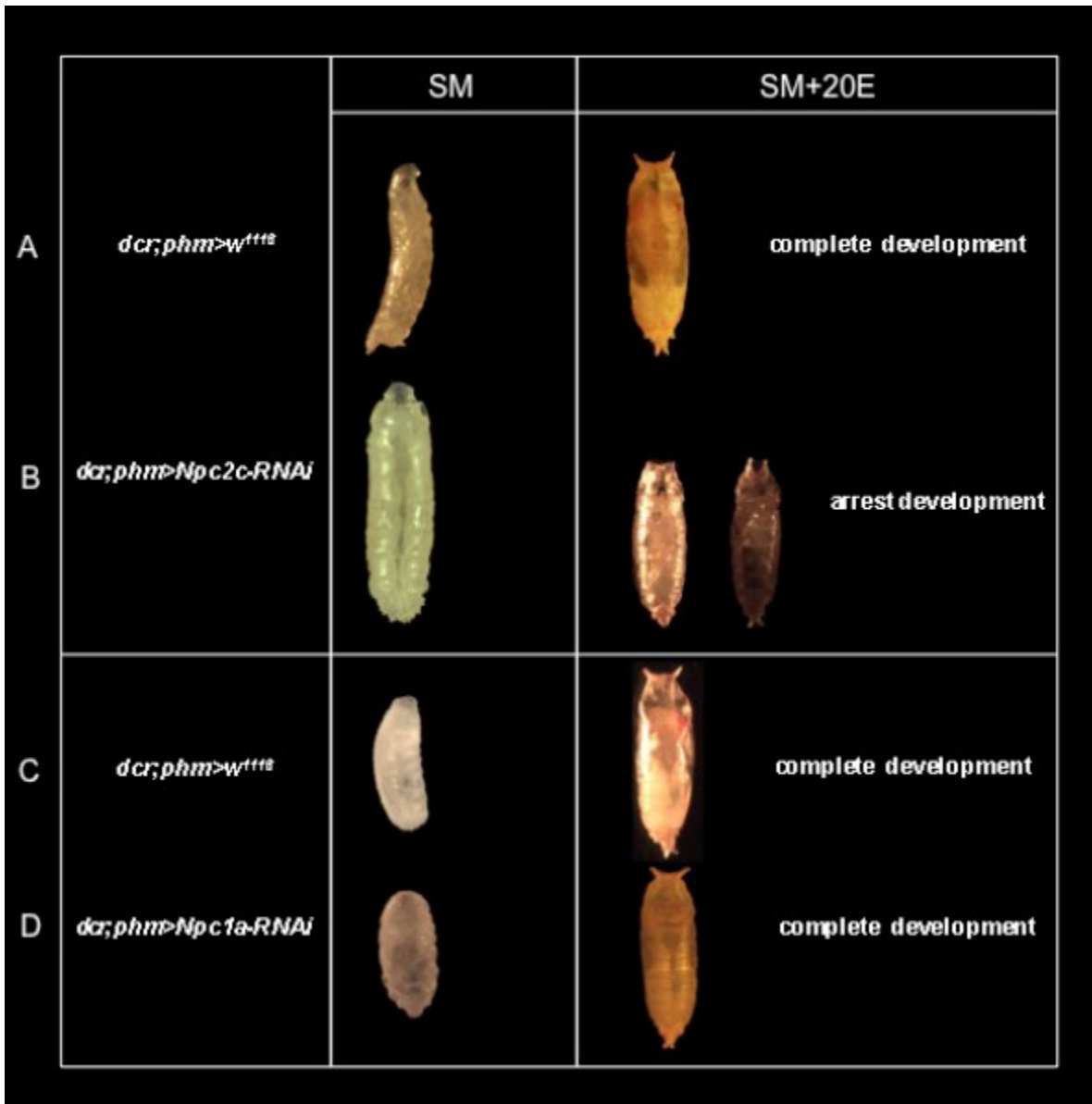
---

\* **Ras**; Rat sarcoma, **RAF**; Rapidly Accelerated Fibrosarcoma, **ERK**; Extracellular signal-regulated kinase, **MAPK**; mitogen-activated protein kinase

these stages until day 10-16 AED. This prolonged larval stage transformed ~85% of the surviving L3s into ‘giant larvae’ (**Figure 5.14**). To test if this apparent failure to pupariate resulted from a hormonal deficiency, I supplemented the SM with 20E, or its precursors C or 7DC, at a range of concentrations: 1.65 mg, 16.5 mg and 33 mg, which however all failed to achieve phenotypic rescue to adulthood (**Figure 5.15**). The 20E-supplemented SM partially rescued ~50% of ‘giant larvae’ to pupae, which were consistently smaller than controls (**Figure 5.14**) and never eclosed to adults, presumably because the diet-derived hormone was insufficient to recapitulate the endogenous ecdysone pulses required for normal development and metamorphosis. To test if *Npc2c* knockdown within the PG correlates with dietary sterol load, I triggered *dcr;phm>Npc2c-RNAi* on the LD medium (**Figure 5.15**), with or without supplemented 20E (100 µg), C or 7DC (200 µg, each). While ~20% of control populations were L2 lethal, due to inherent sterol deprivation on LD medium, these larvae were fully rescued to adults on C or 7DC supplemented diets. In contrast, ~82% and ~18% of *Npc2c-RNAi* animals arrested as L3 and L2, respectively, which continued to survive until 10-13 days AED. ~11% of this L3 population demonstrated the “giant larvae” phenotype, while the majority of the L3s survived as normal-sized larvae until day 12-13 AED, indicating that PG-specific *Npc2c-RNAi* not only recapitulates the ubiquitous *Npc2c* knockdown phenotype, but reveals that *Npc2c* has novel functions in the prothoracic gland related to growth and development. The apparent lack of complete phenotypic rescue by 20E, or its precursors suggests that: *Npc2c* is required in the PG to metabolize dietary cholesterol or a similar metabolite that is involved in the 20E-pathway, and that although ecdysone is sufficient to allow larval molting and metamorphosis to pupal stages, growth and development requires other sterol functions.

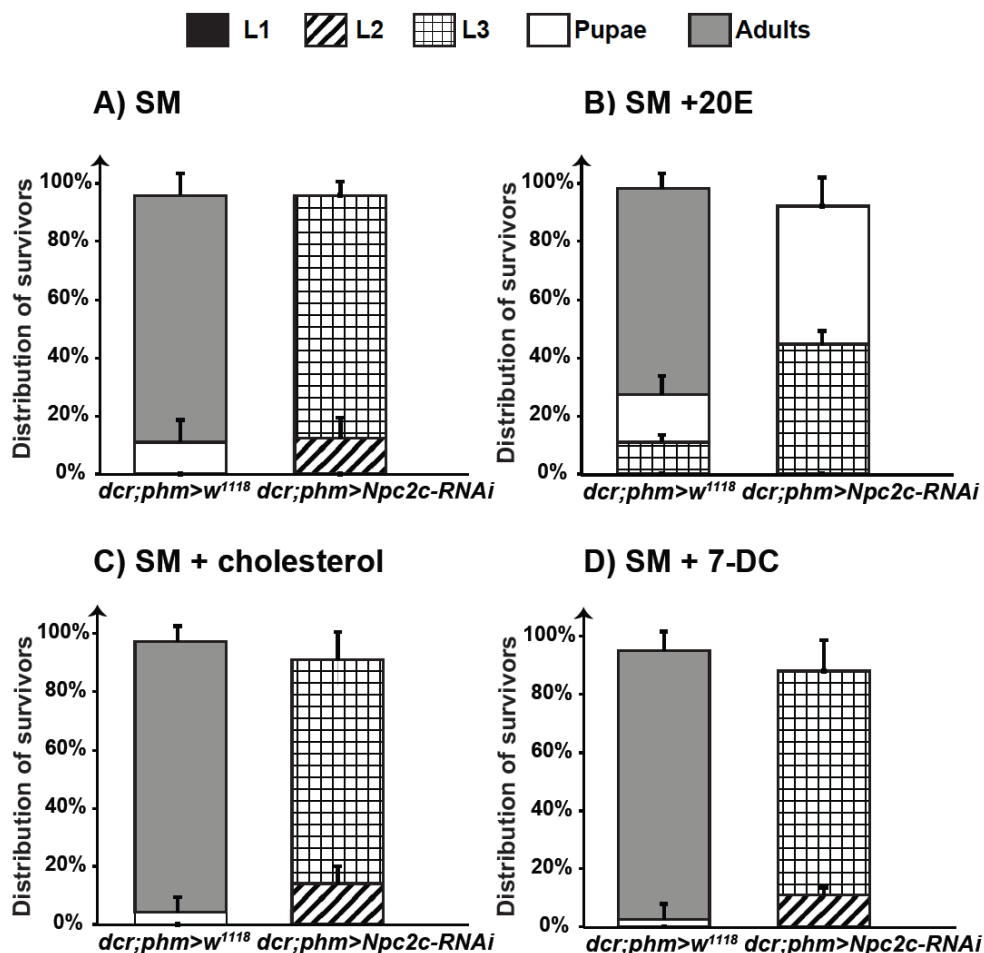
20E supplementation accelerated development of *Npc2c-RNAi* animals and controls by 1-2 days. However, it also resulted in ~10% L2 lethality in controls, a toxicity that aggravated on lipid-depleted medium. In comparison, C and 7DC-supplemented diets caused ~10-20% lethality in controls only at the highest concentration tested on SM (i.e. 33 mg). Additionally, the *dcr;phm-Gal4* stock inherently exhibited ~5-10% pupal lethality. The *phm-Gal4* stock (without the *dicer* transgene), however displayed no phenotypes when crossed to *Npc2c-RNAi* due to a weaker knockdown (40%) of *Npc2c* transcripts (data not shown). Hence I used the *dcr;phm-Gal4* for all further studies in the PG.

Figure 5.14



**Figure 5.14. Summary of the PG-specific *Npc2c*-RNAi developmental phenotypes.** A & B are representative images of the ‘giant larval’ phenotypes of the prothoracic gland-specific knockdown of *Npc2c* on standard medium (SM). Supplementation of SM with 0.33mg 20E partially rescues these giant L3 to pupal stages that never eclose to adult flies. On the other hand, PG-specific knockdown of the another member of the Niemann Pick Disease-Type C family, *Npc1a*, causes L1 lethality that is completely rescued to adult stages by 20E supplementation. 20E; 20-hydroxyecdysone, *act* and *dcr;phm-Gal4* transgenes drives expression ubiquitously and specifically in prothoracic gland cells. The corresponding data are shown in Figure 4.15 (*dcr;phm>Npc2c-RNAi*) and Figure 4.25 (*dcr;phm>Npc1a-RNAi*).

Figure 5.15



**Figure 5.15: Prothoracic gland-specific knockdown of *Npc2c* causes L3 developmental arrest and prolonged feeding.**

Stacked columns represent the proportion of adult survivors in a population versus the proportion of animals that do not develop beyond larval or pupal stages, as indicated: L1; solid black bars, L2; diagonal black stripes, L3; grids, pupae; solid white bars, adults; solid grey bars, respectively. (A-D) 100 embryos of each genotype, as listed on the X-axis, were transferred to either standard media (SM) (A), or SM supplemented with 1.65mg each of 20E (B), cholesterol (C), or 7DC (D). (E-H) 100 embryos of each genotype, as listed on the X-axis, were transferred to standard media supplemented with higher sterol concentrations: 16.5mg of cholesterol (E), or 33mg of cholesterol (F), 16.5mg of 7DC (G), or 33mg 7DC (H). (I-L) 100 embryos of each genotype, as listed on the X-axis, were transferred to either lipid-depleted (LD) media (I), or LD media supplemented with 100 $\mu$ g 20E (J), 200 $\mu$ g cholesterol (K), or 200 $\mu$ g 7DC (L). These populations were scored daily for 12 days by counting the number of viable animals at every developmental stage. Error bars represent standard deviation calculated from 4-5 replicates (each containing 100 embryos). 20E; 20-hydroxyecdysone, 7DC; 7-dehydrocholesterol, *dcr;phm-Gal4* transgene drives expression specifically in the prothoracic gland. The transgenic line used for *Npc2c* knockdown was **VDRC#31139**.

Figure 5.15 contd.

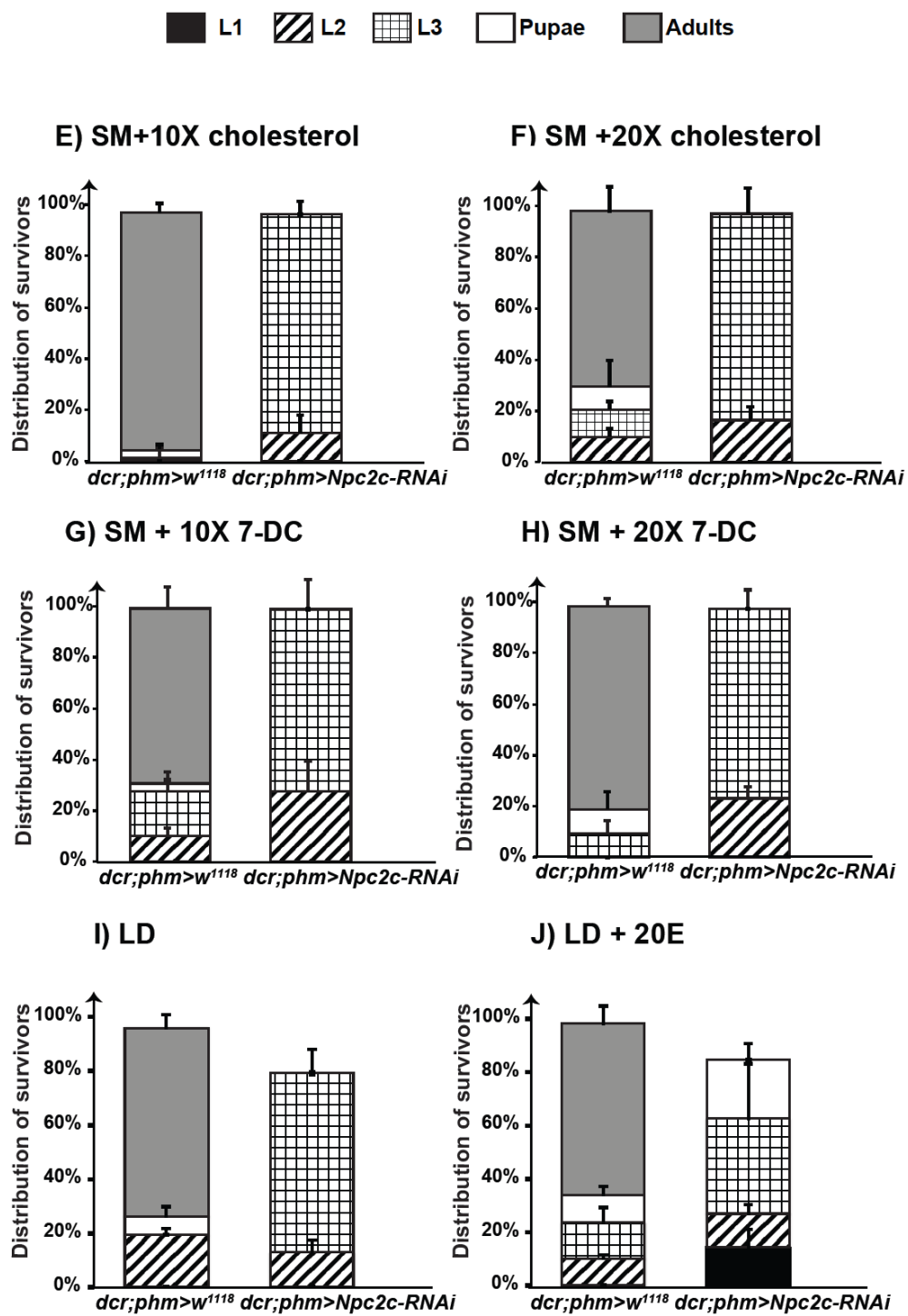
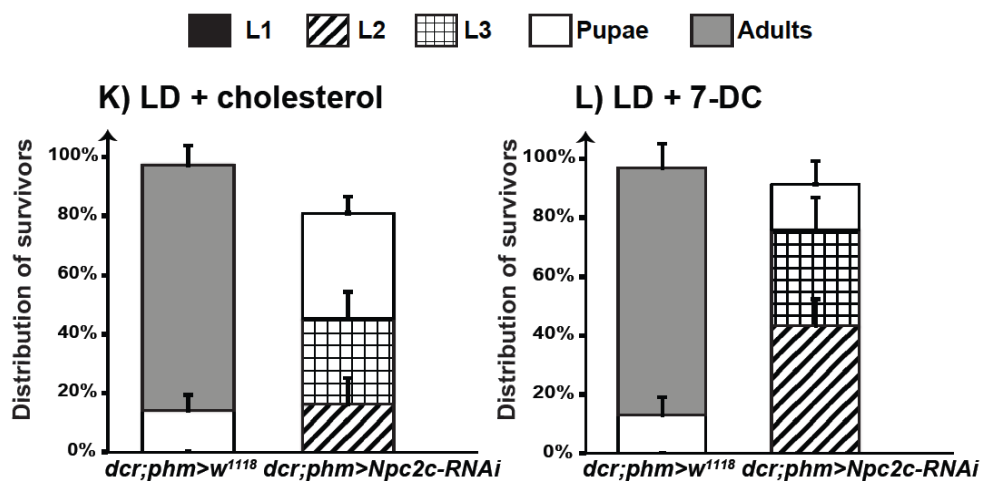


Figure 5.15 contd.



### 5.5.1. Prothoracic gland-specific knockdown of *Npc2c* represses key ecdysone biosynthetic genes

Although the tightly coordinated expression of the steroidogenic enzymes within the PG is well known to be strictly regulated via distinct transcriptional networks, the upstream PG-specific cellular factors that regulate the availability of intracellular cholesterol for entry into the 20E synthesis pathway remains unknown. I hypothesized that *Npc2c* may function within PG cells to make the dietary-derived cholesterol, or a related metabolite, available for utilization, for e.g. 20E production. This may explain why sterol-supplemented diets fail to rescue *Npc2c-RNAi* larval arrest phenotypes. If this notion were true, I asked if PG-specific *Npc2c-RNAi* animals are defective in ecdysone biosynthesis. To test this idea by indirect means, I quantified the expression of key ecdysone biosynthetic genes, namely – *phantom* (*phm*) and *shadow* (*sad*), in brain-ring gland complexes dissected from young (4h after molt) L3 *dcr;phm>Npc2c-RNAi* animals (**Figure 5.16**, fold changes values were calculated for each gene relative to its expression in the control *dcr;phm>w<sup>1118</sup>* that has been normalized to 100% (shown in grey)). PG-specific knockdown of *Npc2c* resulted in ~75% reduction in *Npc2c* transcripts (**Figure 5.16**), which was somewhat less effective than the complete abolishment of *Npc2c* expression by the ubiquitous driver (**Figure 5.5**). In addition, the PG-specific knockdown of *Npc2c* resulted in ~80% repression of *phm* and *sad* expression, indicating that compromising *Npc2c* function within the PG negatively impacts the transcription of crucial ecdysone biosynthetic genes that are normally tightly regulated

to rapidly initiate or block ecdysone production during development, and thus implying that *Npc2c* knockdown within the prothoracic gland likely causes ecdysone deficiency and subsequent developmental arrest. An important future experiment would be to quantify the ecdysteroid titres in these ‘giant larvae’ animals so that we can directly test the hypothesis that knockdown of *Npc2c* in PG affects 20E production.

**Figure 5.16**

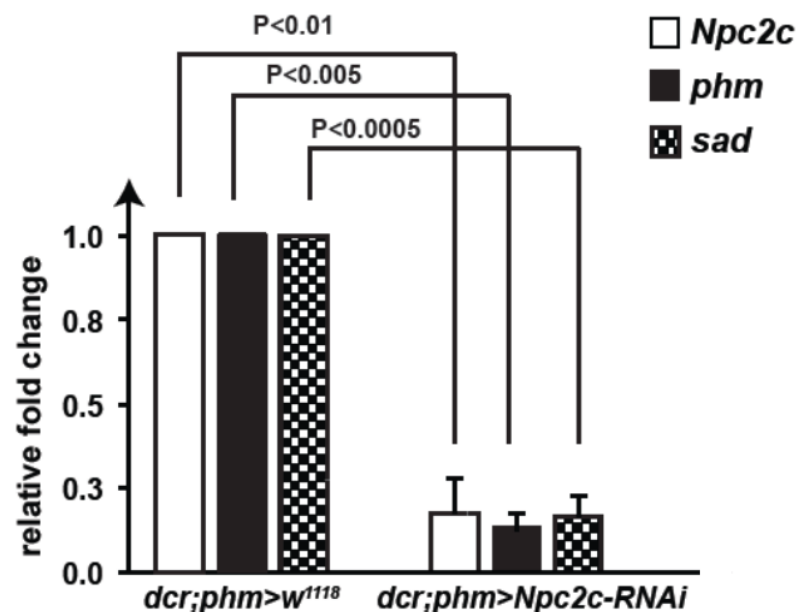


**Figure 5.16. Prothoracic gland-specific *Npc2c*-RNAi represses key ecdysone biosynthetic genes:** qPCR of *Npc2c*, *phantom* (*phm*) and *shadow* (*sad*) transcripts in PG-specific knockdown of *Npc2c*. All RNA samples were collected from brain-ring gland complexes dissected from larvae staged at 4h after L2/L3 molt. Fold changes are relative to *Npc2c* expression in the control *phm;dcr Gal4>w<sup>1118</sup>*. Controls are shown in grey. Error bars represent 95% confidence intervals, and *P*-values were calculated with the unpaired Student's *t*-test.

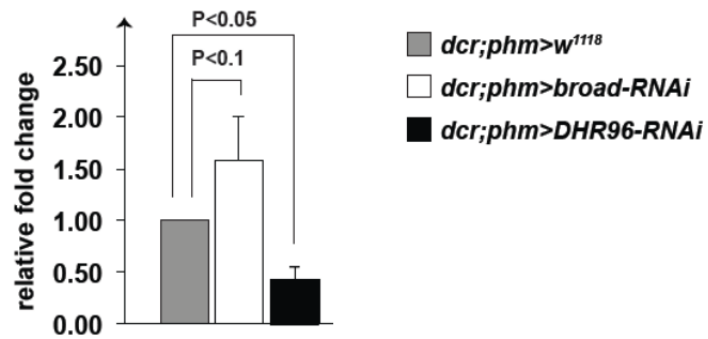
### 5.5.2. Transcriptional regulation of *Npc2c* in the prothoracic gland

To understand how *Npc2c* functions within PG, I wanted to identify the upstream regulators that might control *Npc2c* expression within steroidogenic cells. Whole-body gene expression studies on *DHR96<sup>1</sup>* mutants, (detailed in **chapter 4**) had led to my primary hypothesis that dietary cholesterol modulates *DHR96*-mediated regulation of *Npc2c*. Taken together with my data in **section 5.4** of this chapter, that modulating *Npc2c* expression within midgut cells of *DHR96<sup>1</sup>* mutant partially rescues the *DHR96<sup>1</sup>* mutant phenotype,

suggests that *DHR96* represses *Npc2c* transcription in midgut. In contrast in the prothoracic gland, I observed a strong correlation between reduced *Npc2c* expression to the transcriptional downregulation of key ecdysone biosynthetic genes. Hence I questioned whether *DHR96* had regulatory control of *Npc2c* in the PG.

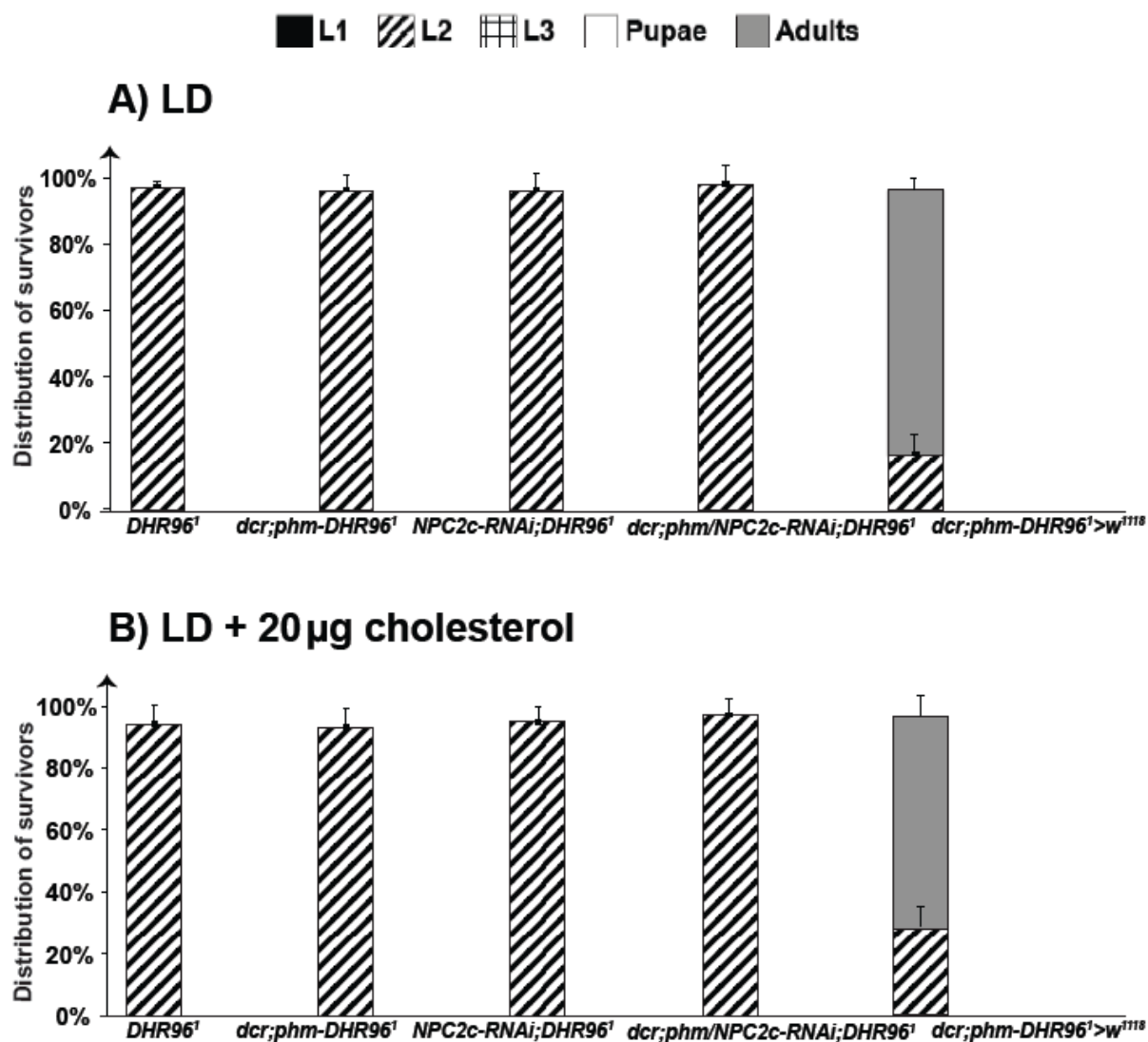
Ou *et al.*, (unpublished) demonstrates that *DHR96* transcripts are highly enriched in the PG. However, immunostaining data by King-Jones *et al.*, (2006) failed to detect DHR96 protein in the PG, raising the question of what might be the functional significance of *DHR96* transcription in this tissue. I tested the hypothesis that DHR96 may regulate *Npc2c* transcription in the PG, by triggering *dcr;phm>DHR96-RNAi* and examining *Npc2c* mRNA levels in brain-ring gland complexes dissected from young (4h after molt) L3 animals whether PG-specific *DHR96-RNAi* recapitulates the transcriptional knockdown of *Npc2c* observed in *DHR96<sup>l</sup>* mutants raised on SM (**Figure 4.3**). Indeed, *Npc2c* is ~2 fold downregulated upon PG-specific knockdown of DHR96, which is consistent with the trend in its expression pattern in *DHR96<sup>l</sup>* mutants on SM (Figure 5.17), supporting the idea DHR96 might regulate *Npc2c* (directly or indirectly) in the PG. To investigate if DHR96 and *Npc2c* interact epistatically in the PG, I tested if the PG-specific knockdown of *Npc2c* might alleviate the *DHR96<sup>l</sup>* mutant phenotype. Unlike the partial rescue of *DHR96<sup>l</sup>* mutants by the midgut-specific knockdown of *Npc2c* (**Figures 5.12 and 5.13**), PG-specific *Npc2c-RNAi* had no effect on *DHR96<sup>l</sup>* mutant survival on LD medium (**Figure 5.18**) suggesting that DHR96 exerts certain degree of regulatory control on *Npc2c* expression, however further studies on the tissue-specific factors will determine whether *DHR96* regulates *Npc2c* similarly in all cell types.

Figure 5.17.

***Npc2c***

**Figure 5.17. PG-specific *broad-RNAi* and *DHR96-RNAi* affect *Npc2c*-transcript levels.** qPCR of *Npc2c* transcripts in PG-specific knockdown of *broad* (white) and *DHR96* (black). All RNA samples were collected from brain-ring gland complexes dissected from larvae staged at 4h after L2/L3 molt. Fold changes are relative to *Npc2c* expression in the control *dcr;phm-Gal4>w<sup>1118</sup>*. Controls are shown in grey. Error bars represent 95% confidence intervals, and p values were calculated with the unpaired Student's *t*-test. *dcr;phm-Gal4* transgene drives expression in the prothoracic gland, with residual expression in the fat body.

Figure 5.18



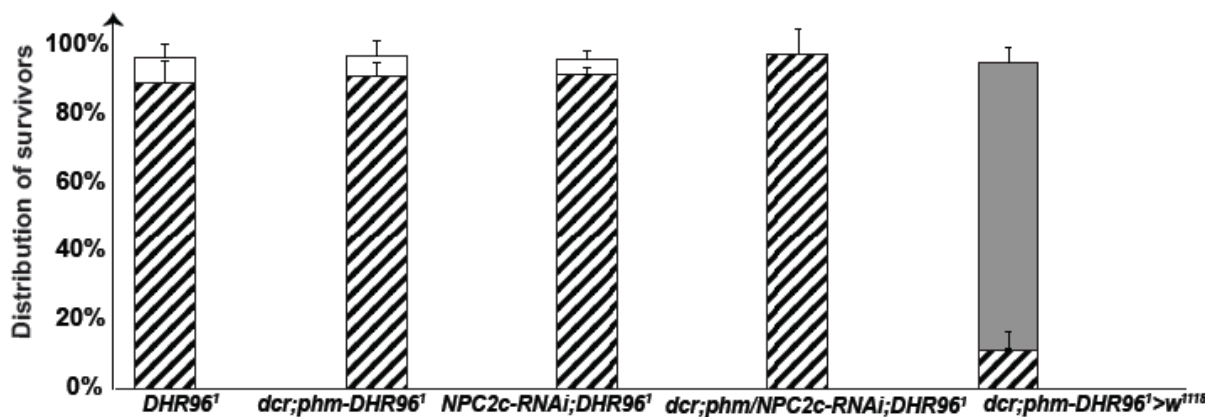
**Figure 5.18. PG-specific knockdown of *Npc2c* has no effects on the survival of *DHR96<sup>1</sup>* mutants on lipid-depleted media.**

Stacked columns represent the proportion of adult survivors in a population versus the proportion of animals that do not develop beyond larvae or pupal stages, as indicated: L1; solid black bars, L2; diagonal black stripes, L3; grids, pupae; solid white bars, adults; solid grey bars, respectively.

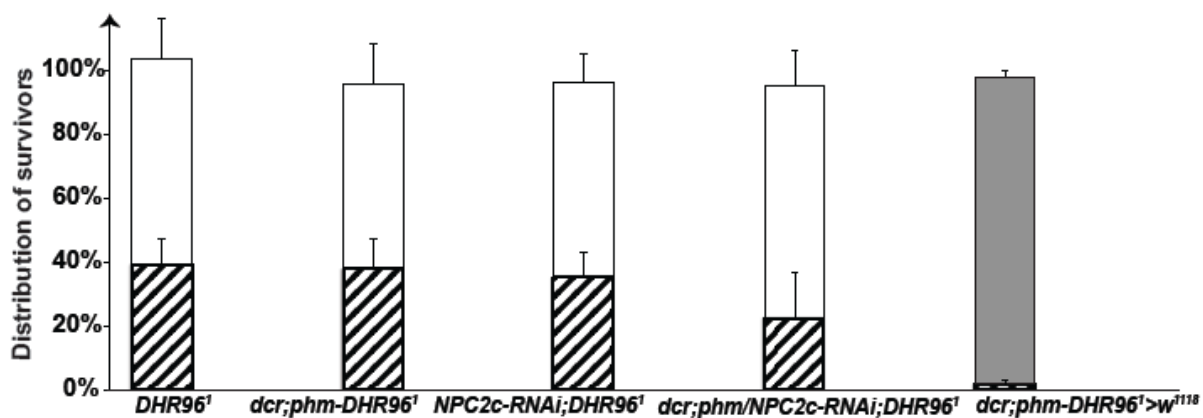
(A-E) 100 embryos of each genotype, as listed on the X-axis, were transferred to either lipid-depleted (LD) media (A), or LD media supplemented with 20 µg cholesterol (B), 40 µg cholesterol (C), 200 µg cholesterol (D), or 100 µg 20E (E). *DHR96<sup>1</sup>* animals arrest development as L2 on LD media and continue to do so in spite of the PG-specific *Npc2c-RNAi*. Error bars represent standard deviation calculated from 3-4 replicates (each containing 50 embryos). 20E; 20-hydroxyecdysone, 7DC; 7-dehydrocholesterol, *dcr;phm-Gal4* transgene drives expression in the prothoracic gland, *DHR96<sup>1</sup>*; *DHR96* mutant.

■ L1    ▨ L2    ▩ L3    □ Pupae    ■ Adults

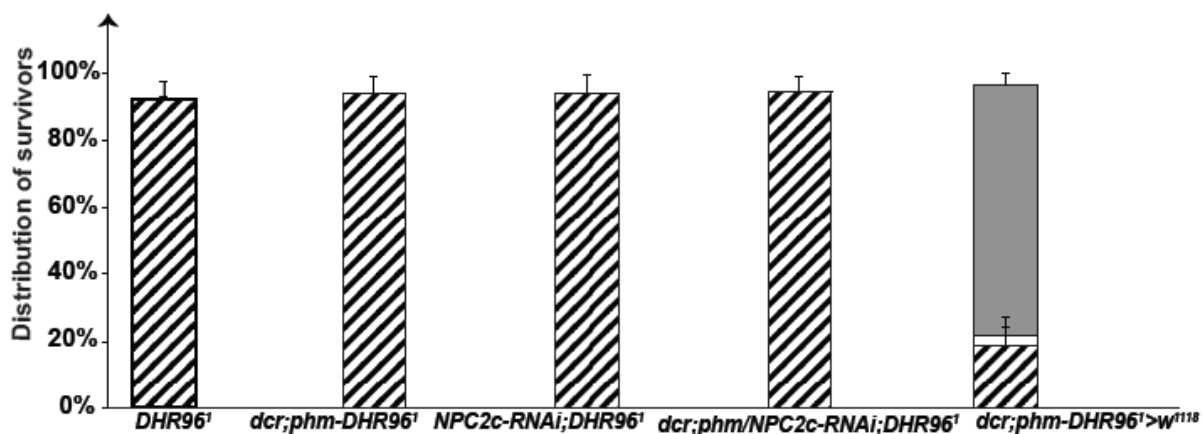
### C) LD + 40 $\mu$ g cholesterol



### D) LD + 80 $\mu$ g cholesterol



### E) LD + 100 $\mu$ g 20E



The ring gland-specific microarrays conducted by Ou *et al.* (unpublished) revealed that under a constitutively active form of Ras, the downstream effector of the PTTH pathway that stimulates ecdysone synthesis strongly represses *Npc2c*. However the repression is not observed in a PG-specific knockdown of the PPTH receptor *torso*, suggesting that the PTTH signaling might regulate *Npc2c* expression within the PG. To test if PTTH regulates *Npc2c* expression, I examined whether *Npc2c-RNAi/torso-RNAi* double knockdown in the PG, could have affect the developmental delay of (PG-specific) *torso-RNAi* animals. However, combining knockdown of *Npc2c* with *torso* aggravated the L2 lethality to ~70%, presumably due to additive effects of their individual *RNAi* phenotypes, causing only ~30% of the progeny to survive as L3, of which ~10% continued to survive for 6 more days to form “giant larvae”. These giant larvae were comparable in size to that of *dcr;phm>Npc2c-RNAi* giant larvae (data not shown). The remaining ~90% of the L3 population failed to survive as L3 for more than 3 days, and thus no progeny pupariated nor eclosed to adult flies. This frequency of this observed L2 lethality was more severe than the PG-specific knockdown of *torso* or *Npc2c*, thus confounding any possible interpretation for/against genetic interaction between *Npc2c* and *torso* based on this data alone.

Work by Xaing and colleagues (2010) demonstrated that PG-specific genes, such as the Niemann Pick disease type 1a (*Npc1a*), Steroid acute regulatory protein-1 (*Start1*) and ecdysone biosynthetic genes such as *phm*, *sad* and *disembodied (dib)*, were significantly repressed in *broad (br)* mutants, suggesting that the transcription factor *broad (br)* has a vital role in regulation of ecdysone biosynthesis. Although we do not know the mechanisms of function of the *Drosophila* Niemann- Pick type C genes, the current working model of mammalian NPC function proposes that the lysosomal luminal NPC2 protein physically interacts with lysosomal membrane NPC1 protein to egress cholesterol out of lysosomes to other subcellular organelles. *Drosophila Npc1a* transcripts are highly expressed in the ring gland and the PG-specific expression of *Npc1a*, or a 20E-supplemented medium is sufficient to fully rescue the *Npc1a* mutant L1 arrest phenotype, indicating that *Npc1a* expression in the PG is indispensable for development. Since vertebrate NPC1 function is closely correlated to its interaction with NPC2, I tested my hypothesis that *broad* expression affects *Npc2c* transcription levels within the PG by quantifying *Npc2c* transcripts in brain-ring gland complexes dissected from young L3 (4h after molt) of *dcr;phm>broad-RNAi* animals

(Figure 5.17). I found that while the PG-specific knockdown of *br* caused only a moderate induction of *Npc2c*, with however sizeable overlapping error bars, it resulted in a strong (~2-fold) repression of *Npc1a* and *Start1* transcripts (Figure 5.19), which is strongly consistent with the transcriptional pattern of broad mutants [174], thus implying that *Npc2c* is unlikely to be regulated by *broad*.

**Figure 5.19**

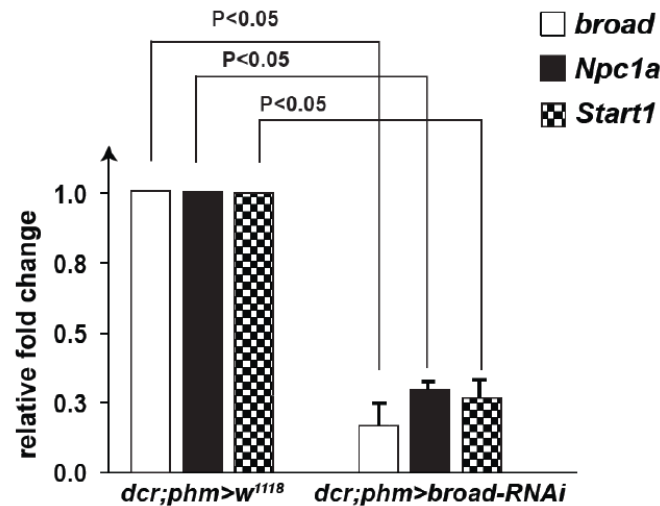


**Figure 5.19. Prothoracic gland-specific *broad-RNAi* represses *Npc1a* and *Start1* transcripts:** qPCR of *broad*, *Npc1a* and *Start1* transcripts in the PG-specific knockdown of *broad*. All RNA samples were collected from brain-ring gland complexes dissected from larvae staged at 4h after L2/L3 molt. Fold changes are relative to expression of the respective genes in the control *phm;dcr-Gal4>w<sup>1118</sup>*. Controls are shown in grey. Error bars represent 95% confidence intervals, and *P*-values were calculated with the unpaired Student's *t*-test. Downregulation of *Npc1a* transcripts by *broad* knockdown is identical to the previous observation by Xaing *et al* (2010). **In summary from Figures 5.12 & 5.13, *Npc1a*, and not *Npc2c*, is significantly misregulated by PG-specific *broad-RNAi*.**

### 5.5.3. Validating the specificity of *Npc2c-RNAi* phenotypes

To characterize the function of *Npc2c*, my studies were entirely based on the available VDRC RNAi-transgenic lines (Figures 5.7 & 5.9). Several studies have previously used gene-specific cDNA clones to rescue gene-specific RNAi phenotypes and demonstrate the specificity of the RNA interference. However, depending on the strength of the cDNA transgene, it is likely that siRNAs also target the cDNA-transgene, thereby overriding the rescue. Moreover, siRNAi species that have off-target effects are also quenched by the cDNA, thereby rescuing both the specific and non-specific effects of the RNAi.

Additionally, overexpression of cDNAs might on their own trigger anomalous cellular responses that could complicate interpretation of the results. To test if the observed *RNAi* mediated knockdown phenotypes were specific only to *Npc2c*, and do not result from off-target effects, I used the fosmid clones containing the *Npc2c* genomic DNA from *D. pseudoobscura* to rescue *Npc2c-RNAi* phenotypes. It has been shown that a 19-bp match in a double stranded RNA target is sufficient for suppressing gene expression [175], [176]. Hence the genomic region for the rescue construct was chosen in such a way that it would be divergent enough to make it resistant to the siRNAi-directed against *D. melanogaster Npc2c*, yet would contain similar amino acid sequences to ensure normal spatiotemporal functioning in the host. **Figure 5.20** shows the fosmid FlyFos046706 (39054bp) containing the genomic region of the *D.pseudoobscura* ortholog of *Npc2c*, named: *GAI7784* (631bp), which was obtained from the Tomancak lab at MPI-CBG TransGeneOmics. The BAC-fosmid clones were injected and transformed into *w<sup>1118</sup>* background, and further recombined with the *UAS-Npc2c-RNAi* transgene to generate the double transgenic stock containing the fosmid rescue-transgene along with the RNAi-transgene. Animals containing two copies of each of these transgenes were lethal, however, one copy of each of the *UAS-Npc2c-RNAi* and fosmid was viable, and was subsequently used for further testing. Upon crossing with the drivers: ubiquitous act-Gal4 and PG-specific *dcr;phm-Gal4*, in triplicates for each cross, I observed that combining the fosmid clone with the *Npc2c-RNAi* in presence of act- or *dcr;phm* - Gal4 drivers caused a significant degree of toxicity. The progeny constituted ~45% L2 arrest and ~55% L3 arrest; of which ~5% survived for 4 more days, and formed “giant L3 larvae” that were identical in size and developmental timing to the *dcr;phm>Npc2c-RNAi* phenotype. Thus, the fosmid clone containing the genomic region of *D.pseudoobscura* homolog of *Npc2c* was unable to render cross-species functionality for *Npc2c* partially lethal when used in combination with the *UAS-Npc2c-RNAi* transgene, and was thus insufficient to rescue the RNAi-mediated phenotypes of *Npc2c*. I have developed an alternate approach to test the specificity of *Npc2c-RNAi* (not tested yet) and discussed it in Chapter 6.



## 5.6. A model for *Npc2c* function

In *Drosophila* PG cells, the dietary-derived cholesterol, must exit the endosomes to the ER and mitochondria where crucial cytochrome P450 enzymes and hydrolases necessary for ecdysteroidogenesis are located. In vertebrates, although this process is hypothesized to be mediated by three proteins: the lysosomal proteins NPC1, NPC2 and the mitochondrial StAR (steroidogenic acute regulatory), the mechanisms by which dietary-derived cholesterol is transported from the lysosome/endosomes to the mitochondrial outer and inner membranes are not well defined. To understand the cellular physiology underlying the *Npc2c* knockdown phenotype, I investigated the functions of the *Drosophila* homologs: *Npc1a* (Flybase CG5722) and *Start1* (FlyBase CG3522), as they would relate to the *Npc2c* (Flybase CG3934) function.

Work by Charman, *et al.*, (2010) [177] on vertebrate lysosomal protein metastatic lymph node protein 64 (MLN64, also called StARD3- Steroid acute regulatory protein) and by Roth, *et al.* [178], who conducted sequence alignments and computational studies on *Drosophila Start1*, have revealed a crucial role for vertebrate MLN64 or *Drosophila Start1* in regulating intracellular cholesterol trafficking between mitochondrial and endosomal organelles. The findings by Roth *et al.* show that the putative *Start1* protein, which is most highly related to the mammalian MLN64, is specifically expressed in larval PG cells and that *Start1* expression is likely regulated by ecdysteroids, thus suggesting a novel role for *Start1* in regulating ecdysone biosynthesis. The study by Huang *et al.* [179] was first to demonstrate that on yeast medium, null mutants of *Npc1a*, which shares 63% identity to human NPC1 protein, are lethal as first instar larvae and are partially rescuable to the second instars by supplementing 20E. Importantly, they identified that these *Npc1a* mutants demonstrated severe sterol accumulation in several tissues including the prothoracic gland cells, the site of ecdysone synthesis. Surprisingly, higher concentrations of cholesterol (C) and 7-dehydrocholesterol (7DC), rescued *Npc1a* mutants to pupal and adulthood respectively. This complete rescue of *Npc1a* mutants by 20E precursors suggested that these supplemented sterols, once within the lysosomes, could circumvent the need for *Npc1a* protein that is predicted to function at the lysosomal membranes to exit the lysosomes and reach the ER and/or mitochondria to complete 20E synthesis.

The early-larval lethality of *Npc1a* mutants, which are fully rescuable to adults by supplementation of a high concentration of ecdysone precursors, C and 7DC, are explained by the ‘sterol-shortage’ model wherein a loss of *Npc1a* function results in endosomal entrapment and accumulation of cholesterol, and subsequent shortage of cellular cholesterol for ecdysone synthesis in the PG. In **section 5.6.1**, I used filipin stain to test whether PG-specific *Npc2c-RNAi* animals display cellular cholesterol accumulation. In contrast, my data shows that PG-specific *Npc2c* knockdown causes late-larval developmental arrest that cannot be rescued by ecdysone or its precursors. This suggested that *Npc2c* and *Npc1a* may be involved in transporting different sterol molecules. In mammalian cells, MLN64 has been shown to bind cholesterol via its StART (StAR-related lipid transfer) domain and mediate cholesterol transport to the mitochondria, independent of NPC1 [177]. Hence, as an approach to understand the reason underlying the developmental arrest of *Npc2c-RNAi* animals, I systematically examined the phenotypic effects and rescue of *Npc1a-RNAi* in the PG to explore the idea that the rescue observed with the *Npc1a* mutant with ecdysone precursors can be credited to the functions of *Start1* and *Npc2c* to mediate and redirect the supplemented sterols to their respective subcellular organelles independent of *Npc1a*. To reliably compare phenotypes of PG-specific *Npc2c-RNAi* to that of *Npc1a* and *Start1*, I used the *dcr;phm-Gal4* driver to trigger *Npc1a-RNAi* (**section 5.6.2**) and *Start1-RNAi* (**sections 5.6.3**) in PG cells and examined their phenotypic effects on defined media. In **section 5.6.4**, I describe the rationale for a future experiment to test whether *Start1* and *Npc2c* are necessary for the observed rescue of *Npc1a* mutants by cholesterol and 7DC.

### **5.6.1. No obvious filipin-positive staining in *Npc2c-RNAi* animals**

The *Npc1a* mutant model by Huang *et al.* demonstrated the sterol accumulation phenotype that is characteristic of mammalian Niemann Pick type C disease. Using filipin staining to visualize intracellular unesterified cholesterol, I investigated whether animals that have a targeted knockdown of *Npc2c* in PG cells may also demonstrate the punctate sterol accumulation pattern (**Figure 5.21**). In agreement with findings by Huang *et al.*, *Npc1a* null mutant tissues demonstrated observable positive filipin staining, characteristic of aberrant cholesterol accumulation, (**Figure 5.21 A**). Although controls did not display any degree of

punctate staining, they exhibited a low degree of background staining that appeared as sporadic, weak spots along the periphery of the brain tissue. On the other hand, filipin images from larval brain ring gland complex of PG-specific *Npc2c-RNAi* animals (**Figure 5.21 B**) displayed no observable punctate pattern or filipin-positive staining, suggesting that the *Drosophila Npc2c* might be involved in transporting sterols or lipids, in addition to, or other than cholesterol, and which are nevertheless crucial for ecdysone synthesis. Mammalian *Npc1* and *Npc2*-deficient cells have been shown to sequester a variety of other lipids in their endosomes [180] [181], raising the possibility that a mere cellular accumulation of cholesterol may not be the primary defect in the *dcr;phm>Npc2c-RNAi* lethality phenotype. Considering that two of the eight *Drosophila Npc2* genes: *Npc2c* and *Npc2g*, have potential significance in the PG, further studies are necessary to understand the NPC physiology in these cells. Below, I have described the preliminary results for a future line of studies that will explore epistatic interactions between *Start1* and *Npc2c*, and whether this putative interaction is critical for trafficking sterols like C and 7DC, specifically within the context of *Npc1a* mutant rescue by C and 7DC.

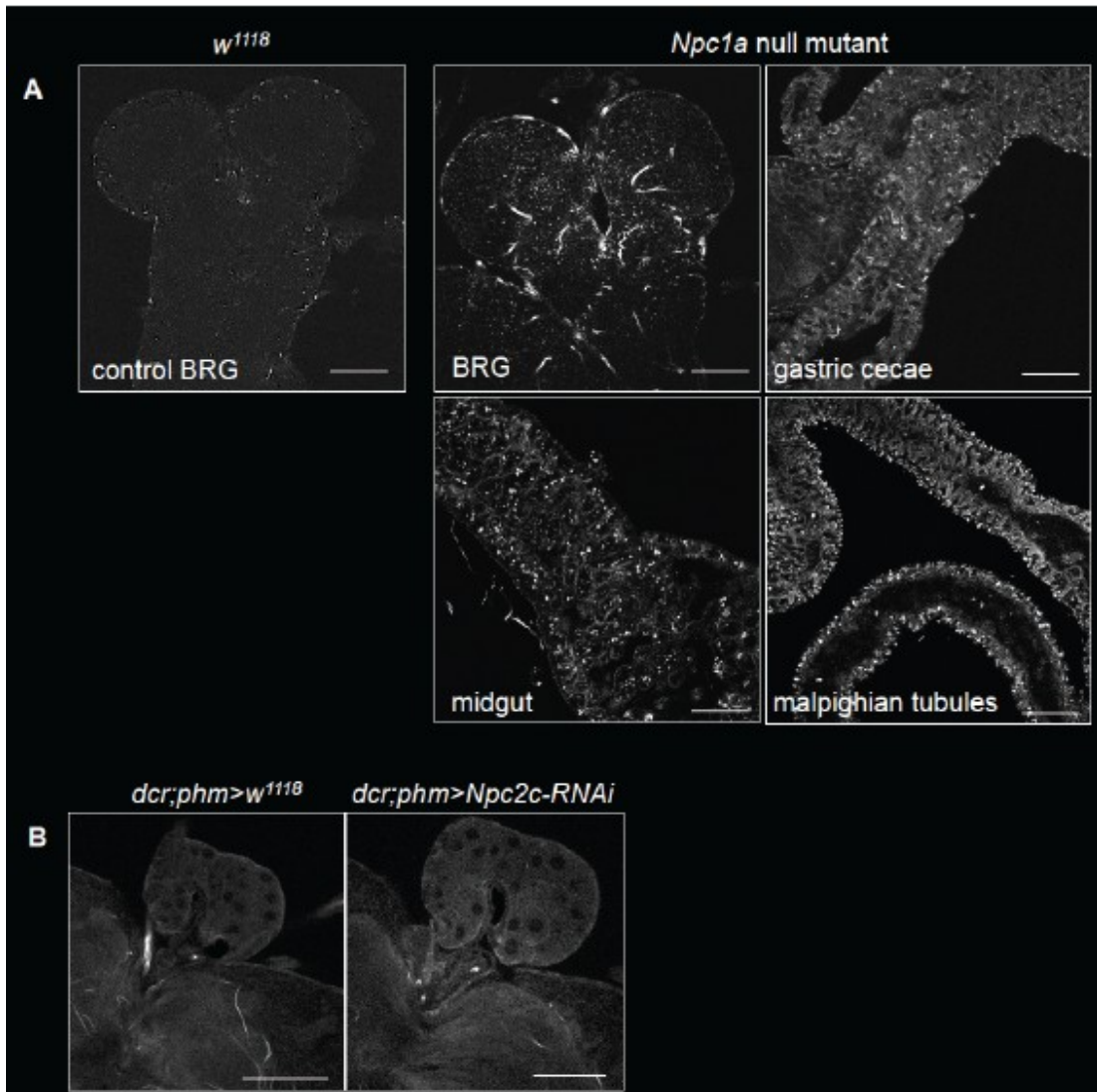


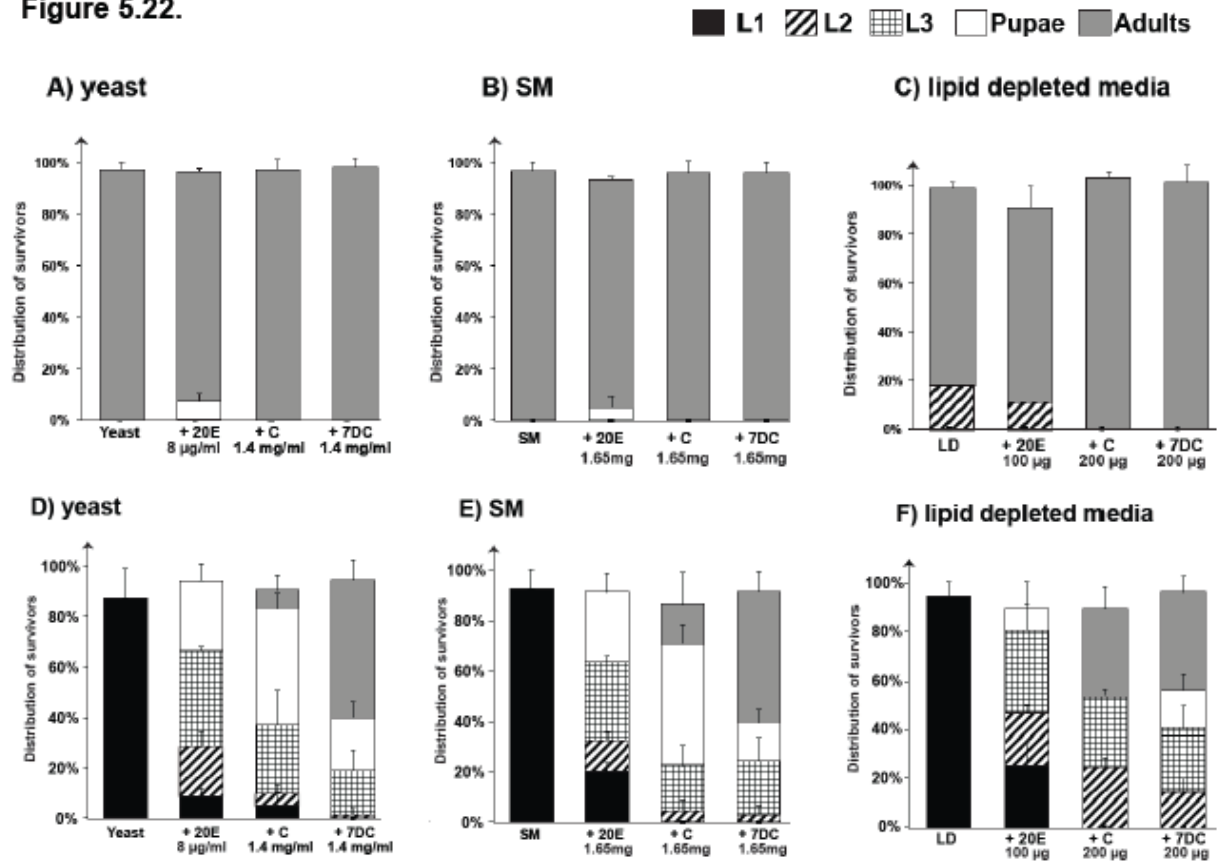
**Figure 5.21. Filipin staining confirms aberrant sterol accumulation in *Npc1a* null mutants.**

First instar larvae (L1) sampled from control *w<sup>1118</sup>* and *Npc1a* null mutants, and mid-wandering L3 larvae from controls *dcr;phm>w<sup>1118</sup>* and PG-specific *Npc2c-RNAi* were stained with Filipin III, and examined by confocal microscopy. Filipin III has been routinely used in the study of Type-C Niemann-Pick disease (Coxey *et al*, 1993) and stains intracellular free cholesterol in blue. All panels in images A and B have been shown in gray scale. scale bars are 25  $\mu$ m. A) Filipin-positive *Npc1a* null mutant L1 larval tissues show a punctate pattern of sterol accumulation in the: gastric cecae, midgut, malpighian tubules and brain/ring-gland complex (BRG). A filipin-negative control image of a first instar BRG is shown on the left. B) PG-specific *Npc2c-RNAi* animals undergo excessive feeding in L3 stages that cause the ‘giant-larvae phenotype’, and result in larger brain/RG than the control *dcr;phm>w<sup>1118</sup>*. In contrast to the pronounced sterol accumulation in *Npc1a*<sup>null</sup> mutant tissues, PG-specific *Npc2c-RNAi* do not demonstrate any observable punctate pattern filipin stain in the prothoracic gland cells.

### 5.6.2. Prothoracic gland-specific *Npc1a*-RNAi recapitulates *Npc1a* mutant phenotypes

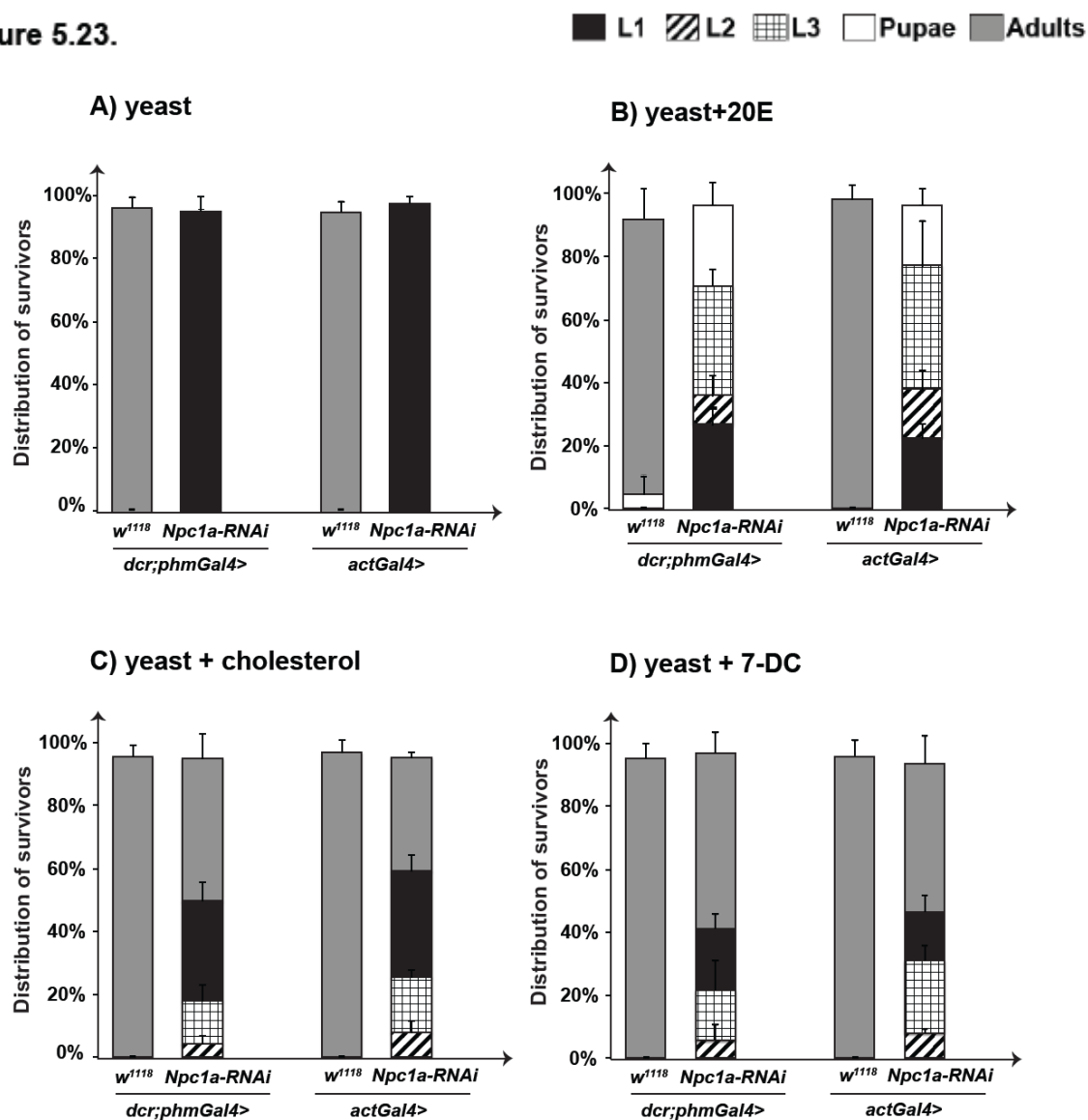
To genetically explore the idea that *Npc2c* and *Start1* play a significant role in the rescue of *Npc1a* mutants by allowing transport of dietary sterols when supplemented in higher concentrations, I used the *dcr;phm-Gal4* driver to trigger *Npc1a*-RNAi and *Start1*-RNAi in PG cells, and examined their phenotypic effects on defined LD and SM. I included *Npc1a* mutant and yeast medium as positive controls, and all concentrations of supplemented sterols: 20E, C and 7DC used for this rescue study were identical to those used in Huang et al., and in my earlier *Npc2c*-RNAi studies on LD and SM (Figures 5.9, 5.11, 5.15). As shown in **Figure 5.22**, feeding 20E (8 µg/ml) with yeast medium partially rescued ~30% of *Npc1a* L1s to pupae, which is a far stronger rescue than the reported ~60% L2 rescue by Huang et al.[110]. Feeding cholesterol (1.4mg/ml) rescued ~10% *Npc1a* mutants to adults, while the rest of the population survived as L1 (~5%), L2 (~5%), L3 (~30%) and pupae (~50%), until day 10-13 AED. This complete rescue by cholesterol is in striking contrast to the partial rescue of the pupal lethality observed by Huang et al. Feeding 7DC (1.4mg/ml) rescued ~60% *Npc1a* mutants to adults, while the remainder of the population survived as L2 (~2%), L3 (~20%) and pupae (~20%) until day 10-13 AED. This rescue of *Npc1a* to ~60% adults by 7DC is twice more than the proportion of adults rescued by 7DC (~30%) in the findings of Huang et al. Unexpectedly I also observed that supplementing LD with cholesterol (200µg) failed to rescue the L1 arrest phenotype, unlike the rescue observed on yeast or SM. The rest of the population continued to survive as L2 (~30%) and, L3 larvae (~25%) as well as pupae (~45%), until day 10-13 AED. On the other hand, 7DC (200µg) consistently rescued ~45% *Npc1a* mutants to adulthood, also on the LD medium, albeit less effectively than the rescue observed on yeast and SM, yet revealing a novel feature that feeding 7DC is more effective than cholesterol to rescue *Npc1a*-RNAi animals on all supplemented diets. In summary, despite a few minor differences, I have recapitulated the *Npc1a* mutant phenotypes reported by Huang et al., on two additional independent nutritional media routinely used in our *Npc2c*-RNAi studies, which indicated that my approach was working.

Figure 5.22.

Figure 5.22. Phenotypic characterization of *Npc1a* null mutants.

Stacked columns represent the proportion of adult survivors in a population versus the proportion of animals that do not develop beyond larval or pupal stages, as indicated: L1; solid black bars, L2; diagonal black stripes, L3; grids, pupae; solid white bars, adults; solid grey bars, respectively. (A-F) 100 wild type embryos (A, C, E), or *Npc1a* null mutant embryos (B, D, F) were transferred to either yeast medium, standard medium (SM), or lipid-depleted (LD) medium, supplemented with 20E, cholesterol or 7DC, as indicated by the respective concentrations on the X-axis labels. These populations were scored daily for 12 days by counting the number of viable animals at every developmental stage. D demonstrates validation of the original observation of the *Npc1a* null mutant phenotype on yeast medium and complete rescue to adulthood exclusively by 7DC supplementation (Huang *et al.*, 2005). One striking difference from the original observation, as indicated in D, is that *Npc1a* null mutant can be rescued to adulthood when supplemented with cholesterol. Error bars represent standard deviation calculated from 4-5 replicates (each containing 100 embryos). 20E; 20-hydroxyecdysone, 7DC; 7-dehydrocholesterol.

Figure 5.23.

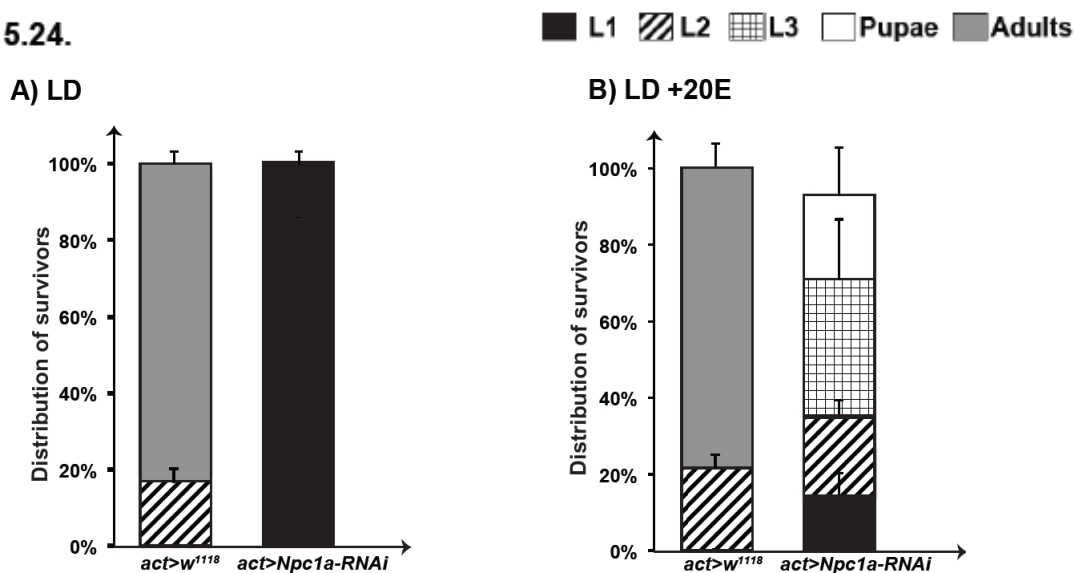


**Figure 5.23. Prothoracic gland-specific *Npc1a*-RNAi is sufficient to fully recapitulate the *Npc1a* null mutant phenotype on yeast medium and subsequent rescue to adulthood by sterol supplementation.**

Stacked columns represent the proportion of adult survivors in a population versus the proportion of animals that do not develop beyond larval or pupal stages, as indicated: L1; solid black bars, L2; diagonal black stripes, L3; large grids, pupae; solid white bars, adults; solid grey bars, respectively. (A-D) 100 embryos of each of *dcr;phm>Npc1a-RNAi* and *act>Npc1a-RNAi* were transferred to either yeast medium (A), yeast medium supplemented with 20E (B), cholesterol (C) or 7DC (D). Controls are *dcr;phm-Gal4>w<sup>1118</sup>* and *act-Gal4>w<sup>1118</sup>* raised on identical conditions. These populations were scored daily for 12 days by counting the number of viable animals at every developmental stage. Error bars represent standard deviation calculated from 4-5 replicates (each containing 100 embryos). 20E; 20-hydroxyecdysone, 7DC; 7-dehydrocholesterol. *dcr;phm-Gal4* and *act-Gal4* transgenes drive expression respectively in the prothoracic gland and ubiquitously.

I expanded these studies to validate the effectiveness of ubiquitous and PG-specific *Npc1a* knockdown (VDRC #105405) and found that the knockdown of *Npc1a-RNAi* in PG cells using the *dcr;phm-Gal4* driver was sufficient to fully recapitulate the *Npc1a* mutant phenotypes on yeast, standard and LD media (**Figures 5.23 and 5.24**). The concentrations of supplemented sterols: 20E, C and 7DC used for rescue of *Npc1a-RNAi* studies were identical to those used in *Npc1a* mutants (**Figure 5.22**). Surprisingly, PG-specific and ubiquitous *Npc1a-RNAi* animals fed on yeast medium containing 7DC (~60%) achieved a better rescue to adulthood than with cholesterol (~50%). Ubiquitous knockdown of *Npc1a* using the *act-Gal4* driver served as a control to compare the effectiveness of RNA interference relative to the *Npc1a* mutant. On the other hand, as also observed with *Npc1a* mutants, while cholesterol failed to rescue *act-Gal4>Npc1a-RNAi* to adult stages on LD medium, 7DC rescued ~50% of *act-Gal4>Npc1a-RNAi* to adult stages, suggesting that 7DC and cholesterol are moved through the cells via different uptake and transport mechanisms. Taken together my data indicates that ubiquitous knockdown of *Npc1a* fully recapitulates *Npc1a* mutant lethality phenotype on yeast, standard and lipid-depleted media, and the subsequent rescue to adulthood by cholesterol and 7DC.

**Figure 5.24.**



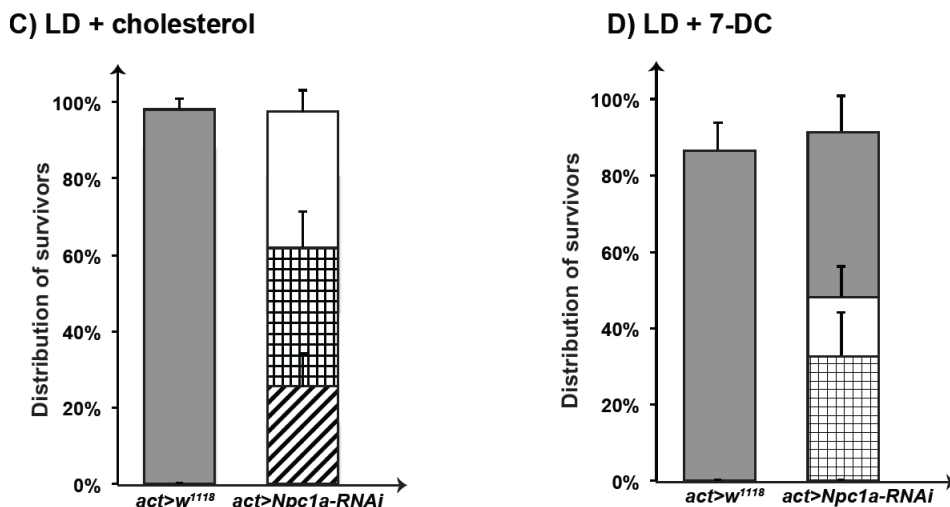


**Figure 5.24. *Npc1a*-RNAi recapitulates *Npc1a* null mutant phenotype on lipid-depleted medium**

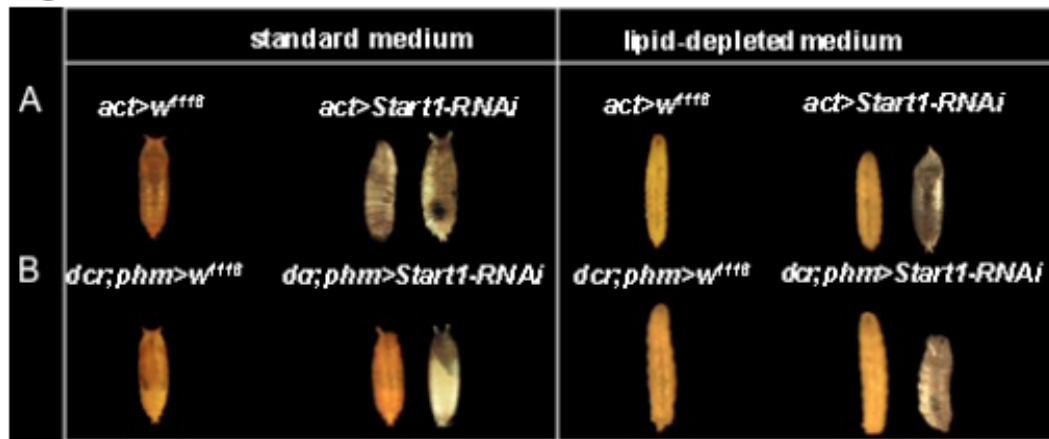
Stacked columns represent the proportion of adult survivors in a population versus the proportion of animals that do not develop beyond larval or pupal stages, as indicated: L1; solid black bars, L2; diagonal black stripes, L3; large grids, pupae; solid white bars, adults; solid grey bars, respectively. (A-D) 100 embryos of *act>Npc1a-RNAi* were transferred to either lipid-depleted medium (A), lipid-depleted medium supplemented with 20E (B), cholesterol (C) or 7DC (D). Controls are *act>w<sup>1118</sup>* raised on identical conditions. These populations were scored daily for 12 days by counting the number of viable animals at every developmental stage. Error bars represent standard deviation calculated from 4-5 replicates (each containing 100 embryos). 20E; 20-hydroxyecdysone, 7DC; 7-dehydrocholesterol. *act-Gal4* transgenes drives expression in ubiquitously. Characterizing the strength of *Npc1a*-RNAi in recapitulating *Npc1a* null mutant phenotype on standard and lipid-depleted media is important to compare *Npc1a* and *Npc2c* phenotypes and test for epistatic between the two genes.

### 5.6.3. *Start1*-RNAi causes late larval developmental arrest that is fully rescuable to adult stages by cholesterol and 7DC

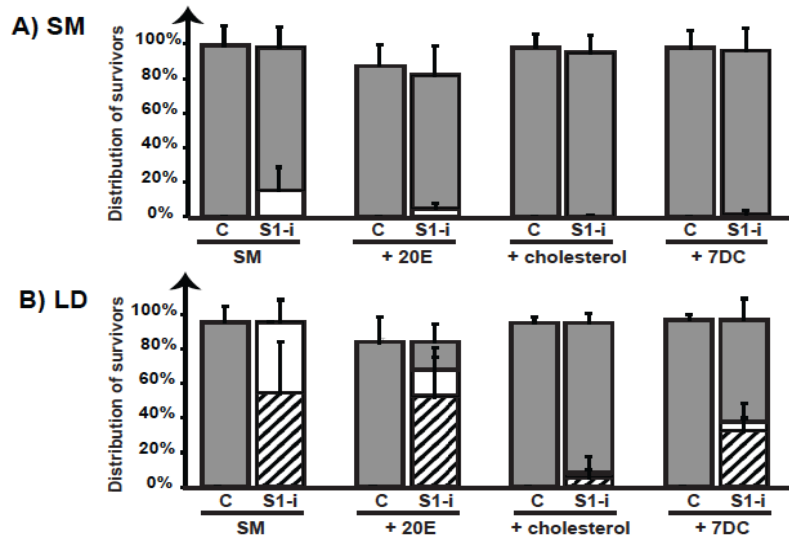
The findings by Roth and colleagues [178] showed that *Start1* transcripts are enriched in the PG. To indirectly test the hypothesis that *Drosophila Start1* may regulate subcellular cholesterol transport for 20E synthesis in PG cells, I tested if PG-specific knockdown of *Start1* (using *dcr;phm-Gal4*) affects cholesterol availability for 20E synthesis. Hence I scored for viability and measured developmental progression of *Start1*-RNAi animals raised on standard and LD media. All results discussed below were knockdown studies performed using the VDRC line #4053. Prior to this, I conducted a pilot study to test an independent VDRC line #109636, which failed to knockdown *Start1*

transcripts and consequently did not affect survival or development. Currently, *Start1* transcripts have been reported to be predominantly expressed in the steroidogenic tissues [178] followed by moderate expression in the digestive system (modENCODE Tissue Expression Data) and in the fat body (FlyAtlas Anatomical Expression Data) tissues of wandering L3 and adult flies. Hence I additionally tested the effects of *Start1* knockdown in whole body (act-Gal4) and fat body cells (*cg-Gal4*). In **Figure 5.25**, ‘C’ denotes the Gal4 driver crossed to  $w^{1118}$  and ‘S1-i’ denoted the corresponding Gal4 driver crossed to *UAS-Start1-RNAi* transgenic animals, respectively.

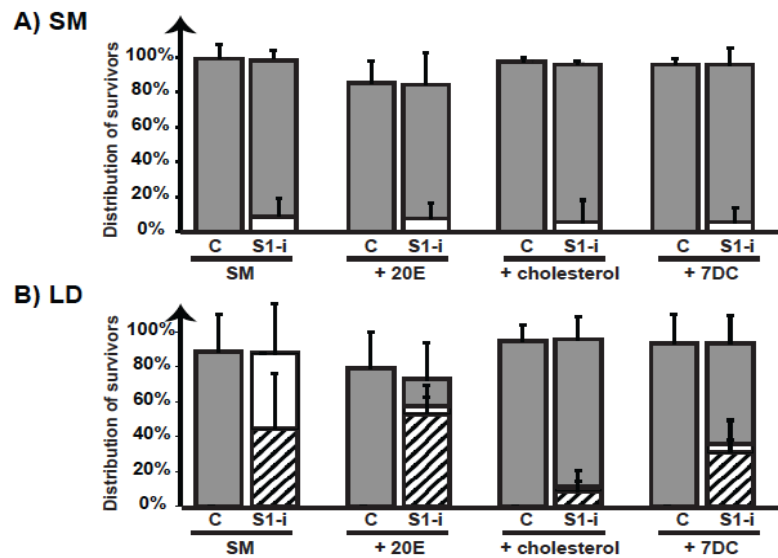
Figure 5.25.



*dcr;phm>Start1-RNAi*      ▨ L3    □ Pupae    ■ Adults



*act>Start1-RNAi*



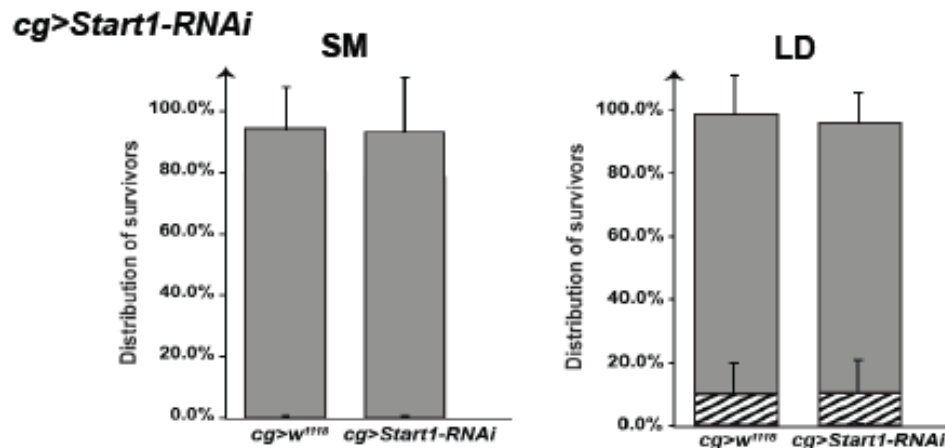


**Figure 5.25: Ubiquitous and prothoracic gland-specific knockdown of *Start1* cause developmental arrest on lipid-depleted (LD) medium.**

(Top panels) Images are representative photographs of the (A) ubiquitous and (B) PG-specific knockdown of *Start1* that result in developmental arrest in pupal stages on standard medium; SM and on lipid-depleted medium; LD. On LD medium, the phenotype is more severe and animals arrest as late L3 to early pupal stages. Images of pupae and L3 from the controls *act>w<sup>1118</sup>* and *dcr;phm>w<sup>1118</sup>* shown on the left.

Stacked columns represent the proportion of adult survivors in a population versus the proportion of animals that do not develop beyond larvae or pupal stages, as indicated: L3; diagonal black stripes, pupae; solid white bars, adults; solid grey bars, respectively. 50 embryos of *dcr;phm>w<sup>1118</sup>* (indicated as 'C'), or *dcr;phm>start1-RNAi* (indicated as 'S1-i'), and 50 embryos of *act>w<sup>1118</sup>* (indicated as 'C'), or *act>start1-RNAi* (indicated as 'S1-i'), were transferred to the following media: standard media (SM), or SM supplemented with 1.65mg of each of 20E, cholesterol, or 7DC, or lipid-depleted (LD) media, or LD media supplemented with 100 $\mu$ g of 20E, 200 $\mu$ g of cholesterol, or 200 $\mu$ g of 7DC. (Lower panel, next page) 50 embryos each of *cg>w<sup>1118</sup>* and *cg>start1-RNAi* were transferred to standard media (SM), or lipid-depleted (LD) media. All aforementioned populations were scored daily for 12 days by counting the number of viable animals at every developmental stage. Error bars represent standard deviation calculated from 3 replicates (each containing 50 embryos). On LD medium, the ubiquitous and prothoracic gland-specific *Start1-RNAi* cause lethality in larval and pupal stages, which are both rescued to adulthood by cholesterol, and to a lesser degree by 7DC. No developmental lethal phenotypes were associated with the fat body-specific knockdown of *Start1*. 20E; 20-hydroxyecdysone, 7DC; 7-dehydrocholesterol, *act-Gal4*, *dcr;phm-Gal4* and *cg-Gal4* transgenes drive expression ubiquitously, in the prothoracic gland and fat body respectively.

On SM, where controls were viable, ~10% of *act>Start1-RNAi* and *dcr;phm>Start1-RNAi* animals arrested development as pupae, which continued to survive until day 10-13 AED, while the remaining ~90% of the population developed into normal healthy adults. Surprisingly, while 20E supplementation (1.6 mg) consistently failed to alleviate the pupal arrest phenotype observed with ubiquitous and PG-specific knockdown of *Start1*, supplementing cholesterol or 7DC (1.6 mg) fully rescued only the PG-specific *Start1-RNAi* animals to adult stages. On the other hand, on lipid-depleted (LD) medium, while ubiquitous knockdown of *Start1* resulted in ~40% pupal and ~40% L3 developmental arrest, the remainder of the population arrested as L2 due to the nature of the LD medium. Supplementing LD medium with cholesterol achieved the best rescue of *act>Start1-RNAi* animals to adults (~80%), followed by supplementation with 7DC (~55%) and 20E (~20%). In a similar manner, PG-specific *Start1-RNAi* resulted in ~50% L3 and ~45% pupal arrest on LD, and could be effectively rescued to ~90% adults by feeding cholesterol, 7DC (~60% adults) or 20E (~20% adults). In all aforementioned conditions, animals that arrested development as L3 or pupae continued to survive in those developmental stages until day 10-13 AED, and supplementing 100 µg of 20E to LD medium, or 1.6 mg of 20E to SM, was relatively toxic and resulted in ~15% reduction in viability of controls and *Start1-RNAi* animals.

Taken together, I found that *Start1* has critical functions in the PG cells that are necessary for normal development and survival on sterol-rich SM and lipid-depleted media. The observation that *Start1-RNAi* phenotypes can be more effectively rescued by the sterol precursor of 20E, i.e. cholesterol, than 20E itself, suggests that *Start1* is required for regulating cellular cholesterol availability in the PG, in addition to 20E biosynthesis.

On the other hand, fat body-specific *Start-RNAi* produced no adverse effects on survival or developmental timing on standard and LD media, indicating that it plays a relatively significant and specific role in the PG.

#### **5.6.4. Are *Start1* and *Npc2c* necessary for the observed rescue of *Npc1a* mutants by cholesterol and 7DC?**

The apparent inability of 20E and its precursor sterols C and 7DC to rescue the developmental arrest of PG-specific *Npc2c-RNAi* animals is intriguing. *Npc1a* mutants on the other hand, which additionally display the sterol-accumulation phenotype characteristic of Niemann-Pick disease, are completely rescued by cholesterol and 7DC, suggesting that the supplemented sterols are somehow efficiently transported between subcellular organelles to complete 20E synthesis in PG cells, independent of *Npc1a*. However, this scenario may not be feasible under *Npc2c* knockdown conditions. To test my hypothesis that *Start1* and *Npc2c* that key players in the rescue of *Npc1a* mutants by cholesterol, future experiments should reassess the *Npc1a* mutant rescue by doubly knocking down *Start1* with or without *Npc2c-RNAi* in PG cells. If we observe that supplemented sterols display a weaker rescue of *Npc1a* mutant, the follow-up studies will help shed a new light on the cellular function of *Npc2c*, specifically with respect to intracellular sterol transport and 20E synthesis within PG cells.

### 5.7. Prothoracic gland-specific screen of the *Npc2* gene family

*Drosophila* has a subfamily of eight *Npc2*-like genes, named *Npc2a-h*, whose exact molecular functions are entirely unknown. While *Npc2a* and *Npc2b* single mutants have been demonstrated [182] to be viable, double mutants display a range of larval, pupal and adult lethality, all of which are fully rescued to adult stages by feeding either 20E, cholesterol or 7-DC, implying that *Npc2a* and *Npc2b* might have redundant roles in 20E synthesis. Our data indicates that *Npc2c* has an essential function within the prothoracic gland (PG) cells. Hence, I explored whether the larval arrest phenotype observed with *Npc2c-RNAi* is exclusive to *Npc2c* function, or whether other *Npc2* genes might have overlapping roles in this tissue. I triggered RNAi-mediated knockdown of all *Npc2* genes in PG using the *dcr;phm-Gal4* driver (**Figure 5.26**) and screened for effects on developmental timing, animal size and survival, relative to the controls *dcr;phm>w*<sup>1118</sup>. With the exception of *Npc2g*, the PG-specific knockdown of *Npc2a*, *-2b*, *-2d*, *-2e*, *-2f* and *-2h*, produced no phenotypic effects on development, regardless of the media they were reared on (LD or SM). Specifically, PG-specific knockdown of *Npc2g* on standard and LD media (**Figure 5.27**) demonstrated a range of phenotypes, presumably due to the variability in strength of the RNAi-mediated silencing. The VDRC line #104942 demonstrated higher penetrance and stronger *RNAi* phenotypic effects than #6523 and resulted in pupal arrest (~60% on SM and 100% on LD media), revealing a novel role for *Npc2g* within the PG. This observation substantiates the previous observation by Ou et al, that torso and ras, both regulators of PTTH signaling modulate *Npc2g* transcripts in brain-ring gland complexes. Importantly, the degree of *dcr;phm>Npc2g-RNAi* phenotypic arrest worsens in conditions of dietary sterol deprivation, i.e. LD medium, suggesting that *Npc2g* function might be closely related to changes in cellular sterol levels.

	<i>npc2</i> gene	RNAi line(s) tested	Transcript knockdown quantified by qPCR		Observed phenotypes		Figure references
					LD	SM	
<i>dcr; phm-Gal4 &gt;</i>	<i>npc2a-RNAi</i>	(VDRC) 30722	no		none	none	none
	<i>npc2b-RNAi</i>	(VDRC) 101233	no		none	none	none
	<i>npc2c-RNAi</i>	(VDRC) 31139, 31140	yes	>4 fold knockdown	L3 arrest		Figure 5.8
		(VDRC) 101583	yes	RNAi ineffective	L3 arrest (<10% penetrant)		Figure 5.6
	<i>npc2d-RNAi</i>	(VDRC) 31095	yes	>2 fold knockdown	none	none	none
	<i>npc2e-RNAi</i>	(VDRC) 28594, 100445	yes	>2 fold knockdown	none	none	
	<i>npc2f-RNAi</i>	(VDRC) 12915, 102172	no		none	none	none
	<i>npc2g-RNAi</i>	(VDRC) 50722, 50721	no		none	none	none
		(VDRC) 6523			Pupal arrest		Figure 5.27
		(VDRC) 104942					
<i>npc2h-RNAi</i>	(VDRC) 38273, 46905	no		none	none	none	

**Figure 5.26: Summary of results from the prothoracic gland-specific RNAi screen of the members of the *npc2* gene family.**

RNAi-transgenic lines of each of eight members of the *npc2* gene family, i.e. *npc2a*, *2b*, *2c*, *2d*, *2e*, *2f*, *2g* and *-2h*, were obtained from VDRC and crossed to *dcr;phm-Gal4*. 50 embryos of each genotype were transferred to lipid-depleted (LD) medium and standard medium (SM), and were scored daily for any effects on developmental timing, size and survival. Controls are *dcr;phm>w<sup>1118</sup>*. Each genotype was tested in triplicates for each media type. *dcr;phm-Gal4* transgene drives expression in the prothoracic gland.

**Figure 5.27: Prothoracic gland-specific knockdown of *Npc2g* is pupal lethal.** Images (top panel) are representative photographs of the PG-specific knockdown of *Npc2g* using the independent VDRG transgenic lines #6523 and #104942, that cause developmental arrest as pupae on standard medium; SM and on lipid-depleted medium; LD. Vertically stacked columns (lower panel) represent the proportion of adult survivors in the population versus the proportion of animals that fail to develop beyond larvae or pupal stages, as indicated: L1; solid black bars, L2; diagonal black stripes, L3; grids, pupae; solid white bars, adults; solid grey bars, respectively. 50 embryos of *dcr;phm>w<sup>1118</sup>* and *dcr;phm>Npc2g-RNAi*, were transferred to either SM or LD media. Populations were scored daily for 12 days by counting the number of viable animals at every developmental stage. Error bars represent standard deviation calculated from 3 replicates. *dcr;phm-Gal4* transgene drives expression in the prothoracic gland. VDRG #104942 exhibited higher penetrance than the #6523 line.

Figure 5.27

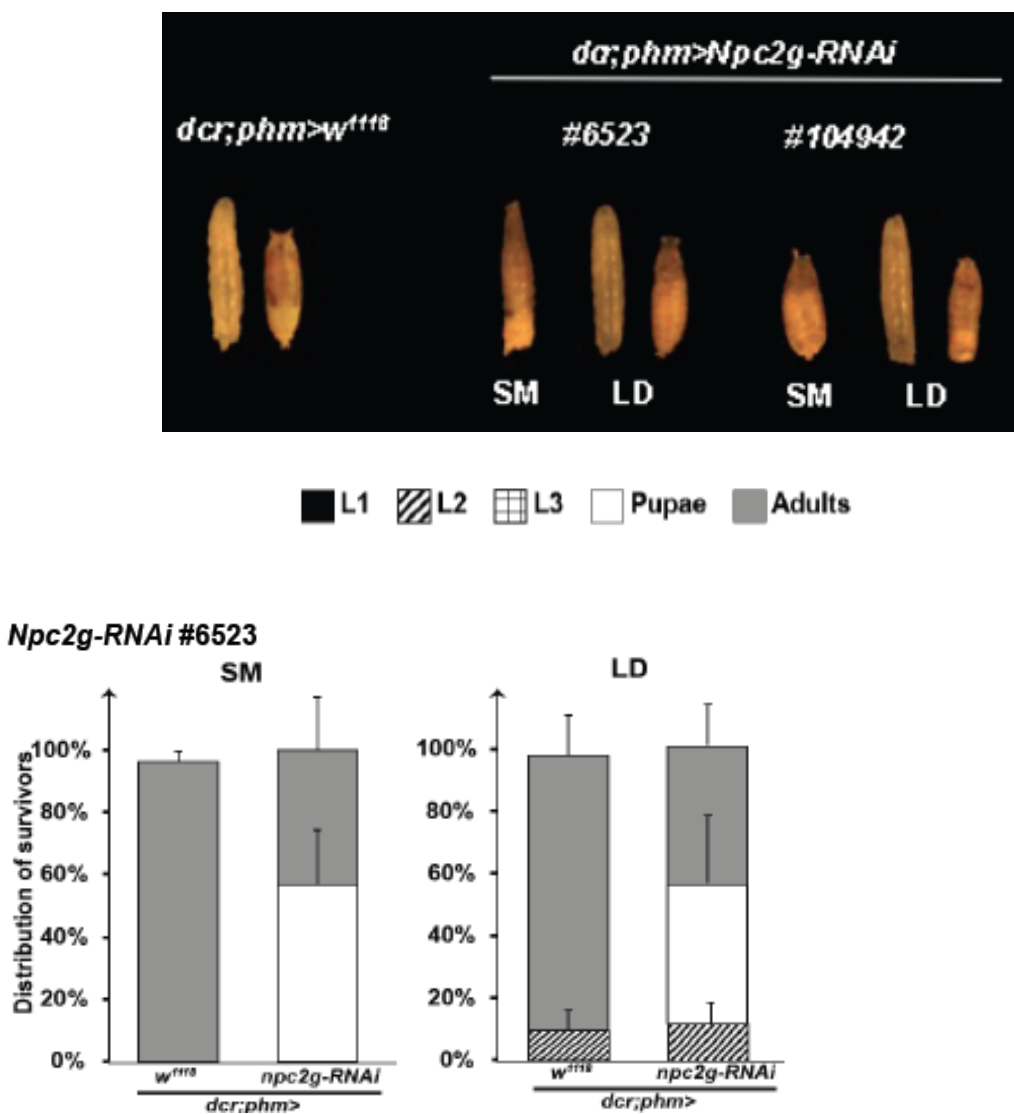
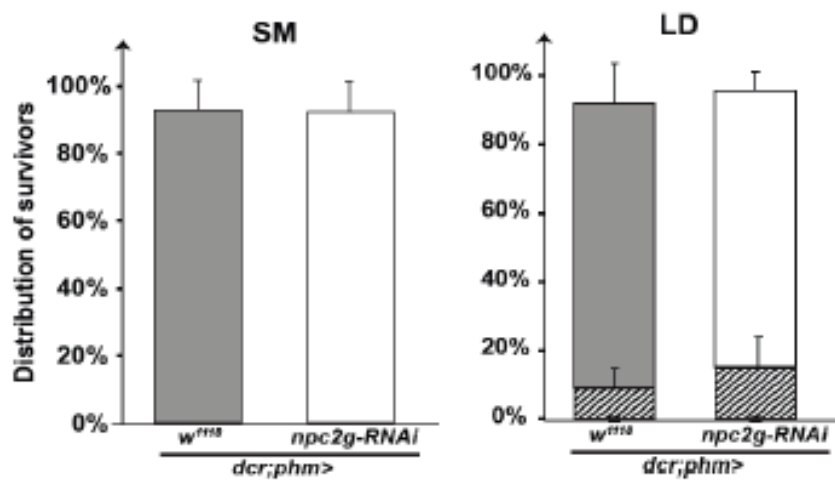


Figure 5.27 (contd.)

■ L1   ▨ L2   ▩ L3   □ Pupae   ■ Adults

***Npc2g-RNAi* #104942**

**CHAPTER 6. DISCUSSION**

### 6.1. *DHR96*<sup>1</sup> mutants as a tool to study *Drosophila* sterol biology

It is a well established that insects cannot synthesize sterols *de novo* and thus have an obligate requirement for dietary sterols to complete development [183][184]. The known functions of cholesterol in *Drosophila* include: (i) steroid hormone 20E biosynthesis, (ii) structural modification of hedgehog (hh) protein to mediate developmental signaling processes [68], [136], [185]–[187] and (iii) in bulk amounts in cell membranes to maintain stability and sterol-dependent membrane microdomains that can in turn regulate a wide range of signaling pathways [188], [189]. I have shown that wild type *Drosophila* fail to survive on diets containing a combination of sterol analogs, despite supplementing sterol analogs that can be utilized by *Drosophila* to functionally replace known functions of cholesterol in insects (**Figure 3.11**). This finding suggested that *Drosophila* requires cholesterol (itself) or a related sterol metabolite to fulfill a previously uncharacterized sterol function necessary to complete adult development. Under severe dietary sterol shortage, *Drosophila* arrest growth and development by drastically reducing average membrane sterol levels [73], presumably to conserve sterols for other metabolic functions. Intriguingly, these animals were found to increase production of sphingolipids and hydroxylated fatty acids – lipid molecules that are known to structurally substitute for cholesterol in myelin and gut apical membranes, revealing that *Drosophila* has evolved to utilize a range of lipids to substitute for sterols in membranes [190] [191]. Indeed, *Drosophila* can use stigmasterol and ergosterol for growth and survival, presumably via modifications to the C22 double bond, which explains why I observed that *DHR96*<sup>1</sup> mutants can be fully rescued to adult stages on LD by supplementing ergosterol and stigmasterol, in a manner identical to that achieved by cholesterol supplementation. **This indicated that the loss of *DHR96* does not affect the animal's ability to utilize a range of sterols (Figure 3.3).** *Drosophila melanogaster*, although closely related phylogenetically to *Musca domestica* (house fly), is incapable of dealkylation. Nutritional studies in several phytophagous insects such as *Bombyx mori* (silk moth), *Aedes aegypti* (mosquito larvae), and *Pyralidae nubilalis* (corn borer) have shown that supplementing ergosterol was more effective than cholesterol in promoting growth and survival [192], whereas stigmasterol was somewhat less effective than cholesterol as shown by some studies carried out in *Drosophila melanogaster* [193].

Nevertheless, there are no reports testing the purity of the sterols used in these historical studies. This has led to large gaps in our knowledge of the sterol requirements and metabolism of *Drosophila*, raising the need to conduct more defined nutritional experiments using high purity sterols and fly media.

20-hydroxyecdysone (20E), a C27-ecdysteroid, has been classically considered the major active steroid hormone in *Drosophila*. However, *in vitro* studies on wandering larvae demonstrate that the *Drosophila* ring gland synthesizes and secretes  $\alpha$ -ecdysone and 20-deoxymakisterone (both C28-ecdysteroids), and can enzymatically convert them to 20E and makisterone A, respectively, in peripheral tissues such as fat body [194]. Importantly, the relative proportions of these circulating ecdysteroids solely depend on the sterol composition of the diets on which the larvae were reared. **Campesterol, the phytosterol derived from maize, is considered the likely precursor of makisterone A in *Drosophila*** and in honeybees [195]. Given the fact that *Drosophila* cannot dealkylate C28-phytosterols to produce cholesterol, larvae fed on yeast-based diets (that predominantly contain ergosterol) produce another steroid hormone, the 24-epi-makisterone A. In contrast, larvae reared on standard fly medium supplemented with (as low as 0.0005%) cholesterol seem to preferentially use cholesterol and exclusively synthesize 20E, suggesting that although *Drosophila* can utilize a range of sterols as substrates for steroid hormones, cholesterol is the preferred substrate. Interestingly, makisterone A and 20E are the most abundant ecdysteroids during pupariation in *Drosophila* [139]. Since these ecdysteroids display different affinities and potency to bind the ecdysteroid receptor (EcR), future work will be important to fully understand the signaling pathways regulating the synthesis of these ecdysteroids and their physiological significance in development.

I have attempted to explore which aspects of *Drosophila* sterol biology require dietary cholesterol, particularly within the context of development and survival on sterol-depleted diets. I have demonstrated that the prohormone  $\alpha$ -ecdysone has a previously uncharacterized role in *Drosophila* development. The first evidence that insects utilize  $\alpha$ -ecdysone for a unique function came through the work by Champlin and Truman [88], who showed that a high-titer of  $\alpha$ -ecdysone promotes extensive proliferation during optic lobe neurogenesis in *Manduca sexta*. In this insect, ring glands secrete 3-dehydroxyecdysone and convert it to  $\alpha$ -ecdysone in the hemolymph. Studies based on the transcriptional activities of

$\alpha$ -ecdysone using reporter genes, showed that  $\alpha$ -ecdysone has differential responsiveness to mosquito versus *Drosophila* EcR-USP heterodimers [196] and that it may mediate its signaling via DHR38 rather than the canonical EcR/USP [197]. The fact that  $\alpha$ -ecdysone has lower binding affinity and potency for EcR may suggest that in the presence of 20E, a higher concentration of putative  $\alpha$ -ecdysone ligand molecules are required to exert a competitive advantage towards EcR binding. This supports my observation that in order to utilize  $\alpha$ -ecdysone (for a yet unidentified purpose) when supplemented in combination with 20E, wild type animals require relatively higher concentrations of  $\alpha$ -ecdysone than 20E to survive on lipid-depleted diets (**Figure 3.11**). This is even more pronounced under conditions of limited sterol availability, where a higher 20E:  $\alpha$ -ecdysone ratio may inadvertently become more disruptive to development. This could explain why I consistently see a higher proportion of adult survivors when  $\alpha$ -ecdysone is supplemented at a higher concentration than 20E levels (**Figure 3.11**). Arguably, the supplemented  $\alpha$ -ecdysone is also being converted to 20E in peripheral tissues, suggesting that there exists a critical balance in the *in vivo* titres of  $\alpha$ -ecdysone: 20E and that both ecdysteroids have exclusive functions in *Drosophila* development and survival.

The work presented here suggests that DHR96 is necessary to trigger transcriptional changes in response to changing dietary cholesterol levels. DHR96 appears to function as a critical sensor of low cellular cholesterol and orchestrates genome wide transcriptional programs to overcome the cellular cholesterol paucity induced on sterol-depleted diets. The main question is why *DHR96*<sup>l</sup> mutants arrest development on a low-cholesterol diet, and given that supplementation of cholesterol is sufficient to fully rescue this lethal phenotype, I asked what function of cholesterol is being rescued in these mutants? I report the first evidence that *DHR96*<sup>l</sup> mutant lethal phenotype can be rescued on lipid-depleted diets without any added cholesterol and that a combination of bulk membrane sterol (desmosterol), the physiologically active steroid hormone (20E) and  $\alpha$ -ecdysone is sufficient to fully and functionally substitute for cholesterol. The observation that *DHR96*<sup>l</sup> mutants absolutely require both  $\alpha$ -ecdysone and 20E (in addition to membrane sterols) is in sharp contrast to our studies on single isolated wild type larvae that can survive on lipid-depleted diets supplemented with membrane sterol and  $\alpha$ -ecdysone alone (**Figure 3.10**). Since *DHR96*<sup>l</sup> mutants have always displayed a higher sterol requirement than wild type (**Figure**

3.3 & 3.5), it is not necessarily surprising that a similar contrast from wild type sterol requirements exists. However, the fact that *DHR96* mutant phenotypes can be fully rescued by a combination of two steroid hormones (and membrane sterols) raises the possibility that DHR96 may have an autonomous or non-autonomous regulatory role in the prothoracic gland (PG) – the site of ecdysone synthesis. As a result of *RNAi* epistasis experiments (Figure 5.12), and gene expression analyses (Figure 4.3, 4.5-4.7), I hypothesized that the Niemann-Pick type C gene, *Npc2c* is a likely target of DHR96. This member of the *Npc2* gene family is predicted to perform an indispensable function in intracellular cholesterol trafficking, similar to the vertebrate homolog, NPC2. Knockdown of *Npc2c* in the PG causes larval lethality that is partially rescued by 20E supplementation, suggesting that *Npc2c* knockdown affects distribution of cellular cholesterol, which in turn impairs ecdysone synthesis within the PG by down regulating key ecdysone biosynthetic genes (Figure 4.16), which ultimately affects *Drosophila* metamorphosis (Figure 4.14). Interestingly, PG-specific knockdown of DHR96 downregulates *Npc2c* expression (Figure 4.17), closely resembling the repression of *Npc2c* in *DHR96<sup>l</sup>* mutants relative to wild type on standard medium (Figure 4.3B), thus supporting the hypothesis that *Npc2c* may be a direct target of DHR96. However, transgenic expression of *DHR96* or *Npc2c* within PG cells of the mutant fails to rescue the *DHR96<sup>l</sup>* lethal mutant phenotype (Figure 4.8), raising the need for future work to address the tissue—specific factors regulating *Npc2c* expression.

In addition, *in vitro* studies have indicated that a wide range of ecdysteroids including 20E, makisterone A,  $\alpha$ -ecdysone, fail to have any significant effect on the activity of DHR96, which along with the fact that DHR96 protein has not been detected in the PG or the brain, weakens the argument for a direct autonomous role for DHR96 in the PG. On the other hand, DHR96 has been indicated to interact with EcR to trigger ‘glue’ synthesis in response to a 20E signal, suggesting that DHR96 may have additional roles in peripheral tissues such as the fat body where 20E is synthesized and has downstream molecular effects on larval development. Therefore, future work addressing the functional significance of  $\alpha$ -ecdysone and insights into the spatio-temporal regulation of DHR96 targets genes will be critical to better understand *Drosophila* sterol biology and how this ties into sterol metabolism and development.

## 6.2. Cholesterol regulates gene expression in *Drosophila*

Studies by Horner *et al.*, indicate that DHR96 binds cholesterol, suggesting that *DHR96* functions as a cellular sensor for varying sterol levels and that cholesterol itself, or a structurally similar metabolite thereof acts as a ligand for DHR96. Thus the plausible reasoning for the observed lethality of *DHR96<sup>l</sup>* mutants is that they are unable to sense that they are ingesting a low-cholesterol diet and therefore fail to implement the transcriptional programs that are necessary to adapt to conditions of severe cholesterol scarcity, specifically to maintain cellular cholesterol homeostasis. On standard medium, cholesterol-metabolizing genes are dynamically regulated to likely maintain coordinated influx and efflux of cellular cholesterol (**Figure 4.3 and 4.5**). Sterol-depleted diets, such as the LDC424 that I have developed, or the ‘low cholesterol’, commercially available, ‘C424’ medium, pose a survival threat since *Drosophila* cannot synthesize cholesterol *de novo*. In such conditions when dietary cholesterol concentrations decline, wild type animals are likely to maximize absorption of available dietary sterols to protect cells from drastic cholesterol deprivation. This would explain why wild type animals reared on C424 media transcriptionally upregulated genes such as *Npc1b* and *Lip3*, which are involved in increasing cellular cholesterol levels, and repressed genes such as *Npc2c* and *ACAT* (**Figures 4.3A-C, E-G and I; black bars**). *Npc1b*, the *Drosophila* ortholog of mammalian NPC1L1 [109] is a midgut-specific putative target of DHR96 necessary for dietary cholesterol absorption, while, *Lip3* is predicted to hydrolyze cholesteryl esters to free cholesterol, a crucial step in utilizing stored cholesterol reserves to meet cellular cholesterol functions. On the other hand, *Npc2c*, encodes a putative lysosomal cholesterol trafficking protein and *ACAT*, encodes an enzyme predicted to esterify free cellular cholesterol for storage and future utilization. Importantly, neither of these genes responded in this manner in *DHR96<sup>l</sup>* mutants that were fed C424 medium, suggesting that these transcriptional responses are strongly *DHR96*-dependent. In spite of the apparent failure of *DHR96<sup>l</sup>* mutants to express genes that increase cellular cholesterol levels or repress genes that deplete free available cellular cholesterol (**Figures 4.3A-C, E-G and I; grey bars**), *DHR96<sup>l</sup>* mutants did not seem to suffer from insufficient absorption of dietary cholesterol, since the total cholesterol and cholesteryl ester levels were only 20% lower than wild type[54]. Rather, it appears that *DHR96<sup>l</sup>* mutants fail to

upregulate *Npc1b* and *Lip3* because at the cellular level, mutant cells still function as though they had sufficient sterol levels (**Figure 6.5**). Similarly, *DHR96*<sup>l</sup> mutants fail to repress *Npc2c* and *ACAT*, likely because they actively reduce cellular cholesterol levels under conditions of low dietary cholesterol concentrations. Instead, *DHR96*<sup>l</sup> mutant cells likely continue to efflux cholesterol, as they would do on a sufficiently sterol rich diet, thus aggravating the cellular cholesterol paucity resulting from low dietary cholesterol.

By employing high-throughput microfluidic qPCR (**Figures 4.5-4.7**), I have shown that feeding a *high cholesterol* diet (1% w/v cholesterol) transcriptionally phenocopies the genome-wide effects of a mutation in *DHR96*. Since *DHR96* is only required for survival when animals are reared on lipid-depleted (LDC424) or low-cholesterol diets (C424), we proposed that *DHR96* is actively transcribing downstream target genes under low cellular cholesterol conditions. Our findings to date appear to indicate that cholesterol, or a similar metabolite, acts as an inverse agonist by inactivating *DHR96* upon binding. An inverse agonist differs from an antagonist, because unlike an antagonist ligand, an inverse agonist can not only bind to the same receptor and interfere with the agonist-mediated response, it can also provoke a biological response on its own that is opposite to that of the agonist. Loss of *DHR96* function via a mutation thus causes mutant cells to transcriptionally behave as though they are feeding on a *high cholesterol* diet, which explains why *DHR96*<sup>l</sup> mutant stocks are healthy and viable on the sterol rich standard medium, indicating that *DHR96* is not required for survival when cholesterol concentrations are sufficiently high, likely because *DHR96* may be rendered inactive by the abundance of its putative ligands on this medium. Conversely, without *DHR96*, cells are unable to sense the drop in their cellular cholesterol levels and fail to execute the transcriptional programs necessary to survive under low cholesterol conditions. A similar inverse agonist mechanism is demonstrated by one of the three vertebrate nuclear receptor orthologs of *DHR96*, the constitutive androstane receptor (*CAR*) that is constitutively active in the absence of its ligand - androstane metabolites [40], [198]. Given that *DHR96* binds cholesterol [113], this inverse agonist model best fits the argument that cholesterol (or a cholesterol metabolite) regulates *DHR96* activity and indicating that *DHR96* thus functions as a cellular low-cholesterol sensor. Feeding sterol-depleted diets results in a drop in the cellular levels of putative *DHR96* ligands, likely cholesterol, and triggers allosteric changes in *DHR96* that manifest as

differences in target gene regulation to counteract the cholesterol paucity. This model for *DHR96* function differs from its mammalian homolog, the Liver X Receptor (LXR $\alpha$ ), which is activated by endogenous oxidized derivatives of cholesterol, called oxysterols, to protect cells from *high cholesterol* levels.

A case in support of this model is my finding that we can reverse the direction of gene regulation (fold change values) of putative *DHR96* targets by merely switching the dietary sterol availability. I ectopically expressed *DHR96* in wild type animals reared on standard or LDC424 media (**Figure 4.7**), such that the genotypes tested were similar in terms of *DHR96* expression, and resulting transcriptional changes are in response to dietary sterol levels. On standard medium, some genes were induced (*Lip3*), repressed (*ACAT*, *FANCL*, *Npc1b*) or unaffected (*ABCA1*, *hh*) by *DHR96* overexpression. Strikingly, the same genes were induced (*Lip3*, *Npc2c*, *ABCA1* and *hh*) or de-repressed (*ACAT*, *FANCL*) on lipid-depleted media. This implied that the sterol compositions and concentrations between LDC424 and standard medium were responsible for the transcriptional responses in genes associated with different aspects of cholesterol homeostasis. We have observed that *DHR96* transcripts are repressed in response to increasing cholesterol levels [54] which demonstrate that cholesterol may modulate *DHR96* function presumably by direct binding as a ligand, or via regulating *DHR96* transcription, which strengthens my argument that cholesterol functions as an inverse agonist to *DHR96* activity. Since *DHR96* protein may regulate its own transcripts via a feedback mechanism, it is likely that increasing cholesterol levels can reduce *DHR96* protein activity, which in turn could modulate *DHR96* mRNA levels by an autoregulatory loop.

My doctoral work provides new information on genes that have critical functions in maintaining cellular cholesterol homeostasis in *Drosophila*. I have used standard *Drosophila* media and developed new sterol supplemented diets as a strategy to identify genes that function in sterol metabolic pathways. Employing a nutrigenomics approach based on diets supplemented with fats other than cholesterol (**Figure 4.7**), I identified that the expression of at least six genes are strongly dependent on dietary cholesterol levels and *DHR96* function. These include four Niemann-Pick genes – *Npc1b*, *Npc2c*, *-2d*, and *-2e*, the midgut-specific lipase; *Magro* (*CG5932*), and *LpRI*; a LDL-receptor-related protein. A follow-up study demonstrated that *DHR96*<sup>l</sup> mutants are resistant to diet-induced obesity and

that DHR96 maintains triacylglycerol (TAG) homeostasis and systemic cholesterol clearance via direct regulation of *Magro* expression. Moreover, the *Drosophila Npc2* genes - *Npc2d* and *Npc2e*, which are the most highly down- and upregulated genes in *DHR96<sup>l</sup>* mutants and in wild type animals in response to a *high cholesterol* diet, are both homologs of vertebrate NPC2, which is a known target of LXR $\alpha$ . This suggested that *DHR96* might function analogous to its mammalian nuclear receptor, LXR $\alpha$ . Many DHR96-regulated genes such as members of the *Npc2* family and *FANCL* are grouped in clusters (e.g. the 85F8 cytogenetic locus), suggesting that the encoded products are likely functionally related and possibly coordinately regulated. From a molecular standpoint, future efforts in defining the DNA-binding sites of DHR96, identifying its binding partners, and tissue-specific transcriptional regulatory elements are crucial to understanding the mechanism by which the DHR96 nuclear receptor maintains cholesterol homeostasis. This is particularly important since DHR96 appears to simultaneously regulate the expression of a diverse array of cholesterol-responsive genes through transcriptional activation as well as repression. The molecular basis for this bimodal activity could be attributed to its promoter context and the availability (and choice) of binding partners in *DHR96*-mediated transcriptional regulation. For example, the activator activity of ligand-inducible transcription factors RAR, the retinoic acid receptor and RXR, the retinoid X receptors, which regulate transcription of retinoid-responsive genes, have been shown to be largely dependent on promoter context [199].

### **6.3. *DHR96* controls cellular cholesterol homeostasis via the Niemann Pick type C genes**

I have identified that *DHR96* regulates several genes that have homologs with known functions in vertebrate cholesterol metabolism (**Figure 4.2**). Importantly, the fact that four of these eight genes, i.e. *Npc1b*, *Npc2c*, *Npc2d* and *Npc2e* belong to the 10 member Niemann Pick Disease Type C family of lysosomal cholesterol transporters is highly significant (*P* value, 6.5E-124). This led to the idea that DHR96 controls cellular cholesterol distribution and homeostasis by transcriptionally regulating *Npc* genes, although no studies have yet determined the exact functions of these genes. The modENCODE RNA-Seq data [200] indicated that the top genes affected by dietary cholesterol and mutation in *DHR96*, displayed maximal expression in the gut of larvae and adults (**Figure 6.3**), implying that

they play critical roles in dietary sterol absorption, secondary cellular sterol uptake and metabolism. Tying this in to the observation that expression of *DHR96* in the midgut is sufficient to rescue the mutant lethal phenotype on LD (**Figure 4.8**) indicates that DHR96 plays an essential role in controlling at least some aspects of dietary cholesterol absorption and secondary cellular uptake.

I tested whether the transcriptional profiles of *Npc2c* in *DHR96<sup>l</sup>* mutants, or the reciprocal expression patterns between *Npc2d* and *Npc2e* in wild type animals in response to high cholesterol, are functionally significant. I used RNAi transgenic constructs of *Npc2c*, -*2d*, and -*2e*, and found that the knockdown of only *Npc2c* either ubiquitously, in the midgut or in the PG severely affects viability resulting in developmental arrest phenotypes (**Figure 5.8, 5.11, 5.15**). If *Npc2c* is important in trafficking cellular cholesterol within the midgut, it is likely that it is also involved in early steps in dietary cholesterol absorption and could directly affect systemic whole body cholesterol levels. If true, this might explain why higher levels of supplemented dietary sterols fail to rescue the midgut-specific *Npc2c-RNAi* lethal phenotype. This can be tested using the Amplex Red kit (Molecular Probes), which measures levels of total cholesterol and cholesteryl esters in lipid extracts. Interestingly, I observed that midgut-specific *Npc2c* knockdown partially rescues *DHR96<sup>l</sup>* mutants on LD medium (**Figures 4.12 and 4.13**), suggesting that the induction of *Npc2c* in *DHR96<sup>l</sup>* mutants relative to wild type (**Figure 4.3 B**) on C424 medium could contribute to the *DHR96<sup>l</sup>* mutant lethal phenotype. Based on the function of its mammalian homolog, I predict that *Npc2c* may be necessary for the subcellular movement of cholesterol or similar sterols to other cellular destinations for its utilization. Taken together with the model that *DHR96* functions as a custodian for low cellular cholesterol concentrations, I hypothesize that *DHR96* may transcriptionally repress *Npc2c* in midgut to conserve cellular cholesterol reserves under sterol-deprived conditions. The characteristic ‘giant larvae’ phenotype of PG-specific *Npc2c-RNAi* animals although a developmental arrest, resulted in extended third instar larval stage wherein arrested larvae continued to survive as L3 for about ten days without metamorphosis. It is likely that during this extended phase, larvae continued feeding, resulting in increased body sizes. There are several methods currently being developed to accurately measure food intake in *Drosophila*. Labeling fly food with a radioactive tracer or colorimetric dye to monitor their feeding and gut clearing status could

help understand whether a prolonged feeding stage caused the ‘giant L3’ size defects. Alternatively, *Npc2c* function in the CNS is critical for other 20E-associated pathways that could affect growth and development.

Other cholesterol-binding transporter proteins have been implicated in the regulation of key steps in 20E synthesis. For example, *Drosophila Npc1a* is critical to ensure sufficient availability of sterol substrates for 20E synthesis in the PG [201], which is why *Npc1a* mutants can be fully rescued by supplementing excess cholesterol or 7-dehydrocholesterol (**Figures 5.25 - 5.27**), similar to *Npc2a* and *Npc2b* mutants [182]. The *Npc1a* mutants display a distinct filipin-positive cholesterol-accumulation phenotype (**Figure 5.24**), which is explained by the paradoxical ‘sterol-shortage’ model [179]. According to this model, a loss of *Npc1a* function results in endosomal entrapment and accumulation of cholesterol, and subsequent shortage of cellular cholesterol for ecdysone synthesis in the PG. In contrast to *Npc1a*, my data on PG-specific *Npc2c-RNAi* do not demonstrate a positive filipin staining (**Figure 5.24**). Instead, *Npc2c-RNAi* causes late-larval developmental arrest that cannot be rescued by ecdysone or its precursors, suggesting that *Npc2c* and *Npc1a* may be involved in transporting different sterol molecules. Mammalian NPC2 has been shown to bind a range of different types of sterols and lipids, raising the possibility that the *Npc2c-RNAi* lethality might arise from a cellular accumulation of critical sterols that may not be reliably detected using the classical filipin [202] stain that is widely used as a histochemical marker for cholesterol. Currently, newer techniques are being developed to better visualize cellular sterol metabolites [203]–[205]. Moreover, with eight *Npc2*-like genes in *Drosophila*, functional redundancy and the variety of sterols that their encoded proteins could bind to, can cloud these phenotypic interpretations. Moreover my preliminary data indicates that in addition to *Npc2c*, *Npc2g* might have critical PG-specific roles. Thus further studies are necessary to validate these findings in null mutants to rule out incorrect interpretations by false positive or negative results common to *RNAi* [206].

The *Drosophila* PTTH signal is well known to trigger the synthesis and release of ecdysone in the PG, and thus directly controls the timing of developmental transitions and larval body size [79]. PTTH binds its receptor Torso, and activates ecdysone production via

the Ras, Raf and ERK/MAPK\* pathway [167] [168]. A related study from our lab indicated that constitutively active form of *Ras* (*Ras<sup>v12</sup>*), repressed *Npc2c*, and conversely, that the PG-specific knockdown of the PTTH receptor torso relieved the repression, suggesting that the PTTH signaling cascade might itself regulate *Npc2c* expression within the PG (**Chapter 5, Supplemental Figure 5B**). If *Npc2c* were to function analogously to vertebrate *Npc2*, then it represents one of the final steps of the pathway critical for effluxing lysosomal cholesterol for ecdysone synthesis in the PG. Consequently, affecting the PTTH signaling cascade could coordinately interfere with other endocrine pathways that directly control larval feeding and growth during the final instar stages [207] [208].

My preliminary data also indicates that the *Drosophila Start1* gene predicted to encode the cholesterol-binding mitochondrial Start1 protein, is crucial within the PG for normal development and survival, and that supplementing excess 20E or its precursor cholesterol can fully rescue the *Start1-RNAi* phenotypes (**Figure 5.25**). Future efforts focused on systematically characterizing the cellular roles of *Start1* and the *Npc2* genes will shed light on the intracellular movement and transport of cholesterol.

RNA interference (RNAi)-mediated knockdown of target mRNA has been extensively used in *Drosophila* to interpret gene function. It is however critical to confirm the specificity of the interference by distinguishing nonspecific phenotypes that might have arisen from off-target effects (OTEs). The core machinery of RNA interference involves activation of the RNA-induced silencing complex (RISC) via the incorporation of small interfering (siRNAs), recognition of target mRNA (by siRNA-mRNA base pairing) and its subsequent cleavage by Argonaute/Slicer. Hence the length and sequence of the siRNA are vital to ensure specificity of silencing and eliminate OTEs. Apart from hybridization of siRNAs with unintentional nucleic acids, short sequence matches of 6-7 nucleotides can function as the seed sequence in a micro (miRNA) and cause translational repression of many off-target genes. It is possible that the siRNA functions unintentionally as a miRNA, causing also OTEs. Intriguingly, while OTEs have not yet been reported in *Caenorhabditis elegans*, there have been several observations in *Drosophila* [209], [210]. I have used transgenic *RNAi* lines extensively for my studies on the *Npc2c*, *-2d*, and *-2e* genes, of which

---

\* **Ras**; Rat sarcoma, **RAF**; Rapidly Accelerated Fibrosarcoma, **ERK**; Extracellular signal-regulated kinase, **MAPK**; mitogen-activated protein kinase

the knockdown of only *Npc2c* (using *Npc2c*<sup>GD6798</sup>) resulted in tissue-specific developmental defects. To ascertain that this is not a result of an off-target effect, I tested the validity of these *Npc2c-RNAi*-induced phenotypes by four approaches. Firstly, *Npc2c*<sup>GD6798</sup> had no effect on the mRNA levels of the predicted off-target CG16720 (serotonin receptor-1A). Secondly, an independent *RNAi* line (*Npc2c*<sup>KK103904</sup>), which only weakly repressed *Npc2c* transcripts (**Figure 5.5**), demonstrated incomplete penetrance and still yet, only partially recapitulated the L3 larval lethal phenotype observed with the *Npc2c*<sup>GD6798</sup> line (**Figure 5.5**). In my third approach to establish the specificity of *Npc2c*<sup>GD6798</sup>, the rescue construct, which contained the genomic region of *D. pseudoobscura* homolog of *Npc2c* (**Figure 5.20**), was lethal when used in combination with the *UAS-Npc2c-RNAi* transgene. This transgene resulted in neomorphic lethal phenotype and thus obscured the interpretation of a possible rescue of *Npc2c-RNAi* phenotypes. This raised the question whether the rescuing construct was functionally inactive, possibly due to lack of its natural cis-regulatory elements, nucleosomal structures or other transcriptional/translational machinery. One could test whether the *D. pseudoobscura* transgene mimics expression of its wild type ortholog by using a combination of *Npc2c* null mutant allele, reporter-tagged versions of the rescue construct to quantify its protein levels, or test the mRNA levels (by qPCR) to validate whether the expression of the rescuing construct is unaffected by the siRNA targeting the *D. melanogaster* gene. I have also generated transgenic flies harboring *Drosophila Npc2c*-cDNA carrying silent mutations in the stretch targeted by *Npc2c*<sup>GD6798</sup> siRNA so as to render them RNAi-resistant. Future work will determine whether this synthetic rescue construct is functionally active enough to rescue the *Npc2c-RNAi* phenotypes and establish *RNAi* specificity by ruling out off-target effects.

Although gene expression studies (described in **Chapter 4**), and the finding that midgut-specific knockdown of *Npc2c* partially rescued *DHR96*<sup>l</sup> mutants, strongly suggest that *Npc2c* is transcriptionally regulated by *DHR96*, I do not have direct evidence to demonstrate whether or how this regulation might occur. I have tested a series of overlapping, varying lengths of upstream promoter constructs of *Npc2c* fused to reporter (*lacZ*) to identify cis-regulatory elements most crucial for *Npc2c* expression (**Figure 6.2**). However, I was unable to identify the functional elements required for transcriptional activation of *Npc2c*, since even the largest upstream region to *Npc2c* failed to recapitulate

wild type *Npc2c* expression patterns on defined media with or without cholesterol (**Figure 6.4**). By employing a transgenic line expressing DHR96 fused to the VP16 activation domain, preliminary (unpublished) data from our lab suggests that DHR96 may bind (~2.6 kb) upstream of *Npc2c* transcription start site, thus providing a viable research direction for future work on the molecular mechanisms by which DHR96 coordinates target gene transcription.

The presence of eight *Drosophila Npc2*-like genes suggests that this gene family encodes highly similar gene products with similar or identical cellular functions and is therefore regulated by shared regulatory pathways. Such redundancies of gene function, particularly arising from gene duplication events such as in the *Npc2* gene family [182], greatly confound phenotypic studies as they may mask or functionally compensate for the loss of function of other related genes. Sequence alignment data [182] indicates that members of this *Npc2* family contain 0 - 3 introns, and that these intron positions are nearly identical to that of the vertebrate *Npc2* gene. This supports the idea that members of this gene family are a result of gene duplication events, and may exhibit a certain degree of functional redundancy. Moreover, *Npc2c*, *-2d*, and *-2e* genes are chromosomally clustered at the cytogenetic locus 85F8 on chromosome III, which strongly suggest that these three genes may be transcriptionally regulated via shared regulatory element.

The expression patterns of these genes in response to RNAi constructs predicted to target their gene-specific transcripts only (**Figure 5.1**), revealed that knockdown of *Npc2c* exclusively reduced *Npc2c* transcripts significantly, whereas the loss or gain of *Npc2d*, and/or *Npc2e* expression affected the mRNA levels of all three genes. Oddly, combining the ubiquitous knockdown of *Npc2d* with *Npc2e* expression, repressed *Npc2e* by ~70% in spite of the *Npc2e* -cDNA transgene. I verified the RNAi specificity of each of *Npc2c*, *-2d*, and *-2e* RNAi constructs using BLAST2 tool to query each of the individual dsRNA double stranded RNA sequence and found that each dsRNA sequence uniquely and exclusively matched only its own specific *Npc2* gene (**Figure 6.3**). Given the fact that I did not observe any phenotypic defects as a result of manipulating *Npc2d* and *-2e* expression patterns, it is likely that *Npc2d* and *Npc2e* are more closely coordinately regulated than *Npc2c*, presumably due to overlapping functions. Future work focused on defining the complete function of each of these *Npc* genes may benefit from the development of new tools for

conditional inactivation, null mutants, double or triple knockout or knockdown of these genes to reveal redundancies in their gene functions.

Figure 6.1

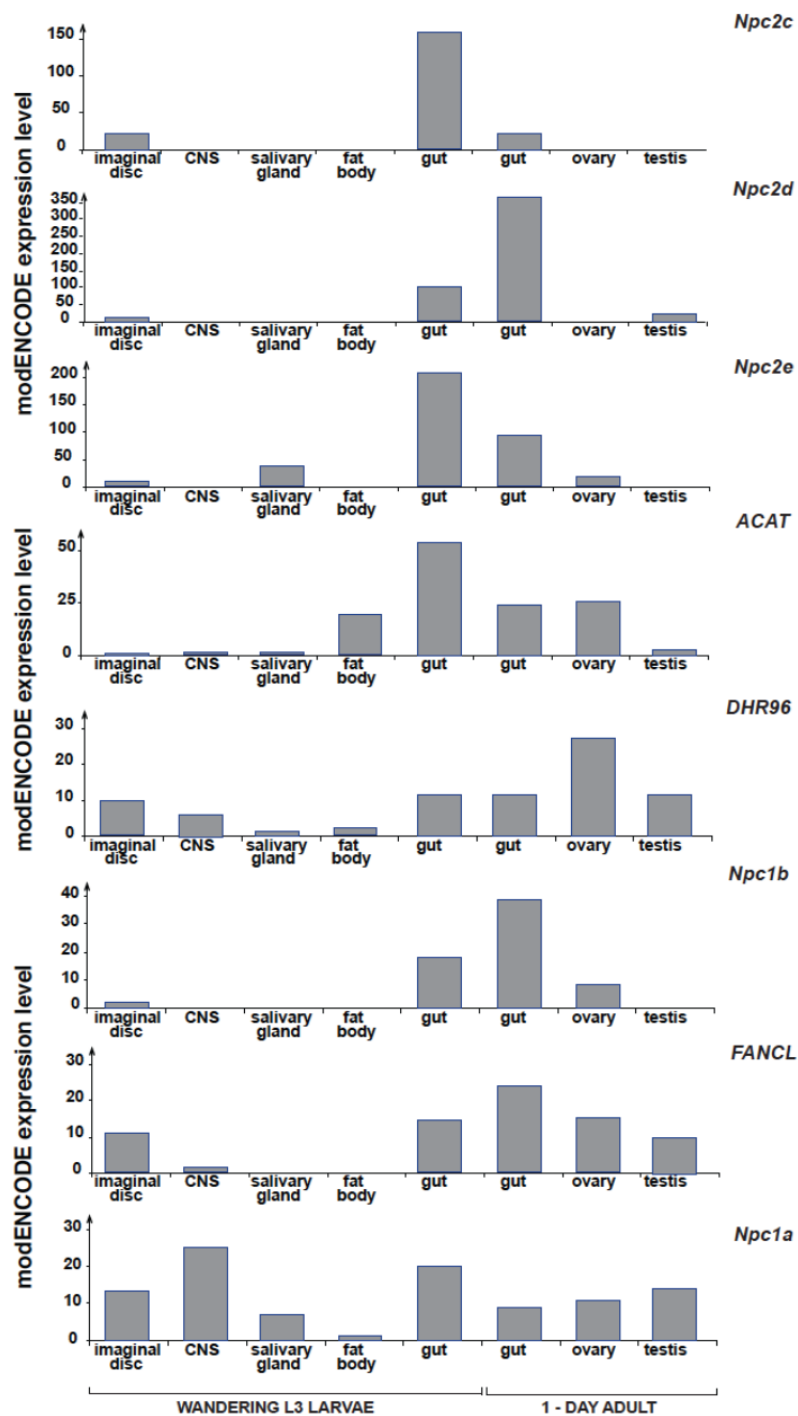
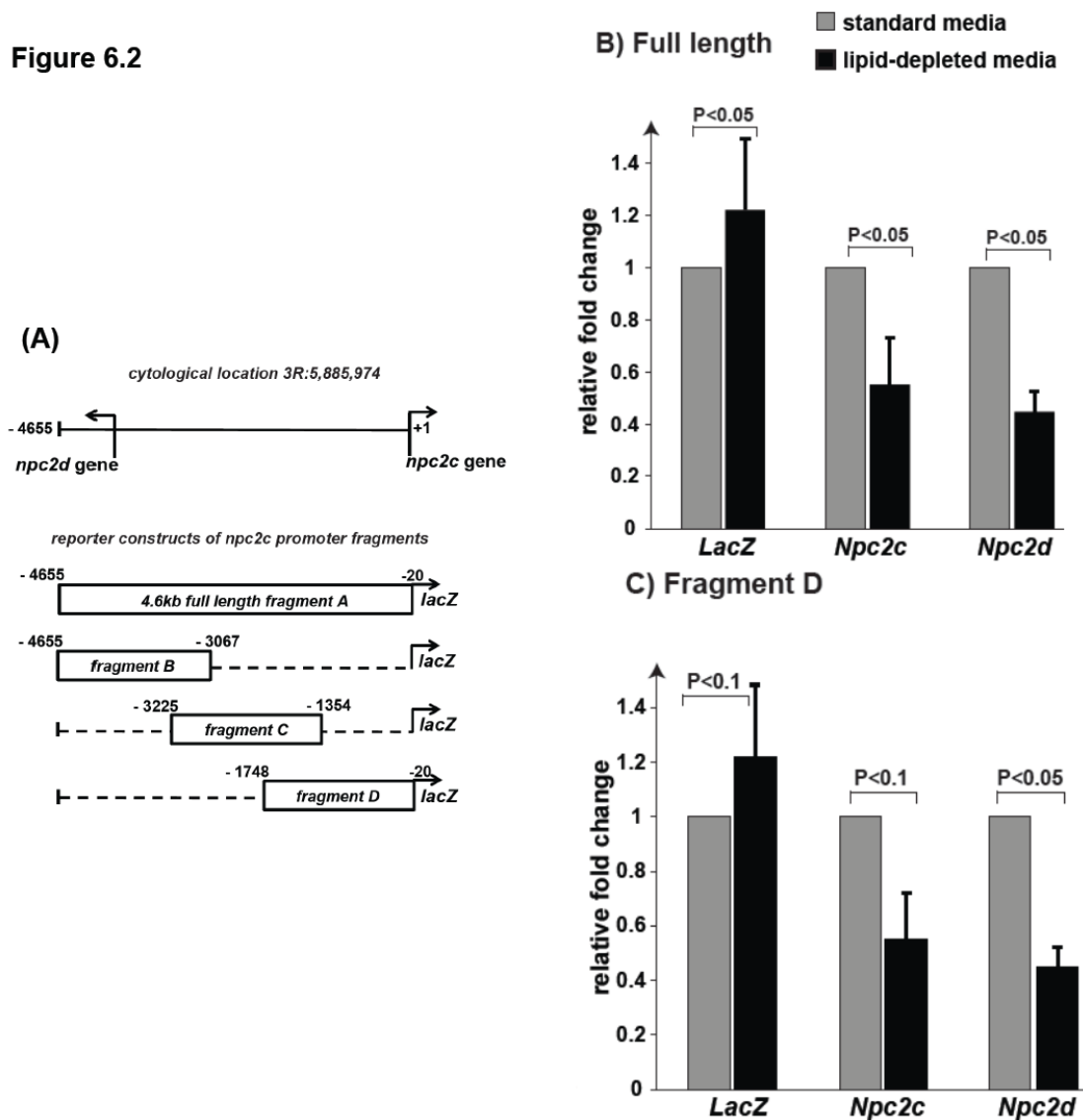


Figure 6.1. modENCODE tissue expression data of top candidate genes regulated by *DHR96* and cholesterol.

Figure 6.2



**Figure 6.2. Promoter analysis of *npc2c* upstream regions.** (A) *lacZ* reporter constructs generated by *N. Farboodi* (unpublished) spanning overlapping sequences upstream of *npc2c*. The full length fragment spans 4.65 kb upstream of *npc2c* which includes 504 bp into the *npc2d* gene region. Fragments B, C,D were constructed as depicted and all fragments were directionally cloned into *placZattB* integration vector and subsequently transformed to generate transgenic flies used for qPCR analysis shown in (B) and (C). (B and C) qPCR on transgenic flies carrying the full-length (B) or fragment D (C). Whole body RNA was collected from third instar wandering larvae staged at 40 h after L2/L3 molt, raised on standard media (grey bars) or raised on lipid depleted media (black bars). Fold changes are relative to expression of *lacZ*, *Npc2c* or *Npc2d* in the full-length or fragment D carrying transgenic flies on standard media. Error bars represent 95% confidence intervals, and P values were calculated with the unpaired Student's *t* test.

dsRNA sequence	Genomic sequence		
	<i>Npc2c</i>	<i>Npc2d</i>	<i>Npc2e</i>
<i>Npc2c</i>	100%	0%	0%
<i>Npc2d</i>	0%	100%	0%
<i>Npc2e</i>	0%	0%	100%

**Figure 6.3.** BLAST2 tool search result: Percentage of match in a BLAST2 search result using double stranded RNA sequence of each of *Npc2c*, *-2d*, *2e* RNAi constructs as 'query' and the cDNA sequence of each of the *Npc2c*, *-2d*, *2e* genes as 'subject'.

#### 6.4. Future directions

There are gaps in our understanding of the sterol requirements of *Drosophila*. In this study, I have conducted survival studies using high purity sterols and defined media, and identified that the prohormone alpha-ecdysone might have novel functions in *Drosophila*. Presumably, wild type *Drosophila* larvae possess mechanisms to maintain the same optimal cellular sterol levels, despite variations in the dietary sterol amounts. Hence exploring the regulatory mechanisms that maintain optimal cellular cholesterol levels will help understand how *Drosophila* utilizes sterols for growth and survival. It is unknown whether the LD medium supplemented with cholesterol is sufficient to nutritionally sustain subsequent generations of *DHR96<sup>1</sup>* mutants and wild type populations, without any adverse effects on fertility. Future work using direct measurements of sterol analytes (by gas chromatography-mass spectrometry (GC-MS)) or ecdysteroids (by Enzyme Immunoassay (EIA) measurements) or using labeled dietary sterols will help complement the phenotypic studies on wild type animals raised on sterol-supplemented lipid-depleted diets and address the effects of supplemented sterols on circulating sterol/steroid titres. This will also allow direct comparison of lipid compositions between wild type and mutants' whole body or specific tissues, under different developmental stages, and reared on different sterol-supplemented diets. Biochemical studies focusing on the signaling pathways that affect the synthesis and downstream effects of sterol-derived ecdysteroids will shed light on the physiological and nutritional significance of different sterols in *Drosophila* development and metabolism.

The work presented here describes that the nuclear receptor DHR96 is necessary to trigger transcriptional changes in response to changing dietary cholesterol levels, suggesting

that DHR96 exerts a regulatory control on gene products involved in maintaining optimal cellular cholesterol levels. In this study, I demonstrated that the expression of selective genes is strongly dependent on dietary cholesterol levels and *DHR96* function. Follow-up work focused using direct methods to identify direct and indirect targets of DHR96 such as chIP-seq will aid in characterizing the molecular pathways controlled by DHR96. In addition, such genome-wide approaches will also provide the direction for further studies in identifying the structural elements involved in DHR96-mediated regulation: such as, identifying DNA-binding sites of DHR96 and exploring its binding partners under different dietary, genetic or even tissue-specific parameters. It will be important to generate DHR96-specific antibodies that can reliably recognize native protein. This is crucial for the aforementioned biochemical approaches and for complementary microscopic methods to visualize the subcellular localization and potential interactions of DHR96 under varying dietary cholesterol levels. Similarly at the cellular level, the advent of new techniques such as the biotinylated  $\theta$ -toxin to visualize cellular sterol metabolites are suggested to present greater sensitivity and selectivity to quantify cellular sterol content, and can ultimately advance our understanding of the mechanisms that regulate cellular cholesterol levels.

## CONCLUSION

Cholesterol is best known for its adverse effects such as stroke and atherosclerosis in humans. However, cholesterol is an essential component of animal cell membranes and the precursor for steroid hormones. The roles of cholesterol in *Drosophila* are beginning to be understood, however the mechanisms by which cellular cholesterol is sensed, transported and metabolized remain unknown. I report my findings that the prohormone  $\alpha$ -ecdysone has a novel role in *Drosophila* sterol biology that is necessary to complete adult development. I demonstrate that the *Drosophila* nuclear receptor DHR96 is a cellular-low cholesterol sensor that has an essential role for survival on sterol-deprived diets. Cholesterol exerts regulatory control on the expression of several genes with predicted roles in cholesterol homeostatic pathways, including vertebrate orthologs of *Npc1b*, *ABCA1* and *Npc2*-genes. Cholesterol, or a related metabolite thereof, has been demonstrated to bind DHR96. Our data indicates that binding to this putative ligand decreases the transcription of *DHR96* and thereby likely rendering it functionally inert or inactive. Among several candidate genes identified in this study, members of the Niemann Pick disease type C (NPC) family of cholesterol transporters demonstrated distinct transcriptional responses to dietary cholesterol in a *DHR96*-dependent manner. The *Niemann-Pick disease type C-2c* (*Npc2c*) gene is necessary to ensure normal developmental progression and survival, and that its spatio-temporal expression is likely regulated by different cell-type specific factors. Follow up studies using direct biochemical methods such as chIP-Seq, and the use of null mutants of *NPC* genes will aid in identifying tissue-specific transcriptional targets of DHR96 in response to dietary cholesterol, and further explore how DHR96 regulates cellular cholesterol homeostasis.

I have used a combination of defined nutritional studies, high throughput gene expression studies and tissue-specific rescue studies, to explore the transcriptional network controlled by *DHR96*. Future work expanding on these studies will ultimately advance our understanding of how the human counterparts of DHR96, i.e. VDR, CAR, SXR, and LXR $\alpha$  contribute to the mechanisms that promote the development of cardiovascular diseases.

## BIBLIOGRAPHY

- [1] F. R. Maxfield, G. van Meer, and G. Van Meer, "Cholesterol, the central lipid of mammalian cells.," *Curr. Opin. Cell Biol.*, vol. 22, no. 4, pp. 422–9, Aug. 2010.
- [2] D. Huster, H. a Scheidt, K. Arnold, A. Herrmann, and P. Müller, "Desmosterol may replace cholesterol in lipid membranes.," *Biophys. J.*, vol. 88, no. 3, pp. 1838–44, Mar. 2005.
- [3] D. J. Peet, S. D. Turley, W. Ma, B. a Janowski, J. M. Lobaccaro, R. E. Hammer, and D. J. Mangelsdorf, "Cholesterol and bile acid metabolism are impaired in mice lacking the nuclear oxysterol receptor LXR alpha.," *Cell*, vol. 93, no. 5, pp. 693–704, May 1998.
- [4] C. F. Garland, E. D. Gorham, S. B. Mohr, and F. C. Garland, "Vitamin D for cancer prevention: global perspective.," *Ann. Epidemiol.*, vol. 19, no. 7, pp. 468–83, Jul. 2009.
- [5] E. J. Squires, T. Sueyoshi, and M. Negishi, "Cytoplasmic localization of pregnane X receptor and ligand-dependent nuclear translocation in mouse liver.," *J. Biol. Chem.*, vol. 279, no. 47, pp. 49307–14, Nov. 2004.
- [6] P. D. Evans, A. Bayliss, and V. Reale, "GPCR-mediated rapid, non-genomic actions of steroids: comparisons between DmDopEcR and GPER1 (GPR30).," *Gen. Comp. Endocrinol.*, vol. 195, pp. 157–63, Jan. 2014.
- [7] K. Simons and E. Ikonen, "How Cells Handle Cholesterol," *Sci.*, vol. 290, no. 5497, pp. 1721–1726, Dec. 2000.
- [8] E. Ikonen, "Mechanisms for Cellular Cholesterol Transport: Defects and Human Disease," *Physiol. Rev.*, vol. 86, no. 4, pp. 1237–1261, Oct. 2006.
- [9] T. Plösch, J. K. Kruit, V. W. Bloks, N. C. A. Huijkman, R. Havinga, G. S. M. J. E. Duchateau, Y. Lin, and F. Kuipers, "Reduction of Cholesterol Absorption by Dietary Plant Sterols and Stanols in Mice Is Independent of the Abcg5/8 Transporter," *J. Nutr.*, vol. 136, no. 8, pp. 2135–2140, Aug. 2006.
- [10] B. Feng, P. M. Yao, Y. Li, C. M. Devlin, D. Zhang, H. P. Harding, M. Sweeney, J. X. Rong, G. Kuriakose, E. a Fisher, A. R. Marks, D. Ron, and I. Tabas, "The endoplasmic reticulum is the site of cholesterol-induced cytotoxicity in macrophages.," *Nat. Cell Biol.*, vol. 5, no. 9, pp. 781–92, Sep. 2003.
- [11] C. Iribarren, "Low Total Serum Cholesterol and Intracerebral Hemorrhagic Stroke: Is the Association Confined to Elderly Men?," *Stroke*, vol. 27, pp. 1993–1998, 1996.
- [12] G. E. Herman, "Disorders of cholesterol biosynthesis: prototypic metabolic malformation syndromes," *Hum. Mol. Genet.*, vol. 12, no. 90001, p. 75R–88, Apr. 2003.

- [13] D. S. Ory, "The niemann-pick disease genes; regulators of cellular cholesterol homeostasis.," *Trends Cardiovasc. Med.*, vol. 14, no. 2, pp. 66–72, Feb. 2004.
- [14] K. Lu, M.-H. Lee, and S. B. Patel, "Dietary cholesterol absorption; more than just bile," *Trends Endocrinol. Metab.*, vol. 12, no. 7, pp. 314–320, Sep. 2001.
- [15] P. Takizawa, "Cellular Control of cholesterol," *Yale Sch. Med.*, 2010.
- [16] M. Hao, S. X. Lin, O. J. Karylowski, D. Wüstner, T. E. McGraw, and F. R. Maxfield, "Vesicular and non-vesicular sterol transport in living cells. The endocytic recycling compartment is a major sterol storage organelle.," *J. Biol. Chem.*, vol. 277, no. 1, pp. 609–17, Jan. 2002.
- [17] B. Mesmin and F. R. Maxfield, "NIH Public Access," vol. 1791, no. 7, pp. 636–645, 2010.
- [18] S. S. Dixit, D. E. Sleat, A. M. Stock, and P. Lobel, "Do mammalian NPC1 and NPC2 play a role in intestinal cholesterol absorption?," *Biochem. J.*, vol. 408, no. 1, pp. 1–5, Nov. 2007.
- [19] R. E. Infante, M. L. Wang, A. Radhakrishnan, H. J. Kwon, M. S. Brown, and J. L. Goldstein, "NPC2 facilitates bidirectional transfer of cholesterol between NPC1 and lipid bilayers, a step in cholesterol egress from lysosomes.," *Proc. Natl. Acad. Sci. U. S. A.*, vol. 105, no. 40, pp. 15287–92, Oct. 2008.
- [20] M. C. Patterson, C. J. Hendriksz, M. Walterfang, F. Sedel, M. T. Vanier, and F. Wijburg, "Recommendations for the diagnosis and management of Niemann-Pick disease type C: an update.," *Mol. Genet. Metab.*, vol. 106, no. 3, pp. 330–44, Jul. 2012.
- [21] C. M. Ramirez, A. M. Lopez, L. Q. Le, K. S. Posey, A. G. Weinberg, and S. D. Turley, "Ontogenic changes in lung cholesterol metabolism, lipid content, and histology in mice with Niemann-Pick type C disease.," *Biochim. Biophys. Acta*, vol. 1841, no. 1, pp. 54–61, Jan. 2014.
- [22] X.-H. Yu, N. Jiang, P.-B. Yao, X.-L. Zheng, F. S. Cayabyab, and C.-K. Tang, "NPC1, intracellular cholesterol trafficking and atherosclerosis.," *Clin. Chim. Acta.*, vol. 429, pp. 69–75, Feb. 2014.
- [23] T.-Y. Chang, P. C. Reid, S. Sugii, N. Ohgami, J. C. Cruz, and C. C. Y. Chang, "Niemann-Pick Type C Disease and Intracellular Cholesterol Trafficking," *J. Biol. Chem.*, vol. 280, no. 22, pp. 20917–20920, Jun. 2005.
- [24] M. Di, A. Dardis, A. Madeo, R. Barone, A. Fiumara, and M. Di Rocco, "Early miglustat therapy in infantile niemann-pick disease type C.," *Pediatr. Neurol.*, vol. 47, no. 1, pp. 40–3, Jul. 2012.

- [25] J. E. Vance and K. B. Peake, "Function of the Niemann-Pick type C proteins and their bypass by cyclodextrin.," *Curr. Opin. Lipidol.*, vol. 22, no. 3, pp. 204–9, Jun. 2011.
- [26] A. C. Berger, T. H. Vanderford, K. M. Gernert, J. W. Nichols, V. Faundez, A. H. Corbett, L. E. U. Cen, and W. Nichols, "Saccharomyces cerevisiae Npc2p Is a Functionally Conserved Homologue of the Human Niemann-Pick Disease Type C 2 Saccharomyces cerevisiae Npc2p Is a Functionally Conserved Homologue of the Human Niemann-Pick Disease Type C 2 Protein , hNPC2 †," *Society*, vol. 4, no. 11, pp. 1851–1862, 2005.
- [27] K. Higaki, D. Almanzar-Paramio, and S. L. Sturley, "Metazoan and microbial models of Niemann-Pick Type C disease.," *Biochim. Biophys. Acta*, vol. 1685, no. 1–3, pp. 38–47, Oct. 2004.
- [28] R. Van Der Kant, I. Zondervan, L. Janssen, and J. Neefjes, "Cholesterol-binding molecules MLN64 and ORP1L mark distinct late endosomes with transporters ABCA3 and NPC1," vol. 54, 2013.
- [29] K. Uusi-Rauva, A. Kyttälä, R. van der Kant, J. Vesa, K. Tanhuanpää, J. Neefjes, V. Olkkonen, and A. Jalanko, "Neuronal ceroid lipofuscinosis protein CLN3 interacts with motor proteins and modifies location of late endosomal compartments," *Cell. Mol. Life Sci.*, vol. 69, no. 12, pp. 2075–2089, 2012.
- [30] M. Dean, a Rzhetsky, and R. Allikmets, "The human ATP-binding cassette (ABC) transporter superfamily.," *Genome Res.*, vol. 11, no. 7, pp. 1156–66, Jul. 2001.
- [31] E. Ikonen, "Mechanisms for Cellular Cholesterol Transport : Defects and Human Disease," *Physiol. Rev.*, pp. 1237–1261, 2006.
- [32] J. A. Whitsett, S. E. Wert, and T. E. Weaver, "Alveolar Surfactant Homeostasis and the Pathogenesis of Pulmonary Disease," *Annu. Rev. Med.*, vol. 61, no. 1, pp. 105–119, Jan. 2010.
- [33] E. Rigamonti, L. Helin, S. Lestavel, a L. Mutka, M. Lepore, C. Fontaine, M. a Bouhlef, S. Bultel, J. C. Fruchart, E. Ikonen, V. Clavey, B. Staels, and G. Chinetti-Gbaguidi, "Liver X receptor activation controls intracellular cholesterol trafficking and esterification in human macrophages.," *Circ. Res.*, vol. 97, no. 7, pp. 682–9, Sep. 2005.
- [34] a Chawla, J. J. Repa, R. M. Evans, and D. J. Mangelsdorf, "Nuclear receptors and lipid physiology: opening the X-files.," *Science*, vol. 294, no. 5548, pp. 1866–70, Nov. 2001.
- [35] P. Tontonoz and D. J. Mangelsdorf, "Liver X receptor signaling pathways in cardiovascular disease.," *Mol. Endocrinol.*, vol. 17, no. 6, pp. 985–93, Jun. 2003.
- [36] R. E. Soccio and J. L. Breslow, "Intracellular cholesterol transport.," *Arterioscler. Thromb. Vasc. Biol.*, vol. 24, no. 7, pp. 1150–60, Jul. 2004.

- [37] S. M. Grundy, "Absorption and metabolism of dietary cholesterol.," *Annu. Rev. Nutr.*, vol. 3, pp. 71–96, Jan. 1983.
- [38] A. Tanatani, "[Development of novel nuclear receptor ligands based on receptor-folding inhibition hypothesis]," *Yakugaku Zasshi*, vol. 127, no. 2, pp. 341–51, Feb. 2007.
- [39] J. S. Carroll, C. a Meyer, J. Song, W. Li, T. R. Geistlinger, J. Eeckhoutte, A. S. Brodsky, E. K. Keeton, K. C. Fertuck, G. F. Hall, Q. Wang, S. Bekiranov, V. Sementchenko, E. a Fox, P. a Silver, T. R. Gingeras, X. S. Liu, and M. Brown, "Genome-wide analysis of estrogen receptor binding sites.," *Nat. Genet.*, vol. 38, no. 11, pp. 1289–97, Nov. 2006.
- [40] K. Kobayashi, T. Sueyoshi, K. Inoue, R. Moore, and M. Negishi, "Cytoplasmic accumulation of the nuclear receptor CAR by a tetratricopeptide repeat protein in HepG2 cells.," *Mol. Pharmacol.*, vol. 64, no. 5, pp. 1069–75, Nov. 2003.
- [41] E. Enmark and J. a Gustafsson, "Comparing nuclear receptors in worms, flies and humans.," *Trends Pharmacol. Sci.*, vol. 22, no. 12, pp. 611–5, Dec. 2001.
- [42] V. Laudet, "Evolution of the nuclear receptor superfamily: early diversification from an ancestral orphan receptor.," *J. Mol. Endocrinol.*, vol. 19, no. 3, pp. 207–26, Dec. 1997.
- [43] S. A. Thomson, W. S. Baldwin, Y. H. Wang, G. Kwon, and G. A. Leblanc, "Annotation, phylogenetics, and expression of the nuclear receptors in *Daphnia pulex*," *BMC Genomics*, vol. 14, pp. 1–14, Jan. 2009.
- [44] N. Shibata and C. K. Glass, "Macrophages, Oxysterols and Atherosclerosis," *Circ. J.*, vol. 74, no. 10, pp. 2045–2051, 2010.
- [45] B. Liu, S. D. Turley, D. K. Burns, A. M. Miller, J. J. Repa, and J. M. Dietschy, "Reversal of defective lysosomal transport in NPC disease ameliorates liver dysfunction and neurodegeneration in the npc1<sup>-/-</sup> mouse.," *Proc. Natl. Acad. Sci. U. S. A.*, vol. 106, no. 7, pp. 2377–82, Feb. 2009.
- [46] A. C. Calkin and P. Tontonoz, "Liver x receptor signaling pathways and atherosclerosis.," *Arterioscler. Thromb. Vasc. Biol.*, vol. 30, no. 8, pp. 1513–8, Aug. 2010.
- [47] C. Zhao and K. Dahlman-Wright, "Liver X receptor in cholesterol metabolism.," *J. Endocrinol.*, vol. 204, no. 3, pp. 233–40, Mar. 2010.
- [48] M. Baranowski, "BIOLOGICAL ROLE OF LIVER X RECEPTORS," *J. Physiol. Pharmacol.* 2008, 59, Suppl 7, 31–55.
- [49] a Chawla, W. a Boisvert, C. H. Lee, B. a Laffitte, Y. Barak, S. B. Joseph, D. Liao, L. Nagy, P. a Edwards, L. K. Curtiss, R. M. Evans, and P. Tontonoz, "A PPAR gamma-LXR-ABCA1 pathway in macrophages is involved in cholesterol efflux and atherogenesis.," *Mol. Cell*, vol. 7, no. 1, pp. 161–71, Jan. 2001.

- [50] Y. Wang, P. M. Rogers, C. Su, G. Varga, K. R. Stayrook, and T. P. Burris, "Regulation of cholesterologenesis by the oxysterol receptor, LXRalpha.," *J. Biol. Chem.*, vol. 283, no. 39, pp. 26332–9, Sep. 2008.
- [51] L. Calpe-Berdiel, N. Rotllan, C. Fiévet, R. Roig, F. Blanco-Vaca, and J. C. Escolà-Gil, "Liver X receptor-mediated activation of reverse cholesterol transport from macrophages to feces in vivo requires ABCG5/G8," *J. Lipid Res.*, vol. 49, no. 9, pp. 1904–1911, Sep. 2008.
- [52] R. Geyeregger, M. Zeyda, and T. M. Stulnig, "Liver X receptors in cardiovascular and metabolic disease," *Cell. Mol. Life Sci.*, vol. 63, no. 5, pp. 524–539, 2006.
- [53] C. Hong and P. Tontonoz, "Liver X receptors in lipid metabolism: opportunities for drug discovery," *Nat Rev Drug Discov*, vol. 13, no. 6, pp. 433–444, Jun. 2014.
- [54] A. Gopalakrishnan, E. Nally, K. King-jones, M. Bujold, A. Gopalakrishnan, E. Nally, and K. King-jones, "Nuclear receptor DHR96 acts as a sentinel for low cholesterol concentrations in *Drosophila melanogaster*," *Mol. Cell. Biol.*, vol. 30, no. 3, pp. 793–805, Feb. 2010.
- [55] R. Clayton, "The utilization of sterols by insects," *J.Lipid Res.*, vol. 15, pp. 3–19, 1964.
- [56] K. Yen, T. T. Le, A. Bansal, S. D. Narasimhan, J.-X. Cheng, and H. a Tissenbaum, "A comparative study of fat storage quantitation in nematode *Caenorhabditis elegans* using label and label-free methods.," *PLoS One*, vol. 5, no. 9, Jan. 2010.
- [57] W. R. Svoboda, J.A., Imberski, R.B., Lusby, "Drosophila melanogaster does not dealkylate [14C]sitosterol.," *Exp.* 45, 983 – 985., 1989.
- [58] K. H. HEED WB, "UNIQUE STEROL IN THE ECOLOGY AND NUTRITION OF DROSOPHILA PACHEA.," *Sci.* 13 August 1965 Vol. 149 no. 3685 pp. 758-761 DOI10.1126/science.149.3685.758.
- [59] T. V Kurzchalia and S. Ward, "Why do worms need cholesterol?," *Nat. Cell Biol.*, vol. 5, no. 8, pp. 684–8, Aug. 2003.
- [60] V. C. Henrich, "Comparison of ecdysteroid production in *Drosophila* and *Manduca*: pharmacology and cross-species neural reactivity.," *Arch. Insect Biochem. Physiol.*, vol. 30, no. 2–3, pp. 239–54, Jan. 1995.
- [61] J. a Svoboda and G. F. Weirich, "Sterol metabolism in the tobacco hornworm, *Manduca sexta*--a review.," *Lipids*, vol. 30, no. 3, pp. 263–7, Mar. 1995.
- [62] a Radhakrishnan and H. M. McConnell, "Chemical activity of cholesterol in membranes.," *Biochemistry*, vol. 39, no. 28, pp. 8119–24, Jul. 2000.

- [63] F. R. Maxfield and D. Wüstner, "Analysis of cholesterol trafficking with fluorescent probes," *Methods Cell Biol.*, vol. 108, pp. 367–93, Jan. 2012.
- [64] J. Bełtowski, "Liver X receptors (LXR) as therapeutic targets in dyslipidemia.," *Cardiovasc. Ther.*, vol. 26, no. 4, pp. 297–316, Jan. 2008.
- [65] P. Sengupta, B. Baird, and D. Holowka, "Lipid rafts, fluid/fluid phase separation, and their relevance to plasma membrane structure and function.," *Semin. Cell Dev. Biol.*, vol. 18, no. 5, pp. 583–90, Oct. 2007.
- [66] P. W. Ingham, "Hedgehog signaling: a tale of two lipids.," *Science*, vol. 294, no. 5548, pp. 1879–81, Nov. 2001.
- [67] W. Palm, M. M. Swierczynska, V. Kumari, M. Ehrhart-bornstein, S. R. Bornstein, and S. Eaton, "Secretion and Signaling Activities of Lipoprotein- Associated Hedgehog and Non-Sterol-Modified Hedgehog in Flies and Mammals," vol. 11, no. 3, 2013.
- [68] F. Wendler, X. Franch-Marro, and J.-P. Vincent, "How does cholesterol affect the way Hedgehog works?," *Development*, vol. 133, no. 16, pp. 3055–61, Aug. 2006.
- [69] K. Simons and E. Ikonen, "Functional rafts in cell membranes.," *Nature*, vol. 387, no. 6633, pp. 569–72, Jun. 1997.
- [70] and B. J. L. Mitchell, D. C., M. Straume, J. L. Miller, "Modulation of metarhodopsin formation by cholesterol-induced ordering of bilayer lipids," *Biochem. 299143–9149*.
- [71] J. Ayala-Sanmartin, "Cholesterol enhances phospholipid binding and aggregation of annexins by their core domain.," *Biochem. Biophys. Res. Commun. 28372–79*.
- [72] Z. Ma, Z. Liu, and X. Huang, "Membrane phospholipid asymmetry counters the adverse effects of sterol overloading in the Golgi membrane of *Drosophila*." *Genetics*, vol. 190, no. 4, pp. 1299–308, Apr. 2012.
- [73] M. Carvalho, D. Schwudke, J. L. Sampaio, W. Palm, I. Riezman, G. Dey, G. D. Gupta, S. Mayor, H. Riezman, A. Shevchenko, T. V Kurzchalia, and S. Eaton, "Survival strategies of a sterol auxotroph.," *Development*, vol. 137, no. 21, pp. 3675–85, Nov. 2010.
- [74] I. Y. Dobrosotskaya, a C. Seegmiller, M. S. Brown, J. L. Goldstein, and R. B. Rawson, "Regulation of SREBP processing and membrane lipid production by phospholipids in *Drosophila*." *Science*, vol. 296, no. 5569, pp. 879–83, May 2002.
- [75] A. Rietveld, S. Neutz, K. Simons, and S. Eaton, "Association of Sterol- and Glycosylphosphatidylinositol-linked Proteins with *Drosophila* Raft Lipid Microdomains \*," vol. 274, no. 17, pp. 12049–12054, 1999.

- [76] S. J. Day and P. a Lawrence, "Measuring dimensions: the regulation of size and shape.," *Development*, vol. 127, no. 14, pp. 2977–87, Jul. 2000.
- [77] N. Alic, T. D. Andrews, M. E. Giannakou, I. Papatheodorou, C. Slack, M. P. Hoddinott, H. M. Cochemé, E. F. Schuster, J. M. Thornton, and L. Partridge, "Genome-wide dFOXO targets and topology of the transcriptomic response to stress and insulin signalling.," *Mol. Syst. Biol.*, vol. 7, no. 502, p. 502, Jan. 2011.
- [78] A. D. Rother KI, "Role of insulin receptors and IGF receptors in growth and development.," *Pediatr Nephrol* 14:558–561., 2000.
- [79] Z. McBrayer, H. Ono, M. Shimell, J.-P. Parvy, R. B. Beckstead, J. T. Warren, C. S. Thummel, C. Dauphin-Villemant, L. I. Gilbert, and M. B. O'Connor, "Prothoracicotropic hormone regulates developmental timing and body size in *Drosophila*.,," *Dev. Cell*, vol. 13, no. 6, pp. 857–71, Dec. 2007.
- [80] L. I. Gilbert, "Halloween genes encode P450 enzymes that mediate steroid hormone biosynthesis in *Drosophila melanogaster*.,," *Mol. Cell. Endocrinol.*, vol. 215, no. 1–2, pp. 1–10, Feb. 2004.
- [81] M. L. Grieneisen, J. T. Warren, and L. I. Gilbert, "Early steps in ecdysteroid biosynthesis: evidence for the involvement of cytochrome P-450 enzymes.," *Insect Biochem. Mol. Biol.*, vol. 23, no. 1, pp. 13–23, Jan. 1993.
- [82] T. Yoshiyama-yanagawa, S. Enya, Y. Shimada-niwa, S. Yaguchi, Y. Haramoto, T. Matsuya, K. Shiomi, Y. Sasakura, S. Takahashi, M. Asashima, H. Kataoka, and R. Niwa, "The Conserved Rieske Oxygenase DAF-36 / Neverland Is a Novel Cholesterol-metabolizing Enzyme \* □," vol. 286, no. 29, pp. 25756–25762, 2011.
- [83] R. Niwa, T. Namiki, K. Ito, Y. Shimada-Niwa, M. Kiuchi, S. Kawaoka, T. Kayukawa, Y. Banno, Y. Fujimoto, S. Shigenobu, S. Kobayashi, T. Shimada, S. Katsuma, and T. Shinoda, "Non-molting glossy/shroud encodes a short-chain dehydrogenase/reductase that functions in the 'Black Box' of the ecdysteroid biosynthesis pathway," *Dev.*, vol. 137, no. 12, pp. 1991–1999, Jun. 2010.
- [84] J. Terashima, K. Takaki, S. Sakurai, and M. Bownes, "Nutritional status affects 20-hydroxyecdysone concentration and progression of oogenesis in *Drosophila melanogaster*," *J. Endocrinol.*, vol. 187, no. 1, pp. 69–79, Oct. 2005.
- [85] A. De Loof, G. Baggerman, M. Breuer, I. Claeys, A. Cerstiaens, E. Clynen, T. Janssen, L. Schoofs, and J. Vanden Broeck, "Gonadotropins in insects: An overview," *Arch. Insect Biochem. Physiol.*, vol. 47, no. 3, pp. 129–138, Jul. 2001.
- [86] L. I. Gilbert, R. Rybczynski, and J. T. Warren, "CONTROL AND BIOCHEMICAL NATURE OF THE ECDYSTEROIDOGENIC PATHWAY," *Annu. Rev. Entomol.*, vol. 47, no. 1, pp. 883–916, Jan. 2002.

- [87] R. B. Beckstead, G. Lam, and C. S. Thummel, "Specific transcriptional responses to juvenile hormone and ecdysone in *Drosophila*," *Insect Biochem. Mol. Biol.*, vol. 37, no. 6, pp. 570–8, Jun. 2007.
- [88] D. T. Champlin and J. W. Truman, "Ecdysteroid control of cell proliferation during optic lobe neurogenesis in the moth *Manduca sexta*," *Dev.*, vol. 125, no. 2, pp. 269–277, Jan. 1998.
- [89] M. F. Feldlaufer, G. F. Weirich, R. B. Imberski, and J. a Svoboda, "Ecdysteroid production in *Drosophila melanogaster* reared on defined diets," *Insect Biochem. Mol. Biol.*, vol. 25, no. 6, pp. 709–12, Jun. 1995.
- [90] P. Leopold and N. Perrimon, "*Drosophila* and the genetics of the internal milieu," *Nature*, vol. 450, no. 7167, pp. 186–8, Nov. 2007.
- [91] N. Buchon, N. a Broderick, and B. Lemaitre, "Gut homeostasis in a microbial world: insights from *Drosophila melanogaster*," *Nat. Rev. Microbiol.*, vol. 11, no. 9, pp. 615–26, Sep. 2013.
- [92] A. C.-N. Wong, A. J. Dobson, and A. E. Douglas, "Gut microbiota dictates the metabolic response of *Drosophila* to diet," *J. Exp. Biol.*, no. February, Feb. 2014.
- [93] J. A. T. Dow, "The versatile stellate cell - more than just a space-filler," *J. Insect Physiol.*, vol. 58, no. 4, pp. 467–72, Apr. 2012.
- [94] M. McCarron, J. O'Donnell, A. Chovnick, B. S. Bhullar, J. Hewitt, and E. P. M. Candido, "ORGANIZATION OF THE ROSY LOCUS IN *DROSOPHILA MELANOGASTER*: FURTHER EVIDENCE IN SUPPORT OF A CIS-ACTING CONTROL ELEMENT ADJACENT TO THE XANTHINE DEHYDROGENASE STRUCTURAL ELEMENT," *Genet.*, vol. 91, no. 2, pp. 275–293, Feb. 1979.
- [95] A. J. Hilliker, B. Duyf, D. Evans, and J. P. Phillips, "Urate-null rosy mutants of *Drosophila melanogaster* are hypersensitive to oxygen stress," *Proc. Natl. Acad. Sci.*, vol. 89, no. 10, pp. 4343–4347, May 1992.
- [96] K. a Hamby, R. S. Kwok, F. G. Zalom, and J. C. Chiu, "Integrating circadian activity and gene expression profiles to predict chronotoxicity of *Drosophila suzukii* response to insecticides," *PLoS One*, vol. 8, no. 7, p. e68472, Jan. 2013.
- [97] J. McGettigan, R. K. J. McLennan, K. E. Broderick, L. Kean, A. K. Allan, P. Cabrero, M. R. Regulski, V. P. Pollock, G. W. Gould, S.-A. Davies, and J. A. T. Dow, "Insect renal tubules constitute a cell-autonomous immune system that protects the organism against bacterial infection," *Insect Biochem. Mol. Biol.*, vol. 35, no. 7, pp. 741–54, Jul. 2005.
- [98] K. D. Baker and C. S. Thummel, "Diabetic larvae and obese flies-emerging studies of metabolism in *Drosophila*," *Cell Metab.*, vol. 6, no. 4, pp. 257–66, Oct. 2007.

- [99] E. Gutierrez, D. Wiggins, B. Fielding, and A. P. Gould, "Specialized hepatocyte-like cells regulate *Drosophila* lipid metabolism.," *Nature*, vol. 445, no. 7125, pp. 275–80, Jan. 2007.
- [100] E. Bier and R. Bodmer, "Drosophila, an emerging model for cardiac disease.," *Gene*, vol. 342, no. 1, pp. 1–11, Nov. 2004.
- [101] M. Frasch, "Intersecting signalling and transcriptional pathways in *Drosophila* heart specification.," *Semin. Cell Dev. Biol.*, vol. 10, no. 1, pp. 61–71, Feb. 1999.
- [102] L. E. Canavoso, Z. E. Jouni, K. J. Karnas, J. E. Pennington, and M. A. Wells, "FAT METABOLISM IN INSECTS," *Annu. Rev. Nutr.*, vol. 21, no. 1, pp. 23–46, Jul. 2001.
- [103] E. L. Arrese, L. E. Canavoso, Z. E. Jouni, J. E. Pennington, K. Tsuchida, and M. A. Wells, "Lipid storage and mobilization in insects: current status and future directions," *Insect Biochem. Mol. Biol.*, vol. 31, no. 1, pp. 7–17, Jan. 2001.
- [104] E. Parra-Peralbo and J. Culi, "Drosophila lipophorin receptors mediate the uptake of neutral lipids in oocytes and imaginal disc cells by an endocytosis-independent mechanism.," *PLoS Genet.*, vol. 7, no. 2, p. e1001297, Jan. 2011.
- [105] M. Brankatschk and S. Eaton, "Lipoprotein particles cross the blood-brain barrier in *Drosophila*." *J. Neurosci.*, vol. 30, no. 31, pp. 10441–7, Aug. 2010.
- [106] D. Pistillo, a Manzi, a Tino, P. P. Boyl, F. Graziani, and C. Malva, "The *Drosophila melanogaster* lipase homologs: a gene family with tissue and developmental specific expression.," *J. Mol. Biol.*, vol. 276, no. 5, pp. 877–85, Mar. 1998.
- [107] S. T. Shindou H, "Acyl-CoA:lysophospholipid acyltransferases.," *J Biol Chem*, 2009.
- [108] M. Buszczak, X. Lu, W. A. Segraves, T. Y. Chang, and L. Cooley, "Mutations in the midway Gene Disrupt a *Drosophila* Acyl Coenzyme A :," 2002.
- [109] S. P. Voght, M. L. Fluegel, L. A. Andrews, and L. J. Pallanck, "Drosophila NPC1b promotes an early step in sterol absorption from the midgut epithelium.," *Cell Metab.*, vol. 5, no. 3, pp. 195–205, Mar. 2007.
- [110] X. Huang, K. Suyama, J. Buchanan, A. J. Zhu, and M. P. Scott, "A *Drosophila* model of the Niemann-Pick type C lysosome storage disease: *dnpc1a* is required for molting and sterol homeostasis.," *Development*, vol. 132, no. 22, pp. 5115–24, Nov. 2005.
- [111] X. Huang, J. T. Warren, and L. I. Gilbert, "New players in the regulation of ecdysone biosynthesis.," *J. Genet. Genomics*, vol. 35, no. 1, pp. 1–10, Jan. 2008.
- [112] K. King-jones, M. A. Horner, G. Lam, and C. S. Thummel, "The DHR96 nuclear receptor regulates xenobiotic responses in *Drosophila*." *Cell Metab.*, vol. 4, no. 1, pp. 37–48, Jul. 2006.

- [113] M. A. Horner, K. Pardee, S. Liu, K. King-jones, G. Lajoie, A. Edwards, H. M. Krause, and C. S. Thummel, "The *Drosophila* DHR96 nuclear receptor binds cholesterol and regulates cholesterol homeostasis," *Genes Dev.*, pp. 2711–2716, 2009.
- [114] K. J. Livak and T. D. Schmittgen, "Analysis of relative gene expression data using real-time quantitative PCR and the 2(-Delta Delta C(T)) Method.," *Methods*, vol. 25, no. 4, pp. 402–8, Dec. 2001.
- [115] L. R. Marek and A. E. Bale, "Drosophila homologs of FANCD2 and FANCL function in DNA repair.," *DNA Repair (Amst.)*, vol. 5, no. 11, pp. 1317–26, Nov. 2006.
- [116] M. D. Phillips and G. H. Thomas, "Brush border spectrin is required for early endosome recycling in *Drosophila*," *J. Cell Sci.*, vol. 119, no. Pt 7, pp. 1361–70, Apr. 2006.
- [117] K. M. Hennig, J. Colombani, and T. P. Neufeld, "TOR coordinates bulk and targeted endocytosis in the *Drosophila melanogaster* fat body to regulate cell growth.," *J. Cell Biol.*, vol. 173, no. 6, pp. 963–74, Jun. 2006.
- [118] S. Roy, L. S. Shashidhara, and K. VijayRaghavan, "Muscles in the *Drosophila* second thoracic segment are patterned independently of autonomous homeotic gene function.," *Curr. Biol.*, vol. 7, no. 4, pp. 222–7, Apr. 1997.
- [119] S. Terhzaz, P. Cabrero, V. R. Chintapalli, S.-A. Davies, and J. a T. Dow, "Mislocalization of mitochondria and compromised renal function and oxidative stress resistance in *Drosophila* SesB mutants.," *Physiol. Genomics*, vol. 41, no. 1, pp. 33–41, Mar. 2010.
- [120] J. a T. Dow, "Insights into the Malpighian tubule from functional genomics.," *J. Exp. Biol.*, vol. 212, no. Pt 3, pp. 435–45, Feb. 2009.
- [121] M. G. C. (MGC) P. Team, "Generation and initial analysis of more than 15,000 full-length human and mouse cDNA sequences," *Proc. Natl. Acad. Sci.*, vol. 99, no. 26, pp. 16899–16903, Dec. 2002.
- [122] E. N. Moriyama and J. R. Powell, "Codon usage bias and tRNA abundance in *Drosophila*," *J. Mol. Evol.*, vol. 45, pp. 514–523, 1997.
- [123] M. D. Krasowski, A. Ni, L. R. Hagey, and S. Ekins, "Evolution of promiscuous nuclear hormone receptors: LXR, FXR, VDR, PXR, and CAR.," *Mol. Cell. Endocrinol.*, vol. 334, no. 1–2, pp. 39–48, Mar. 2011.
- [124] L. Arnqvist, P. C. Dutta, L. Jonsson, and F. Sitbon, "Reduction of Cholesterol and Glycoalkaloid Levels in Transgenic Potato Plants by Overexpression of a Type 1 Sterol Methyltransferase cDNA 1," vol. 131, no. April, pp. 1792–1799, 2003.
- [125] J. Sang, *The nutritional requirements of Drosophila*. 1978, pp. 159–190.

- [126] W. a Smith and L. I. Gilbert, "Early events in peptide-stimulated ecdysteroid secretion by the prothoracic glands of *Manduca sexta*," *J. Exp. Zool.*, vol. 252, no. 3, pp. 264–70, Dec. 1989.
- [127] M. F. Feldlaufer, E. W. H. Jr, and J. A. Svoboda, "Makisterone a," vol. 15, no. 5, pp. 3–6, 1985.
- [128] C. P. Redfern, "Evidence for the presence of makisterone A in *Drosophila* larvae and the secretion of 20-deoxymakisterone A by the ring gland," *Proc. Natl. Acad. Sci. U. S. A.*, vol. 81, no. 18, pp. 5643–7, Sep. 1984.
- [129] J. N. Kaplanis, S. R. Dutky, W. E. Robbins, M. J. Thompson, E. L. Lindquist, D. H. Horn, M. N. Galbraith, A. J. N. Kaplanis, and S. Horn, "Makisterone A: a 28-carbon hexahydroxy molting hormone from the embryo of the milkweed bug," *Science*, vol. 190, no. 4215, pp. 681–2, Nov. 1975.
- [130] S. J. BEGG M, "A method for collecting and sterilizing large numbers of *Drosophila* eggs," *Sci. 1950 Jul 7;112(2897)11-2*.
- [131] J. T. Warren, J. Wismar, B. Subrahmanyam, and L. I. Gilbert, "Woc (without children) gene control of ecdysone biosynthesis in *Drosophila melanogaster*," *Mol. Cell. Endocrinol.*, vol. 181, no. 1–2, pp. 1–14, Jul. 2001.
- [132] a J. Clark and K. Block, "The absence of sterol synthesis in insects," *J. Biol. Chem.*, vol. 234, no. 10, pp. 2578–82, Oct. 1959.
- [133] E. Canavoso, Z. E. Jouni, K. J. Karnas, E. James, and M. A. Wells, "Etabolism in," pp. 23–46, 2001.
- [134] K. E. Bloch, "Sterol structure and membrane function," *CRC Crit. Rev. Biochem. 14*, 47–92., 1983.
- [135] L. I. Gilbert and K. F. Rewitz, "The Function and Evolution of the Halloween Genes : The Pathway to the Arthropod Molting Hormone," *Evolution (N. Y.)*, pp. 231–269, 2009.
- [136] S. Eaton, "Multiple roles for lipids in the Hedgehog signalling pathway," *Nat. Rev. Mol. Cell Biol.*, vol. 9, no. 6, pp. 437–45, Jul. 2008.
- [137] R. K. Mann and P. a Beachy, "Novel lipid modifications of secreted protein signals," *Annu. Rev. Biochem.*, vol. 73, pp. 891–923, Jan. 2004.
- [138] J. T. Warren, A. Petryk, G. Marques, M. Jarcho, J.-P. Parvy, C. Dauphin-Villemant, M. B. O'Connor, and L. I. Gilbert, "Molecular and biochemical characterization of two P450 enzymes in the ecdysteroidogenic pathway of *Drosophila melanogaster*," *Proc. Natl. Acad. Sci. U. S. A.*, vol. 99, no. 17, pp. 11043–8, Aug. 2002.

- [139] K. D. Baker, J. T. Warren, C. S. Thummel, L. I. Gilbert, and D. J. Mangelsdorf, "Transcriptional activation of the *Drosophila* ecdysone receptor by insect and plant ecdysteroids.," *Insect Biochem. Mol. Biol.*, vol. 30, no. 11, pp. 1037–43, Nov. 2000.
- [140] H. Ono, "Ecdysone differentially regulates metamorphic timing relative to 20-hydroxyecdysone by antagonizing juvenile hormone in *Drosophila melanogaster*." *Dev. Biol.*, vol. 391, no. 1, pp. 32–42, Jul. 2014.
- [141] B. Blumberg, W. Sabbagh, H. Juguilon, J. Bolado, C. M. van Meter, E. S. Ong, and R. M. Evans, "SXR, a novel steroid and xenobiotic-sensing nuclear receptor.," *Genes Dev.*, vol. 12, no. 20, pp. 3195–205, Oct. 1998.
- [142] B. M. Forman, I. Tzamelis, H. S. Choi, J. Chen, D. Simha, W. Seol, R. M. Evans, and D. D. Moore, "Androstane metabolites bind to and deactivate the nuclear receptor CAR-beta.," *Nature*, vol. 395, no. 6702, pp. 612–5, Oct. 1998.
- [143] R. R. Nofsinger, P. Li, S.-H. Hong, J. W. Jonker, G. D. Barish, H. Ying, S.-Y. Cheng, M. Leblanc, W. Xu, L. Pei, Y.-J. Kang, M. Nelson, M. Downes, R. T. Yu, J. M. Olefsky, C.-H. Lee, and R. M. Evans, "SMRT repression of nuclear receptors controls the adipogenic set point and metabolic homeostasis.," *Proc. Natl. Acad. Sci. U. S. A.*, vol. 105, no. 50, pp. 20021–6, Dec. 2008.
- [144] L. a Solt, P. R. Griffin, and T. P. Burris, "Ligand regulation of retinoic acid receptor-related orphan receptors: implications for development of novel therapeutics.," *Curr. Opin. Lipidol.*, vol. 21, no. 3, pp. 204–11, Jun. 2010.
- [145] L. Palanker, A. S. Necakov, H. M. Sampson, R. Ni, C. Hu, C. S. Thummel, and H. M. Krause, "Dynamic regulation of *Drosophila* nuclear receptor activity in vivo.," *Development*, vol. 133, no. 18, pp. 3549–62, Sep. 2006.
- [146] G. Mengus, M. May, L. Carre, P. Chambon, and I. Davidson, "Human TAF(II)135 potentiates transcriptional activation by the AF-2s of the retinoic acid, vitamin D3, and thyroid hormone receptors in mammalian cells.," *Genes Dev.*, vol. 11, no. 11, pp. 1381–1395, Jun. 1997.
- [147] F. M. Sladek, "What are nuclear receptor ligands?," *Mol. Cell. Endocrinol.*, pp. 1–11, Jul. 2010.
- [148] J. Cooke and J. H. Sang, "Utilization of sterols by larvae of *Drosophila melanogaster*," *J. Insect Physiol.*, vol. 16, no. 5, pp. 801–812, May 1970.
- [149] C. Curtis, G. N. Landis, D. Folk, N. B. Wehr, N. Hoe, M. Waskar, D. Abdueva, D. Skvortsov, D. Ford, A. Luu, A. Badrinath, R. L. Levine, T. J. Bradley, S. Tavaré, and J. Tower, "Transcriptional profiling of MnSOD-mediated lifespan extension in *Drosophila* reveals a species-general network of aging and metabolic genes.," *Genome Biol.*, vol. 8, no. 12, p. R262, Jan. 2007.

- [150] Y. Matsuzaki, V. Besnard, J. C. Clark, Y. Xu, S. E. Wert, M. Ikegami, and J. a Whitsett, "STAT3 regulates ABCA3 expression and influences lamellar body formation in alveolar type II cells.," *Am. J. Respir. Cell Mol. Biol.*, vol. 38, no. 5, pp. 551–8, May 2008.
- [151] M. H. Sieber and C. S. Thummel, "The DHR96 nuclear receptor controls triacylglycerol homeostasis in *Drosophila*," *Cell Metab.*, vol. 10, no. 6, pp. 481–90, Dec. 2009.
- [152] M. Jmoudiak and A. H. Futerman, "Gaucher disease: pathological mechanisms and modern management.," *Br. J. Haematol.*, vol. 129, no. 2, pp. 178–88, Apr. 2005.
- [153] I. Ron and M. Horowitz, "Intracellular cholesterol modifies the ERAD of glucocerebrosidase in Gaucher disease patients.," *Mol. Genet. Metab.*, vol. 93, no. 4, pp. 426–36, Apr. 2008.
- [154] A. M. Gurtan, P. Stuckert, and A. D. D'Andrea, "The WD40 repeats of FANCL are required for Fanconi anemia core complex assembly.," *J. Biol. Chem.*, vol. 281, no. 16, pp. 10896–905, Apr. 2006.
- [155] T. R. Hartman, T. I. Strohlic, Y. Ji, D. Zinshteyn, and A. M. O. Reilly, "Diet controls," vol. 201, no. 5, pp. 741–757, 2013.
- [156] S. M. Shreve, S. Yi, and R. E. Lee, "INCREASED DIETARY CHOLESTEROL ENHANCES COLD TOLERANCE IN *Drosophila melanogaster*," vol. 28, no. 1, pp. 33–37, 2007.
- [157] M. J. Lee, M. S. Park, S. Hwang, Y. K. Hong, G. Choi, Y. S. Suh, S. Y. Han, D. Kim, J. Jeun, C.-T. Oh, S.-J. Lee, S.-J. Han, D. Kim, E. S. Kim, G. Jeong, and K. S. Cho, "Dietary hempseed meal intake increases body growth and shortens the larval stage via the upregulation of cell growth and sterol levels in *Drosophila melanogaster*," *Mol. Cells*, vol. 30, no. 1, pp. 29–36, Jul. 2010.
- [158] R. O'Brian, *Fats and oils: formulating and processing for applications*. 2004, pp. 2nd ed., p. 31–34. CRC Press, Boca Raton, FL.
- [159] W. J. Etges, C. L. Veenstra, L. L. Jackson, and and L. L. J. Etges, W. J., C. L. Veenstra, "Premating isolation is determined by larval rearing substrates in cactophilic *Drosophila mojavensis*. VII. Effects of larval dietary fatty acids on adult epicuticular hydrocarbons.," *J. Chem. Ecol.*, vol. 32, no. 12, pp. 2629–46, Dec. 2006.
- [160] H. K. A. Boey, "The regulation and function of the *Drosophila melanogaster* Cytochrome P450 gene, *Cyp12d1*. PhD thesis, Department of Genetics, The University of Melbourne."
- [161] K. J. Patel and H. Joenje, "Fanconi anemia and DNA replication repair.," *DNA Repair (Amst.)*, vol. 6, no. 7, pp. 885–90, Jul. 2007.

- [162] A. C. Jung, B. Denholm, H. Skaer, and M. Affolter, "Renal tubule development in *Drosophila*: a closer look at the cellular level.," *J. Am. Soc. Nephrol.*, vol. 16, no. 2, pp. 322–8, Feb. 2005.
- [163] S. M. Linton and M. J. O'Donnell, "Contributions of K<sup>+</sup>:Cl<sup>-</sup> cotransport and Na<sup>+</sup>/K<sup>+</sup>-ATPase to basolateral ion transport in malpighian tubules of *Drosophila melanogaster*," *J. Exp. Biol.*, vol. 202, no. 11, pp. 1561–1570, Jun. 1999.
- [164] M. J. O'Donnell, J. A. Dow, G. R. Huesmann, N. J. Tublitz, and S. H. Maddrell, "Separate control of anion and cation transport in malpighian tubules of *Drosophila Melanogaster*," *J. Exp. Biol.*, vol. 199, no. 5, pp. 1163–1175, May 1996.
- [165] M. J. O'Donnell and J. H. Spring, "Modes of control of insect Malpighian tubules: synergism, antagonism, cooperation and autonomous regulation.," *J. Insect Physiol.*, vol. 46, no. 2, pp. 107–117, Feb. 2000.
- [166] M. J. O'Donnell, M. R. Rheault, S. A. Davies, P. Rosay, B. J. Harvey, S. H. P. Maddrell, K. Kaiser, and J. A. T. Dow, "Hormonally controlled chloride movement across *Drosophila* tubules is via ion channels in stellate cells," vol. 274, no. 4, pp. R1039–R1049, Apr. 1998.
- [167] Q. Ou, A. Magico, and K. King-Jones, "Nuclear receptor DHR4 controls the timing of steroid hormone pulses during *Drosophila* development.," *PLoS Biol.*, vol. 9, no. 9, p. e1001160, Sep. 2011.
- [168] K. F. Rewitz, N. Yamanaka, L. I. Gilbert, and M. B. O. Connor, "Activates Receptor Tyrosine Kinase Torso to Initiate Metamorphosis," *Science (80-. )*, vol. 326, no. December, 2009.
- [169] K. Subramanian and W. E. Balch, "NPC1/NPC2 function as a tag team duo to mobilize cholesterol.," *Proc. Natl. Acad. Sci. U. S. A.*, vol. 105, no. 40, pp. 15223–4, Oct. 2008.
- [170] H.-L. Liou, S. S. Dixit, S. Xu, G. S. Tint, A. M. Stock, and P. Lobel, "NPC2, the protein deficient in Niemann-Pick C2 disease, consists of multiple glycoforms that bind a variety of sterols.," *J. Biol. Chem.*, vol. 281, no. 48, pp. 36710–23, Dec. 2006.
- [171] M. L. Wang, M. Motamed, R. E. Infante, L. Abi-Mosleh, H. J. Kwon, M. S. Brown, and J. L. Goldstein, "Identification of surface residues on Niemann-Pick C2 essential for hydrophobic handoff of cholesterol to NPC1 in lysosomes.," *Cell Metab.*, vol. 12, no. 2, pp. 166–73, Aug. 2010.
- [172] N. Friedland, H.-L. Liou, P. Lobel, and A. M. Stock, "Structure of a cholesterol-binding protein deficient in Niemann-Pick type C2 disease.," *Proc. Natl. Acad. Sci. U. S. A.*, vol. 100, no. 5, pp. 2512–7, Mar. 2003.

- [173] D. C. Ko, J. Binkley, A. Sidow, and M. P. Scott, "The integrity of a cholesterol-binding pocket in Niemann-Pick C2 protein is necessary to control lysosome cholesterol levels.," *Proc. Natl. Acad. Sci. U. S. A.*, vol. 100, no. 5, pp. 2518–25, Mar. 2003.
- [174] Y. Xiang, Z. Liu, and X. Huang, "Br Regulates the Expression of the Ecdysone Biosynthesis Gene *Npc1*," *Dev. Biol.*, vol. 344, no. 2, pp. 800–8, Aug. 2010.
- [175] S. Kondo, M. Booker, and N. Perrimon, "Cross-species RNAi rescue platform in *Drosophila melanogaster*," *Genetics*, vol. 183, no. 3, pp. 1165–73, Nov. 2009.
- [176] R. K. Ejsmont, M. Sarov, S. Winkler, K. A. Lipinski, and P. Tomancak, "BRIEF COMMUNICATIONS A toolkit for species gene engineering in *Drosophila*," vol. 6, no. 6, 2009.
- [177] M. Charman, B. E. Kennedy, N. Osborne, and B. Karten, "MLN64 mediates egress of cholesterol from endosomes to mitochondria in the absence of functional Niemann-Pick Type C1 protein.," *J. Lipid Res.*, vol. 51, no. 5, pp. 1023–34, May 2010.
- [178] G. E. Roth, M. S. Gierl, L. Vollborn, M. Meise, R. Lintermann, and G. Korge, "The *Drosophila* gene *Start1*: a putative cholesterol transporter and key regulator of ecdysteroid synthesis.," *Proc. Natl. Acad. Sci. U. S. A.*, vol. 101, no. 6, pp. 1601–6, Feb. 2004.
- [179] X. Huang, K. Suyama, J. Buchanan, A. J. Zhu, and M. P. Scott, "A *Drosophila* model of the Niemann-Pick type C lysosome storage disease: *dnpc1a* is required for molting and sterol homeostasis.," *Development*, vol. 132, no. 22, pp. 5115–24, Nov. 2005.
- [180] S. U. Walkley and K. Suzuki, "Consequences of NPC1 and NPC2 loss of function in mammalian neurons.," *Biochim. Biophys. Acta*, vol. 1685, no. 1–3, pp. 48–62, Oct. 2004.
- [181] E. Lloyd-Evans, A. J. Morgan, X. He, D. A. Smith, E. Elliot-Smith, D. J. Sillence, G. C. Churchill, E. H. Schuchman, A. Galione, and F. M. Platt, "Niemann-Pick disease type C1 is a sphingosine storage disease that causes deregulation of lysosomal calcium," *Nat Med*, vol. 14, no. 11, pp. 1247–1255, Nov. 2008.
- [182] X. Huang, J. T. Warren, J. Buchanan, L. I. Gilbert, and M. P. Scott, "Drosophila Niemann-Pick type C-2 genes control sterol homeostasis and steroid biosynthesis: a model of human neurodegenerative disease.," *Development*, vol. 134, no. 20, pp. 3733–42, Oct. 2007.
- [183] J. Cooke and J. H. Sang, "Cooke, J. & Sang, J. H.," *J. Insect Physiol.* 16, 801–812, vol. 16, no. 5, pp. 801–812, May 1970.
- [184] R. P. Hobson, "On a fat-soluble growth factor required by blow-fly larvae: identity of the growth factor with cholesterol," *J. Biochem.*, vol. 29, pp. 2023–2026, 1935.

- [185] M. M. Swierczynska, V. Lamounier-Zepter, S. R. Bornstein, and S. Eaton, "Lipoproteins and Hedgehog signalling--possible implications for the adrenal gland function.," *Eur. J. Clin. Invest.*, vol. 43, no. 11, pp. 1178–83, Nov. 2013.
- [186] W. Palm, J. L. Sampaio, M. Brankatschk, M. Carvalho, A. Mahmoud, A. Shevchenko, and S. Eaton, "Lipoproteins in *Drosophila melanogaster*--assembly, function, and influence on tissue lipid composition.," *PLoS Genet.*, vol. 8, no. 7, p. e1002828, Jan. 2012.
- [187] M. Carvalho, J. L. Sampaio, W. Palm, M. Brankatschk, S. Eaton, and A. Shevchenko, "Effects of diet and development on the *Drosophila* lipidome.," *Mol. Syst. Biol.*, vol. 8, no. 600, p. 600, Jan. 2012.
- [188] L. J. Pike, "Growth factor receptors, lipid rafts and caveolae: an evolving story.," *Biochim. Biophys. Acta*, vol. 1746, no. 3, pp. 260–73, Dec. 2005.
- [189] H. a Lucero and P. W. Robbins, "Lipid rafts-protein association and the regulation of protein activity.," *Arch. Biochem. Biophys.*, vol. 426, no. 2, pp. 208–24, Jun. 2004.
- [190] H. Löfgren and I. Pascher, "Molecular arrangements of sphingolipids. The monolayer behaviour of ceramides," *Chem. Phys. Lipids*, vol. 20, no. 4, pp. 273–284, Dec. 1977.
- [191] S. Carolina, "NIH Public Access," vol. 49, no. 1, pp. 153–161, 2009.
- [192] W. D. Nes, "Biosynthesis of cholesterol and other sterols.," *Chem. Rev.*, vol. 111, no. 10, pp. 6423–51, Oct. 2011.
- [193] C. Parkin and B. Burnet, "Growth arrest of *Drosophila melanogaster* on *erg-2* and *erg-6* sterol mutant strains of *Saccharomyces cerevisiae*," *J. Insect Physiol.*, vol. 32, no. 5, pp. 463–471, 1986.
- [194] A. J. N. Kaplanis, S. R. Dutky, W. E. Robbins, M. J. Thompson, E. L. Lindquist, S. Horn, and M. N. Galbraith, "Makisterone A : A 28-Carbon Hexahydroxy Molting Hormone from the Embryo of the Milkweed Bug Published by : American Association for the Advancement of Science Stable URL : <http://www.jstor.org/stable/1741206> Makisterone A : A 28-Carbon Hexahydroxy Molting," *Adv. Sci.*, vol. 190, no. 4215, pp. 681–682, 2010.
- [195] in: J. K. (Ed. . M.F. Feldlaufer, "Ecdysone—From Chemistry to Mode of Action.," *Georg Thieme Verlag, Stuttgart, 1989, p. 308.*
- [196] S. Wang, S. Ayer, W. A. Segraves, R. Williams, A. S. Raikhel, and D. R. Williams, "Molecular Determinants of Differential Ligand Sensitivities of Insect Ecdysteroid Receptors Molecular Determinants of Differential Ligand Sensitivities of Insect Ecdysteroid Receptors," 2000.

- [197] K. D. Baker, L. M. Shewchuk, T. Kozlova, M. Makishima, A. Hassell, B. Wisely, J. A. Caravella, M. H. Lambert, J. L. Reinking, H. Krause, C. S. Thummel, T. M. Willson, D. J. Mangelsdorf, M. Drive, N. Carolina, and E. Street, "The Drosophila Orphan Nuclear Receptor DHR38 Mediates an Atypical Ecdysteroid Signaling Pathway," vol. 113, pp. 731–742, 2003.
- [198] T. M. Willson and S. a. Kliewer, "Pxr, Car and Drug Metabolism," *Nat. Rev. Drug Discov.*, vol. 1, no. 4, pp. 259–266, Apr. 2002.
- [199] A. Higazi, M. Abed, J. Chen, and Q. Li, "Promoter context determines the role of proteasome in ligand-dependent occupancy of retinoic acid responsive elements.," *Epigenetics*, vol. 6, no. 2, pp. 202–211, Feb. 2011.
- [200] B. R. Graveley, A. N. Brooks, J. W. Carlson, M. O. Duff, J. M. Landolin, L. Yang, C. G. Artieri, M. J. van Baren, N. Boley, B. W. Booth, J. B. Brown, L. Cherbas, C. A. Davis, A. Dobin, R. Li, W. Lin, J. H. Malone, N. R. Mattiuzzo, D. Miller, D. Sturgill, B. B. Tuch, C. Zaleski, D. Zhang, M. Blanchette, S. Dudoit, B. Eads, R. E. Green, A. Hammonds, L. Jiang, P. Kapranov, L. Langton, N. Perrimon, J. E. Sandler, K. H. Wan, A. Willingham, Y. Zhang, Y. Zou, J. Andrews, P. J. Bickel, S. E. Brenner, M. R. Brent, P. Cherbas, T. R. Gingeras, R. A. Hoskins, T. C. Kaufman, B. Oliver, and S. E. Celniker, "The developmental transcriptome of *Drosophila melanogaster*," *Nature*, vol. 471, no. 7339, pp. 473–479, Mar. 2011.
- [201] M. L. Fluegel, T. J. Parker, and L. J. Pallanck, "Mutations of a *Drosophila* NPC1 gene confer sterol and ecdysone metabolic defects.," *Genetics*, vol. 172, no. 1, pp. 185–96, Jan. 2006.
- [202] A. Takamura, N. Sakai, M. Shinpoo, A. Noguchi, T. Takahashi, S. Matsuda, M. Yamamoto, A. Narita, K. Ohno, T. Ohashi, H. Ida, and Y. Eto, "The useful preliminary diagnosis of Niemann-Pick disease type C by filipin test in blood smear.," *Mol. Genet. Metab.*, vol. 110, no. 3, pp. 401–4, Nov. 2013.
- [203] S. Sugii, P. C. Reid, N. Ohgami, Y. Shimada, R. A. Maue, H. Ninomiya, Y. Ohno-Iwashita, and T.-Y. Chang, "Biotinylated  $\theta$ -toxin derivative as a probe to examine intracellular cholesterol-rich domains in normal and Niemann-Pick type C1 cells," *J. Lipid Res.*, vol. 44, no. 5, pp. 1033–1041, May 2003.
- [204] R. Ishitsuka, T. Saito, H. Osada, Y. Ohno-Iwashita, and T. Kobayashi, "Fluorescence image screening for chemical compounds modifying cholesterol metabolism and distribution," *J. Lipid Res.*, vol. 52, no. 11, pp. 2084–2094, Nov. 2011.
- [205] A. A. Waheed, Y. Shimada, H. F. G. Heijnen, M. Nakamura, M. Inomata, M. Hayashi, S. Iwashita, J. W. Slot, and Y. Ohno-Iwashita, "Selective binding of perfringolysin O derivative to cholesterol-rich membrane microdomains (rafts)," *Proc. Natl. Acad. Sci.*, vol. 98, no. 9, pp. 4926–4931, Apr. 2001.

- [206] M. Booker, A. A. Samsonova, Y. Kwon, I. Flockhart, S. E. Mohr, and N. Perrimon, “False negative rates in *Drosophila* cell-based RNAi screens: a case study.,” *BMC Genomics*, vol. 12, no. 1, p. 50, Jan. 2011.
- [207] K. Hiruma and Y. Kaneko, “Hormonal regulation of insect metamorphosis with special reference to juvenile hormone biosynthesis.,” *Curr. Top. Dev. Biol.*, vol. 103, pp. 73–100, Jan. 2013.
- [208] X. Zhou, “Overexpression of broad: a new insight into its role in the *Drosophila* prothoracic gland cells,” *J. Exp. Biol.*, vol. 207, no. 7, pp. 1151–1161, Mar. 2004.
- [209] Y. Ma, A. Creanga, L. Lum, and P. a Beachy, “Prevalence of off-target effects in *Drosophila* RNA interference screens.,” *Nature*, vol. 443, no. 7109, pp. 359–63, Sep. 2006.
- [210] J. Moffat, J. H. Reiling, and D. M. Sabatini, “Off-target effects associated with long dsRNAs in *Drosophila* RNAi screens.,” *Trends Pharmacol. Sci.*, vol. 28, no. 4, pp. 149–51, Apr. 2007.
- [211] C. Blais, T. Blasco, A. Maria, C. Dauphin-Villemant, and R. Lafont, “Characterization of ecdysteroids in *Drosophila melanogaster* by enzyme immunoassay and nano-liquid chromatography-tandem mass spectrometry.,” *J. Chromatogr. B. Analyt. Technol. Biomed. Life Sci.*, vol. 878, no. 13–14, pp. 925–32, Apr. 2010.